INSTITUTE OF SEISMOLOGY
UNIVERSITY OF HELSINKI

REPORT S-73

LITHOSPHERE 2024

THIRTEENTH SYMPOSIUM ON THE STRUCTURE, COMPOSITION AND EVOLUTION OF THE LITHOSPHERE

Vuorimiehentie 5 Auditorium, Espoo, Finland
November 12-14, 2024

PROGRAMME AND EXTENDED ABSTRACTS

edited by

Perttu Mikkola, Toni Veikkolainen, Suvi Heinonen, Hannu Koivula, Kaisa Nikkilä, Jochen Kamm, David Whipp, Riikka Kietäväinen and Hanna Silvennoinen

Helsinki 2024

Series Editor-in-Chief: Suvi Heinonen

Guest Editors: Perttu Mikkola, Toni Veikkolainen, Suvi Heinonen, Hannu Koivula, Kaisa Nikkilä, Jochen Kamm, David Whipp, Riikka Kietäväinen and Hanna Silvennoinen

Publisher: Institute of Seismology
P.O. Box 68
FI-00014 University of Helsinki
Finland
Phone: +358-294-1911 (switchboard)
Email: seismo@helsinki.fi
https://www.seismo.helsinki.fi

ISSN 0357-3060
ISBN 978-952-10-9614-3 (PDF)

LITHOSPHERE 2024

THIRTEENTH SYMPOSIUM ON THE STRUCTURE, COMPOSITION AND EVOLUTION OF THE LITHOSPHERE

PROGRAMME AND EXTENDED ABSTRACTS

Vuorimiehentie 5 Auditorium, Espoo, Finland
November 12 – 14, 2024

CONTRIBUTING ORGANIZATIONS

Finnish National Committee of the International Lithosphere Programme (ILP)
Geological Survey of Finland (GTK)
National Land Survey of Finland, Finnish Geospatial Research Institute (FGI)
University of Helsinki
Åbo Akademi University
University of Oulu

ORGANIZING COMMITTEE AND EDITORS

Perttu Mikkola	Geological Survey of Finland (perttu.mikkola@gtk.fi)
Toni Veikkolainen	University of Helsinki (toni.veikkolainen@helsinki.fi)
Suvi Heinonen	University of Helsinki (suvi.heinonen@helsinki.fi)
Hannu Koivula	National Land Survey of Finland (hannu.koivula@nls.fi)
Kaisa Nikkilä	Åbo Akademi University (kaisa.nikkila@abo.fi)
Jochen Kamm	Geological Survey of Finland (jochen.kamm@gtk.fi)
David Whipp	University of Helsinki (david.whipp@helsinki.fi)
Riikka Kietäväinen	University of Helsinki (riikka.kietavainen@helsinki.fi)
Hanna Silvennoinen	University of Oulu (hanna.silvennoinen@oulu.fi)

References of Lithosphere Symposia Publications

Pesonen, L.J., Korja, A. and Hjelt, S.-E., 2000 (Eds.). Lithosphere 2000 - A Symposium on the Structure, Composition and Evolution of the Lithosphere in Finland. Programme and Extended Abstracts, Espoo, Finland, October 4-5, 2000. Institute of Seismology, University of Helsinki, Report S-41, 192 pages.

Lahtinen, R., Korja, A., Arhe, K., Eklund, O., Hjelt, S.-E. and Pesonen, L.J., 2002 (Eds.). Lithosphere 2002 – Second Symposium on the Structure, Composition and Evolution of the Lithosphere in Finland. Programme and Extended Abstracts, Espoo, Finland, November 12-13, 2002. Institute of Seismology, University of Helsinki, Report S-42, 146 pages.

Ehlers, C., Korja A., Kruuna, A., Lahtinen, R. and Pesonen, L.J., 2004 (Eds.). Lithosphere 2004 – Third Symposium on the Structure, Composition and Evolution of the Lithosphere in Finland. Programme and Extended Abstracts, November 10-11, 2004, Turku, Finland. Institute of Seismology, University of Helsinki, Report S-45, 131 pages.

Kukkonen, I.T., Eklund, O., Korja, A., Korja, T., Pesonen, L.J. and Poutanen, M., 2006 (Eds.). Lithosphere 2006 – Fourth Symposium on the Structure, Composition and Evolution of the Lithosphere in Finland. Programme and Extended Abstracts, Espoo, Finland, November 9-10, 2006. Institute of Seismology, University of Helsinki, Report S-46, 233 pages.

Korja, T., Arhe, K., Kaikkonen, P., Korja, A., Lahtinen, R. and Lunkka, J.P., 2008 (Eds.). Lithosphere 2008 – Fifth Symposium on the Structure, Composition and Evolution of the Lithosphere in Finland. Programme and Extended Abstracts, Oulu, Finland, November 5-6, 2008. Institute of Seismology, University of Helsinki, Report S-53, 132 pages.

Heikkinen, P., Arhe, K., Korja, T., Lahtinen, R., Pesonen, L.J. and Rämö, T., 2010 (Eds.). Lithosphere 2010 – Sixth Symposium on the Structure, Composition and Evolution of the Lithosphere in Finland. Programme and Extended Abstracts, Helsinki, Finland, October 27-28, 2010. Institute of Seismology, University of Helsinki, Report S-55, 154 pages.

Kukkonen, I.T., Kosonen, E., Oinonen, K., Eklund, O., Korja, A., Korja, T., Lahtinen, R., Lunkka, J.P. and Poutanen, M., 2012 (Eds.). Lithosphere 2012 – Seventh Symposium on the Structure, Composition and Evolution of the Lithosphere in Finland. Programme and Extended Abstracts, Espoo, Finland, November 6-8, 2012. Institute of Seismology, University of Helsinki, University of Helsinki, S-56, 116 pages.

Eklund, O., Kukkonen, I.T., Skyttä, P., Sonck-Koota, P., Väisänen, M. and Whipp, D., 2014 (Eds.). Lithosphere 2014 – Eighth Symposium on the Structure, Composition and Evolution of the Lithosphere in Finland. Programme and Extended Abstracts, Turku, Finland, November 4-6, 2014. Institute of Seismology, University of Helsinki, S-62, 126 pages.

Kukkonen, I.T., Heinonen, S., Oinonen, K., Arhe, K., Eklund, O., Karell, F., Kozlovskaya, E., Luttinen, A., Lahtinen, R., Lunkka, J., Nykänen, V., Poutanen, M., Tanskanen, E. and Tiira T. (Eds.), 2016. Lithosphere 2016 – Ninth Symposium on the Structure, Composition and Evolution of the Lithosphere in Finland. Programme and Extended Abstracts, Espoo, Finland, November 9-11, 2016. Institute of Seismology, University of Helsinki, Report S-65, 156 pages.

Kukkonen, I.T., Heinonen, S., Silvennoinen, H., Karell, Kozlovskaya, E., Luttinen, A., Nikkilä, K., Nykänen, V., Poutanen, M., Skyttä, P., Tanskanen, E., Tiira, T. and Oinonen, K. (Eds.), 2018. Lithosphere 2018 – Tenth Symposium on the Structure, Composition and Evolution of the Lithosphere. Programme and Extended Abstracts, Oulu, Finland, November 14-16, 2018. Institute of Seismology, University of Helsinki, Report S-67, 134 pages.

Kukkonen, I.T., Veikkolainen, T., Heinonen, S., Karell, F., Kozlovskaya, E., Luttinen, A., Nikkilä, K., Nykänen, V., Poutanen, M., Skyttä, P., Tanskanen, E. and Tiira, T. (Eds.), 2021. Lithosphere 2021 – Eleventh Symposium on the Structure, Composition and Evolution of the Lithosphere in Finland. Programme and Extended Abstracts, January 19-20, 2021. Institute of Seismology, University of Helsinki, Report S-71, 164 pages (pdf).

Skyttä, P., Nikkilä, K., Heilimo, E., Kukkonen, I.T., Veikkolainen, T., Karell, F., Kozlovskaya, E., Luttinen, A., Nykänen, V., Poutanen, M., Tanskanen, E., and Tiira, T. (Eds.), 2022. Lithosphere 2022 – Twelfth Symposium on the Structure, Composition and Evolution of the Lithosphere. Programme

and Extended Abstracts, November 15-17, 2022. Institute of Seismology, University of Helsinki, Report S-72, 200 pages.

Mikkola, P., Veikkolainen, T., Heinonen, S., Koivula, H., Nikkilä, K., Kamm, J., Whipp, D., Kietäväinen, R., and Silvennoinen, H. (Eds.), 2022. Lithosphere 2024 – Thirteenth Symposium on the Structure, Composition and Evolution of the Lithosphere. Programme and Extended Abstracts, November 12-14, 2024. Institute of Seismology, University of Helsinki, Report S-73, 133 pages.

Keywords (GeoRef Thesaurus, AGI): lithosphere, crust, upper mantle, Fennoscandia, Finland, Precambrian, Baltic Shield, symposia

TABLE OF CONTENTS

PREFACE

The Finnish National committee of the International Lithosphere Programme (ILP) has organized the biannual LITHOSPHERE (LITO) symposium since 2000. The LITO symposium provides a forum for solid earth geoscientists to present their results and reviews to an audience consisting of both geologists and geophysicists, inspiring interdisciplinary discussions and networking. The thirteenth symposium - LITHOSPHERE 2024 - comprises 37 presentations with topics varying from the deep biosphere to the ancient tectonic margins of Fennoscandia. The extended abstracts in this volume provide an overview of current research in Finland, focusing on the structure and processes within the solid Earth. Prof. Alireza Malehmir (Uppsala University, Sweden) will share insights into the novel developments of seismic data acquisition in his keynote talk. An invited talk by Prof. Gregor Hillers (University of Helsinki) will discuss the possibilities offered by dense array seismology and Stefan Luth (Geological Survey of Sweden) will share how structural geologists can utilize data produced by geophysicists.

The three-day symposium is jointly hosted by the Geological Survey of Finland and National Land Survey of Finland, and it will take place at Vuorimiehentie 5, Otaniemi, Espoo on November 12-14, 2024. The symposium is sponsored by Loimu (The Union of Professionals in Natural, Environmental and Forestry Sciences). In addition to oral presentations, the LITO symposium will have a traditional poster session. In each LITO symposium, posters prepared by graduate and postgraduate students are evaluated and the student with the best poster will receive an award.

This special volume “LITHOSPHERE 2024” contains the programme and extended abstracts of the symposium in alphabetical order by the first author’s last name. Enjoy reading the current developments of lithosphere-related research in Finland.

Helsinki, October 31, 2024

Perttu Mikkola, Toni Veikkolainen, Suvi Heinonen, Hannu Koivula, Kaisa Nikkilä, Jochen Kamm, David Whipp, Riikka Kietäväinen and Hanna Silvennoinen

Lithosphere 2024 Organizing Committee

LITHOSPHERE 2024 Symposium
Programme

Tuesday, Nov 12

12:00–13:00 Registration and hanging up posters, Vuorimiehentie 5, Espoo, ground floor

13:00–13:05 Opening: Suvi Heinonen
13:05–13:15 Jarkko Koskinen, Deputy Director General, National Land Survey
Aku Heinonen, Research Director, Geological Survey of Finland

13:15–14:30 Session 1: Fennoscandian crustal development
Chair: Toni Veikkolainen

13:15–13:40 **J. M. Pownall, K.A. Cutts, K. Hiltunen & V. Yliknuussi**
The Lapland Granulite Belt: new P–T–t results and tectonic ideas
13:40–14:05 **T. Slagstad, E.A.F. Østnes & B.E. Sørensen**
Tectonic assembly of the SW Fennoscandian margin
14:05–14:30 **J.D. Solano-Acosta, A. Soesoo, R. Hints & S. Graul**
Is the Estonian Alutaguse Section of Eastern Fennoscandia a continuation of the Southern Svecofennian Finnish Terranes, or is it akin to the Swedish Bergslagen region?

14:30–14:55 Session 2: Poster teasers

14:30–14:40 **S. Luth, J. Köykkä & E. Torgersen (Keynote poster)**
Lithotectonic map of Fennoscandia: An ongoing project
14:40–14:55 Other posters, 1 slide per poster (see list below)

14:55–16:00 Coffee/Tea, poster viewing

POSTERS

P01. S. Luth, J. Köykkä and E. Torgersen (Keynote poster): Lithotectonic map of Fennoscandia: An ongoing project

P02. S. Aatos and the NDCAF team: Developing the digital core archive of Finland
P03. T. Elminen: Rapakivi related thermal effect in nearby shear zones in the capital area, southern Finland
P04. A. Harjulehto, J. Kamm, P. Mishra and J. Salminen: Three-dimensional resistivity model of Svecofennian collision zone in Bothnian region

P05. **V. Laakso and S. Heinonen:** Seismic reflection profiling for studying lithosphere in Finland

P06. **A. C. Nascimento, D. C. Oliveira and E. Heilimo:** Metamorphic insights into the Archean Basement of the Carajás Province and its Affinity with the Karelia and Kola Provinces

P07. **M. Nuppunen-Puputti, R. Kietäväinen, L. Purkamo, I. Kukkonen and M. Bomberg:** Rock surface attaching deep biosphere microbes and their functionality (DEEPFUN)

P08. **C. Patzer, T. Luhta, M. Cyz, E. Koskela, V. Laakso, M. Malinowski, J. Mursu and T. Luoto:** Structural studies of Wiborg rapakivi batholith in Geoenergialoikka -project to support utilization of geothermal energy in Kymenlaakso

P09. **S. Silvennoinen, T. Luoto, J. Näränen, H. Pettersson, A. Riihelä, T. Rämö, T. Tiira, L. Tuomi, P. Uotila, J. Uusikivi and H. Vanhamäki:** International Union of Geodesy and Geophysics (IUGG)

P10. **J.D. Solano-Acosta, A. Soesoo and R. Hints:** Geophysical and Geochemical characterisation of the Märjamaa Rapakivi granite, Estonia

P11. **A. Tsampas, A. Korja, E. Moen and EPOS-Finland Consortium:** EPOS-FI - The Finnish node of the European Plate Observing System

P12. **J. Tuomiranta, C. Patzer, J. Kamm and J. Salminen:** Magnetotellurics over Kainuu belt, Finland

16:00–17:25 **Session 3**
Chair: Hannu Koivula

16:00–16:25 **M. Poutanen**
The Contribution of the IAG to Lithosphere Research

16:25–17:25 **Alireza Malehmir (Keynote)**
Imaging impossible in GPS-denied environment: in-mine seismic studies for hardrock exploration

17:30–late **Ice breaker**
Otapas Bar, Otakaari 27, 300 m walk from the meeting venue

Wednesday, Nov 13

09:00–10:35 **Session 4: Modelling in different scales and Ds**
Chair: Perttu Mikkola

09:00–09:35 **S. Luth & J. Jönberger (Invited)**
3D geological modelling and combined XCT-XRF drill core scanning of the Enåsen Au-Cu-(Te-Ag) deposit, Central Sweden

09:35–10:00 **S. Heinonen**
Seismic reflection profiling in hardrock terrains: interpreting complex reflectivity patterns in Fennoscandia

10:00–10:25 **M. Malinowski, T. Niiranen, T. Luhta & L. Sito**
A new regional reflection seismic profile across the Peräpohja belt, northern Finland

10:25–10:50 **D. Whipp, M. Häkkinen, L. Tuikka, A.-K. Maier, E. Muñoz & S. Laaksonen**
Exploring the life and death of ancient orogens

10:50–11:35 Coffee/Tea, poster viewing

11:35–12:10 **Gregor Hillers (Invited)**
Passive seismic imaging with dense arrays

12:10–13:00 Session 5: Fractures, cleavages and faults
Chair: Alan Bischoff

12:10–12:35 **J. Engström, P. Jänkävaara, N. Nordbäck, N. Ovaskainen, K. Nikkilä, H. Hansson, T. Kauti, P. Skyttä, E. Heilimo & A. Bischoff**
How does preexisting ductile structures effect brittle deformation in crystalline bedrocks, insights from Kisko and Paimio area in SW Finland?

12:35–13:00 **K. Nikkilä, P. Skyttä, N. Nordbäck & J. Engström**
Generation of faults and associated damage zones in crystalline rocks

13:00–14:00 Lunch, poster viewing

14:00–15:15 Session 6: Geothermal
Chair: Kaisa Nikkilä

14:00–14:25 **A. Bischoff, D. Carbajal, M. Heap, S. Vuoriainen, T. Luoto, T. Reuschlé, J. Kuva & K. Cutts**
Crystal clear: A petrophysical databank of crystalline rocks for assessing deep geothermal reservoirs in Finland and beyond

14:25–14:50 **D. Carbajal-Martinez, A. Bischoff, S. Vuoriainen, T. Luoto, E. M. Jolis, J. Kuva, J. Engström, E. Kortunov & Nicklas Nordbäck**
Fracturing and Hydrothermal Alteration in Faulted Granites: Impact on Fluid Flow and Geothermal Energy at the Kivetty Site

14:50–15:15 **N. Nordbäck, A. Bischoff, K. Nikkilä, D. Carbajal-Martinez, J., Engström, P. Skyttä, A. Nicol, N. Ovaskainen & S. Burchardt**
Strike-Slip Brittle Deformation and Hydrothermal Alteration in the Vehmaa Rapakivi Batholith: Insights into Reservoirs in Crystalline Rocks and Geothermal Potential in Southern Finland

15:15–15:40 **EPOS movie moment**

15:40–16:10 Coffee/Tea, poster viewing

16:10–17:25 Session 7: Raw materials
Chair: Jochen Kamm

16:10–16:35 **S. Graul, S. Nirgi, A. Soesoo, J-D, Solano-Acosta, R. Hints, T. Hands & C. Hernandez-Moreno**
DEXPLORE Horizon EU project: Investigation of CRM potential of Estonian basement

16:35–17:00 **Soesoo, A.; Nirgi, S. & Acosta, J.**
Critical raw materials of the Estonian Precambrian basement: Any new targets?

17:00–17:25 **N. Coint, E. T. Mansur, Y. Wang., A. C. R. Miranda, F. Szitkar, P. Acosta-Gongora, V. Baranwal, A. Nazuti & M. H. Huyskens**
Prospectivity for Fe-Ti-P-(REE) mineralization in alkaline monzonite and syenite: example from the Southern Oslo Rift, Norway

18:30 Conference Dinner. i.e. beer and something
Oluthuone Kaisla, Vilhonkatu 4, near metrostation Helsingin Yliopisto

Thursday, Nov 14

09:00–10:35 Session 8: Deep geobiosphere
Chair: Riikka Kietäväinen

09:00–09:25 **I.T. Kukkonen, R. Kietäväinen, V. Nenonen, M. Bomberg, H. Miettinen, M. Nyyssönen, M. Nuppunen-Puputti, A. Karjalainen & J. Rytkönen**
Research application of the St1 superdeep boreholes in Espoo, southern Finland

09:25–09:50 **H. Miettinen, M. Nyyssönen, M. Nuppunen-Puputti , R. Kietäväinen, I. Kukkonen, V. Nenonen, A. Karjalainen, J. Rytkönen & M. Bomberg**
Microbiological aspects of sampling the St1 superdeep boreholes in Espoo, southern Finland

09:50–10:15 **M. Bomberg, M. Nuppunen-Puputti, L. Purkamo, M. Nyyssönen, H. Miettinen & R. Kietäväinen**
Biological sulfur cycling in Finland’s deep groundwater

10:15–10:40 **M. Nyyssönen, M. Nuppunen-Puputti, M. Kuusiluoma, A. Delgado, M. Bomberg & R. Kietäväinen**
Dark oxygen in the deep geobiosphere of the geological repository (DODGE)

10:40–11:10 Coffee/tea

11:10–12:25 Session 9: Magmatism through time
Chair: David Whipp

11:10–11:35 **A. Costa do Nascimento, D. Carvalho de Oliveira & E. Heilimo**
Origin and tectonic significance of Archean sanukitoids: correlation between the Carajás and Karelia Provinces

11:35–12:00 **A.E. Johnson, J.S. Heinonen & O. Eklund**
Intraorogenic magmatism in southern Finland – new evidence from geochemistry and dating

12:00–12:25 **O. Teräs, K. Nikkilä, P. Mikkola, A. Kotilainen, O. Eklund & O.T. Rämö**
Influence of the Transscandinavian Igneous Belt on the post-orogenic shoshonitic magmatism in Finland

12:25–13:00 Closing of symposium, forthcoming meetings, other short announcements and poster award
Chair: Suvi Heinonen

13:00– Lunch

EXTENDED ABSTRACTS

The publication is electronically available at https://www.seismo.helsinki.fi/ilp/lito2024/.

Developing the digital core archive of Finland

S. Aatos[1] and the NDCAF team

[1]Geological Survey of Finland, P.O. Box 1237, 70211 Kuopio, Finland
E-mail: Soile.Aatos@gtk.fi

Geological Survey of Finland (GTK) acquired a large collection of drill core hyperspectral imaging (HSI) data in 2018 as a test, and later, from 2021 to 2023, to further develop electronic drill core archive of Finland. The total length of core imaged was 175 km. Additionally, a test set of 173 m of drill core was scanned with laser-induced breakdown spectroscopy (LIBS) in 2022-2023.

Keywords: HSI, LIBS, electronic archives, drill cores, Finland

1. HSI

Geological Survey of Finland (GTK) and TerraCore International (TerraCore) have developed a large drill core hyperspectral imaging (HSI) data repository for Finland (Table 1) in two phases. Initially, pilot projects funded both publicly and jointly by private and public sectors were carried out in 2018 (Ojala & Vuollo, 2019, Aatos et al., 2023). This was followed by the data acquisition for a publicly funded National Digital Core Archive of Finland (NDCAF) from 2021 to 2023 (MinMatKa project, https://projektit.gtk.fi/minmatka/en/ndcaf/), with local subcontracting by GeoPool Oy. In selection of scanned targets, ones with battery mineral potential and nuclear waste disposal site studies were prioritised.

The HSI process, along with data storage and location-independent delivery, offers a non-destructive method to swiftly analyse large amounts of drill core and obtain detailed mineralogical data from them. These data were provided in quality-controlled spectral form and were either automatically processed or interpreted by human experts, depending on the service level ordered (Table 1). The SWIR or LWIR responses of the data ranged from moderate to good, for many silicate and non-silicate group minerals. However, minerals such as zircon, magnetite, and sulphides were non-diagnostic.

For GTK employees the prepared HSI datasets are viewable and partly downloadable online via the IntelliCore graphic user interface, offered by TerraCore as a service (Figure 1 A-C). In spring 2023, metadata and most locations of the GTK 2021-2022 HSI data were published via the GTK Mineral Deposits and Exploration (MDaE) online map service (https://gtkdata.gtk.fi/mdae/index.html).

The first scientific paper based on the NDCAF HSI data was published by Hamedianfar et al. (2023), utilising the results from the HypeLAP project (Korhonen et al., 2022).

2. LIBS

A small LIBS scanning, and data processing pilot campaign was carried out in 2022-2023 (Table 1). Length of drill core scanned with the novel LASO-LIBS method and instrumentation developed and operated by Lumo Analytics Oy was 173 m in total from two drill cores.

Compared to the HSI methodology, LIBS was a slightly destructive analysis technique due to the use of an erosive laser beam. During the LIBS scanning project, automating the mineralogical interpretation required verifying references at a microscopic scale, such as image analysis data from prepared samples from drill cores of a current exploration target.

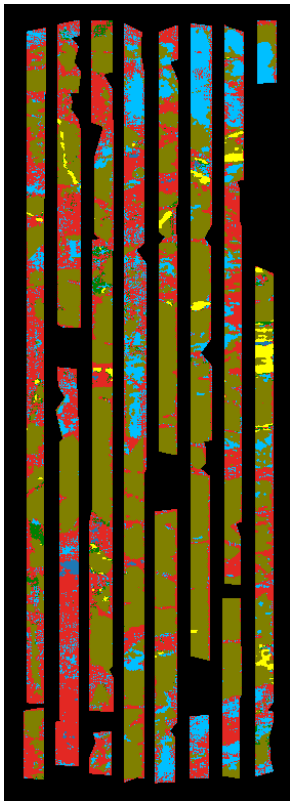
a)
Amphibole
Amphibole-1
Carbonate
Clinopyroxene
Feldspar
MgOH Minerals
Quartz
QTZ-Fsp-Phy
Qtz-Phy
Unclassified
Whitemica

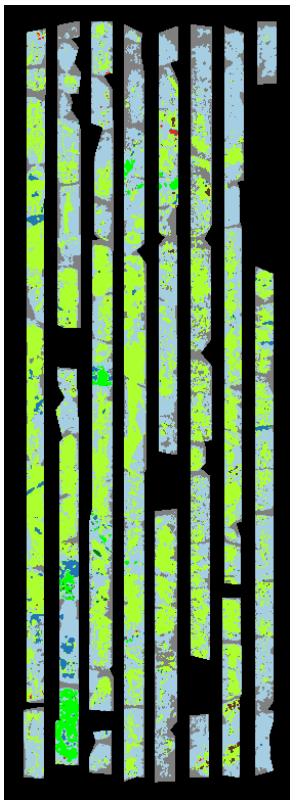
b)
Amphibole
Biotite
Carbonate
Chlorite
Clinopyroxene
Serpentine
Talc
Tourmaline
Unclassified
Wmca-Chl
Zeolite


c)

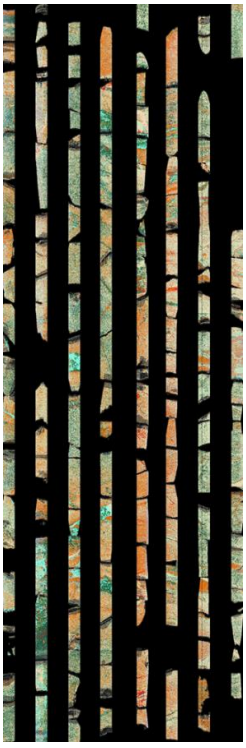
d)


e)


f)

Figure 1. Processed images of spectral scanning results from the drill core KTÄ-PV-33 (depth 62.35-69.90 m) originating from Pahtavuoma, Kittilä, Finland. A) A dominant mineral map from hyperspectral LWIR imaging. B) A dominant mineral map from hyperspectral VN-SWIR imaging. C) A high-resolution RGB image (IntelliCore). D) A mineral summary map from LIBS scanning. Mineral group colours: carbonates = aqua, feldspars = light grey-, light pink, micas = red-purple, quartz = light beige, amphiboles = dark green. E) A sulphide mineral map from LIBS scanning. F) Sulphur concentration map from LIBS scanning. HSI images were delivered via IntelliCore online service by TerraCore. LIBS scanning images were provided by Lumo Analytics Oy. Both scanning methods offered original spectral data and high-resolution RGB images of the drill core boxes for scientific use.

Although the data acquisition speed of the LIBS is slower and its drill core area coverage narrower than that of HSI, it offers better resolution and a wider parameter repertoire, including chemical elements and the ability to diagnose sulphur-bearing minerals (Figure 1 D-F). The automated interpretation of minerals was immediately run, and the results were deliverable, like the HSI data preparation phase. By the time of the LIBS test scanning project, the company had also announced plans to develop an online database service for future users.

3. Future scenarios

The use of spectral data is expected to grow in future collaborations with companies and research organisations. These entities will benefit from the processed digital observation data of rocks and minerals, e.g., for exploration and mining, environmental studies, or other branches of applied geology. To utilise large spectral archives, information, data storage, and delivery systems need to be developed. Additionally, individual users may be interested in learning methods for interpreting spectral data more thoroughly for scientific use.

In recent years, spectral studies of microscopic scale have expanded beyond the visible light wavelength range (e.g., XRF, LIBS). Simultaneously, 2D-3D interpretation of digital mineralogical data has been evolving towards automation, even on the microscopic scale. At GTK, the next phase of development is expected to focus on digitising Finland's thin section archives.

Acknowledgements

For all of those who identify themselves as having taken part in this ground-breaking endeavour in one way or another – your effort and support are much appreciated.

References:

Aatos, S., Kuikka, J., Kuosmanen, E., Leskelä, T., Niiranen, T., Niskanen, M., Nousiainen, M., Ojala, J., Rauhala, J., Salo, A. & Torppa, J. 2023. Hattu Schist Belt 3D Mineral System (Hattu 3D) – Project Report. Geological Survey of Finland, Open File Research Report 29/2020, 79 p. Available at: https://tupa.gtk.fi/raportti/arkisto/29_2020.pdf

Hamedianfar, A., Laakso, K., Middleton, M., Törmänen, T., Köykkä, J., Torppa, J. 2023. Leveraging High-Resolution Long-Wave Infrared Hyperspectral Laboratory Imaging Data for Mineral Identification Using Machine Learning Methods. Remote Sens. 15, 4806. https://doi.org/10.3390/rs15194806

Korhonen, M., Laakso, K., Torppa, J., Köykkä, J., Törmänen, T., Heilimo, V., Middleton, M., Hamedianfar, A., Tuusjärvi, K., Hautala, S., Torppa, A., Rauhala, R., Haavikko, S., Jolis, E., Lukkari, S., Laitala, J. & Nykänen, V. 2022. Hyperspectral Lapland (HypeLAP) – project report. Geological Survey of Finland, Open File Work Report 49/2022, 71 p. Available at: http://projects.gtk.fi/export/sites/projects/hypelap/documents/HypeLAP-Project-Report.pdf

Ojala, J. & Vuollo, J. 2019. Hyperspektriskannauspilotointi 2018. Geological Survey of Finland. Unpublished report. 25 p. (in Finnish)

Table 1. Key figures of the first stages of large-scale acquisition of HSI of drill cores (2018, 2021-2023) with an extension of testing LIBS scanning (2022-2023) for GTK.

Year	**2018**	**2021**	**2022**	**2023**	**In total**
Number of drill holes[1] HSI (LIBS)	244	338	307 (2)	361	1250 (2)
HSI (m)	27939[2]	44138[3]	44975[3]	45669[3]	162721
HSI additional processing[4] (m)		4009	4458	4193	12660
LIBS test scanning[5] (m)			173		173

[1] Preliminary count of public drill hole IDs (GTK)
[2] Test phase image processing (TerraCore)
[3] Level 2 image processing including data acquisition (level 0), data QC and corrections, automated minerals maps (level 1), and data preparation, i.e. masking (TerraCore)
[4] Level 4 image processing including the previous (level 2), spectral processing (level 3), and spectral interpretation (TerraCore)
[5] 3D point cloud data collected in 2022 were processed automatically in 2023 (Lumo Analytics Oy)

Crystal clear: A petrophysical databank of crystalline rocks for assessing deep geothermal reservoirs in Finland and beyond

A. Bischoff[1,2], D. Carbajal[1], M. Heap[3], S. Vuoriainen[1], T. Luoto[1], T. Reuschlé[3], J. Kuva[1] and K. Cutts[1]

[1]Geological Survey of Finland
[2]University of Turku, Finland
[3]University of Strasbourg, France
E–mail: alan.bischoff@gtk.fi

We performed multiple laboratory experiments and analytical techniques to define the petrophysical characteristics and understand the formation of deep crystalline reservoirs in Finland. Our results indicate that fracturing and mineral dissolution can create exceptional reservoirs with porosity and permeability values of up to 31.5% and 1.5 × 10^{-11} m^2 (15.2 Darcy), respectively. Hydrothermal alteration and tectonic processes are responsible for the formation of these reservoirs, which must date back to Precambrian times. Our findings could represent a significant shift in geothermal exploration within ancient crystalline cratons, expanding target prospects beyond the conventional focus on volcanic and rifting areas.

Keywords: crystalline reservoirs, geothermal energy, petrophysics, hydrothermal alteration

1. Geological background and geothermal opportunities

Finland's crystalline bedrock consists of various Precambrian igneous, metamorphic, and supracrustal rocks that typically exhibit low porosity and low permeability. Consequently, these rocks have little reservoir potential mainly due to the interlocking nature of their minerals typically formed under or rearranged at high pressure and temperature conditions. However, during its geological evolution, the Finnish crystalline crust experienced multiple tectonic and hydrothermal events that created secondary pore networks (Figure 1), enabling fluid flow within these rocks. The circulation of fluids in the upper crust is widely known as one of the main drivers facilitating heat extraction and the development of geothermal energy prospects (e.g. Jolie et al. 2021). As part of the Deep-HEAT-Flows project (https://deep-heat-flows.voog.com), we are compiling a comprehensive geological and petrophysical databank for crystalline rocks across Finland, evaluating their potential as deep (>1 km) reservoirs. Our databank will provide valuable information for assessing geothermal opportunities in Finland and in similar crystalline settings affected by tectonic and hydrothermal activity.

2. Methods

Our investigations involve a range of laboratory-based experiments, including measurements of rock density, elastic wave velocity, electrical resistivity, magnetic susceptibility, porosity and permeability under various confining pressures, and thermal properties of over 300 samples of crystalline rocks collected from diverse outcrop locations and boreholes across Finland. Additionally, we employ detailed mineral and pore space characterization techniques, including thin-section petrography, micro-XRF spectrometry, SEM-EDS, X-ray CT scans, and isotope dating, to better understand the processes that control the formation of crystalline reservoirs. Our focus is on defining petrophysical variations in the architecture of fault zones, offering a unique dataset that details the characteristics and reservoir properties typically found in the fault core, damage zone, and host blocks of crystalline rocks subjected to brittle deformation and hydrothermal alteration. This information has been compiled into comprehensive spreadsheets and will be made available through various scientific publications over the course of the project, which is set to conclude in 2027.

3. Petrophysical parameters of crystalline reservoirs

Our preliminary findings highlight a consistent trend among various petrophysical parameters: rock density, electric resistivity, elastic wave velocity, magnetic susceptibility, thermal conductivity, and heat capacity typically decrease as porosity increases (Figure 2), a pattern classically observed across sedimentary and volcanic rocks. Additionally, porosity and permeability are usually directly proportional and governed by the extent of brittle deformation and alteration processes affecting the crystalline rocks. Thus, altered rocks have the higher porosity and permeability values, up to 31.5% and 1.5×10^{-11} m^2 (15.2 Darcy), respectively; brecciated and fractured rocks have moderate porosity ranging from 1 to 10% and permeability up to 8.38×10^{-13} m^2 (849 millidarcy); while massive rocks recorded the lowest porosity (<2%) and permeability (<1.23×10^{-17} m^2) values. Markedly, these rocks are consistently distributed across diverse parts of fault zones. Typically, altered, brecciated, and fractured rocks are found in the fault core and damage zone, while massive rocks occur within the host block. However, massive rocks can also occur in the damage zone and fault core. Notably, all rocks with porosity above 10% are highly altered and consistently located within the fault core, a zone characterized by intense deformation where most of the fault displacement occurs. This observation highlights that porosity (and consequently other properties such permeability, density, resistivity, elastic wave velocity, and thermal parameters) systematically varies following the fault architecture, providing a valuable prospective model for locating geothermal reservoirs in crystalline settings. In detail, the quality of crystalline reservoir (i.e. their suitability for geothermal energy extraction) is primarily revealed by the morphology and connectivity of diverse pore types (Bischoff et al. 2024). Massive rocks typically have dispersed and disconnected pores and thus have little reservoir potential. Their value in geothermal systems relies on their ability to store and transfer heat by conduction, due to abundant minerals such as quartz and feldspar, as well as to generate heat through the decay of radioactive elements like uranium, thorium, and potassium. Conversely, rocks dominated by fractures typically have low porosity (<5%) but can exhibit extremely high permeability (nearly 10^{-12} m^2) at low confining pressure, which sharply decreases to 10^{-19} m^2 when confining pressure exceeds 20–30 MPa, corresponding to depths of around 700–1000 meters. According to our dataset, only fractures with irregular walls commonly resulting from mineral dissolution and brecciation can sustain permeability above 10^{-16} m^2 at high confining pressures of 50 MPa, simulating depths of approximately 2 km. Consequently, rocks that have undergone brecciation and hydrothermal alteration are the most promising deep geothermal reservoirs because they show comparatively milder porosity and permeability reduction even under high confining pressures of 50 MPa.

4. Crystalline reservoir formation in Fennoscandia

Throughout most subsets of rocks transected by faults and fractures, a consistent pattern emerge: mafic minerals including biotite, pyroxene and amphibole are commonly replaced by chlorite and epidote, indicating hydrothermal alteration processes at relatively high temperatures (200–300 °C). Additionally, altered peraluminous granites, migmatites and gneisses display a replacement order of garnet→biotite→chlorite→titanite, which is consistent with retrograde metamorphism and hydration also at relatively high temperature. We observe that the effects of hydrothermal alteration and leaching of mafic mineral phases, plagioclase, and garnet are often associated with the generation of secondary porosity. This includes the development of moldic, intracrystal, and sieve pores, typically achieving 60% and up to 96% pore connectivity at an 11 µm CT scan resolution. As thermal and tectonic events of great magnitude have not been reported to substantially affect the Fennoscandian upper crust in the last billion years, most faulting and hydrothermal alteration must date from Precambrian times. We perform U-Pb isotope dating of secondary titanite to serve as a proxy for the age of porosity

formation at a location in the Karelian Craton. The age results cluster at 2200-2140 Ma and 1900-1750 Ma, confirming a temporal correlation with the Paleoproterozoic rifting of the Karelian Craton and the Svecofennian orogeny. Although the relationship between hydrothermal alteration and secondary porosity exerts a first-order control throughout our dataset, the overprinting effects of weathering due to the exposure of the crystalline rocks to meteoric water and organic fluids is also commonly observed, particularly in rock samples collected from outcrops or from shallow (<500 m) borehole sections. In light of our observations, we describe the formation of crystalline reservoirs as a dynamic process that likely involves multiple interrelated tectonic, thermal, and chemical stages: Initially, massive rocks were fractured and brecciated by tectonic forces or hydro-mechanical stress, creating pathways for fluid circulation. Hydrothermal fluids then use these fracture pathways and interact with primary minerals, inducing chemical alterations and leaching, which lead to the generation of secondary porosity. When finally exposed to meteoric and organic fluids, the porosity initially created at higher temperature conditions is further reshaped by additional mineral dissolution processes and the precipitation of new mineral phases and oxides. These processes can be repeated multiple times as faults are reactivated under new stress regimes or during younger magmatic and orogenic events.

5. Implications for geothermal exploration

The identification of hydrothermally altered rocks as potential deep geothermal reservoirs could represent a significant shift in geothermal exploration within crystalline regions, expanding target prospects beyond the conventional focus on volcanic and rifting areas. Our results are crucial for identifying highly productive permeable zones within crustal fault transecting crystalline terrains. Brecciation, cataclasis, fracturing, and mineral dissolution collectively contribute to the creation of exceptional reservoir properties, which have been widely overlooked in deep setting of crystalline cratons. Additionally, our results have the potential to support the advancement of Enhanced Geothermal Systems, which could prioritize creating more intricate fracture networks through thermal and chemical stimulation, mimicking the natural formation of crystalline reservoirs in the Fennoscandia Craton.

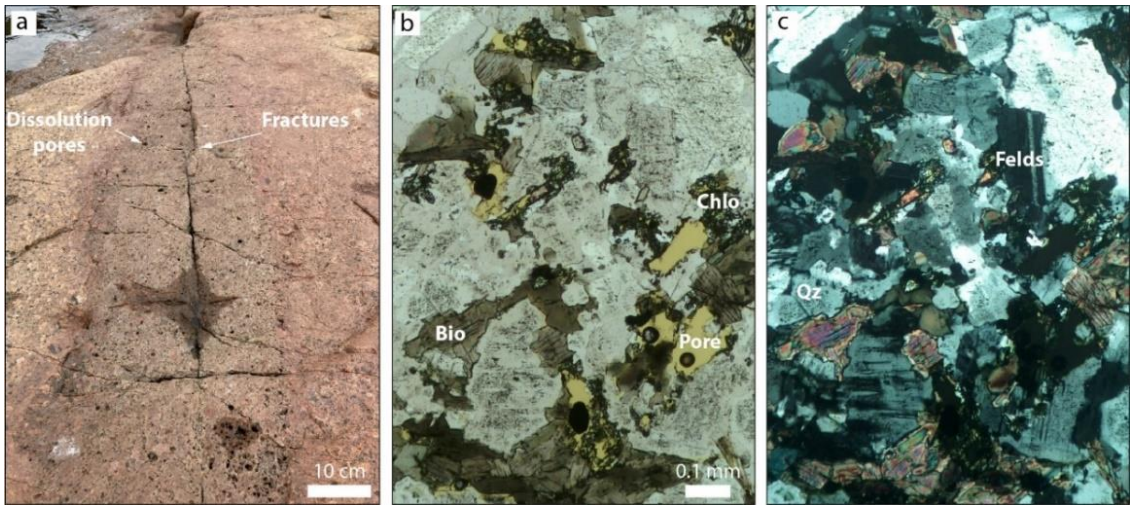

Figure 1. Examples of crystalline rocks affected by fracturing and hydrothermal alteration. (a) Rapakivi granite from the Vehmaa Batholith, Southern Finland. Microphotographs in natural (b) and plain polarized light (c) of an altered granite collected from a depth of 1620 m from the Koillismaa borehole, Eastern Finland.

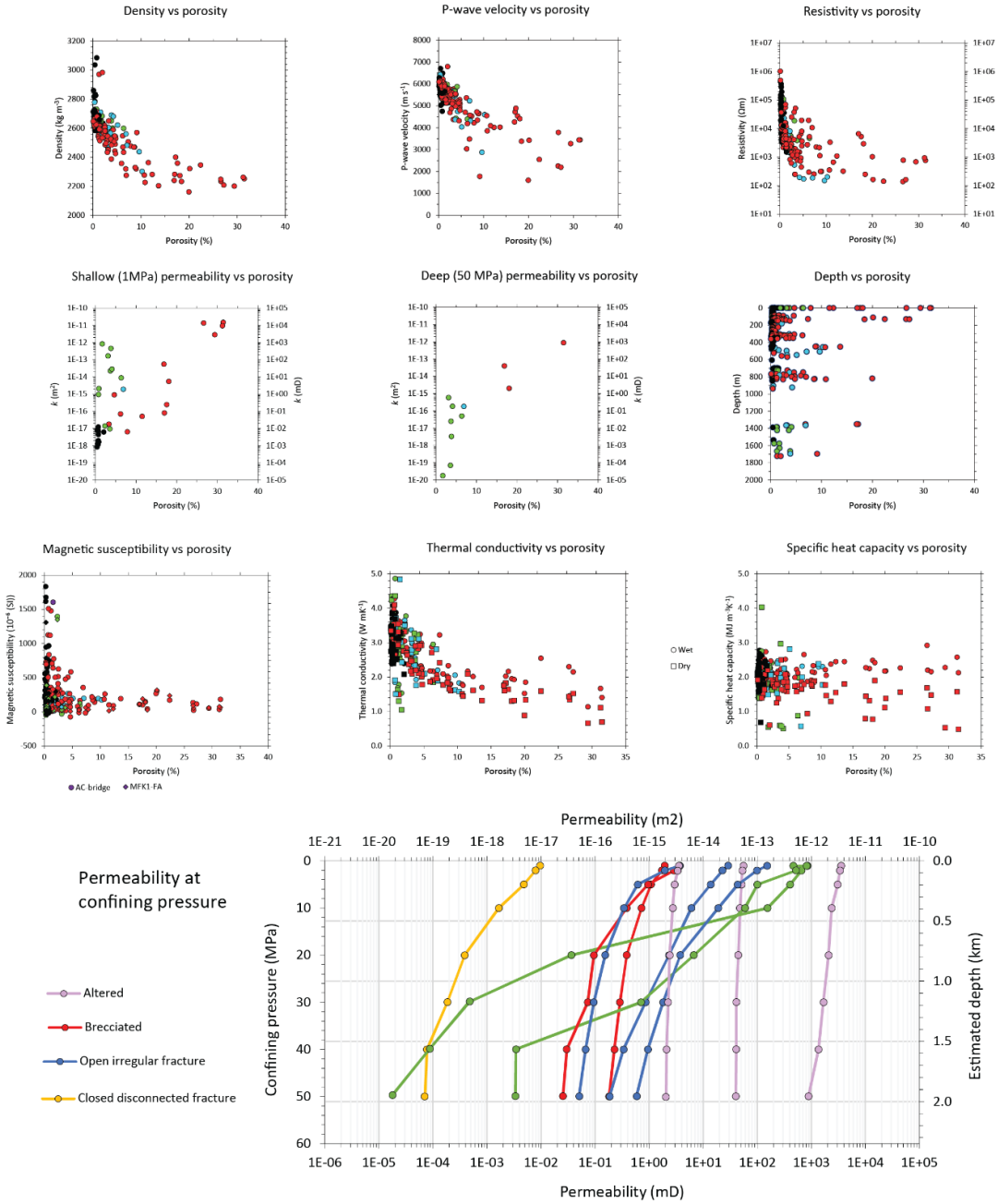

Figure 2. Main petrophysics trends observed on Finnish crystalline rocks, sorted by their texture and structure. Black dot = massive; green = fracture; blue = brecciated; red = altered.

References:

Bischoff, AP., Heap, MJ., Mikkola, P., Kuva, J., Reuschlé, T., Jolis, EM., Engström, J., Reijonen, H., Leskelä, T. (2024). Hydrothermally altered shear zones: a new reservoir play for the expansion of deep geothermal exploration in crystalline settings. Geothermics. https://doi.org/10.1016/j.geothermics.2023.102895

Jolie, E., Scott, S., Faulds, J. et al. (2021). Geological controls on geothermal resources for power generation. Nat Rev Earth Environ 2, 324–339. https://doi.org/10.1038/s43017-021-00154-y

Biological sulfur cycling in Finland's deep groundwater

M. Bomberg[1], M. Nuppunen-Puputti[1], L. Purkamo[2], M. Nyyssönen[1], H. Miettinen[1], and R. Kietäväinen[3]

[1]VTT, Espoo, Finland
[2]GTK, Espoo, Finland
[3]Dept. of Geosciences and Geography, University of Helsinki, Finland
E-mail: malin.bomberg@vtt.fi

The sulfur cycle is key for microbial life in the deep subsurface, where sulfate is one of the few electron acceptors available. Sulfate reducing bacteria (SRB) are commonly found in Finnish deep groundwater, but the complete biological cycling of sulfur compounds is still not well known. Despite the assumed lack of oxygen in deep groundwaters, studies hint at oxygen production that might support oxygen-requiring microbial processes, such as sulfide oxidation, although this hasn't been studied in detail yet. This study examined groundwater samples from six sites in the Finnish part of the Fennoscandian Shield, covering depths from 100 to 2400 meters. The research used uniform molecular analysis techniques, including qPCR for bacterial and SRB abundance and metagenomics for microbial metabolisms. Results show varied bacterial and SRB abundance across sites, with the highest numbers in Kopparnäs and Liminka and the lowest in Pyhäsalmi. Community composition varied, with distinct clusters identified. Metagenomic analyses revealed pathways for sulfate reduction and thiosulfate and sulfide oxidation in several sites, indicating active sulfur cycling, including both anoxic and oxygen-demanding processes.

Keywords: sulfate reduction, sulfide oxidation, deep biosphere, *dsr*B gene, bacteria, Fennoscandian Shield

1. Introduction

The sulfur cycle is one of the most important elemental cycles for microbial life in oligotrophic deep subsurface environment, where electron acceptors other than sulfate are scarce. Sulfate reducing bacteria (SRB) have been shown to be ubiquitously detected in Finnish deep groundwater (Purkamo et al., 2016; Bomberg et al., 2015; Noroaho, 2022), but sulfur and sulfide oxidizing bacteria have also been found (Bell et al., 2020). Sulfate in Finnish deep groundwater originates from ancient seawater or is generated by oxidation of sulfide minerals, or have a yet unknown origin (Pitkänen et al., 1996). Sulfides and other reduced sulfur compounds are products of the reduction of oxidized sulfur compounds, such as sulfate. Sulfide may react with metal ions, forming metal sulfides, which precipitate removing toxic metals from the habitat. Nevertheless, sulfides may serve as electron donors in the deep subsurface, keeping an active biological sulfur cycle going. Many of the microbe driven biochemical reactions of the sulfur cycle, such as biological sulfide and thiosulfate oxidation, require oxygen, which in principle is absent in the deep subsurface environment. However, new studies show that oxygen may be produced at quantities sufficient for oxygen-requiring microbial metabolic processes to occur, even in anoxic environments (Ruff et al., 2023). How the biological sulfur cycle and the possibility of oxygen requiring metabolisms occur has not been extensively studied in Finnish deep crystalline bedrock environments to date, although several studies exist showing active sulfur cycling in several sites in Finland (e.g. Purkamo et al., 2016; Bomberg et al., 2015; Blomberg et al., 2016).

The continental subsurface contains an estimated 12 – 20% of Earth's biomass (Magnabosco et al., 2018). In deep rock environments, this biomass is dwelling in the aqueous spaces, fractures and pores, of the rock and is either attached to rock surfaces in biofilms or free-living in the fluids. Some meta-analyses exist striving to identify a core deep biosphere microbiome, or to identify what parameters affect the microbial community size and

composition by collecting available data, but face issues such as difference in sampling procedures, DNA extraction methods, negative control protocols, primers used for sequencing etc., which may introduce false variation. Here we studied the Finnish part of the Fennoscandian Shield, collecting groundwater samples from 6 sites, Kopparnäs R307, Outokumpu Deep Borehole, Pyhäsalmi Mine boreholes R2247 and R2250, Loviisa borehole KR4, Liminka Tupos and Pori Po-1, covering depths between 100 to 2400 m below surface between the years 2009 – 2022. Some of the sites have deep groundwater that has resided in the Earth crust for more than 50 Ma, whereas in other places the groundwater is considerably younger (Kietäväinen et al., 2014). We emphasised the use of the same molecular analysis techniques for the study, starting from DNA extraction to primers, enzymes and sequencing technology and hydrogeochemical analyses. The bacterial community size was estimated using 16S rRNA gene targeting quantitative PCR (qPCR) and the abundance of sulfate reducing bacteria (SRB) by *dsr*B gene targeting qPCR. The SRB community composition was characterised with *dsr*B gene targeted amplicon sequencing and the microbial metabolisms of the microbial communities was analysed using metagenomics.

2. Results and Discussion

The abundance of bacteria varied greatly between sites, with the highest numbers found in Kopparnäs at approximately 130 m depth and in Liminka at 400 – 700 m depth, with bacterial 16S rRNA gene copy numbers in the range of 10^6 mL^{-1} (Figure 1a). The lowest numbers were detected in Pyhäsalmi samples, with less than 10^0 gene copies mL^{-1} (Figure 1a). The amount of SRB varied likewise between sites, the highest *dsr*B gene copy numbers found in Liminka at 400 – 700 m depth, exceeding 10^5 copies mL^{-1}, and 10^4 copies mL^{-1} in Pori at 100 m depth. *Dsr*B gene copies were also detected by qPCR in Kopparnäs and Outokumpu, above 1800 m depth, but were below the detection limit of the assay in the other samples. Interestingly, the concentration of sulfate or TDS did generally not affect the abundance of SRB (Figure 1a).

*Dsr*B gene amplicons were produced from all sites, although not all samples, even when the number of *dsr*B gene had been shown to be below the detection limit of the *dsr*B qPCR assay. The Principal coordinates Analysis (PCoA) comparing the relative abundance and general distribution of different *dsr*B gene types between the different sites showed that the community composition between sites varied (Figure 1b). In the PCoA, the SRB communities separated into four distinct groups, clustering Outokumpu, Pori and two Loviisa samples into separate clusters from each other and the rest of the communities, while Liminka, Kopparnäs, Pyhäsalmi and one Loviisa sample formed their own tight group.

The metagenomic analyses showed that the full metabolic pathway for sulfate reduction potential was present in Kopparnäs, Outokumpu to the depth of 1500 m, Pyhäsalmi, Loviisa and Liminka 400 – 700m, but not detected in the other samples (Figure 1c). A full pathway for thiosulfate oxidation was identified in Kopparnäs, Pyhäsalmi and Liminka (400 – 700 m). Sulfhydrogenase for reduction of S^0 to sulfide using H_2 as electron donor was detected in Kopparnäs, Outokumpu to a depth of 1200 m and in Liminka (400 – 700 m) and sulfur dioxygenase oxidizing S^0 using oxygen and was detected in Kopparnäs and Outokumpu to 1500 m depth, indicating that a source of oxygen would be present in these fluids. Sulfite dehydrogenase, which produce sulfate from sulfite, was detected only in Kopparnäs and in Outokumpu at 1200 m depth. The capacity for sulfide oxidation, which is an oxygen consuming process, was detected in Kopparnäs, Outokumpu to 1500 m depth, Pyhäsalmi, Loviisa and Liminka (400 – 700 m depth). These results indicate that the capacity for microbially catalysed sulfur cycling is present generally in the deep subsurface, including both anoxic as well as oxygen demanding processes in an environment that has been considered strictly oxygen-free.

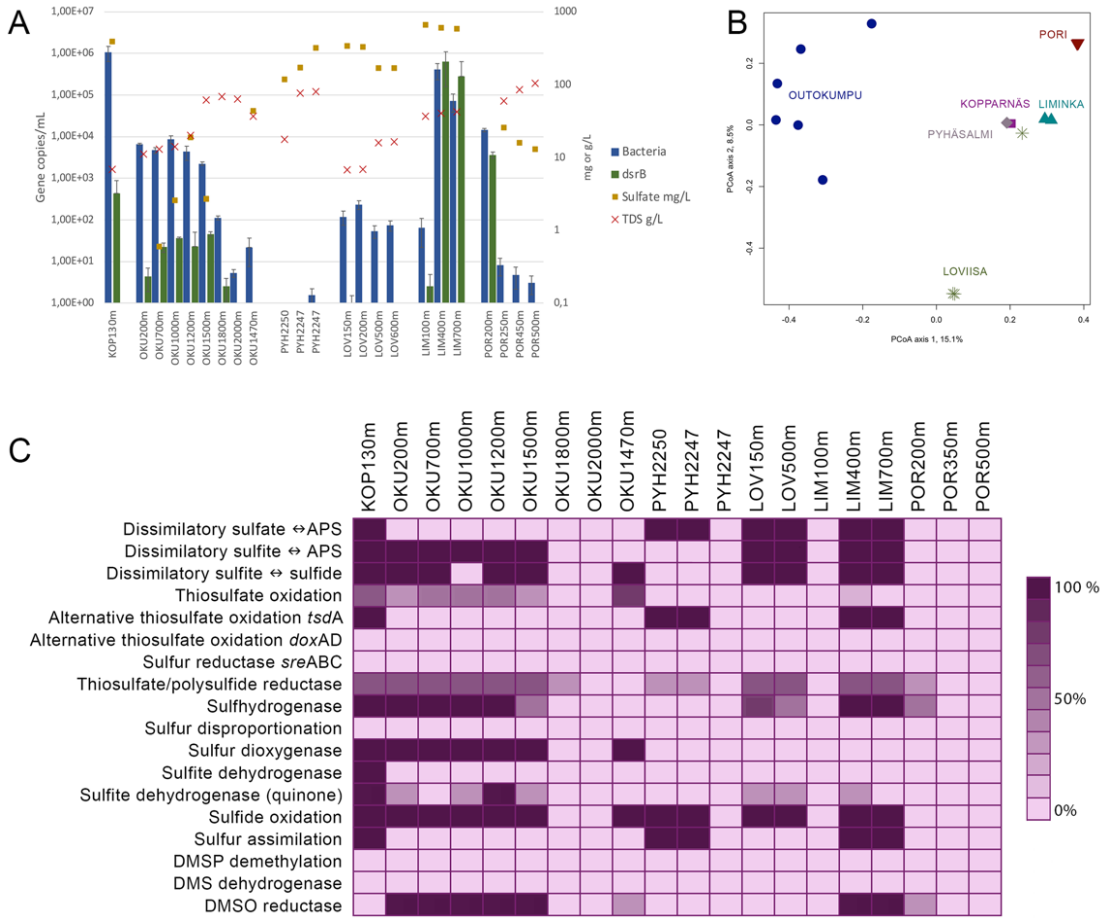

Figure 1. A) The average number of bacterial 16S rRNA gene (blue bars) and *dsr*B gene (green bars) copies mL-1 groundwater in Kopparnäs (KOP), Outokumpu (OKU), Pyhäsalmi (PYH), Loviisa (LOV), Liminka (LIM) and Pori (POR) deep groundwater. The sampling depths are indicated in the sample names except for the PYH samples, where the two boreholes R2250 and R2247 reach a total depth of 2400m and 2200m below ground surface, respectively. The concentration of sulfate (mg/L) and TDS (g/L) are indicated by squares and crosses, respectively with the concentrations on the right-side y-axis. All values are shown on a logarithmic scale. B) Principal coordinates Analysis (PCoA) showing the variance between the different sulfate reducing communities detected by *dsr*B gene amplicon sequencing from the different sites. The values on the x- and y-axes show % variance. C) The estimated microbial sulfur cycling metabolisms detected by metagenomic sequencing in the different sites. The colour of the squares indicates percentage of completeness of a particular metabolic pathway detected, with the darkest colour indicating high completeness and lightest colour that no genes needed for a specific metabolic pathway to proceed were found.

3. Conclusions

Biological cycling of sulfur compounds, comprising both reducing and oxidising reactions, is a process found in many deep subsurface sites in Finland. The concentration of sulfate in the water does not determine the abundance of SRB, i.e. in these groundwaters sulfate is not the limiting factor for the abundance of SRB. The sulfur cycling communities vary between sites.

4. Acknowledgements

This work has received funding from KYT2022 (MIMOSA, BIKES) and SAFER2028 (DODGE). We would like to thank Lasse Ahonen and Arto Pullinen for invaluable help and knowledge sharing in the sampling campaigns, and Mirva Pyrhönen for her magic in the laboratory.

5. References

Bell, E., Lamminmäki, T., Alneberg, J., Andersson, A. F., Qian, C., Xiong, W., ... & Bernier-Latmani, R. (2020). Active sulphur cycling in the terrestrial deep subsurface. The ISME journal, 14(5), 1260-1272.

Blomberg, P., Itävaara, M., Marjamaa, K., Salavirta, H., Arvas, M., Miettinen, H., Vikman, M. 2017. Metabolic Pathways of Deep Groundwater Microbiomes and Sulphide Formation at Olkiluoto. Posiva Working Report 2017-11, Posiva Oy, Eurajoki, 150 p.

Bomberg, M., Nyyssönen, M., Pitkänen, P., Lehtinen, A., & Itävaara, M. (2015). Active microbial communities inhabit sulphate-methane interphase in deep bedrock fracture fluids in Olkiluoto, Finland. *BioMed research international*, *2015*(1), 979530.

Kietäväinen, R., Ahonen, L., Kukkonen, I. T., Niedermann, S., & Wiersberg, T. (2014). Noble gas residence times of saline waters within crystalline bedrock, Outokumpu Deep Drill Hole, Finland. *Geochimica et Cosmochimica Acta*, *145*, 159-174.

Magnabosco, C., Lin, L. H., Dong, H., Bomberg, M., Ghiorse, W., Stan-Lotter, H., ... & Onstott, T. C. (2018). The biomass and biodiversity of the continental subsurface. Nature Geoscience, 11(10), 707-717.

Noroaho, K. 2022. Syvän pohjaveden rikkiyhdisteet Limingan alueen savikivimuodostumassa. MSc Thesis, Department of Geosciences and Geography, University of Helsinki, 62 p. (In Finnish with an English abstract)

Pitkänen, P., Vuorinen, U., & Snellman, M. (1996). On the origin and chemical evolution of ground water at the Olkiluoto site (No. POSIVA--96-04). Posiva Oy.

Purkamo, L., Bomberg, M., Kietäväinen, R., Salavirta, H., Nyyssönen, M., Nuppunen-Puputti, M., ... & Itävaara, M. (2016). Microbial co-occurrence patterns in deep Precambrian bedrock fracture fluids. *Biogeosciences*, *13*(10), 3091-3108.

Ruff, S.E., Humez, P., de Angelis, I.H. et al. 2023. Hydrogen and dark oxygen drive microbial productivity in diverse groundwater ecosystems. Nature Communications 14, 3194

Fracturing and Hydrothermal Alteration in Faulted Granites: Impact on Fluid Flow and Geothermal Energy at the Kivetty Site

Daniel Carbajal-Martinez[1], Alan Bischoff[1,2], Satu Vuoriainen[1], Toni Luoto[1], Ester M. Jolis[1], Jukka Kuva[1], Jon Engström[1], Evgenii Kortunov[1], Nicklas Nordbäck[1]

[1]Geological Survey of Finland
[2]University of Turku, Finland
E-mail: daniel.carbajal@gtk.fi

This research aims to deepen our understanding of the complex interactions between mineral alterations and hydraulic conductivity in faulted crystalline rocks. It focuses on their impact on porosity, permeability, and petrophysical properties, key for defining prolific geothermal reservoirs. We observed that fracturing and mineral alterations within fault zones increase porosity (up to 20%), permeability (up to 10^{-12} m^2), and connectivity of crystalline rocks (at least 500 m sections). These discoveries highlight the potential of the Kivetty site as a valuable case study for understanding large-scale heat and fluid flow in fault zones to form amagmatic geothermal reservoirs, crucial knowledge for advancing clean energy production and heating solutions on a global scale.

Keywords: Faults zones, fracturing, hydrothermal alteration, fluid flow, geothermal energy

1. Introduction

Crystalline rocks in fault zones, altered by heat and deformation, often create favorable conditions for hosting geothermal reservoirs with high porosity and permeability (Bischoff et al., 2024). The Kivetty site, located 80 km north of Jyväskylä in the town of Äänekoski (Figure 1), provides a valuable case study for understanding the relationship between fracturing and hydrothermal alteration and their impact on large-scale hydraulic conductivity within fault zones in crystalline rocks. During the 1980s and 1990s, 13 boreholes were drilled to 250–1000 m depths to explore a nuclear waste repository, intersecting various crystalline rocks from the Central Finland Granitoid Complex (~1.8 Ga; Anttila et al., 1999). Several steeply dipping fault zones and hydrothermally altered areas were identified (Figures 1 and 2). While these structures pose a challenge to nuclear waste disposal, they present an opportunity for geothermal use due to their typical high hydraulic conductivity for fluid flow and heat. Understanding the processes that increase fluid flow is essential to unraveling the potential of geothermal reservoirs in crystalline settings and achieving sustainable energy solutions.

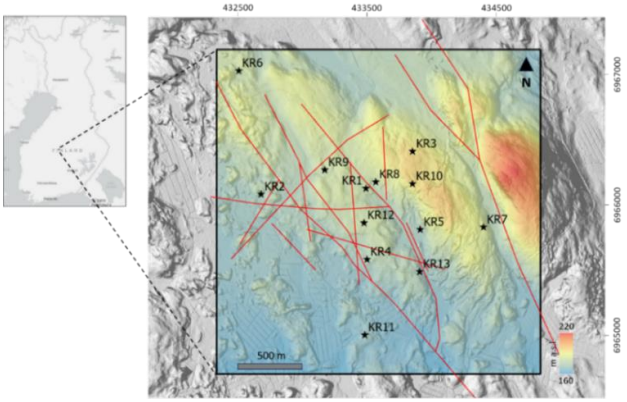

Figure 1. Location of 13 boreholes in the Kivetty site, Finland. Elevation is visualized using LiDAR data (National Land Survey of Finland, 2019), with faults marked in red lines (Anttila et al., 1999).

2. Methods and Materials

Complementing legacy studies from Posiva Oy's nuclear waste repository, we collected 92 core samples from six boreholes (KR1, KR3, KR4, KR5, KR12, and KR13) at the National Drill Core Archive of Finland. The selected samples, primarily granites and granodiorites, represent various rock facies, including massive, mylonitic, fractured, brecciated, and altered rocks. Various laboratory tests were employed at the Research Laboratory of the Geological Survey of Finland in Espoo to assess the key petrophysical properties, alterations, and fluid flow characteristics of these rocks. These techniques included petrophysical laboratory experiments (e.g., porosity, resistivity, density, elastic wave velocity, and thermal conductivity), scanning micro-XRF (μXRF) with the Advanced Mineral Identification and Characterization System (AMICS) software and computed tomography (CT scan). Additionally, hydraulic conductivity tests conducted by Posiva Oy in the boreholes at 2 m packer intervals were compared with our laboratory measurements, enhancing our understanding of the reservoir characteristics.

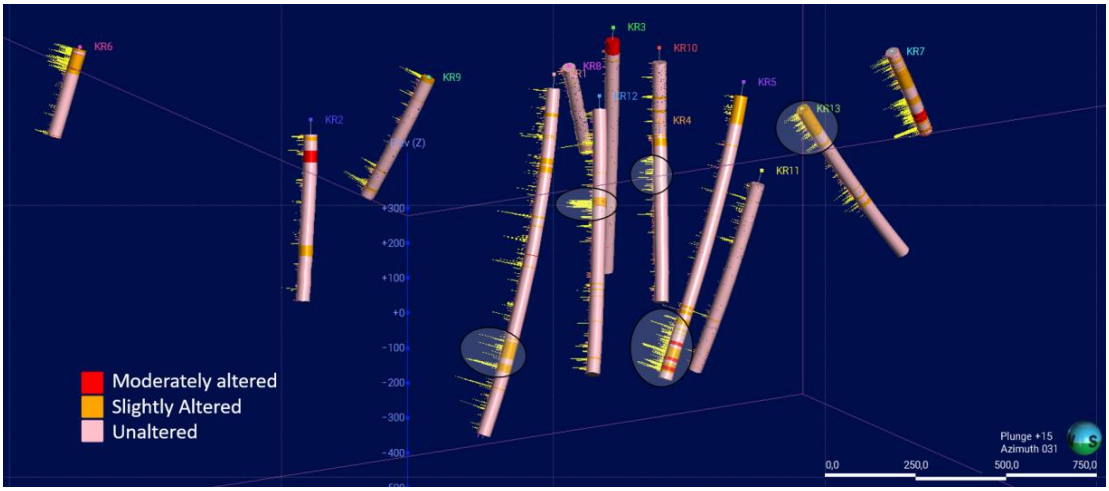

Figure 2. Directional boreholes at the Kivetty site, showing the degree of alteration and fracture frequency (yellow bars parallel to boreholes). Ovals highlight areas with high alteration and fracture frequency, indicating highly permeable connectivity zones.

3. Results and Discussion

3.1 Mineral Alteration and Petrophysical Properties

Our results show a wide range in porosity across different rock facies. Massive granites showed a low porosity (0.9%), brecciated granites exhibited a moderate porosity (9.0%), and altered granites reached a high porosity of 20% (Figure 3A). The AMICS mineralogical maps revealed that the increased porosity primarily results from the dissolution of feldspar, K-feldspar, quartz, and biotite (Figure 3A). Additionally, altered minerals, such as chlorite, epidote, Fe-oxides, Ti-oxides, and muscovite, were identified, indicating hydrothermal alteration processes at relatively high temperatures (>200 °C). These mineralogical changes significantly affect the rock properties, particularly in altered rock types. As shown in Figure 3B, higher porosity was associated with a marked decrease in density, electrical resistivity, P-wave velocity, and thermal conductivity. These changes reflect the overall alteration of the rock matrix due to the replacement of primary minerals with secondary minerals and the increase in pore spaces.

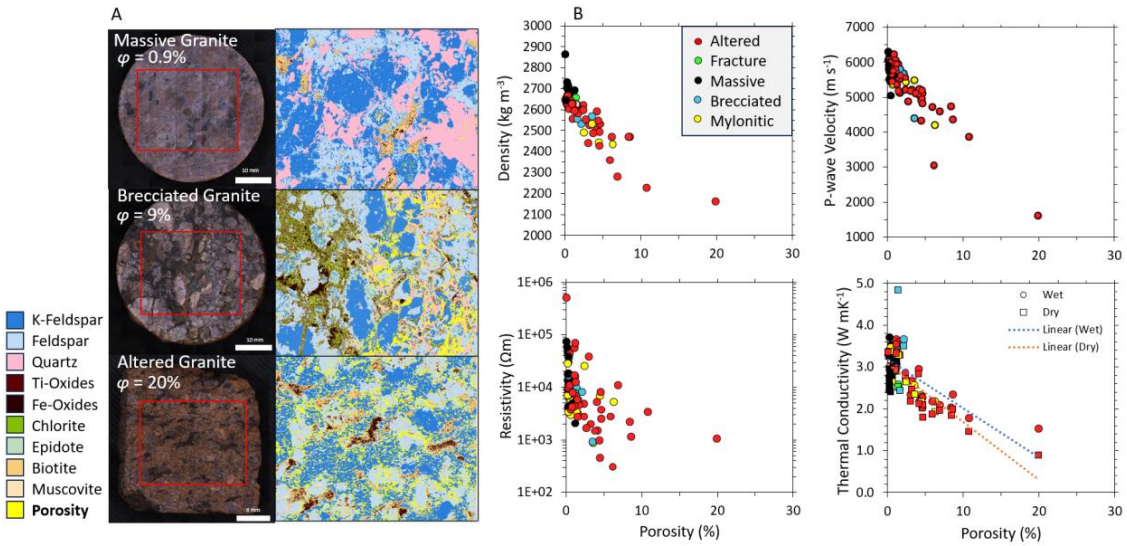

Figure 3. (A) Mineralogical maps illustrating mineral dissolution that leads to increased porosity in brecciated and altered granites. (B) Petrophysical trends show a higher porosity linked to lower density, resistivity, P-wave velocity, and thermal conductivity.

3.2 Permeability and Connectivity of Fault Zones

Hydraulic tests reveal significant permeability (k) changes across different facies, particularly between massive and altered rocks. Massive rocks have low permeability ($k = <10^{-17}$ m^2), while altered within faulted zones exhibit much higher values, approximately five times greater ($k = 1 \times 10^{-12}$ m^2 at depths of 720–850 m) (Figure 4). These structural changes, coupled to alteration and fracturing, promote enhanced fluid flow in these zones. Computed tomography scans, conducted at a resolution of 11 microns, indicate high pore connectivity of up to 94% (Figure 4) in the most altered rocks. Additionally, Posiva Oy's in situ cross-well pumping tests confirmed that these highly permeable zones are hydraulically connected over at least 500 meters sections, particularly in areas dominated by altered and fractured rocks (Figure 2; Anttila et al., 1999). This high connectivity supports the potential for extensive fluid circulation within the fault zones, enhancing the outcome of geothermal energy prospects.

3.3 Geothermal Potential within Fault Zones in Crystalline Rocks

To have a first-order estimation of the geothermal potential of these fault zones, we compare our results with the United Downs Deep Geosystems in Cornwall, UK. There, geothermal energy is extracted from a fault zone within granite, with production wells reaching temperatures of 180 °C at a depth of ~5.2 km. This site is expected to generate between 1–3 megawatts of electrical power (MWe), assuming a fault of 200 m width and a permeability of 1×10^{-13} m^2 (Ledingham and Cotton, 2021). In contrast, permeability at the Kivetty site is an order of magnitude higher than in Cornwall, and the fault width is ~100 m (Figure 4), which highlights the significant potential of fault zones to form geothermal reservoirs. Although the plumbing test depths at Kivetty and Cornwall differ, laboratory tests demonstrate that altered rocks have a minimal reduction in permeability as confining pressures increase, indicating that these rocks within fault zones can act as deep geothermal reservoirs (Bischoff et al., 2024).

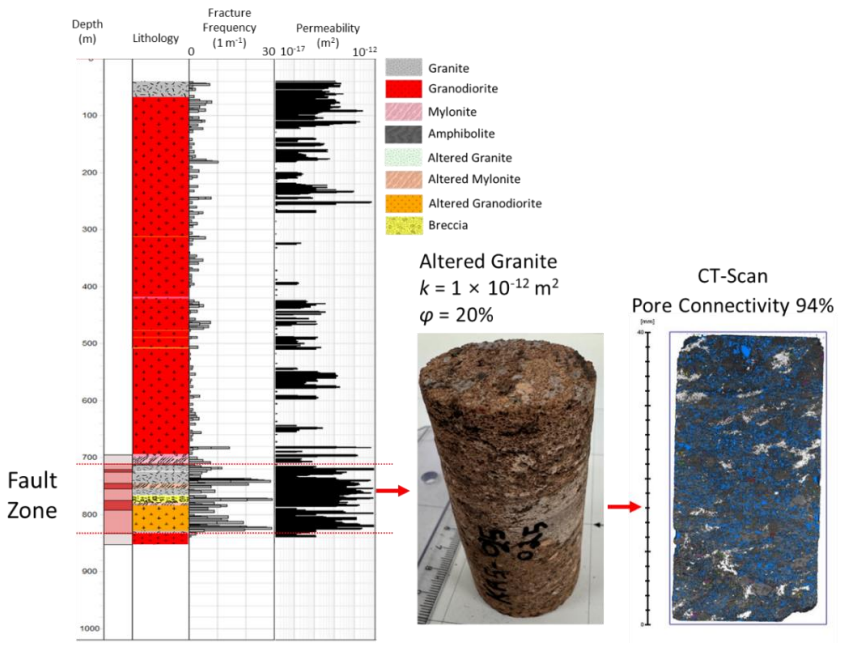

Figure 4. Borehole KR5 at the Kivetty site, Finland, showing lithology, fracture frequency, and permeability test results. The right side features a rock sample from the most permeable zone, with a computed tomography scan highlighting pore space in blue.

5. Conclusion

This study increases our understanding of the behavior of fracturing and hydrothermal alteration in the faulted granites of the Kivetty site. We found that hydrothermal alteration and fracturing significantly change the petrophysical properties of the crystalline rocks, enhancing their likelihood for deep geothermal reservoirs. While massive granite has low permeability, altered granite within fault zones shows high permeability and large-scale connectivity (at least 500 m sections) for heat and fluid flow transport, making these zones ideal sites for forming geothermal reservoirs. These findings contribute to understanding amagmatic geothermal systems within fault zones, highlighting their ideal targets in locations lacking magmatism and crustal extension, crucial information for advancing sustainable energy solutions.

6. Acknowledgement

We thank Posiva Oy and Teollisuuden Voima Oy for providing access to the Kivetty site reports.

References:

Anttila, P., Ahokas, H., Front, K., Heikkinen, E., Hinkkanen, H., Johansson, H., Paulamäki, S., Riekkola, R., Saari, J., Saksa, P., Snellma, M., Wiketrom, L., & Öhberg, A. (1999). *Final Disposal of Spent Nuclear Fuel in Finnish Bedrock - Kivetty Site Report* (Vols. 99–09).

Bischoff, A., Heap, M. J., Mikkola, P., Kuva, J., Reuschlé, T., Jolis, E. M., Engström, J., Reijonen, H., Leskelä, T. (2024). Hydrothermally altered shear zones: A new reservoir play for the expansion of deep geothermal exploration in crystalline settings. *Geothermics*, *118*(September 2023). https://doi.org/10.1016/j.geothermics.2023.102895

Ledingham, P., Cotton, L. (2021). The United Downs Deep Geothermal Power Project. *World Geothermal Congress*, *October*, 1–11.

National Land Survey of Finland. (2019). *Laser scanning 2008-2019 by National Land Survey of Finland*. https://www.maanmittauslaitos.fi/en/maps-and-spatial-data/expert-users/product-descriptions/laser-scanning-data

Prospectivity for Fe-Ti-P-(REE) mineralization in alkaline monzonite and syenite: example from the Southern Oslo Rift, Norway

N. Coint[1], E. T. Mansur[1], Y. Wang[1]., A. C. R. Miranda[1], F. Szitkar[1], P. Acosta-Gongora[1], V. Baranwal[1], A. Nazuti[1] and M. H. Huyskens[1].

[1]Leiv Erikssons vei 39, 7040 Trondheim, Norway
E-mail: Nolwenn.Coint@ngu.no

Iron-Ti-P mineralization of magmatic origin are mostly associated with Anorthosite in Anorthosite Mangerite Charnockite Granite (AMCG) suites. In Norway, however, they can be found in alkaline monzonite and syenite of the Permo-Caboniferous Oslo Rift. This project aims at characterizing this unconventional type of Fe-Ti-P-mineralization and developing/testing new tools across geological disciplines to assess the critical metals prospectivity of the southern part of the Oslo rift. Results from U-Pb geochronology and igneous petrology studies show that Fe-Ti-P-(REE) mineralization are not restricted to the Larvik Plutonic Complex, as previously thought, but instead can be associated with monzonitic and syenitic intrusions further north. The prospectivity map generated through machine learning, using regional geophysics and whole-rock geochemical datasets, provide valuable information to guide future mineral exploration in the area, although understanding the petrogenesis of the mineralization is essential to interpret the results.

Keywords: Oslo Rift, Fe-Ti-P-(REE) mineralization, Mineral prospectivity mapping

1. The Oslo Rift and associated Fe-Ti-P-(REE) mineralization

The Oslo rift is a NNW-SSE 220 x 60 km-large graben resulted from an extensional tectonic setting stretching from Scandinavia to Northern Germany from the late Carboniferous to early Permian.

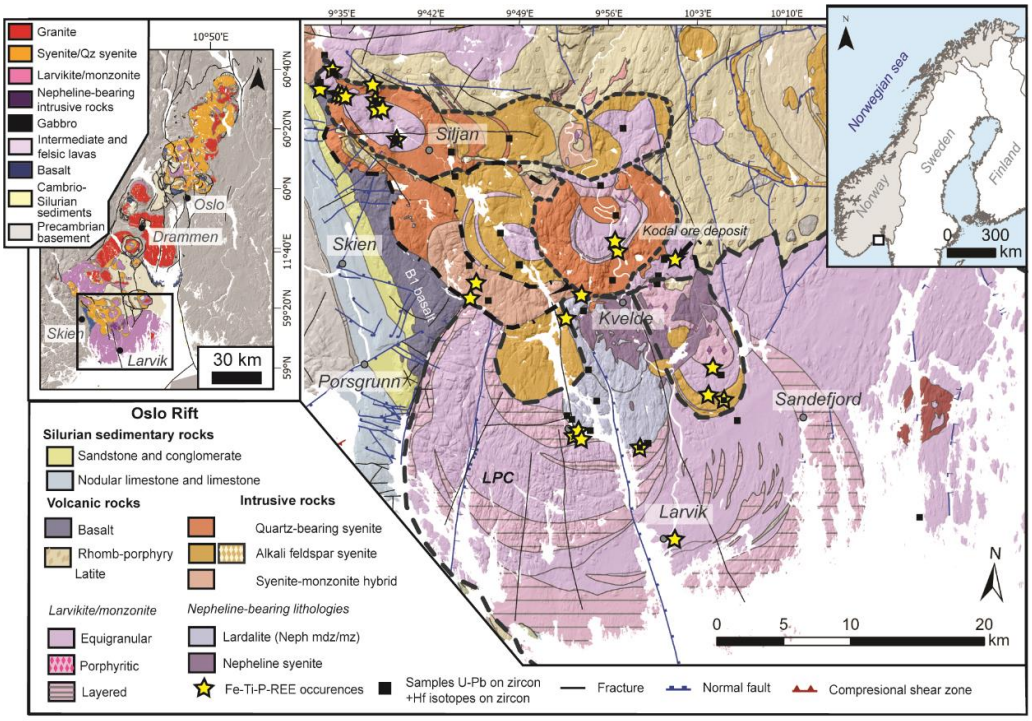

Figure 1. Geologic map of the study area (modified from Mansur et al., submitted).

Magmatism in the rift started with emplacement of alkaline to tholeiitic basaltic flows, the formation of a 3 km-thick latitic rhomb-porphyry lava plateau around 300 Ma, followed by the emplacement of a series of shallow nested intrusions. The youngest and most voluminous of them, the Larvik Plutonic complex (LPC thereafter-Fig.1), was emplaced between 299-288 Ma (Mansur et al., submitted; Rämö et al., 2023) and range from silica-saturated monzonite to silica-undersaturated nepheline syenite (Neumann, 1980). Magmatism continued towards the north with emplacement of silica-saturated monzonite, syenite and granite (284 to 278 Ma), occasionally associated with caldera collapse structures.

Previous studies indicate the LPC intrusion hosts several occurrences of Fe-Ti-P-(Rare Earth Elements - REE) mineralization (Ihlen et al., 2014) consisting of centimeter to 20-25 m scale pods, schlieren and lenses of titanomagnetite, ilmenite, apatite and various proportions of diopside hosted by a coarse-grained monzonite (locally called larvikite). The largest known mineralization in the area, Kodal consists of a 2000 x 30 m large zone where massive ore lenses are concentrated. The deposit has a JORC compliant total indicated and inferred resources of 48.9 Mt at 4.77 wt% P_2O_5. Furthermore, apatite is enriched in Rare Earth Elements (REE) with concentrations ranging from 0.92 to 1.29 wt% TREO (total Rare Earth Oxides) (Decrée et al., 2023).

Examples of Fe-Ti-P-(REE) occurrences hosted in monzonitic to syenitic rocks have been described in the Lofoten-Vesterålen AMCG suite (Coint et al., 2020), where mineralization formed through silicate-liquid immiscibility from a monzodioritic magma. An on-going study indicates that the same process likely happened in the monzonitic rocks hosting the Kodal deposit (Miranda et al., 2023). These results suggest that other intrusions in the area might be prospective for Fe-Ti-P-(REE) as well. In both regions, Fe-Ti-P-(REE) mineralization is found in mingling zones where several magmas interacted.

2. Geochronology

A regional U-Pb geochronology study in the targeted area constrains the timing of magmatism (Mansur et al., submitted).

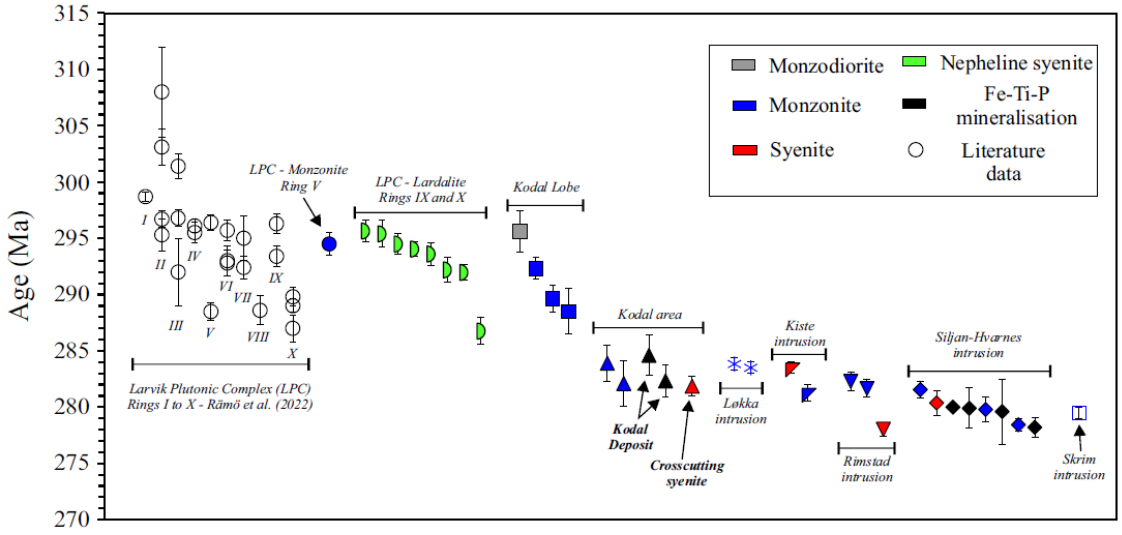

Figure 2. New U-Pb in zircon ages acquired by LA ICP-MS (Mansur et al., submitted).

New U-Pb ages show that the Kodal deposit (284-282 Ma) is younger than the LPC (299-288 Ma), intrusion previously assumed to host the deposit based on its location on the geological

map. Instead, the deposit belongs to the group of intrusion further north, reenforcing the hypothesis that mineralization can be associated with silica-saturated monzonitic and syenitic intrusive systems of the Oslo rift.

3. Prospectivity mapping and machine learning

In view of the results presented above, the study area for prospectivity mapping was extended to the intrusions north of the LPC (Fig. 1).

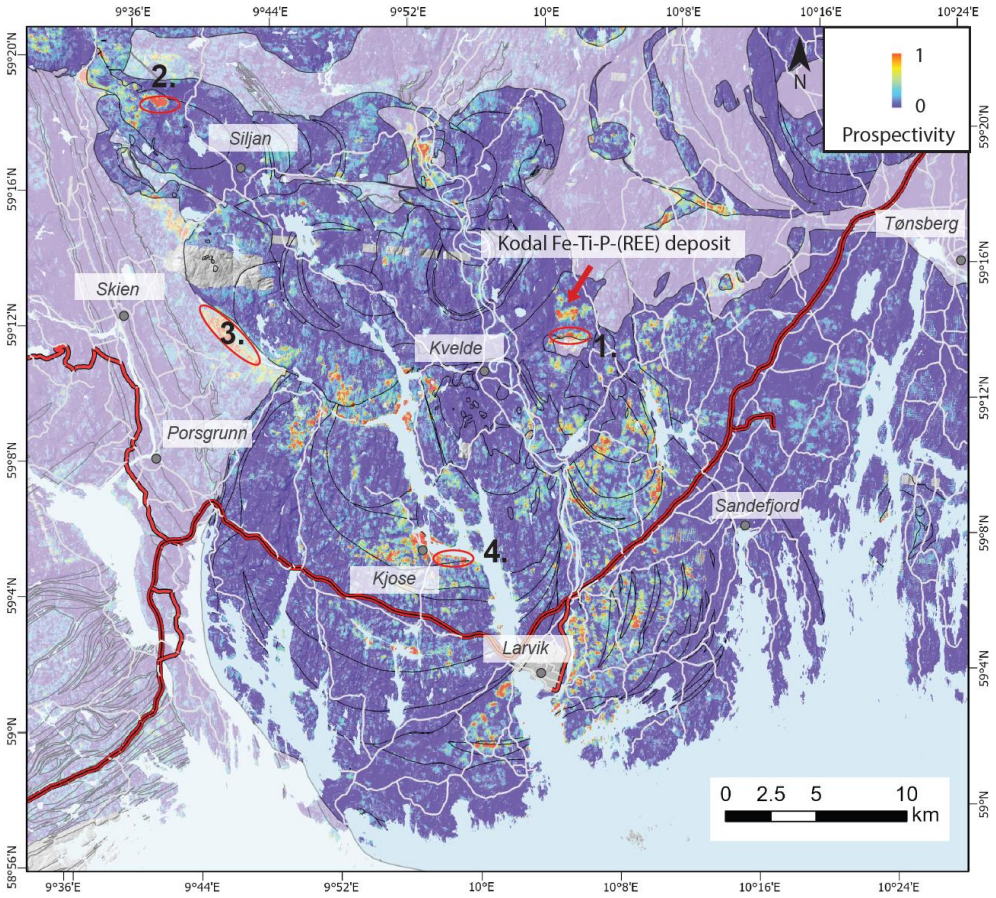

Figure 3. Prospectivity map for Fe-Ti-P-(REE) mineralization (from Wang et al., 2024).

Strong petrophysical contrast exists between the mineralized rocks and their host owing to their different mineralogy. Monzonite and syenite are dominated by feldspar (potassium-rich phase), whereas mineralization contains abundant magnetite and rare feldspars. We used available datasets within a supervised machine learning framework, resulting in a predictive prospectivity map at a regional scale (Fig. 3). The predictors include data derived from airborne magnetic and radiometric (uranium, potassium, thorium) surveys, in addition to topographical information. The training dataset consists of 400 whole-rock analyses of samples collected for petrogenetic purposes that have been categorized based on their phosphorous concentration. Below 4 wt% P_2O_5 samples were considered as barren, whereas above this value, they were labelled as mineralized.

4. Field validation

The choice of a geographical area covered by continuous datasets resulted in a prospective map for the whole area, even where the geology is not appropriate for hosting such mineralization. Zone 3 is for example a false-positive where basalt, rocks poor in potassium and rich in magnetite, like Fe-Ti-P-(REE)-rich rocks crop out. The results from such a study must therefore be carefully assessed. We used bedrock maps to shade the polygons where the lithology was not compatible with the presence of Fe-Ti-P-(REE) mineralization, such as basalt, sediments and volcanic rocks.

Zones 1, 2 and 4, classified as high prospectivity areas on the map were however promising, and we confirmed the presence of Fe-Ti-P-(REE) mineralization at the surface. It is noteworthy however that this product only shows areas with geophysical properties similar to the ones encountered in mineralized areas and that it does not provide any information on the phosphorous or REE content of the mineralization. Furthermore, only a proper drilling campaign can assess the size and quality of the newly discovered occurrences.

5. Conclusion

- Understanding the ore petrogenesis provides important constraints on the extent of the prospective area. Additional U-Pb ages indicate that silica-saturated monzonite and syenite of the Oslo rift are also prospective for Fe-Ti-P-(REE) mineralization, whereas petrological study will confirm the petrogenetic processes behind the formation of the mineralization and help define the target areas (mingling zones between two different magma batches).
- Supervised machine learning provides a new tool to integrate available datasets at a regional scale, however good geological understanding is necessary to interpret the data.

References:

Coint, N., Keiding, J.K. and Ihlen, P.M. (2020). "Evidence for Silicate–Liquid Immiscibility in Monzonites and Petrogenesis of Associated Fe–Ti–P-rich rocks: Example from the Raftsund Intrusion, Lofoten, Northern Norway." Journal of Petrology 61(4).

Decrée, S., N. Coint, Debaille, V., Peter-Hagen, G., Leduc, T. and Schiellerup, H. (2023). "The potential for REEs in igneous-related apatite deposits in Europe." Geological Society, London, Special Publications 526(1): SP526-2021-2175.

Ihlen, P. M., Schiellerup, H., Gautneb, H and Skår, Ø. (2014). "Characterization of apatite resources in Norway and their REE potential — A review." Ore Geology Reviews 58: 126-147.

Mansur, E.T., Coint, N., Slagstad, T., Miranda, A.C., Huyskens, M. and Andersen, T. (submitted). Temporal, spatial and compositional relationships between alkaline intrusions and associated Fe-Ti-P mineralization in the southern Oslo Rift, Norway: constraints from whole-rock geochemistry and U-Pb and Hf isotopes systematics in zircon, Geosphere.

Miranda, A.C.R., Coint, N., Dare, S. and Mansur, E.T. (2023). Iron-Ti oxide and apatite mineralization associated with alkaline monzonitic rocks: An example from the Kodal deposit, Permian Oslo Rift, Norway. In: Proceedings of the 17th SGA Biennial Meeting, 28 August – 1 September 2023, 3:229–232.

Neumann, E.R., (1980). "Petrogenesis of the Oslo region larvikites and associated rocks." Journal of Petrology 21(3): 499-531.

Rämö, O. T., T. Andersen and Whitehouse, M. (2022). "Timing and Petrogenesis of the Permo-Carboniferous Larvik Plutonic Complex, Oslo Rift, Norway: New Insights from U-Pb, Lu-Hf and O Isotopes in Zircon." Journal of Petrology 63: 1-29.

Wang, Y., Coint, N., Mansur, E.T., Acosta-Gongora P., Miranda, A.C.R., Nasuti, A. and Baranwal, V. (2024). "Leveraging Domain Expertise in Machine Learning for Critical Metal Prospecting in the Oslo Rift: A Case Study for Fe-Ti-P-Rare Earth Element Mineralization." Minerals 14(4): 377.

Rapakivi related thermal effect in nearby shear zones in the capital area, southern Finland

T. Elminen

Geological Survey of Finland, P.O. Box 96, FI-02151 Espoo, Finland
E-mail: Tuija.Elminen@gtk.fi

This article introduces Ar-Ar-ages from southern Finland in NE-trending shear zones in the vicinity of c. 1640 Ma rapakivi plutons. The aim of the study was to date the mylonites but the Ar-Ar ages are scattered around the rapakivi U-Pb ages and probably show the thermal effect of the magmatism in the area.

Keywords: shear zones, rapakivi, $^{40}Ar/^{39}Ar$, Southern Finland

1. Background

The extensive bedrock construction work and bedrock utilization in capital area has added interest in the structural formations and geological history, especially in faults that can cause trouble in rock engineering during construction. There are different generations of shear and fault zones in the capital area and they often show multiple reactivation (Elminen et al. 2008). The NE-SW-oriented Porkkala-Mäntsälä (PM) and N-S-oriented Vuosaari-Korso (VK) shear and fault zones are the major structures in capital area and the wedge between them contain subordinate NE-SW orientated shear zones (Figure 1). The sampling of the faults was targeted to date the first, ductile phase of the NE-structures. Reactivation in cataclastic conditions is evident in the major shear zones, therefore the sampling was directed into the smaller zones that showed only ductile mylonite structures. Two sampling sites were in NE-SW oriented zones, one sample was from a NNE-SSW structure close to VK shear zone, and one was from an older E-W-trending mylonite zone which is cut by NE-SW orientated zone c. 200 m to the west. The samples were taken from 20 to 50 cm wide ultramylonite zones and from their country rocks about one or more metres apart (Saalman and Elminen 2006).

The capital area is situated in southernmost part of the Svecofennian domain in a 100 km broad ENE-SSW-trending southern Finland granite zone consisting of various plutonic and supracrustal rocks. The age range from >1.9 Ga to ~1.8 Ga in different rocks shows the long Svecofennian history. In this southern part, the last metamorphic peak was achieved about 1.83 Ga ago when migmatization was extensive (Korsman et al. 1999), and late granites and pegmatites of that age have been dated (Kurhila et al. 2005). According to Pajunen et al. (2008) after extensional conditions there was ESE-WNW contraction c. 1.8 Ga ago. Strain partitioning in late stages caused the formation of NE-trending shear zones that occur roughly at 50 km intervals in southern Finland. Structural studies at the NE-SW shear zones show low to medium grade mylonitization and SE-side up movements (Elminen et al. 2008). Next well-established ages are 1.65 – 1.4 Ga rapakivi granites and related rocks that cut these rocks in the Gulf area (Koistinen, T ed. 1994). By that time, the deformation was already brittle.

The $^{40}Ar/^{39}Ar$ dating of the fault zones was carried out in 2007 at the same time as dating of a shear zone controlled mineralization in the Häme Belt (Saalman & Elminen, 2006; Saalmann et al. 2009). Sample preparation was made in GTK, Espoo, Finland and the laboratory work was done in the University of Rennes, France. The method and laboratory work are described in Saalman et al 2009.

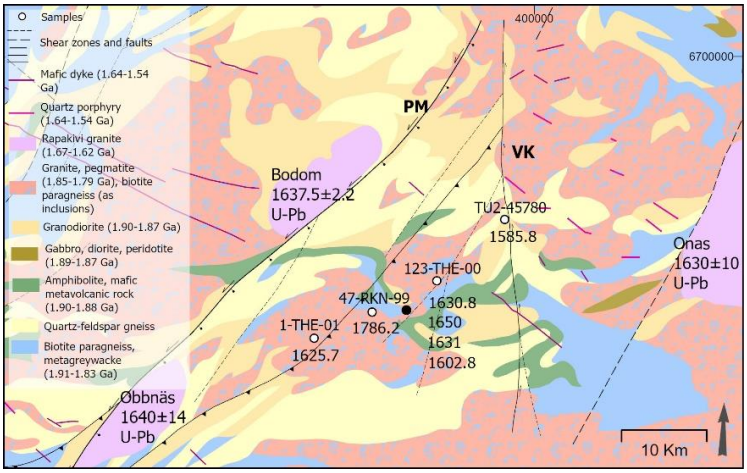

Figure 1. Sampling sites, lithology and some shear and fault zones around the study area. Sample sites as white dots. Numbers on rapakivi plutons mean U-Pb ages in Ma. Numbers below the study sites mean Ar-Ar ages. PM= Porkkala-Mäntsälä shear/fault zone, VK = Vuosaari-Korso shear/fault zone. Black dot is on Helsinki centre. Bedrock map of Finland 1:1 000 000, GTK

2. Age results

Altogether 12 different samples were analysed and two of them were reanalysed. 7 samples gave proper spectra, while 5 samples were chloritised or otherwise altered. In all sites, at least one sample gave a result. The succeeded analyses came from host rocks and the E-W mylonite but none from the actual NE-SW mylonites. $^{40}Ar/^{39}Ar$ plateaus or pseudo-plateau ages are shown in Figure 2.

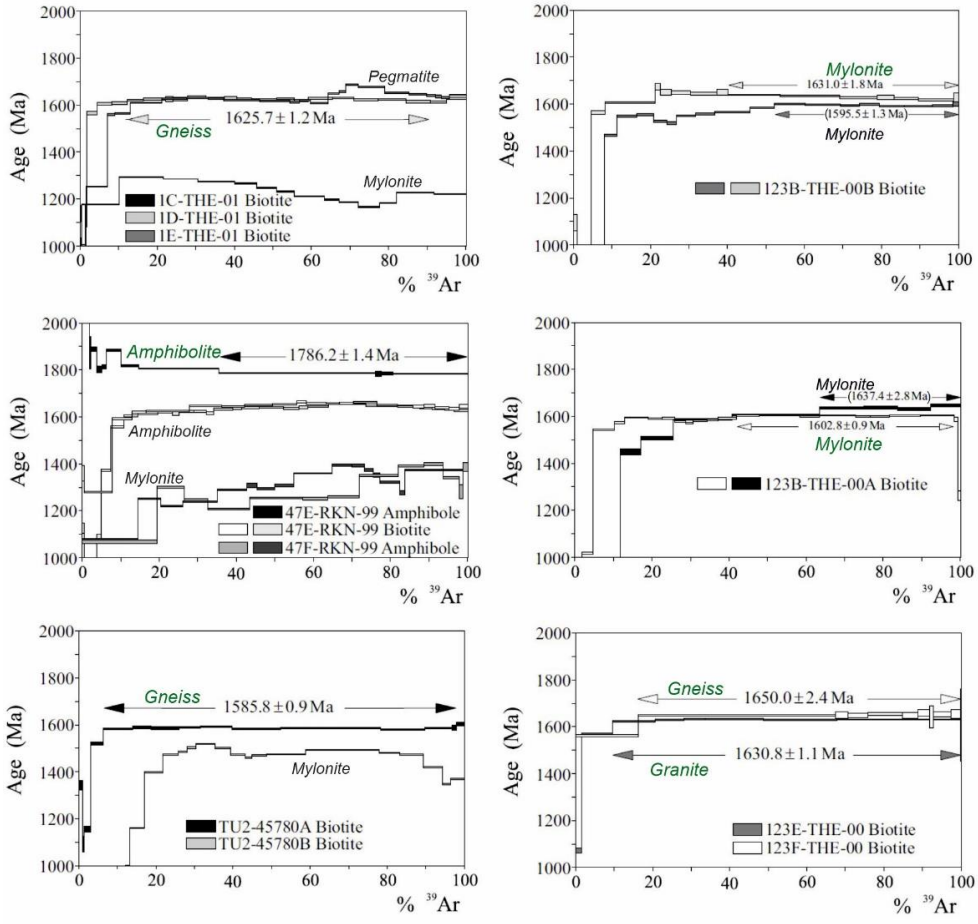

Figure 2. Age spectra from the analysed samples. The fair outcome of the analyses is marked as green color on the rock type.

The age results from the samples are summarized below:

1-THE-01, Iso Vasikkasaari, NE-SW shear zone, biotite. The biotitic ultramylonite (1C-THE-01) had recoil effect and the biotite in pegmatitic host rock sample (1E-THE-01) was cloritized. The only plateau was from the biotite in host rock granodiorite gneiss (1D-THE-01) and it showed an age of 1625.7 ±1.2 Ma.

47-RKN-99 Lemissaari, *NE-SW shear zone, amphibole and biotite.* The amphibole was altered in the ultramylonite (47F-RKN-99) and no result was gained from the mylonite. Also, the biotite from the host rock amphibolite, sample (47E-RKN-99) was chloritized. However, the amphibole from host rock (47E-RKN-99) gave a plateau age 1786.2 ±1.4 Ma.

TU2-45780 Länsisalmi, NNE-SSW shear zone, biotite. (Close to VK zone, in a tunnel). The biotite in ultramylonite (TU2-45780B) was chloritized. Mica gneiss (TU2-45780A) gave a plateau age of 1585.8 ±0.9 Ma.

123-THE-00 Kivinokka, E-W shear zone, biotite. (c. 200 m from a supposed undersea NE-SW shear zone). Kivinokka was the only site where also the mylonitic sample in addition to the host rock sample gave results and both rocks had comparable age range. Acceptable results in mylonites are 1602.8 ±0.9 Ma (123B-THE-00A) and 1631.0 ±1.8 Ma (123B-THE-00B). The plateau age in host rock granite (123E-THE-00) was 1630.8 ±1.1 Ma. The biotite in mica gneiss inclusion (123F-THE-00) in granite had a plateau age of 1650.0 ±2.4 Ma.

3. Discussion

The samples were taken from small shear zones between PM and VK shear/fault zones showing only one generation of movements to avoid resetting of the Ar in younger events. Biotite and amphibole in the mylonitized samples were recrystallised in mylonitization in ductile conditions. Although not seen in microscope all samples of the mylonitic rocks proved to be somewhat chloritized or otherwise altered, and the age results did not succeed. However, the host rocks gave eight succeeded age results which are discussed here.

Closure temperature for the Ar-Ar system in biotite is c. 300 ºC . Ages 1650 ±2.4 to 1585.8 ± 0.9 Ma were derived from biotite in the host rocks and this indicates rapakivi related processes. U-Pb ages for rapakivi granites surrounding the area are Bodom pluton 1637.5±2.2 Ma (Kosunen, 2004) in SW, Obbnäs pluton 1640±14 Ma (Kosunen, 2004) in NW and Onas 1630±10 Ma (Laitala, 1984) in the east (Figure 1). Bodom and Obbnäs are situated alongside the PM shear zone. The ~5 km x 15 km wide Bodom and Obbnäs rapakivi plutons are more than 10 km away from the closest samples. The larger, about 20 km x 20 km wide Onas rapakivi granite is located 20 km from Länsisalmi site. The temperature in rapakivi magmas is relatively high and Kosunen (2004) concluded that in Bodom rapakivi, the younger of two existing generations of zircons (1637 Ma) was formed after magma intrusion into cooler country rocks. The zircon crystallization temperature is high, about 750 ºC. It is suggested that the heat from rapakivi magmatism has reset the argon in biotite in these samples.

Subjotnian events have been documented also by paleomagnetic studies. A magnetic pole component close to the known 1.63 Ga key pole has been detected in Lemissaari site, the same sampling site and shear zone as in this study (Mertanen et al. 2008). The component was isolated in temperatures 200-400 ºC, thus certain magnetic minerals in the mylonite have preserved this c. 1.63 “age” but in biotite the Ar-Ar system has been disturbed. It also appeared that magnetization values in mylonite and host rock within one metre distance were lower than in the surroundings, indicating reactivation and hydrothermal alteration. At the PM zone the paleomagnetic samples showed 1.58 Ga magnetic component (Mertanen et al. 2008) indicating to later episodes in the fault area.

The closure temperature for Ar-Ar system in amphibole is commonly about 600 °C. The only measurements in amphibole come from Lemissaari site and also there the mylonite was

too altered. Instead, the host rock amphibole had an age result of 1786 ± 1.4 Ma. Because the rock was intact and hydrothermal events would not heat the rocks up to c.a. 600 ºC, it is probable that this age indicates cooling of the crustal section through the closure temperature of Ar-Ar system in amphibole after the Svecofennian orogeny.

Hydrothermal activity in major fault zones is likely to occur long time after their formation. Whether the measured c. 300 °C thermal event at c.1630 Ma occurred just in and close to the shear/fault zones (in which case also the small mylonite zones have been reactivated in brittle conditions after all), or if it affected a much larger area, is not resolved in this study. It is also possible that there are more rapakivi plutons that produced heat and fluids beneath the exposed bedrock in the capital area.

4. Conclusion

Two different ages were obtained by $^{40}Ar/^{39}Ar$ studies in the bedrock of capital area, southern Finland. 1786 Ma Ar-Ar age from amfibole in amphibolite next to a NE mylonite zone points to post-orogenic cooling of the crust to temperatures below 600°C at that time. C. 1630 Ma Ar-Ar ages from biotite in gneisses and E-W-trending older mylonite point to thermal effect of rapakivi magmatism recording c. 300°C temperatures in the capital area during that time.

References:

Elminen, T., Airo, M.-L., Niemelä, R., Pajunen, M., Vaarma, Wasenius, P. and Wennerström, M., 2008. Fault structures in Helsinki area, Southern Finland. Geological Survey of Finland, Special Paper 47, 185-213.

Kurhila, M., Vaasjoki, M., Mänttäri, I., Rämö, T. and Nironen, M., 2005. U-Pb ages and Nd isotope characteristics of the lateorogenic migmatizing microcline granites in southwestern Finland. Bulletin of the Geological Society of Finland. vol 77, 2, 105-128.

Koistinen, T. (ed.) 1994. Precambrian basement of Gulf of the Finland and surrounding area 1:1 000 000. Geological Survey of Finland, Special maps 31.

Korsman, K., Korja, T., Pajunen, M. & Virransalo, P., 1999. The GGT/SVEKA transect: structure and evolution of the continental crust in the Paleoproterozoic Svecofennian orogen in Finland. International Geology Review 41, 287–333.

Kosunen, P., 2004. Petrogeneisis of mid-Proterozoic A-type granites: Case studies from Fennoscandia (Finland) and Laurentia (New Mexico). PhD thesis, University of Helsinki, Department of Geology. 21p.

Laitala, M., 1984. Pellingin ja Porvoon alueen kartta-alueiden kallioperä. Summary: Pre-Quaternary rocks of the Pellinki and Porvoo map-sheet areas. Geological map of Finland 1: 100 000, Explanation to the maps of Pre-Quaternary rocks, Sheets 3012 and 3021, 53 pg.

Mertanen, S., Airo, M.-L., Elminen, T., Niemelä, R., Pajunen, M., Wasenius, P. & Wennerström, M. 2008. Paleomagnetic evidence for Mesoproterozoic – Paleozoic reactivation of the Paleoproterozoic crust in southern Finland. Geological Survey of Finland, Special Paper 47, 215–252.

Saalman, K. and Elminen, T., 2006. 40Ar/39Ar dating of Svecofennian mineralization episodes and late- to post-Svecofennian shearing in southern Finland. Geological Survey of Finland, unpublished report, K 21.42/2006/1. 14 p.

Saalmann, K; Mänttäri, I; Ruffet, G ; Whitehouse, M. J. 2009. Age and tectonic framework of structurally controlled Palaeoproterozoic gold mineralization in the Häme belt of southern Finland, Precambrian Research, vol 174, 1-2, 53-77

Pajunen M., Airo M.-L., Elminen T., Mänttäri I., Niemelä R., Vaarma M., Wasenius P., Wennerström, M., 2008. Tectonic evolution of the Svecofennian crust in southern Finland. Geological Survey of Finland, Special Paper 47, 15–184.

How does preexisting ductile structures effect brittle deformation in crystalline bedrocks, insights from Kisko and Paimio area in SW Finland?

Jon Engström[1], Patrik Jänkävaara[2], Nicklas Nordbäck[1], Nikolas Ovaskainen[1], Kaisa Nikkilä[3], Helena Hansson[3], Tuomas Kauti[4], Pietari Skyttä[4], Esa Heilimo[2], Alan Bischoff[1,2]

[1]Geological Survey of Finland
[2]University of Turku, Finland
[3]Åbo Akademi University, Turku, Finland
[4]Structural Geology Company, Turku, Finland
E-mail: jon.engstrom@gtk.fi

This study aims to deepen our understanding of how preexisting ductile structures in crystalline bedrock setting affects the development of subsequent brittle structures, such as faults and other fracture types. The research has been performed on three different crystalline bedrock outcrops and the initial results indicates that ductile precursors, such as bedding, foliation and semi-ductile shears, affect the subsequent brittle deformation. Understanding the role of preexisting ductile structures is crucial for 3D modelling and for enhancing the geological characterization of areas affected by multiple tectonic events.

Keywords: Ductile deformation, brittle deformation, semi-ductile shears, foliation, fractures, faults.

1. Introduction

Previous research concerning fracture networks in southern Finland have been focused on isotropic crystalline bedrock lacking ductile precursors (Ovaskainen et al., 2023; Nordbäck et al., 2024). The effect of ductile structural anisotropy, such as foliation or folding, in the formation of brittle structures is thus poorly known. The ductile shear zones and pre-existing brittle structures are known to have reactivated in brittle regime (Mattila and Viola, 2014). However, the knowledge of the effect of pre-existing ductile structures during formation of subsequent brittle structures are scarce, especially from the Fennoscandian bedrock. However, a recent study by Nordbäck et al., (2023) defined that fractures and faults are affected by precursors in the bedrock, especially in foliated migmatitic rocks at the Kopparnäs site in Inkoo, southern Finland. The bedrock of the study area in southwestern Finland (Fig. 1) was formed during the Svecofennian orogen from ca. 1.90 to 1.78 Ga (Nironen, 2017). The orogeny initiated with a collisional stage, followed by subsequent tectonic phases that included minor crustal extension and a resumption of orogenic convergence at the latter part of the orogeny (Lahtinen et al., 2023). Thus, the bedrock in studied area has experienced multiple deformation phases that includes development of major shear and fault zones, both in the ductile and brittle regime (Torvela and Kurhila, 2022).

This study is part of the FLOP (FLOw Pathways within faults and associated fracture systems in crystalline bedrock). This part of the project focuses on three outcrops in the vicinity of major shear zones in Paimio and Kisko area, in southwestern Finland (Fig. 1). Two of the outcrops are in Kisko, one (FLOP_02) near the Jyly Shear Zone (JSZ) and the other one (FLOP_03) near the Kisko Shear Zone (KSZ). The third outcrop (FLOP_05) is close to the Paimio Shear Zone (PSZ). These outcrops have been carefully selected to represent brittle structures in different rock types with different types of ductile structures. The aim of this study is to show 1) whether

brittle structures correlate with previous ductile deformation/structures, and 2) whether brittle structures correlate at both outcrop and sawed sample scales.

2. Methods

Our data consists of 1) High resolution 2D orthomosaics images (acquired with Unmanned Aerial Vehicle) of the outcrops, 2) Panorama photographs of sawed hand samples (15 cm * 15 cm * 100 cm) and 3) Scanned thin sections from small drill cores taken from the same locations as the sawed samples. Detailed mapping was performed at outcrops to define all structures, and when applicable, measurements were coupled to the photographs and samples.

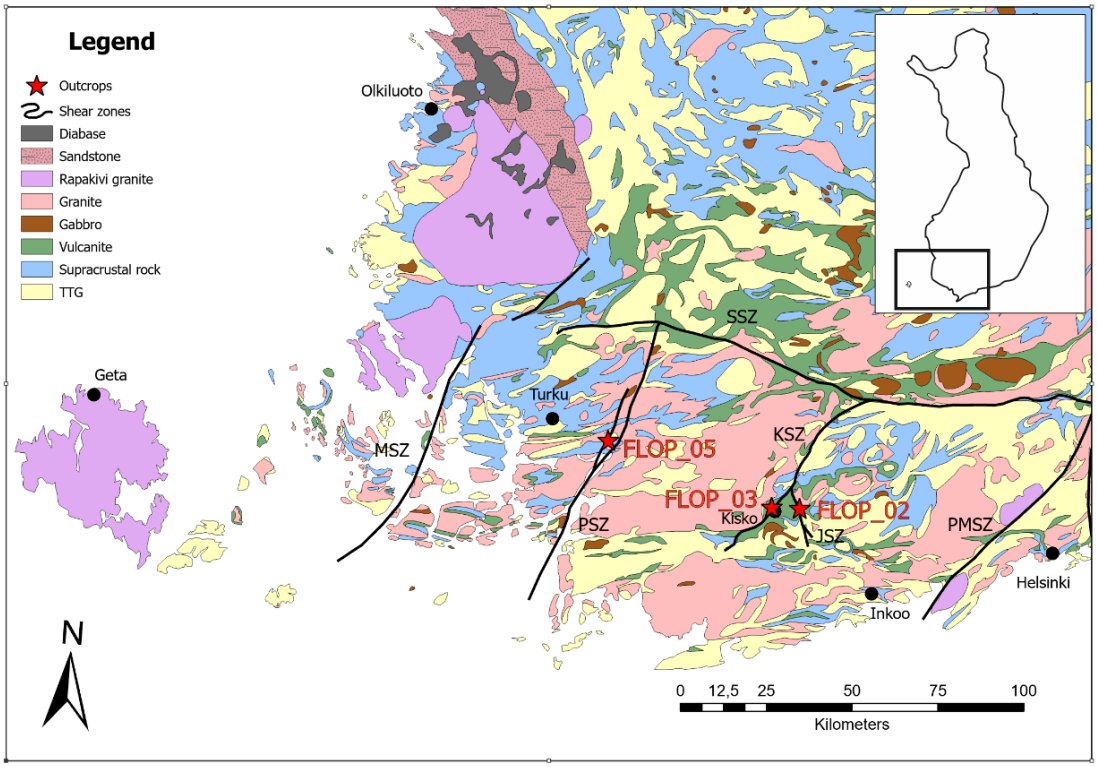

Figure 1. Geological map of southwestern Finland, with major shear zones and location of the outcrops. SSZ = Somero Shear Zone, MSZ = Mynälahti Shear Zone, PSZ = Paimio Shear Zone, KSZ = Kisko Shear Zone, JSZ = Jyly Shear Zone and PMSZ = Porkkala-Mäntsälä Shear Zone.

3. Results

The FLOP_02 outcrop is composed mainly of mafic metavolcanic-sedimentary rocks with recrystallized hornblende and plagioclase. The bedrock has a strong foliation trending NEE–SWW, but at the southern side of the main fault the foliation is rotated towards the fault plane (Fig. 2A). The outcrop contains two main sets of sub-vertical fractures in addition to the main fault, set 1 is trending NNW–SSE and set 2 N–S (Fig. 2B). The outcrop FLOP_03 is dominated by layered mafic metavolcanic rocks with recrystallized hornblende, plagioclase, and minor amounts of biotite (Fig. 2C). The outcrop shows ductile shearing with NE–SW orientation, parallel to the original bedding. The bedding is cut by approximately N–S trending en echelon quartz veins, indicating previous sinistral brittle deformation (Fig. 2C). FLOP_03 is crosscut by several sub-vertical dextral faults, with dextral strike-slip kinematics, parallel to the

shearing. The outcrop has two main sets of sub-vertical fractures. Set 1 is parallel to the foliation and the fault planes while set 2 is E–W trending (Fig. 2D).

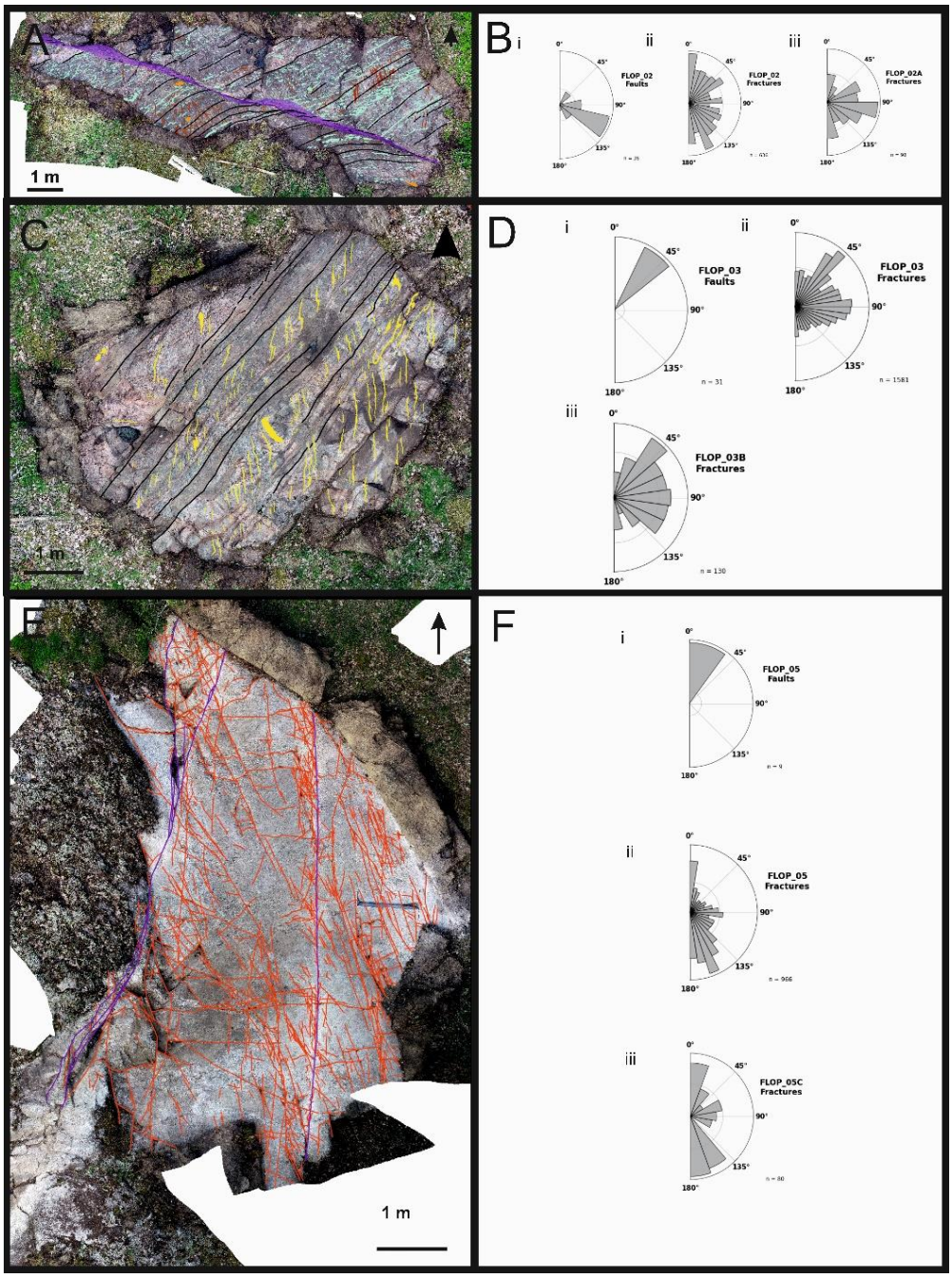

Figure 2. A. FLOP_02 Orthomosaic with digitized fault and foliation; fault = lilac polygons, foliation = black lines. D. Rose diagrams of FLOP_02. C. FLOP_03 Orthomosaic with digitized veins and foliation; Veins = yellow polygons, foliation = black lines. D. Rose diagrams of FLOP_03. E. FLOP_05 Orthomosaic with digitized faults and fractures; fractures = red lines, faults = lilac lines. F. Rose diagrams of FLOP_05.

The FLOP_05 outcrop consist of garnet bearing and altered tonalite with minor amount of slightly folded quartz and pegmatite veins. However, no other signs of the pre-existing ductile

deformation are observed in the outcrop. The outcrop is crosscut by two approximately N–S trending steeply W-dipping faults (Fig. 2E). The kinematics of the faults appear oblique with both sinistral and reverse movement. The outcrop contains three sets of sub-vertical fractures with set 1 trending NNW–SSE, set 2 trending N–S and set 3 trending E–W (Fig. 3F). The faults are linked to each other by mainly extensional set 1 fractures. Set 2 is subparallel to the faults and set 3 perpendicular to the faults.

In addition to the mapping at the outcrops, several sawed samples were examined in more detail and especially across the faults. In this scale the focus was set on fault development and related fracturing but also the alteration coupled to the faults were defined. The sawed samples from FLOP_02 and FLOP_03 show faults with semi-ductile precursors (sheared rock) while these ductile structures are absent in FLOP_05.

4. Conclusion

Based on comparison of the digitized structure orientations and field observations from the three different outcrops the ductile precursor structures, such as bedding, foliation and semi-ductile shears, affect the subsequent brittle deformation, thus fault and fracture development. The FLOP_02 outcrop is dominated by a major ENE–WSW orientated fault that is generated in a mylonitic shear zone. However, the FLOP_03 outcrop is exhibiting a clear bedding with later sub-parallel shears that generates prominent surfaces for development of faults, while the other fracture types are more dispersed. FLOP_05, lacking ductile precursors, shows faults with developed damage zones, but also likely younger joint development similar to the isotropic bedrock studied in the Wiborg rapakivi (Skyttä et al., 2021) and the Åland rapakivi batholith (Nordbäck et al., 2024).

References:

Lahtinen, R., Köykkä, J., Salminen, J., Sayab, M., Johnston, S.T., 2023. Paleoproterozoic tectonics of Fennoscandia and the birth of Baltica. Earth-Science Reviews 246, 104586. https://doi.org/10.1016/j.earscirev.2023.104586

Mattila, J., Viola, G., 2014. New constraints on 1.7 Gyr of brittle tectonic evolution in southwestern Finland derived from a structural study at the site of a potential nuclear waste repository (Olkiluoto Island). Journal of Structural Geology 67, 50–74. https://doi.org/10.1016/j.jsg.2014.07.003

Nironen, M., 2017. Bedrock of Finland at the scale 1:1 000 000 – Major stratigraphic units, metamorphism and tectonic evolution, Geological Survey of Finland, Special Paper 60.

Nordbäck, N., Ovaskainen, N., Markovaara-Koivisto, M., Skyttä, P., Ojala, A., Engström, J., Nixon, C., 2023. Multiscale mapping and scaling analysis of the censored brittle structural framework within the crystalline bedrock of southern Finland. Bulletin of the Geological Society of Finland 95 (1), 5–32. https://doi.org/10.17741/bgsf/95.1.001

Nordbäck, N., Skyttä, P., Engström, J., Ovaskainen, N., Mattila, J., Aaltonen, I., 2024. Mesoproterozoic Strike-Slip Faulting within the Åland Rapakivi Batholith, Southwestern Finland. Τεκτονικα 2, 1–26. https://doi.org/10.55575/tektonika2024.2.1.51

Ovaskainen, N., Skyttä, P., Nordbäck, N., Engström, J., 2023. Detailed investigation of multi-scale fracture networks in glacially abraded crystalline bedrock at Åland Islands, Finland. Solid Earth 14, 603–624. https://doi.org/10.5194/se-14-603-2023

Skyttä, P., Ovaskainen, N., Nordbäck, N., Engström, J., Mattila, J., 2021. Fault-induced mechanical anisotropy and its effects on fracture patterns in crystalline rocks. Journal of Structural Geology 146, 104304. https://doi.org/10.1016/j.jsg.2021.104304

Torvela, T., Kurhila, M., 2022. Timing of syn-orogenic, high-grade transtensional shear zone formation in the West Uusimaa Complex, Finland. Bulletin of the Geological Society of Finland 18. https://doi.org/10.17741/bgsf/94.1.001

DEXPLORE Horizon EU project: Investigation of CRM potential of Estonian basement

S. Graul[1], S. Nirgi[2], A. Soesoo[1,2], J-D, Solano-Acosta[1], R. Hints[1], T. Hands[1], C. Hernandez-Moreno[3]

[1] Department of Geology, Tallinn University of Technology, Tallinn, Estonia
[2] Geological Survey of Estonia, F. R. Kreutzwaldi 5, 44314 Rakvere, Estonia
[3] Iberian Sustainable Mining Cluster, León Technology Park, 24009 Armunia, Spain
E-mail: sophie.graul@taltech.ee

DEXPLORE is a Horizon Europe funded, beginning project which focuses on innovative, deep-land mineral exploration across Spain and Estonia to enhance critical raw material sources knowledge. The project will propose a holistic innovation package, integrating UAV-assisted in-field mineral detection, advanced Earth Observation methods, and novel deep-land geophysics techniques to reach at least 600 m depth. In Estonia, the investigations will be mainly targeted towards the Alutaguse and Jõhvi Zones area, as recent exhaustive geochemical surveys and previous geophysical studies, have shown high anomaly concentrations of critical raw materials, particularly Cu and magnetite for Fe resources. Additionally, Mn and Mo are present in relatively significant concentrations and highest Pb-Zn-Cu concentrations are found over graphitic and sulphides-bearing gneisses and amphibolites. Thus, C and other potential CRMs will also be explored (Ni, Mn, Mo). Later aims of the project include the development of metallogenic ore models along with online platforms for data visualisation and exploitation.

Keywords: Exploration, Metallogeny, Geophysics, Fennoscandia, Estonia

1. General

The Estonian Precambrian basement is considered a southern continuation of the Fennoscandian Shield, and this yields potential similar to that of metal formations found in southern Finland and Sweden, especially with the Bergslagen province and the Central Finland Granitoid Complex (Keitele microcontinent) (Bogdanova et al. 2015, Nirgi and Soesoo, 2021). It is overlain by a 100 to 780m thick cover of sedimentary rocks. Thus, the basement is unavailable for direct observations from the surface, and the present knowledge is based on information of cores from deep drillings and interpretation of potential gravity and magnetic fields. The basement of Estonia comprises metamorphic and igneous rocks and is divided into two major units: the North Estonian amphibolite complex and the Southeast Estonian granulite complex (Figure 1). Significant anomalies of siderochalcophile, graphite-bearing gneisses have also been identified, where Cu, Pb, and Zn reach levels as high as 5.6% (Soesoo et al. 2021). Therefore, mineralisations and ore potentials remain to be explored with deep-land investigations and could lead to the discovery of potential CRM sources for the EU.

The DEXPLORE project regroups a consortium of thirteen partners froSpain, Estonia, Greece, and Italy and is managed by the Iberian Sustainable Mining Cluster (ISMC). The project began in October 2024 and has a planned duration of thirty-six months. The project will focus on the Estonian Precambrian basement, along with two Spanish zones: the fluorite mineralisation of northern Spain and the volcanogenic massive sulphide ore deposits (VSHMS) of the Iberian Pyrite belt. The work to be conducted in Estonia will be the first to compile and assess the current knowledge and available materials for petrology investigations from the Alutaguse and Jõhvi magnetic anomaly zones; and potential other formations such as the Märjamaa pluton (Figure 2, Nirgi and Soesoo, 2021). as well as conduct systematic mineral characterisation and quantification studies and hyperspectral scanning of historical drill cores by the Geological Survey of Estonia.

The first aim of the project is to provide new information for a better understanding and resource distribution in sulphides and graphite-bearing gneisses, which have recently been interpreted as a metasedimentary and metavolcanic system related to back-arc rifting process (Solano-Acosta et al., 2024). To develop a first ore model, a comparative study of the Bergslagen complex of Sweden will be conducted along with Laser Ablation Inductively Coupled Plasma Mass Spectrometry (LAICPMS) imaging analyses for garnet/biotite geothermobarometers and in-situ, semiquantitative investigations of sulphides, which are mainly pyrite, pyrrhotite, arsenopyrite and sphalerite (Figure 3). The ISMC will also develop a compact remote Raman+LIBS+Fluorescence prototype for remote and in situ applications.

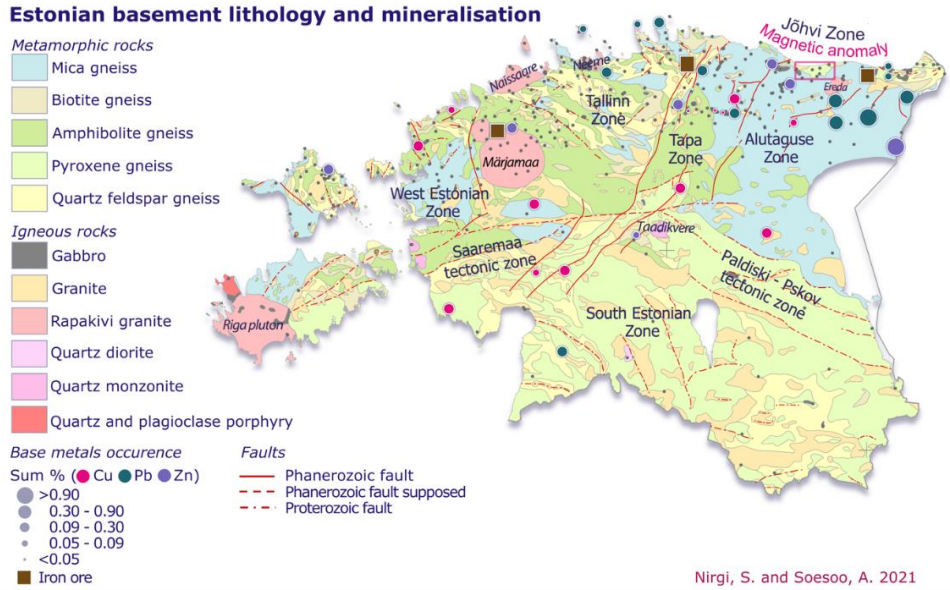

Figure 1. Estonian basement lithology and current investigated mineralisation, after Nirgi and Soesoo (2021).

A pilot geophysical campaign will be organised based on UAV with scalar gravity technology, providing high-resolution and high-quality gravity solutions for mapping and target detection on the Precambrian basement, along with local seismic lines measurements. The identification of density anomalies in the processed data is crucial for defining geological structures and indicating potential mineral deposits. The next step will involves integrating gravimetric data with existing geological maps and information, enabling a correlation between density anomalies and known geological features. Particularly, the correlation between high lead (Pb), zinc (Zn), and copper (Cu) concentrations and the presence of graphitic gneisses will be explored. After running the last validation of the surface and deep-land exploration DEXPLORE technology, the last aim of the project will be to work on the integration of geophysical, petrophysical and mineral information to create an online visualisation and interaction platform along with 3D models with extended Reality tool.

DEXPLORE will be actively involved in several key areas to promote responsible mineral exploration and environmental sustainability. This will include an evaluation of the environmental impact, dissemination, exploitation, and communication. The project has a comprehensive plan to communicate its findings and engage with stakeholders by sharing research results and best practices through workshops, conferences, and publications. The project will involve the general public and stakeholders in educational and engagement

activities in the Estonian and Spanish pilot areas. Three clustering events are planned throughout the project to foster synergies with relevant projects and organisations across a variety of domains, including policies, regulations, standards, and data dissemination.

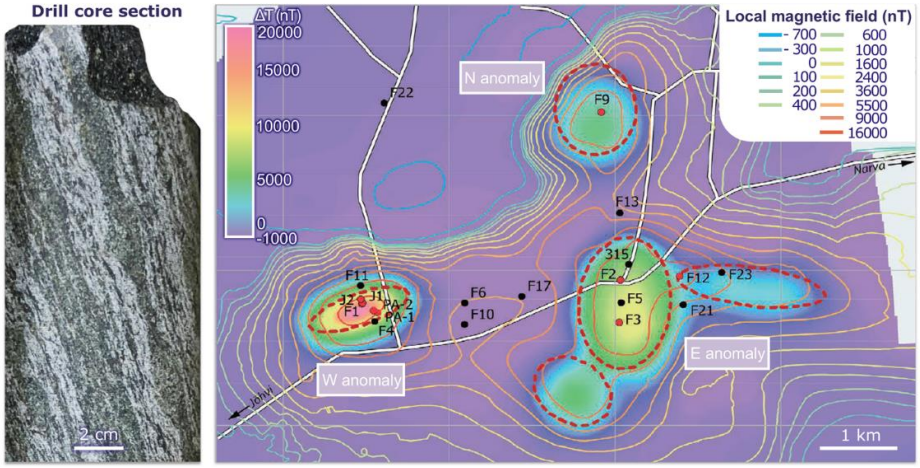

Figure 2. Jõhvi gravimetric magnetic anomaly, after Nirgi and Soesoo (2021); and an example of magnetite-rich gneiss section.

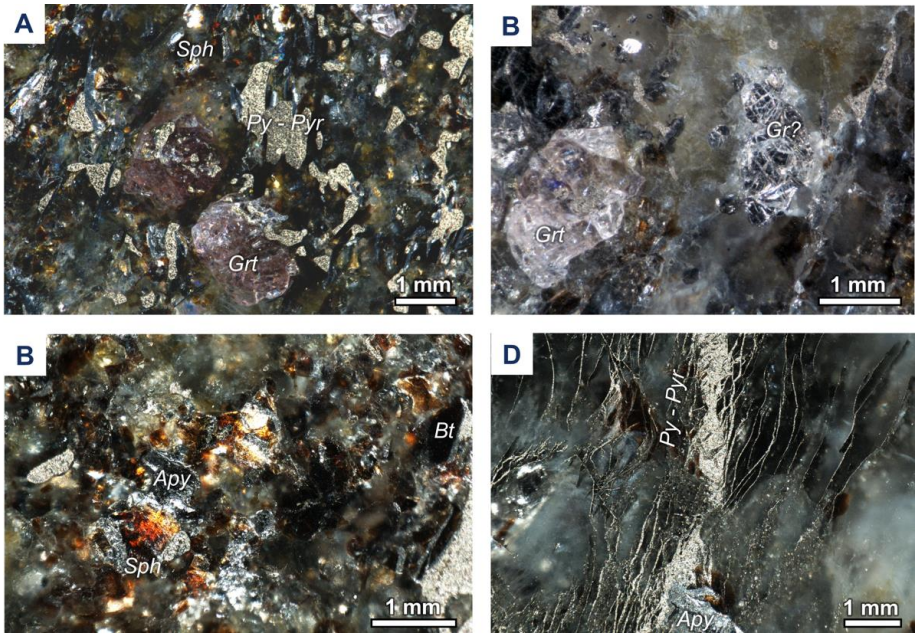

Figure 3. Examples of mineralisation from Alutaguse felsic gneisses. A. Mn-rich garnets with sulphides inclusions. B. Mn-garnet with graphite in quartz matric. B. Sphalerite and arsenopyrite association. D. Small veins of sulphides in a quartz bed.

7. Conclusions

DEXPLORE is an EU Horizon project which will focus on the deep-land investigations of CRM in Western and Eastern Europe craton. In Estonia, geophysical and geochemical exploration will be conducted on sulphides and graphite bearing gneisses of the Precambrian

basement to determine the metallogeny of the Uusimaa-Tallinn belt and potential C-Pb-Zn-Cu resources. The project aims to develop ore genesis model along with 3D visualisation plateforms.

References:

Bogdanova, S., Gorbatschev, R., Skridlaite, G., Soesoo, A., Taran, L., Kurlovitch, D. (2015) Trans-Baltic Palaeoproterozoic correlations towards the reconstruction of supercontinent Columbia/Nuna. *Precambrian Research*. P 5-33. 10.1016/j.precamres.2014.11.023.

Nirgi, S., Soesoo, A. (2021). Geology and geochemistry of the Paleoproterozoic complex of North-Eastern Estonia. *Proceedings of the Karelian Research Centre of the Russian Academy of Sciences*. 10.17076/geo1492

Soesoo, A., Nirgi, S., Urston, K., Volma, M. (2021). Geochemistry, mineral chemistry and pressure–temperature conditions of the Jõhvi magnetite quartzites and magnetite-rich gneisses, Estonia. *Estonian Journal of Earth Sciences*. 70(2):71-93. 10.3176/earth.2021.05

Solano-Acosta, J-D., Soesoo, A., Hints, R. (2022). New insights of the crustal structure across Estonia using satellite potential fields derived from WGM-2012 gravity data and EMAG2v3 magnetic data. *Tectonophysics*. 846(6):229656. 10.1016/j.tecto.2022.229656;

Solano-Acosta, J-D., Soesoo, A., Graul, S., Hints, R. (2024). Geochemistry, provenance, and tectonic setting of Paleoproterozoic metavolcanic and metasedimentary units of the Alutaguse zone, Estonia, a comparative study with the south Svecofennian zones. CRM conference, Tallinn. Poster link.

A three-dimensional resistivity model of the Svecofennian collision zone in the Bothnian region

A. Harjulehto[1], J. Kamm[2], P. Mishra[2] and J. Salminen[1]

[1]Department of Geosciences and geography, P.O. Box 64, 00014 University of Helsinki
[2]Geological Survey of Finland, P.O. Box 96 02151 Espoo, Finland
E-mail: aleksanteri.harjulehto@helsinki.fi

The bedrock of the Bothnian area on the west coast of Finland has been shaped by the Svecofennian orogeny. The area has been studied widely using different geological and geophysical methods. However, no three-dimensional large-scale resistivity model of the area has been available before, despite an extensive collection of magnetotelluric data. In this study old magnetotelluric sites, collected along lines, are combined with freshly collected dataset and a new three-dimensional model of resistivity is created. The new model is used to recognize the vertical continuity of large-scale geological units and compared to earlier two-dimensional models from the area.

Keywords: magnetotellurics, crustal structure, Svecofennian orogeny

1. Introduction

The Svecofennian domain of the Fennoscandian shield was accreted onto the Archean Karelian craton 1.9-1.8 Ga ago during the Svecofennian orogeny as a part of the amalgamation of the Nuna supercontinent. In central Finland, microcontinents and island arcs assembled with newly-formed crust, and the Vaasa migmatitic complex in western Finland is thought to represent the metamorphic core of the Svecofennian orogen.

The accretionary Svecofennian orogen has been intensively studied by a wide range of geological and geophysical methods. Seismic, electric and magnetotelluric studies show that the Svecofennian orogen is characterized by a thick three-layer crust and long, elongated crustal-scale conductors surrounding large resistive units (Korja et al. 1993, Korja and Koivukoski 1994, Korja et al. 2002). Earlier studies, conducted along profiles, show that the Vaasa migmatitic complex and Central Finland Granitoid Complex, are underlain by a large conductivity anomaly (e.g., Korja et al. 1986, Vaittinen et al. 2012, Chopin et al. 2020). The magnetotelluric method has proven to be informative in crustal-scale studies by producing conductivity models with information on the dimensions and orientation of structures if three-dimensional inversion is utilized. With an additional collection of 14 magnetotelluric sites, previous measurement lines were complemented by a dataset suitable for three-dimensional inversion. The goal of the study was to improve the image of resistivity of the whole crust within the Svecofennian collision zone in the Bothnian region.

2. Previous data and measurements

The bedrock at the study site in the Bothnian region consists of four main geological units (Figure 1). The western corner of the area is located in the Vaasa complex, which composed of granitic and granodioritic rocks. The eastern part of the research area is in the Central Finland Granitoid Complex. Between the complexes are the metamorphic Lappfors and Pirttikylä suites. Both magnetotelluric data from previous studies and new magnetotelluric data were used in this study. Most of the data points are from previous studies in the area, including data from the D-Rex project (Kamm et al. 2022), MT-FIRE (Vaittinen et al. 2012), Oulu lines (Korja et al. 1986), the Midcrust project (Chopin et al. 2020) and the SVEKA project (Korja and Koivukoski 1994).

Fourteen new magnetotelluric sites were positioned in the study area between previous measuring lines without data coverage (Figure 1). The target maximum depth of the study was crust-mantle boundary. Following Chopin et al. (2020), the local Moho depth was defined to be vary between 50 to 60 km. Broad-band magnetotelluric soundings were carried out at 14 sites during the summer 2023 using Metronix ADU instruments. Both magnetic and electric fields were measured using the same instrument. Measurements were done using a 128 Hz continuous recording supplemented with a two-hour long 4096 Hz recording and two-minute long 65536 Hz recording. The continuous recording lasted for about 24 hours in each site. A remote reference site was also deployed close to the city of Rovaniemi and was used to reduce the effect of noise in the other recorded sites. The dataset was modeled using the inversion program ModEM (Kelbert et al. 2014), capable of creating three-dimensional models, which is a novelty compared to earlier studies from the area.

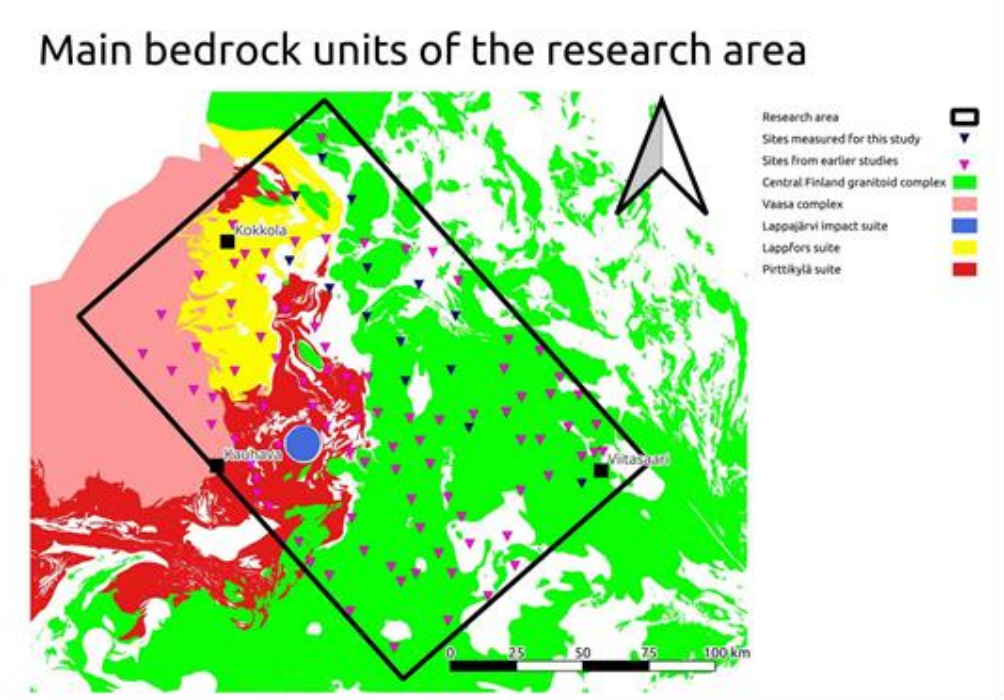

Figure 1. The main bedrock units of the research area, with magnetotelluric sites indicated (triangles). The most significant units are the Vaasa complex (pink), the Central Finland granitoid complex (green), the Lappfors suite (yellow) and the Pirttikylä suite (red). The Lappajärvi impact suite (blue) is included as a reference point to locate the area. White areas are other suites and complexes, that are less important for the study.

3. Results and interpretations

The location of the good conductors are indicated with the 10 Ωm isosurface of the three-dimensional resistivity model (Figure 2). The main part of the model is about 180 km by 120 km wide and 70 km deep. The model also extends beyond the main area, but the results are not reliable due to the lack of recorded data. Conductors in the area are mainly connected to each other and a deeper conductor unit. Also, some individual conductive areas are visible.

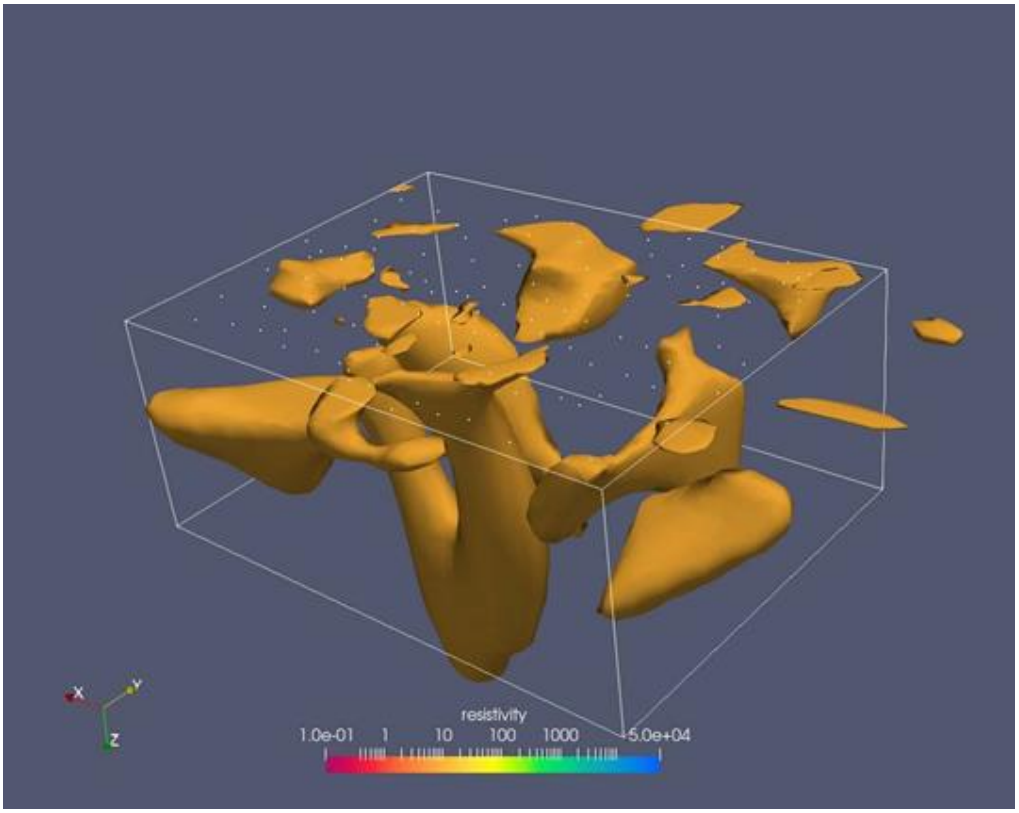

Figure 2. 10 Ω*m* resistivity value isosurface of the model. The white box represents the research area shown on Figure1 and the white points are the study sites. The box is 70 km deep. x is pointing northwest, y points northeast and z points down.

The especially interesting part of the model is the vertical continuity of the Vaasa complex, Pirttikylä suite, Lappfors suite and the Central Finland Granitoid Complex. In the model, conductors are visible under both the Vaasa complex and the Central Finland Granitoid Complex. Chopin et al. (2020) suggested that the Lappfors and Pirttikylä suites seem to continue under both complexes based on their resistivity models. The newly created three-dimensional model is also generally supporting the claim of continuity under the Vaasa complex, but connection between the Pirtttikylä or Lappfors suites and conductors under the Central Finland Granitoid Complex is less clear. In the new model, conductors under the Central Finland Granitoid complex seems to be connected to a deeper conductive anomaly, not shallow metamorphic suites. Generally, the three-dimensional model shows higher resistivity values compared to earlier models, which might be due to characteristics of the used inversion programs.

4. Conclusions

By integrating new and existing magnetotelluric data, a comprehensive three-dimensional resistivity model was developed for the Svecofennian domain in the Bothnian region. The key findings of this work indicate a vertical continuity among the Vaasa complex, the Central Finland Granitoid Complex, and the Lappfors and Pirttikylä suites, supporting the previous suggestion about their interconnections. However a connection between conductors under the Central Finland Granitoid Complex, and the Lappfors or Pirttikylä suite is unclear in the new model.

References

Chopin, F., Korja, A., Nikkilä, K., Hölttä, P., Korja, T., Abdel Zaher, M., Kurhila, M., Eklund, O., and Rämö, T. 2020. The Vaasa Migmatitic Complex (Svecofennian Orogen, Finland): Buildup of a LP-HT Dome During Nuna Assembly. Tectonics 39, e2019TC005583.

Kamm, J., Mishra, P. K., Patzer, C., Autio, U., Vaittinen, K., Smirnov, M., Muhumuza, K., and Hill, G. 2022. 3D Magnetotelluric Study of the Crustal Architecture and Mineral System in Pyhäsalmi, Finland. AGU Fall Meeting Abstracts. Vol. 2022, GP33A–01.

Kelbert, A., Meqbel, N., Egbert, G., and Tandon, K. 2014. ModEM: A modular system for inversion of electromagnetic geophysical data. Comput. Geosci. 66, 40–53.

Korja, A., Korja, T., Luosto, U., and Heikkinen, P. 1993. Seismic and geoelectric evidence for collisional and extensional events in the Fennoscandian Shield implications for Precambrian crustal evolution. Tectonophysics 219, 129–152.

Korja, T. and Koivukoski, K. 1994. Crustal conductors along the SVEKA profile in the Fennoscandian (Baltic) Shield, Finland. Geophys. J. Int. 116, 173–197.

Korja, T., Zhang, P., Pajunpaa, K., et al. 1986. Magnetovariational and magnetotelluric studies of the Oulu anomaly on the Baltic Shield in Finland. J. Geophys. 59, 32–41.

Korja, T., Engels, M., Zhamaletdinov, A., Kovtun, A., Palshin, N., Smirnov, M., Tokarev, A., Asming, V., Vanyan, L., Vardaniants, I., et al. 2002. Crustal conductivity in Fennoscandia-a compilation of a database on crustal conductance in the Fennoscandian Shield. Earth, Planets Space 54, 535–558.

Vaittinen, K., Korja, T., Kaikkonen, P., Lahti, I., and Smirnov, M. 2012. High-resolution magnetotelluric studies of the Archaean-Proterozoic border zone in the Fennoscandian Shield, Finland. Geophys. J. Int. 188, 908–924.

Seismic reflection profiling in hardrock terrains: interpreting complex reflectivity patterns in Fennoscandia

S. Heinonen[1]

[1]Institute of Seismology, University of Helsinki
E-mail: suvi.heinonen@helsinki.fi

Seismic reflection profiling is a powerful tool for imaging subsurface interfaces, though it faces challenges in resolving the complex geological structures typical of hardrock terrains typical of the Fennoscandian shield. Petrophysical measurements provide the basis for interpreting the origin of reflectivity, while insights into structural geology are crucial for understanding the reflectivity patterns observed in such environments. Integrating seismic data with geological and geophysical information is the key to improving the interpretation of seismic profiles, particularly in Precambrian terrains, where folded and faulted structures are common.

Keywords: seismic reflection, seismic interpretation, Fennoscandia

1. Introduction

The seismic reflection method provides high-resolution information about subsurface structures even down to the Moho boundary. In Finland, most seismic surveys are conducted as profiles due to restricted terrain accessibility and economic constraints. Seismic reflection profiling is a powerful tool for imaging subsurface interfaces but faces challenges when imaging the complex three-dimensional (3D) geological structures typical of hardrock terrains. Drill hole data and petrophysical measurements complement seismic surveys by offering a solid basis for interpretation. Integrating seismic data with geological and geophysical information enables the creation of 3D geological models that improve the understanding of crustal structures and tectonic evolution, while also providing more detailed information for applications such as mineral exploration.

2. Seismic interpretation

Petrophysical properties form the basis for interpreting geophysical data, and for seismic reflection interpretation, rock densities and seismic velocities are utilized. In Figure 1, sonic and density logging results from the Outokumpu deep drill hole in Eastern Finland are shown. The figure illustrates how changes in acoustic impedance (the product of P-wave velocity and density) are reflected in synthetic and measured seismic data. The synthetic data were calculated with an Ormsby wavelet using corner frequencies of 20-40-100-150 Hz, while the measured seismic data utilized vibroseis sources with a 30-165 Hz linear upsweep (Kukkonen et al., 2012). Knowledge of the acoustic impedance of typical rock types aids in understanding possible reflective rock contacts: the greater the difference between the acoustic impedance of two rock types, the stronger the reflection from their contact.

Seismic energy propagates as a spherical wave throughout the subsurface, and reflections observed in the profile at a certain travel time (depth) can originate from anywhere within the 3D space at the same travel time (distance) radius. Thus, seismic reflection profiles contain information not only along the vertical section beneath the profile's surface trace but also from the volume of rock surrounding the profile. Based on 2D seismic data alone, it is not always possible to distinguish between a horizontal reflector directly beneath the profile at 1 km depth and a vertical reflector at 1 km distance, for example. This highlights the necessity of

incorporating all available geological and geophysical data into seismic interpretation. Understanding the structural geology of a study area is crucial for robust seismic interpretation.

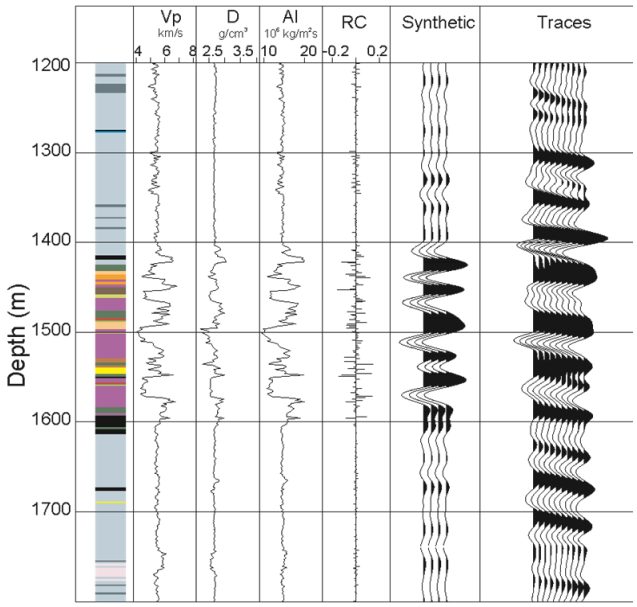

Figure 4. *In Outokumpu, an ophiolite-derived rock sequence embedded in mica schist shows significant variability in seismic P-wave velocity (Vp), density (D), and acoustic impedance (AI) at 1420-1600 m depth. A large reflection coefficient causes prominent reflectivity in both the synthetic seismogram and the traces shown from the seismic profile located near the drill hole. The figure is modified from Kukkonen et al. (2012).*

In Finland, geological structures are typically complex with interfaces folded and faulted due to a polyphase deformation history, which makes interpreting seismic reflection data particularly challenging. In the absence of drill holes, the lack of control points further complicates the geological interpretation and 3D geomodeling. The thickness, orientation, and degree of anisotropy in a given rock unit also causes perturbations to seismic wave propagation. Seismic forward modeling based on assumed subsurface geometries can help identify the origins of observed reflections. Forward modeling results demonstrate how folded geological interfaces can be misinterpreted as horizontal discontinuous layers when the wavefield frequencies are not high enough to image tightly spaced anticlines and synclines (Shaecheng and Changxing, 2006).

Despite the challenges in interpretation, seismic reflection data facilitates understanding of crystalline bedrock. In particular, petrophysical measurements are valuable for estimating which lithological contacts are reflective, and synthetic seismograms provide insight into how lithological changes are expected to appear in measured data. In addition to mapping lithological changes, seismic reflection profiling offers valuable information about large-scale geological structures such as faults.

References

Kukkonen, I.T., Heinonen, S., Heikkinen, P.J., and Sorjonen-Ward, P., 2012. Delineating ophiolite-derived host rocks of massive sulfide Cu-Co-Zn deposits with 2D high-resolution seismic reflection data in Outokumpu, Finland. Geophysics. 77, p. WC213-WC222

Shaocheng, J. and Changxing, L., 2006. Seismic reflection response of folded structures and implications for the interpretation of deep seismic reflection profiles. Journal of Structural Geology, 28, 1380-1387

Passive seismic imaging with dense arrays

G. Hillers[1]

[1]Institute of Seismology, University of Helsinki, Helsinki, Finland
E-mail: gregor.hillers@helsinki.fi

In this presentation I review fundamental concepts that underpin modern noise based passive dense array imaging applications. These include microseisms excitation, propagation length scales and regimes, empirical Green's function estimates, the evolution of the Green's function quality, classic vs. dense or large-N arrays, ambient noise surface wave tomography, resolution, focal spot imaging, and correlation coda based change imaging.

Keywords: Ambient seismic field, microseisms, scattering, cross-correlation, passive surface wave tomography, resolution, coda wave interferometry

1. Summary

Passive seismic imaging refers to imaging applications that are based on the processing of the ambient seismic field or noise, in contrast to using impulsive tectonic signals such as earthquakes, or controlled sources used in geophysical exploration. Dense or large-N seismic arrays become increasingly more available to researchers. Sufficiently powerful data management and computing systems support the implementation of established and the further development of systematic ambient field processing workflows for an improved characterization of the space and time dependent subsurface velocity structure. Passive seismic imaging with dense arrays can enhance a range fundamental research and applied imaging applications in a lithosphere environment that exhibits a comparatively low level of natural seismicity.

2. Fundamental concepts of ambient field based dense array imaging

I review a range of fundamental concepts that are essential for all ambient field based imaging applications. (1) I focus on the double frequency microseisms excitation mechanism. It results from opposite traveling ocean gravity waves that generate a standing pressure wave on the ocean bottom. The effectiveness of the coupling depends on the bathymetry (Kedar et al., 2008). (2) I review the characteristics of the lapse time dependent wave field propagation regimes ballistic, single and multiple scattering, diffusion, and equipartition (Hennino et al., 2001). (3) The Green's function theorem connects the ambient field correlations to the Green's function estimate between two seismic sensors (Campillo, 2006). I discuss the Green's function emergence from correlations of ballistic and scattered waves (Gouédard et al., 2008). (4) The relative lengths of the propagation distance between source and imaging region, scattering and dissipation paths, medium heterogeneity, and wavelength control the ambient field properties and noise correlation characteristics (Hillers et al., 2013). (5) The correlation signal-to-noise ratio depends on the field intensity, and it scales positively with correlation time, wave speed, period, and bandwidth, but negatively with distance (Larose et al., 2007). (6) Classic array designs try to optimize the array response function for f-k and beamforming analysis, whereas modern dense or large-N arrays can be considered brute-force samplers of the wave field (Lin et al., 2013). (7) I present a standard ambient noise surface wave tomography workflow (Mordret et al., 2013) and imaging results from a range of scales. (8) I discuss two approaches to assess the surface wave tomography resolution (Barmin et al., 2001). (9) In contrast to the tomography approaches, the surface wave focal spot method analyses the spatial autocorrelation for local dense array imaging (Tsarsitalidou et al., 2024). (10) I conclude with

a connection to the correlation coda based monitoring and imaging techniques that are characterized by an increased detection or resolution of subsurface changes (Sens-Schönfelder & Wegler, 2006; Obermann et al., 2013).

References:

Kedar, S., M. Longuet-Higgins, F. Webb, N. Graham, R. Clayton, and C. Jones (2008), The origin of deep ocean microseisms in the North Atlantic Ocean, Proc. R. Soc. A, 464, 777–793, doi:10.1098/rspa.2007.0277.

Hennino, R., N. Trégourès, N. M. Shapiro, L. Margerin, M. Campillo, B. A. van Tiggelen, and R. L. Weaver (2001), Observation of equipartitioning of seismic waves, Phys. Rev. Lett., 86(15), 3447–3450, doi:10.1103/PhysRevLett.86.3447.

Campillo, M. (2006), Phase and correlation of 'random' seismic fields and the reconstruction of the green function, Pure Appl. Geophys., 163, 475–502, doi:10.1007/s00024-005-0032-8.

Gouédard, P., P. Roux, M. Campillo, and A. Verdel (2008), Convergence of the two-point correlation function toward the Green's function in the context of a seismic-prospecting data set, Geophysics, 73(6), 47–53, doi:10.1190/1.2985822.

Hillers, G., Y. Ben-Zion, M. Landès, and M. Campillo (2013), Interaction of microseisms with crustal heterogeneity: A case study from the San Jacinto fault zone area, Geochem. Geophys. Geosyst., 14, 2182–2197, doi:10.1002/ggge.20140.

Larose, E., P. Roux, and M. Campillo (2007), Reconstruction of Rayleigh-Lamb dispersion spectrum based on noise obtained from an air-jet forcing, J. Acoust. Soc. Am., 122(6), 3437–3444, doi:10.1121/1.2799913.

Lin, F. C., Li, D., Clayton, R. W., & Hollis, D. (2013). High-resolution 3D shallow crustal structure in Long Beach, California: Application of ambient noise tomography on a dense seismic array. Geophysics, 78(4), Q45-Q56.

Mordret, A., Landès, M., Shapiro, N. M., Singh, S. C., Roux, P., & Barkved, O. I. (2013). Near-surface study at the Valhall oil field from ambient noise surface wave tomography. Geophysical Journal International, 193(3), 1627-1643.

Barmin, M., Ritzwoller, M. & Levshin, A., 2001. A fast and reliable method for surface wave tomography, Pure appl. Geophys., 158(8), 1351–1375.

Tsarsitalidou, C., Hillers, G., Giammarinaro, B., Boué, P., Stehly, L., & Campillo, M. (2024). Long period Rayleigh wave focal spot imaging applied to USArray data. Journal of Geophysical Research: Solid Earth, 129, e2023JB027417. https://doi.org/10.1029/2023JB027417.

Sens-Schönfelder, C. & Wegler, U. (2006). Passive image interferometry and seasonal variations of seismic velocities at Merapi Volcano, Indonesia, Geophys. Res. Lett., 33, doi:10.1029/2006GL027797.

Obermann, A., Planès, T., Larose, E., Sens-Schönfelder, C. & Campillo, M. (2013). Depth sensitivity of seismic coda waves to velocity perturbations in an elastic heterogeneous medium, Geophys. J. Int., 194(1), 372–382.

Intraorogenic magmatism in southern Finland – new evidence from geochemistry and dating

A. E. Johnson, J. S. Heinonen and O. Eklund

Geology and Mineralogy, Åbo Akademi University, Turku, Finland
E-mail: anna.johnson@abo.fi

The ca 1.87–1.84 Ga intraorogenic period of the Svecofennian orogeny (~1.9–1.8 Ga) is poorly understood. A characteristic feature for the intraorogenic mantle-derived magmas is a wide geochemical variation, from highly calc-alkaline to tholeiitic MORB type rocks. This suggests diverse magma sources in variable tectonic environments. This work is a compilation of earlier published hypotheses about the intraorogenic mafic magmatism in southern Finland together with some new findings. The overall tectonic puzzle is addressed.

Keywords: Svecofennian orogeny, intraorogenic mafic magmatism, tectonic models

1. The discovery of the Svecofennian intraorogenic stage

The Svecofennian orogeny in southern Finland has for more than 100 years been known to consist of several different stages of magmatism. Ramsay (1912) and Sederholm (1926) described three separate magmatic events, separated by cross-cutting relationships, in the southern Finland archipelago from Hanko to Ingå and further to the east. From the Pargas-Nagu-Korpo archipelago (Figure 1), Hausen (1944) reported a "late-orogenic" remelting of pre-existing crustal material to form extensive coarse-grained granites and migmatites. In short, the sequency is as follows: early granite/granodiorite formation, emplacement of crosscutting mafic dykes and intrusions and finally a phase of "palingenesis/granitisation" i.e. migmatisation and partial melting of pre-existing crustal material at high T-conditions.

The overall mechanisms of mountain building through plate tectonics were generally accepted during the 1960's, but it was still a new concept when Anna Hietanen (1975) introduced the first tectonic model of the Svecofennian orogeny: collision of an arc-system towards an older continent by northeast-ward subduction.

Simonen (1980) summarises the tectonic model for the Svecofennian orogeny in southwestern Finland as follows: Syn-orogenic (emplacement of synorogenic plutonic rocks, regional metamorphism, deformation and folding) – Intra-orogenic (jointing and intrusion: amphibolite dykes) – Late-orogenic (emplacement of late-orogenic granites, migmatisation, granitisation, diapiric updoming and cross folding) – Post-orogenic (intrusion: granitoids).

Suominen (1991) summarised and added to the already then extensive isotope chronology (U-Pb, Rb-Sr, K-Ar) of the SW archipelago of Finland. He writes that 1) the synorogenic intrusions in southwestern Finland form an age group of 1880 ± 20 Ma; 2) Pyroxene granodiorites are time markers (1862 ± 6 Ma) of the intraorogenic intrusions of the study area; and 3) the late-orogenic granites in southwestern Finland characterized by their monazite content and lack of titanite forming a coherent age group of 1830 ± 10 Ma.

Since then, a significant number of mafic rocks of intraorogenic age and tectonic characteristics have been identified (e.g. Väisänen et al. 2012a, Nevalainen et al. 2014, Kara et al. 2020). The tectonic model of the Svecofennian accretionary orogeny in Finland has been further developed by Lahtinen et al. (2005) and Nironen (2017) among others.

2. The mafic magmatism, geochemistry and field occurrence

The intraorogenic mafic magmas are mantle-derived and show a wide geochemical variation, from calc-alkaline and shoshonitic, to tholeiitic N-MORB, E-MORB and OIB type signatures.

Normally, these magma series occur in different tectonic environments, but they are all found among the intraorogenic rocks in southern Finland (Figures 1, 2). The geotectonic environments has mostly been interpreted as extensional, implying a high degree of partial melting of shallow mantle underneath a thin(ning?) crust. Some rocks show compositions characteristic of more compressive and subduction-related environments.

The mafic intraorogenic magmatism occurs as both plutonic and dyke intrusions. Magma mingling between mafic and felsic components is common. The felsic magma is interpreted to be generated by partial melting of the wall rock into which the mafic magma intruded. Furthermore, rocks close to the larger mafic bodies have undergone dehydration (charnockitisation) which is another indication of the high heat flow connected to the intraorogenic stage. The high-T conditions continued into the late-orogenic stage, producing the late-orogenic granites and migmatites. The intraorogenic mafic rocks are additionally metamorphosed under high-T amphibolite to granulite facies conditions.

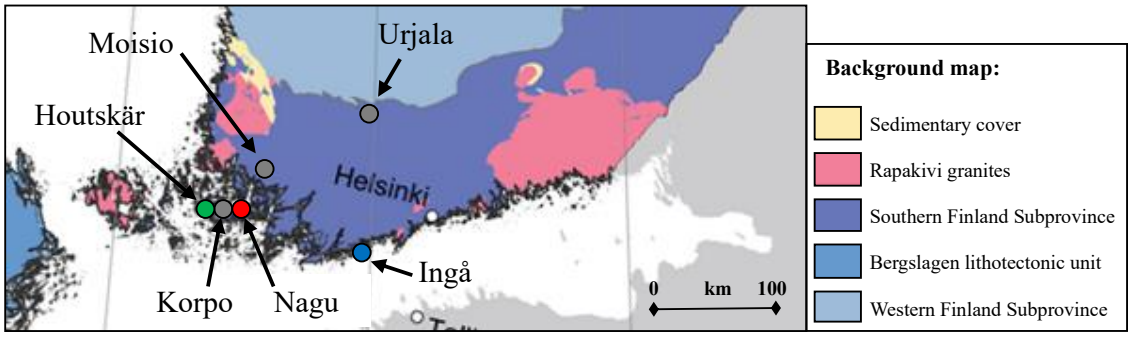

Figure 1. Map showing locations of intraorogenic rocks mentioned in this presentation. Symbols in grey: Väisänen et al. (2012a, Korpo, 1.85 Ga); Nevalainen et al. (2014, Moisio, 1.86 Ga), Kara et al. (2020, Urjala, 1.86 Ga). Red: Johnson et al. (submitted, Kaiplot, Nagu 1.86 Ga); Blue: Rydberg (2024, Ingå, 1.87 Ga); Green: Johnson (unpublished, Houtskär, 1.83 Ga). Background map from Luth et al. (2024).

3. New findings

Johnson et al. (submitted) describe the 1865 ± 2 Ma Kaiplot gabbros in Nagu (Figure 1). These rocks are the most depleted and MORB-BABB-like intraorogenic mafic rocks found so far (Figure 2) and they imply a mature back-arc tectonic environment.

Rydberg (2024) presented new U-Pb ages (1867 ± 5 Ma, 1871 ± 11 Ma and 1878 ± 10 Ma) and geochemistry for three amphibolitic dykes in the Ingå archipelago (Figure 1, 2) that Sederholm (1926) described as evidence of the extensional period. These are older than the Kaiplot gabbros and can be related to the early stages of this possible back-arc extension. The magmas were enriched by assimilation of crustal material and/or by low-degree partial melting of relatively enriched mantle sources.

Ongoing investigations of a gabbroic body in Houtskär (Figure 1, 2) has so far resulted in an age determination of about 1835 Ma which likely represent the timing of metamorphism. It remains to be seen whether a magmatic age can be found. Initial whole rock XRF analysis hints about an extremely depleted MORB-BABB-like original magma type (Figure 2). Further analysis will be done, and the data published in the future.

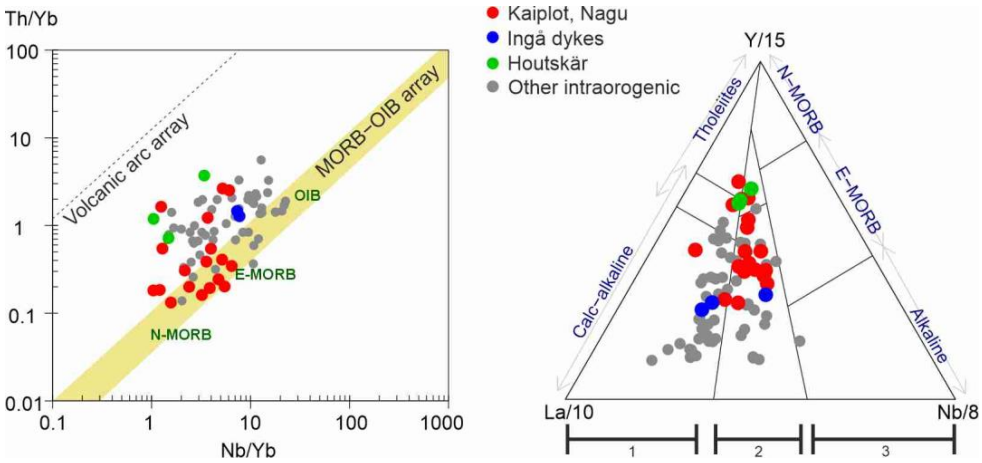

Figure 2. Geochemical data from Finnish intraorogenic mafic rocks shown in diagrams A) Nb-Th-Yb (Pearce 2008) and B) La/10-Y/15-Nb/8 (Cabanis & Lecolle 1989; 1: Orogenic compressive domains (island arcs, active margins); 2: Late- to post-orogenic compressive to distensive intra-continent domains; 3: Anorogenic distensive domains). Grey dots: Väisänen et al. (2012a, Korpo, 1.85 Ga); Nevalainen et al. (2014, Moisio, 1.86 Ga), Kara et al. (2020, Urjala, 1.86 Ga). Red dots: Johnson et al. (submitted, Kaiplot, Nagu 1.86 Ga); blue dots: Rydberg (2024, Ingå, 1.87 Ga); green dots: Johnson (unpublished, Houtskär, 1.83 Ga).

4. Tectonic implications and new ideas

Is there a way to combine all the intraorogenic rocks into a common tectonic model? This rather large area has been subjected to repeated pulses of mantle-derived magma of very different geochemical affinities.

The traditional accretionary model with the syn-intra-late-post-orogenic division (e.g. Simonen 1980, Lahtinen et al. 2005, Nironen 2017) seems to be too simple to include all rock types and ages. Another model that has been applied to the Svecofennian orogeny is tectonic switching with a single subduction zone (e.g. Hermansson et al. 2008, Stephens & Andersson 2015). This model has been applied to the south-central Swedish part of the Svecofennian orogeny, including, in general, the same age ranges and rock types as on the Finnish side.

Lately, a new model including the supercontinent puzzle has been introduced by Mints et al. (2020) among others. This model places the Svecofennian orogeny in a large-scale mobile belt between the Karelia and Superior cratons. This model can include and repeatedly switch between different small-scale local tectonic environments for an extensive period of time, since the cratons are moving and turning in respect to each other while the mobile belt acts as a tectonic buffer zone.

References:

Cabanis, B. & Lecolle, M., 1989. Le diagramme La/10-Y/15-Nb/8: un outil pour la discrimination des series volcaniques et la mise en evidence des processus de melange et/ou de contamination crustale. C.R. Acad. Sci. Ser. II, 309, 2023–2029.

Hausen, H., 1944. Geologische Beobachtungen in Schärenhof von Korpo-nagu, Südwest-Finland, Acta Aca. Aboensis, Math. -Phys. XIV 12. 92 p.

Hermansson, T., Stephens, M.B., Corfu, F., Page, L.M. & Andersson, J., 2008. Migratory tectonic switching, western Svecofennian orogen, central Sweden: constraints from U/Pb zircon and titanite geochronology. Precambrian Research 161, 250–278. https://doi.org/10.1016/j.precamres.2007.08.008.

Hietanen, A., 1975.Generation of potassium-poor magmas in the northern Sierra Nevada and the Svecofennian in Finland. J. Res. U.S. Geol. Surv. 3, 631–644.

Kara, J., Väisänen, M., Heinonen, J.S., Lahaye, Y., O'Brien, H. & Huhma, H., 2020. Tracing arclogites in the Paleoproterozoic Era – A shift from 1.88 Ga calc-alkaline to 1.86 Ga high-Nb and adakite-like magmatism in central Fennoscandian Shield. Lithos, Volumes 372–373. https://doi.org/10.1016/j.lithos.2020.105663

Lahtinen, R., Korja, A. & Nironen, M., 2005. Paleoproterozoic tectonic evolution. In: Lehtinen, M., Nurmi, P.A., Rämö, O.T. (Eds.), Precambrian Geology of Finland – Key to the Evolution of the Fennoscandian Shield. Elsevier B.V., Amsterdam, pp. 481-532. https://doi.org/10.1016/S0166-2635(05)80012-X

Luth, S.W., Torgersen, E. & Köykkä, J. 2024. Lithotectonic map of Fennoscandia. Conference poster, 36th Nordic Geological Winter Meeting, Gothenburg., https://doi.org/10.13140/RG.2.2.20487.37285

Mints, M.V., Glaznev, V.N., Muravina, O.M. & Sokolova, E.Yu., 2020. A 3D model of the Svecofennian Accretionary Orogen and the Karelia Craton based on geology, reflection seismics, magnetotellurics and density modeling: geodynamic speculations. Geosci. Front., 11, 999–1023. https://doi.org/10.1016/j.gsf.2019.10.003

Nevalainen, J., Väisänen, M., Lahaye, Y., Heilimo, E. & Fröjdö, S., 2014. Svecofennian intraorogenic gabbroic magmatism: a case study from Turku, southwestern Finland. Bulletin of the Geological Society of Finland, 86, 93–112.

Nironen, M., 2017. Bedrock of Finland at the scale 1:1000000 – Major stratigraphic units, metamorphism and tectonic evolution. Geological Survey of Finland, Special Paper 60, 41–76.

Pearce, J.A., 2008. Geochemical fingerprinting of oceanic basalts with applications to ophiolite classification and the search for Archean oceanic crust. Lithos 100, 14–48. https://doi.org/10.1016/j.lithos.2007.06.016

Ramsay, W., 1912. Geologiens grunder II, Översikt av den geologiska utvecklingen, Fennoskandias Geologi. G. W. Edlunds förlagsaktiebolag, Helsingfors. Andra upplagan.

Rydberg, M., 2024. Classification of mafic dikes in the Hanko-Ingå archipelago. Master's Thesis, Åbo Akademi university. https://urn.fi/URN:NBN:fi-fe2024051530992

Sederholm, J.J., 1926. On migmatites and associated pre-cambrian rocks of southwestern Finland. Part II: The region around the Barösundsfjärd W of Helsingfors and neighbouring areas. Bulletin de la Commission Géologique de Finland 77, 139 p.

Simonen, A., 1980. The Precambrian in Finland. Geol. Surv. Finland, Bull. 304, 58 p.

Stephens, M.B. & Andersson, J., 2015. Migmatization related to mafic underplating and intra- or back-arc spreading above a subduction boundary in a 2.0–1.8 Ga accretionary orogen, Sweden. Precambrian Research 264, 235-257. https://doi.org/10.1016/j.precamres.2015.04.019

Suominen, V., 1991. The chronostratigraphy of southwestern Finland with special reference to Postjotnian and Subjotnian diabases. Geo. Surv. Finland, Bull. 356, 100 p.

Väisänen, M., Eklund, O., Lahaye, Y., O'Brien, H., Fröjdö, S., Högdahl, K. & Lammi, M., 2012a. Intra-orogenic Svecofennian magmatism in SW Finland constrained by LA-MC-ICPMS zircon dating and geochemistry. GFF 134 (2), 99–114. https://doi.org/10.1080/11035897.2012.680606

Research application of the St1 superdeep boreholes in Espoo, southern Finland

I.T. Kukkonen[1], R. Kietäväinen[1], V. Nenonen[1], M. Bomberg[2], H. Miettinen[2], M. Nyyssönen[2], M. Nuppunen-Puputti[2], A. Karjalainen[3] and J. Rytkönen[3]

[1]Dept. of Geosciences and Geography, University of Helsinki, Finland
[2]VTT, Espoo, Finland
[3]St1 Lähienergia Oy, Espoo, Finland
E-mail: ilmo.kukkonen@helsinki.fi

The St1 Deep Heat Project with its two deep wells extending to 6.2 - 6.4 km depth was the world's deepest industrial geothermal energy project carried out 2014 - 2022. The aim of this pilot was to build an EGS (enhanced geothermal system) heat exchanger at the depth of 5 - 6 km and to produce thermal power to a district heating network. Due to low hydraulic conductivity at the EGS reservoir depth, regardless of hydraulic stimulation, the project did not achieve its economic goal. Now there are two cased superdeep boreholes which provide an excellent opportunity to carry out multidisciplinary experiments at depths very rarely accessible. We review the Deep Heat Project and a recent geothermal-hydrogeological-microbial logging and sampling campaign. Equilibrium temperature logs and fluid samples to 5 km depth for hydrogeochemical, isotope geochemical and microbial analysis of water and gas were carried out successfully in September 2024.

Keywords: geothermal, temperature, saline fluids, microbiology, crystalline rocks, Precambrian

1. Introduction and background

The St1 Deep Heat Project was active in 2014 - 2022. With its two deep wells extending to 6.2 - 6.4 km drilling depth, located in Otaniemi, Espoo, southern Finland, it was the world's deepest industrial geothermal energy pilot. The aim was to build an EGS (enhanced geothermal system) heat exchanger at the depth of about 5 - 6 km and to produce thermal power to a district heating network. Due to the demands of the district heating, the aim was to produce hot fluid at about 100°C and re-inject it to the formation at 50°C. The 100°C temperature goal required drilling to about 6 km depth (Kukkonen et al., 2021). The extreme depth level set significant challenges for drilling and hydraulic stimulation, as well as controlling of induced seismicity. Eventually, the project drilled a 2 km deep completely cored pilot hole (OTN-1), and two superdeep wells, OTN-2 to 6.2 km and OTN-3 to 6.4 km.

The extreme depth of the planned EGS was due to low geothermal gradient in the study area (ancient Precambrian bedrock) and the technical requirements of the district heating system. The reservoir temperature should be at least 100°C, and the re-injected fluid should be about 40 – 50 °C. With a typical geothermal gradient of about 15-17 °C/km, the 100°C temperatures required drilling to about 6 km depth.

In EGS heat is 'mined' by circulating water as a heat transfer fluid in the formation between two deep boreholes. Natural level of hydraulic conductivity is very low at depths of several km and only provided by natural fractures of the rock. In most cases, the natural hydraulic conductivity is too low for EGS production and must be improved. In the Deep Heat Project, it was done by hydraulic stimulation. Due to elastic response of the rock, sufficient improvement in hydraulic conductivity was not achieved and the project was terminated in 2022 (Kukkonen et al., 2023).

2. Applying the St1 superdeep boreholes for research

The company St1 provides an opportunity to access the boreholes for research purposes. As the first *in situ* research application, we carried out temperature logging to 4.8 km depth in OTN-2 and OTN-3 and took fluid and gas samples to 5 km depth for hydrogeochemical, isotope geochemical and microbial studies. The motivation is to obtain undisturbed temperature logs to an unprecedented depth in Finland, to study the extremely saline deep fluids (up to 170 g/l dissolved solids), and to insight the already confirmed microbial life forms in the Otaniemi bedrock (Purkamo et al., 2016). Field work was carried out in September 2024 with the logging team of the GFZ-Potsdam responsible of the logging and pressurized fluid sampling. First results are reviewed in the presentation.

3. ICDP proposal DEEP EGS

An international research team has made an application to the International Scientific Drilling Program (ICDP) about using the St1 superdeep boreholes for a multidisciplinary research project. ICDP has recently accepted the DEEP EGS workshop proposal and we will be able to organize an international open workshop in 2025 for planning of the next step, i.e., the planning of the research project itself. The St1 deep holes provide a unique possibility to establish a deep borehole observatory and geothermal laboratory offering unprecedented possibilities for research in induced seismicity, geothermics, hydraulic properties, deep fluids and gas as well as deep biosphere, helping to understand the behavior of crystalline bedrock at extreme depth. Our aim in the DEEP EGS project is to apply the boreholes and data sets for a thorough analysis of the crystalline bedrock conditions at 5 – 6 km depth, solving problems related to developing EGS in crystalline rock as well as basic research questions. We expect that the project will provide novel and indispensable data for planning new EGS projects.

4. References

Kukkonen, I.T., Pentti, M., and Heikkinen, P.J., 2021. St1 Deep Heat Project: Hydraulic stimulation at 5 – 6 km depth in crystalline rock. In: Kukkonen, I.T., Veikkolainen, T., Heinonen, S., Karell, F., Kozlovskaya, E., Luttinen, A., Nikkilä, K., Nykänen, V., Poutanen, M., Skyttä, P., Tanskanen, E. and Tiira, T. (Eds.), Lithosphere 2021 – Eleventh Symposium on the Structure, Composition and Evolution of the Lithosphere in Finland. Programme and Extended Abstracts, January 19-20, 2021. Institute of Seismology, University of Helsinki, Report S-71, pp. 69 – 72 (extended abstract)

Kukkonen, I.T., Heikkinen, P.J., Malin, P.E., Renner, J., Dresen, G., Karjalainen, A., Rytkönen, J., Solantie, J., 2023. Hydraulic conductivity of the crystalline crust: Insights from hydraulic stimulation and induced seismicity of an enhanced geothermal system pilot reservoir at 6 km depth, Espoo, southern Finland. Geothermics 112 (2023) 102743. https://doi.org/10.1016/j.geothermics.2023.102743

Purkamo, L., Bomberg, M., Kietäväinen, R., Salavirta, H., Nyyssönen, M., Nuppunen-Puputti, M., Ahonen, L., Kukkonen, I., Itävaara, M., 2016. Microbial co-occurrence patterns in deep Precambrian bedrock fracture fluids. Biogeosciences 13, 3091–3108.

Seismic reflection profiling for studying the lithosphere in Finland

V. Laakso[1] and S. Heinonen[2]

[1]Geological Survey of Finland (GTK)
[2] University of Helsinki
E-mail: Viveka.laakso@gtk.fi

Seismic reflection methods, adapted from hydrocarbon exploration to crystalline bedrock, enable imaging of the complex geology typical of hardrock formations. In Finland, crustal-scale seismic imaging of the Precambrian bedrock has established a robust foundation for studying the lithospheric architecture, while high-resolution seismic reflection profiles have proved their utility on identifying rock interfaces and structures in important mining and mineral exploration districts in Fennoscandia.

Keywords: Seismic reflection methods, Mineral Exploration, Fennoscandia, Crystalline bedrock, Mineral systems

1. Introduction

In Finland, seismic reflection profiling has been used for the past two decades to study the crystalline bedrock and its mineral systems (Heinonen and Laakso, 2024). Seismic reflection methods, adapted from hydrocarbon exploration, offer improved depth resolution for imaging complex hardrock geology. Fennoscandia, especially northern Finland, has significant mineral potential and open mines like the Kemi Mine (the EU's only chromium producer), Siilinjärvi Mine (the sole phosphorus producer in the EU) and the Kevitsa Mine supplying key metals like copper and nickel. As easily discoverable ore deposits are less likely to be found, deep exploration technologies are needed. Discovering new deposits at depth near existing mines enhances sustainability by utilizing current infrastructure and protecting untouched natural areas.

2. From FIRE to HIRE

The FIRE project (Finnish Reflection Experiment 2001-2005) provided groundbreaking insights into Precambrian bedrock through over 2000 kilometres of seismic sections, revealing crustal structures down to 80 km and imaging the Moho boundary (Kukkonen and Lahtinen, 2006). This data supports a mineral-system approach to exploration, focusing on lithospheric-scale processes that influence ore deposit formation. Following FIRE, the HIRE (High Resolution Reflection Seismics for Ore Exploration 2007-2010) program advanced the use of high-resolution seismic techniques in 15 sites, successfully identifying mineral-bearing rock interfaces in several regions, including Outokumpu (Kukkonen et al., 2012) and Suhanko, and providing reflection images of the geology at the Olkiluoto nuclear waste disposal site (Kukkonen et al., 2010). Subsequent projects including COGITO-MIN in Kylylahti in 2016 (Heinonen et al., 2019), XSoDEx in Sodankylä in 2017 (Niiranen et al., 2020), Smart Exploration in Siilinjärvi in 2018 (Malehmir et al., 2019), KOSE in Kuusamo in 2018 (Gislason et al., 2018), the Kevitsa Seismic survey in 2022 (Laakso et al., 2022), and SEEMS DEEP in Kuusamo in 2023 (Heinonen et al., 2023) have continued to leverage seismic methods for mineral potential mapping. In recent years GTK has conducted urban seismic surveys, facing challenges such as noise and infrastructure limitations to study subsurface structures for geoenergy development (Cyz et al., 2022 and Koskela et al., 2024).

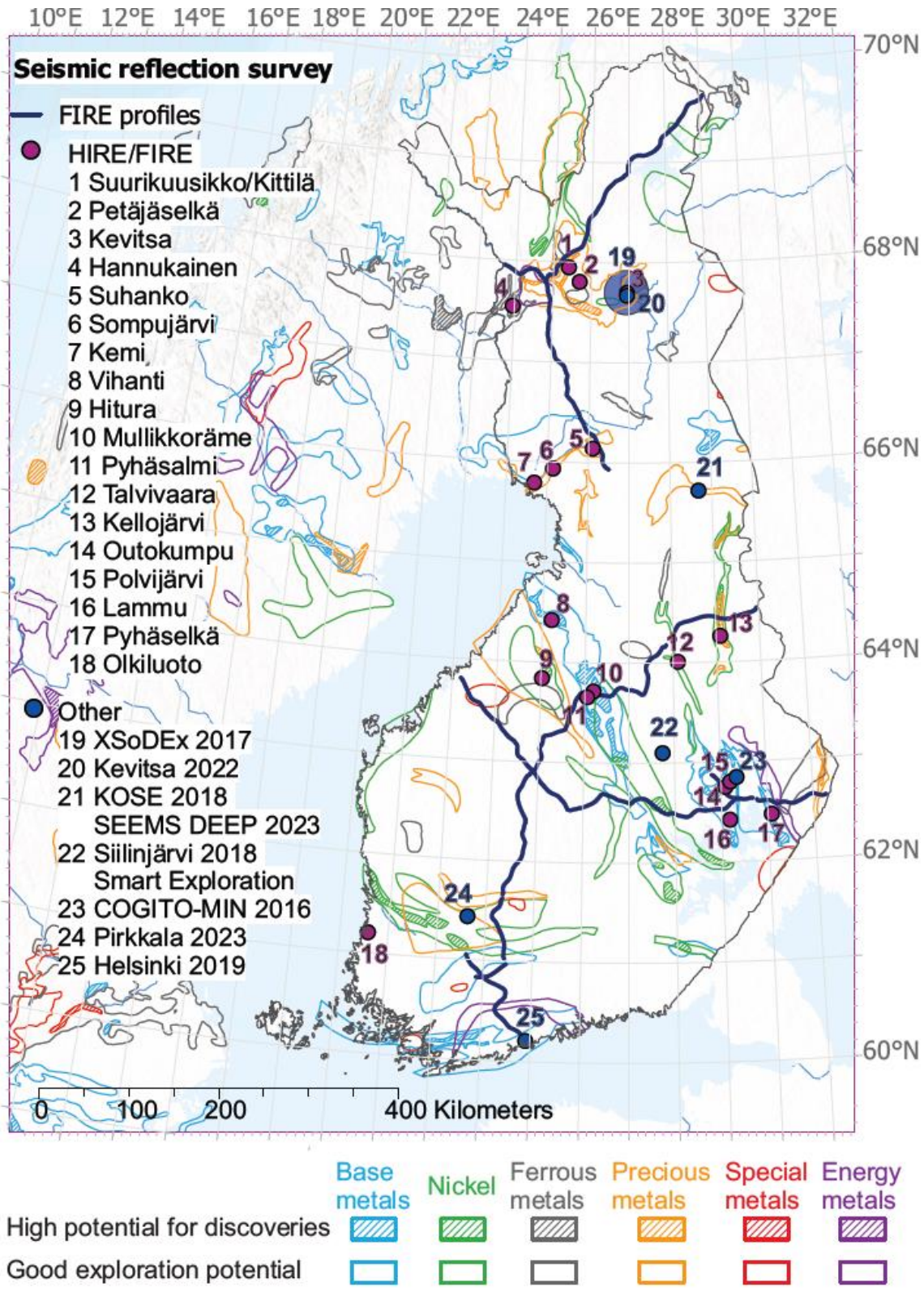

Figure 1. Hardrock seismic reflection surveys conducted over the past two decades overlaid on metallogenic areas in Finland (Heinonen and Laakso 2024).

3. Insights about hardrock settings and future perspectives

With an overview and examples from two decades of hardrock mineral exploration, Heinonen and Laakso (2024) summarized their insights as follows. Seismic data acquisition is most effective before mining begins, as it enhances accessibility, improves the signal-to-noise ratio, and maximizes data utility throughout the mine's life cycle. Seismic reflection data form the basis of 3D geomodels that enhance the understanding of mineral systems. However, these models require additional drill hole and petrophysical data for reliable interpretation.

While 2D seismic data are useful for supporting mineral system modelling, 3D surveys are in many ways preferable, although they face challenges due to higher costs and terrain accessibility. Advances in receiver and seismic source technologies, including lightweight wireless nodes, make seismic methods more viable for the mineral industry. Ongoing developments aim to achieve higher resolution in more accessible locations, utilizing techniques like accelerated weight drops or electric vibroseis systems to effectively map mineral-rich areas down to depths of 800-1500 meters, essential for detailed 3D geomodelling in mineral exploration and mining.

References:

M. Cyz, M. Malinowski, T. Linqvist, E. Virta, S. Heinonen, T. Arola, J. Riissanen, S. Mustonen, J. Hietava and P. Skyttä, 2022. Seismic recognition of the faults for geothermal exploration in crystalline rocks: results from the pilot survey in Helsinki. 12th Symposium on the Structure, Composition and Evolution of the Lithosphere. Åbo Akademi University, Turku, Finland, November 15 – 17, 2022. https://www.seismo.helsinki.fi/ilp/lito2022/Lithosphere_2022_Symposium_Abstract_Volume.pdf

Gislason, G., Heinonen, S., Salmirinne, H., Konnunaho, J. and Karinen, T., 2018. KOSE - Koillismaa Seismic Exploration survey: Acquisition, processing and interpretation. GTK Open File Work Report 101/2018, 36 pages.

Heinonen, S., Malinowski, M., Hlousek, F., Gislason, G., Buske, S., Koivisto, E. and Wojdyla, M., 2019. Cost-effective seismic exploration: 2D reflection profiling at the Kylylahti massive sulfide deposit, Finland. Minerals, 9(5), 263; https://doi.org/10.3390/min9050263

S. Heinonen, J. Kamm, T. Karinen, T. Leskelä and the SEEMS DEEP working group, 2023. SEEMS DEEP - Geophysics based 3D geomodelling for mineral exploration. The 6th European Meeting on 3D geological modelling, Copenhagen, Denmark, 23-26.5.2023. https://www.tilmeld.dk/6theuropeanmeetingon3d/abstracts

Heinonen, S. and Laakso, V. 2024. Insights gained from two decades of seismic reflection profiling for mineral exploration in Finland. First Break, Volume 42, Issue 8, Aug 2024, p. 71 – 76.

Koskela, E. Brodic, B., Malinowski, M., Laakso, V., Martinkauppi, A. and M. Cyz, M., 2024. Seismic methods for geoenergy-related site investigations in crystalline rocks: case study from Pirkkala, Finland. NSG2024 30th European Meeting of Environmental and Engineering Geophysics, Sep 2024.

Kukkonen, I., Heikkinen, P., Paananen, M., Elo, S., Paulamäki, S., Heinonen, S. and Laitinen, J., 2010, HIRE Seismic Reflection Survey in the Olkiluoto area, western Finland. Geological Survey of Finland Report 53, 57 p. https://tupa.gtk.fi/raportti/arkisto/q23_2010_53.pdf

Kukkonen, I.T., Heinonen, S., Heikkinen, P.J., and Sorjonen-Ward, P., 2012. Delineating ophiolite-derived host rocks of massive sulfide Cu-Co-Zn deposits with 2D high-resolution seismic reflection data in Outokumpu, Finland. Geophysics. 77, p. WC213-WC222.

Kukkonen, I.T. and Lahtinen, R. (eds.), 2006. Finnish Reflection Experiment FIRE 2001–2005, Geological Survey of Finland, Special Paper 43, 247 p. https://tupa.gtk.fi/julkaisu/specialpaper/sp_043.pdf

Laakso, V., Heinonen, S., Koskela, E. and Malinowski, M. Reflection seismic profiling in the Kevitsa Ni-Cu-PGE mining area for mineral exploration. LITHOSPHERE 2022 Symposium, November 15-17, Turku. https://www.seismo.helsinki.fi/ilp/lito2022/Lithosphere_2022_Symposium_Abstract_Volume.pdf

Malehmir, A., Holmes, P., Gisselø, P., Socco, L.V., Carvalho, J., Marsden, P., Verboon, A.O. and Loska, M. 2019. Smart Exploration: Innovative ways of exploring for the raw material in the EU. 81st EAGE Conference & Exhibition 2019. 3–6 June 2019, London, UK.

Niiranen, T., Heinonen, S., Karinen, T., Lahti, I., Leväniemi, H., Madetoja, J., and Nykänen, V., 2020. Exploration Lapland 3D (XL3D) - An integrative geomodeling workflow to support exploration. GTK Open File Work Report 47/2020, 90 pages.

3D geological modelling and combined XCT-XRF drill core scanning of the Enåsen Au-Cu-(Te-Ag) deposit, Central Sweden

S. Luth[1] and J. Jönberger[1]

[1] Geological Survey of Sweden (SGU) Villavägen 18, Uppsala, Sweden
E-mail: stefan.luth@sgu.se

3D geological models based on data from structural mapping, magnetic and EM surveys, drill core logging and combined XCT-XRF scanning of drill core samples are presented for the Enåsen Au-Cu-(Te-Ag) deposit in central Sweden. The Paleoproterozoic epithermal gold deposit was mined until 1991 by Boliden Mineral AB and consists of chalcopyrite, gold and tellurides within a highly metamorphosed sillimanite quartzite. Our combined modelling results reveal that mineralization is open in all directions and that a significant amount of gold, copper, tellurium and silver may be left as an economic resource. From the semi-regional modelling result we further postulate that the copper and gold showings around Enåsen all occur in the same folded and faulted stratigraphic sequence. Its association with low resistivity in combination with the proposed structural framework makes this type of mineralization a good target for future mineral exploration.

Keywords: 3D geological modelling, epithermal gold, tellurium. drill core scanning, Enåsen

1. Introduction

Building 3D geological models is a current requirement for mining and exploration. Not the least to expand the lifetime of an active mine or to reopen an abandoned mine, exploring and exploiting deeper-seated orebodies preferably containing a cocktail of polymetallic ore. Significant in the modelling process is the *integration* of geological, geophysical, and geochemical datasets using time- and cost-efficient methods (e.g. Nassar et al. 2020). Integration of datasets may be a joined- or constrained geophysical inversion, or it even may refer to a concept such as “Common Earth Modelling” or “Mineral System Approach”. However, in many cases *data integration* in 3D geological modelling can be deduced to an overall interpretation resulting from a *combined visualization* including multiple datasets, which individually or together provide geological insights on a range of scales.

In this study, we present the result of ongoing research on the geological setting and 3D structural framework of the Enåsen Au-Cu-(Te-Ag) deposit in central Sweden using new and legacy data from geological mapping, geophysical surveys, lithology logs and assays from drilling together with combined XCT-XRF drill core scans.

2. The Enåsen Au-Cu-(Te-Ag) deposit

The Enåsen gold deposit in central Sweden was mined until 1991. Open-pit mining was followed by underground mining with a total production of 1.7 million metric tons of ore with an average of 3 g/t of Au and 1% Cu, but locally exceeding 30 g/t Au and 5% Cu (Hallberg et al. 1994, Boliden Mineral AB). The deposit is drilled by 258 drill holes 1600 meters along strike and down to 370 meters and is open at depth, to the northwest and to the southeast.

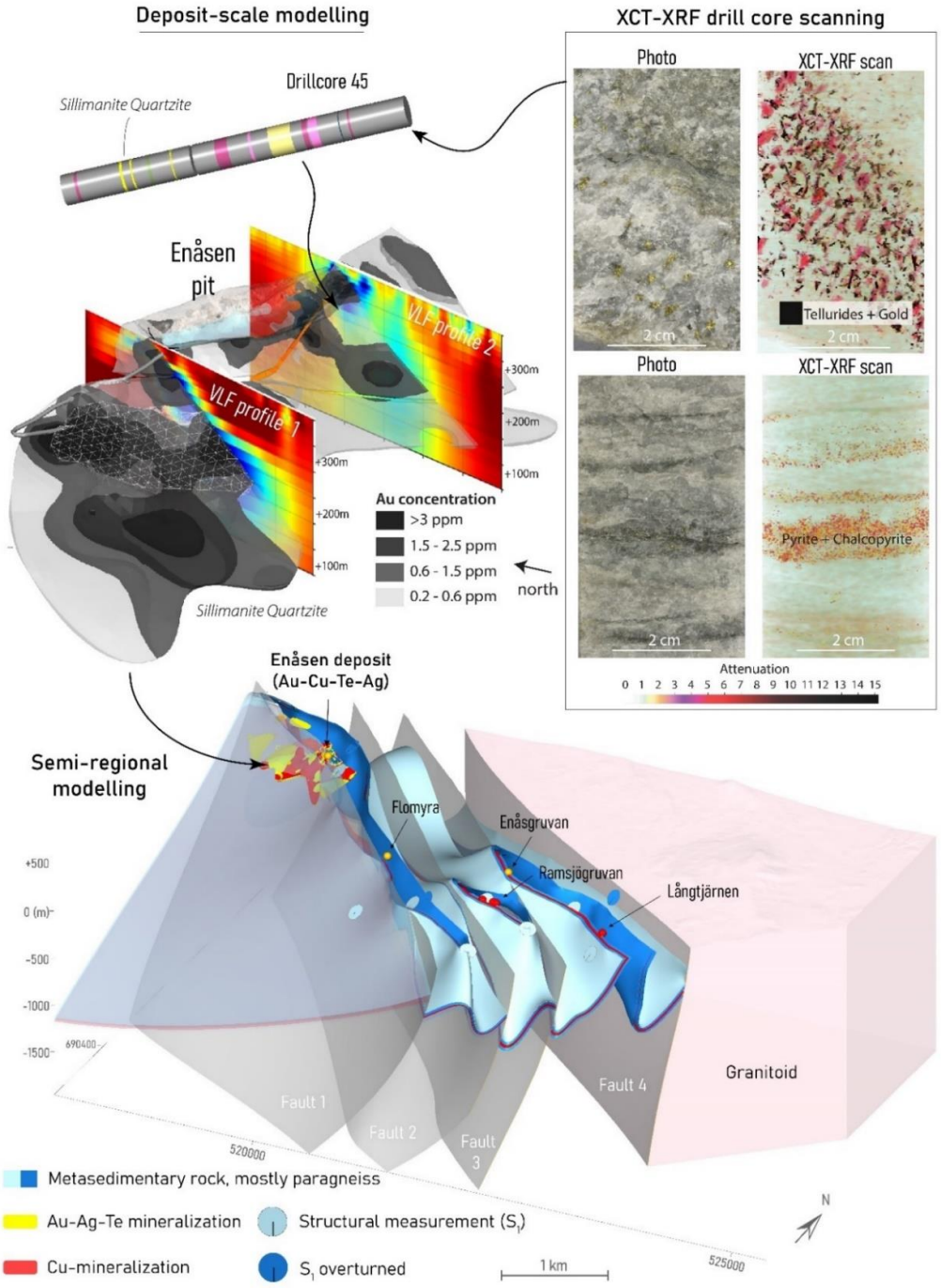

Figure 1. Compilation showing the relationship between multi-scale geological models and resulting imagery from XCT-XRF core scanning of the sillimanite quartzite. From the latter we interpret two different mineralization types of which the upper one shows the highest attenuation values, here interpreted as gold and tellurides, within a 5 cm thick vein. Ore minerals in the lower image are mainly pyrite and chalcopyrite within mm-thick laminae parallel to the main foliation. White polygonal mesh shown in the deposit model refers to the mined-out volume. Blue colour on the VLF-profiles corresponds to low resistivity.

The deposit is a Paleoproterozoic (c. 1.9-1.7 Ga), high sulphidation, epithermal gold deposit and consists of a chalcopyrite, gold, topaz, and tellurides bearing sillimanite quartzite (Hallberg et al. 1994). The surrounding rocks are mainly garnet and mica bearing paragneisses occurring within a supracrustal inlier that can be traced along strike for three kilometres southeast of the Enåsen deposit.

3. Methods & Results

Structural data and rock samples from outcrops were collected in an area within 4 km from Enåsen deposit, including a few additional showings of copper sulphide mineralization at Flomyra, Enåsgruvan, Ramsjögruvan and Långtjärnen. More detailed geological mapping and sampling focussed on outcrops around and within the Enåsen open pit.

In addition to the airborne campaigns, ground magnetic and electromagnetic (VLF) measurements were carried out along a series of profiles intersecting the Enåsen deposit (Figure 1). VLF data was collected with a WADI instrument from ABEM.

Drill core logging and sampling was conducted on 8 holes from around the deposit. Core logging focussed mainly on the verification of the historic lithology logs from Boliden Mineral AB as well as on sampling full and half core bits for petrophysical measurements, whole rock lithogeochemistry, and XCT-XRF drill core scanning.

Combined XCT-XRF drill core scanning was performed at Orexplore Technologies in Kista (Sweden), using their GeoCoreX10 instrument. The instrument utilizes a technique that combines XRF spectra, attenuation and density values derived from tomography imaging and sample weight to calculate for mineral compositions and elemental abundances (Bergqvist et al. 2019; Luth et al. 2022). A precalculated dataset of minerals common for Enåsen was used to correlate measured X-ray attenuations to known mineral attenuation values using cross-section data from PENELOPE-2006 (Salvat et al. 2006).

The obtained scanning data was imported into the Insight software (Orexplore Technologies, 2023), which visualizes the scanned drill core as 3D rotatable imagery (Figure 1). 3D geological modelling was conducted using the implicit modelling software Leapfrog Geo v. 2023.2. A deposit-scale model measuring 2km x 1.5km x 600m was constructed utilizing all drill data, structural measurements and mine-maps. The bottom of the open pit (now waterfilled), the underground infrastructure and the mined-out rooms were digitized directly from the mine maps. Numerical geochemical models were created for gold, copper and silver through interpolation of assay data of which most was provided by Boliden Mineral AB (Figure 1). A semi-regional model measuring 7km x 4km x 2km was built from mapped lithological contacts, structural measurements, VLF-profiles, airborne magnetic- and electromagnetic anomaly maps.

4. Conclusions

Combined XCT-XRF drill core scanning reveals various deformation fabrics and mineralization types within the sillimanite quartzite. We interpret that gold and tellurium occur mainly in discordant, up to 5 cm thick veins, and to a lesser extend within thinner laminae parallel to the main foliation (Figure 1).

3D deposit-scale modelling reveals that the sillimanite quartzite forms a disc-shaped body that extends along strike for approximately 1600 meters and 400 meters deep. The body is open in all directions. The gold and copper content vary significantly within the sillimanite quartzite, and a large amount of these metals, including tellurium and silver, remains today below the mined-out volume at a depth between 200 and 400 meters (Figure 1).

The low resistivity zones observed on the VLF-profiles overlap with the area of mineralization. In addition, slight variations in resistivity along strike (profile 1 vs. profile 2) may be explained by the variation in metal content of the sillimanite quartzite (Figure 1).
The semi-regional geological model shows that several sulphide showings around Enåsen all occur in the same stratigraphic sequence, which is strongly folded and faulted with an overall tectonic vergence towards the northeast.

References:

Bergqvist, M., Landström, E., Hansson, A., and Luth, S., 2019, Access to geological structures, density, minerals and textures through novel combination of 3D tomography, XRF and sample weight: Australian Exploration Geoscience Conference (AEGC), Perth, 2019, Extended Abstracts, v. 1, 1–3.

Hallberg, A., 1994: The Enåsen gold deposit, central Sweden. 1. A Palaeoproterozoic high-sulphidation epithermal gold mineralization. Mineralium Deposita 29, 150–162.

Luth, S., Sahlström, F., Bergqvist, M., Hansson, A., Lynch, E-P., Sädbom, S., Jonsson, E., Andersson, S. and Arvanitidis N., 2022: Combined X-Ray Computed Tomography and X-Ray Fluorescence Drill Core Scanning for 3-D Rock and Ore Characterization: Implications for the Lovisa Stratiform Zn-Pb Deposit and Its Structural Setting, Bergslagen, Sweden. Economic Geology 117, 1255–1273.

Nassar, N.T., Brainard, J., Gulley, A., Manley, R., Matos, G., Lederer, G., Bird, L.R., Pineault, D., Alonso, E., Gambodi, J., and Fortier, S.M., 2020, Evaluating the mineral commodity supply risk of the US manufacturing sector: Science Advances, v. 6, no. 8, doi: 10.1126/sciadv.aay8647.

Orexplore Technologies, 2023, https://orexplore.com

Salvat, F., Fernandez-Varea, J.M., and Sempau, J., 2006, PENELOPE-2006: A code system for Monte Carlo simulation of electron and photon transport: The OECD Nuclear Energy Agency, PENELOPE-2006 Workshop, Barcelona, July 4–7, 2006, Proceedings, v. 4, no. 6222.

Lithotectonic map of Fennoscandia: An ongoing project

S. Luth[1], J. Köykkä[2] and Espen Torgersen[3]

[1]Geological Survey of Sweden (SGU) Villavägen 18, Uppsala, Sweden
[2]Geological Survey of Finland (GTK), Rovaniemi, Finland
[3]Geological Survey of Norway (NGU), Trondheim, Norway
E-mail: stefan.luth@sgu.se

We present an updated version of the lithotectonic map for the onshore solid rock masses of Norway, Sweden and Finland (Figure 1). The map provides a large-scale tectonic framework that includes 2 billion years of geological evolution of Fennoscandia. It subdivides the three main orogens Svecokarelian (1.9 – 1.7 Ga), Sveconorwegian (1.1 − 0.9 Ga) and Caledonide (500 – 400 Ma), into large-scale lithotectonic units which are preliminary defined by their tectonic boundaries.

The map is largely the result of a first-order harmonization between the publicly available NGU, SGU and GTK national bedrock databases as they were in the year 2023 (Luth et al. 2024). The map also builds heavily on - and complements - earlier tectonic synthesis of Fennoscandia, such as published by Stephens et al. (2020), Kohonen et al. (2021), Torgersen et al. (2021) and Lahtinen et al. (2023).

The lithotectonic map is treated as a dynamic framework that may change over time as new data and knowledge becomes available. A new consensus may be reached on terminology and the connection between border-crossing units and tectonic boundaries. Until then, the map here presented will serve the need to place other national geological- and geophysical datasets, such as the occurrences of energy- and mineral resources of the Nordic countries, into a wider tectonic context.

References

Kohonen, J., Lahtinen, R., Luukas, J., Nironen, M. 2021: Classification of regional-scale tectonic map units in Finland. In: Kohonen, J., Tarvainen, T. (eds) Developments in map data management and geological unit nomenclature in Finland. Geological Survey of Finland, Bulletin 412, 33–80.

Lahtinen, R., Köykkä, J., Salminen. J., Sayab, M., Johnston, S.T. 2023: Paleoproterozoic tectonics of Fennoscandia and the birth of Baltica. Earth-Science Reviews, 104586.

Luth, S., Torgersen, E., Köykkä, J. 2024: Lithotectonic map of Fennoscandia. *In*: Regnéll, C., Zack, T., Holme, K. & Andersson, J. (Eds.) 2024: 36th nordic geological winter meeting, Göteborg, January 10–12 2024, Abstract volume. *Geologiska Föreningen Specialpublikation* 5, 558 pp.

Stephens, M.B., Bergman Weihed, J. (eds) 2020: Sweden: Lithotectonic Framework, Tectonic Evoluation and Mineral Resources. *Geological Society, London, Memoirs,* 50.

Torgersen, E., Svendby, A K., Bingen, B., Nilsson, C., Gasser, D., Petttersen, Eirik., Gunleiksrud, I H., Rasmussen, M C., Arntsen, M L. 2021:. Bedrock map of Norway 1:1 350 000 m. *Geological Survey of Norway.*

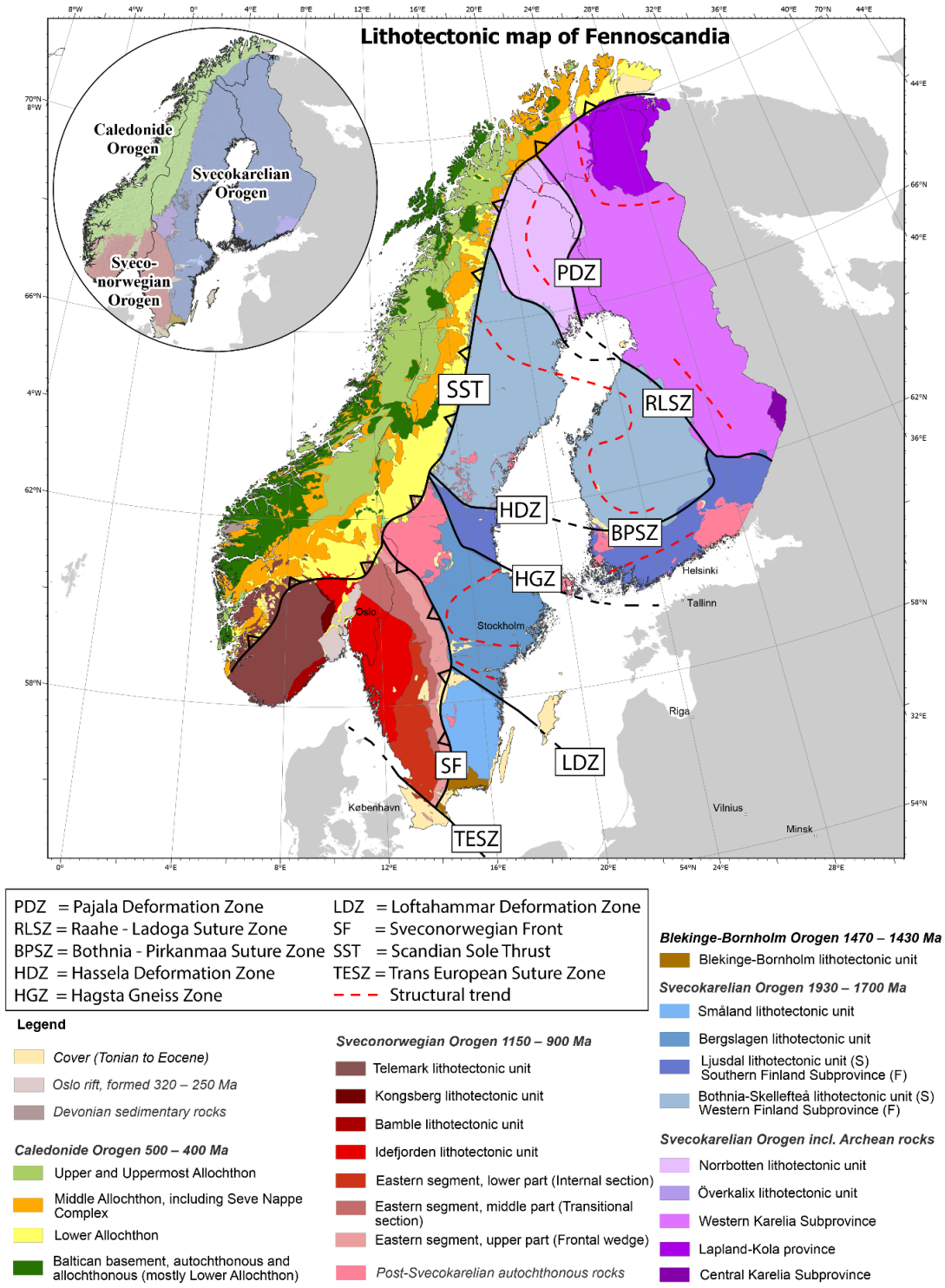

Figure 1. Lithotectonic map of Fennoscandia showing the orogens (inset map) and their internal lithotectonic units (main map). Theses units are primarily defined by their tectonic boundaries (labels). Notice that these boundaries are not labelled within the Sveconorwegian and Caledonide orogens. (S), (F) in legend refers to the names of the same unit in Sweden and Finland, respectively.

Imaging impossible in GPS-denied environment: in-mine seismic studies for hardrock exploration

A. Malehmir[1]

[1]Dept. of Earth Sciences, Uppsala University, Uppsala, Sweden
E-mail: alireza.malehmir@geo.uu.se

In this work, a development work using a GPS-time prototype is presented. The system allows time-synchronized surveys in GPS denied underground mining environment. With a maximum drift on the order of only a portion of microsecond per day, the system transmits simulated false or real GPS-time signal without cabling from the surface. This provides opportunities for geophysical surveys in deep exploration and mining tunnels where access to such a signal is cost ineffective via surface cabling or even sometimes impractical. A background to how such a system was realized first is presented and then two surveys showcasing how-to and what-for. The first case is from the Neves-Corvo mine (Portugal) at 650 m depth and the second one from the South Deep gold mine (South Africa) at approximately 3000 m. The synchronized recorders so far include nodal, central acquisition, and fiber-optic interrogators, source zero time, a few to mention. The system is currently planned to be ruggedized for more extensive passive and active surveys within the scope of Hub1-Green Sensing Tech of the Smart Exploration Research Center.

Keywords: GPS, time, exploration, imaging, deep targeting

1. Introduction

Mineral exploration industry regards the future to be underground mining and at great depths of >800 m specially for precious and base metals. To extend life-of-mine and avoid environmental footprints (as well as licensing and permitting issues) and for financial reasons, exploration expenditure is primarily focused on brownfield and near-mine exploration. Technical challenges (e.g., logistics and operational noise) around an operating mine limit what exploration techniques can be utilized, hence, in-mine exploration becomes in most cases limited to mainly drilling and based on drill core observations. Exploration tunnels are usually excavated in the hanging-wall of the mineralization to be utilized for down-dip drilling work. To improve exploration at depth and in operating mines, improved geophysical solutions are needed. Innovative solutions are more than ever needed for improved targeting but also for public perceptions (Malehmir et al., 2024). Moreover, exploration should also help exploitation to be effectively done to avoid ore block loss and possible geological surprises during the mining operation. Mining and exploration infrastructure such as exploration tunnels and boreholes can greatly be used to tackle these issues.

Inspired by an earlier study where we were tasked to image vertical fracture systems between surface and an access tunnel for infrastructure-planning projects, we prototyped a GPS-time transmitter system for denied GPS-time environments to allow exploration and mining infrastructures to be used for deep targeting and rock mass characterization. The prototype was invented (Malehmir et al., 2020), and after several trials, it was utilized in 2018 for an upscaling work at the Neves-Corvo mine in Portugal and more recently (in 2023) in the South Deep gold mine in South Africa. Here, the system and the two case studies are presented.

2. GPS-time transmitter system

The GPS-time system (Figure 1) is a hardware solution (physical prototype) that comes with expert-knowledge experiments/surveys (how-to solutions). The system transmits false or real simulated GPS-time signals in denied spaces (e.g., tunnels) for several recorders (10-1000s) readily available in the market sensors (e.g., within 1-3 days) in an easy and practical manner

(1-2 persons and no requirement for extensive cabling from surface to the underground spaces). The solution is based on off-the-shelf components that are readily available in the market but not assembled for such a purpose. There are components in the development that are unique such as the ability to provide time signal for a distributed array of sensors (not only for a single point), practical in the sense that it does not need extensive cabling.

Combined with fibre-optic technologies, attenuations of the GPS-time signal are considerably reduced for longer sensor arrays or going from one level of depth to another. If needed, multiple systems can be used in different depth levels independently without a cabling requirement at depth. A great benefit of the system is that one does not need to modify existing recording sensors, which is a substantial cost saving.

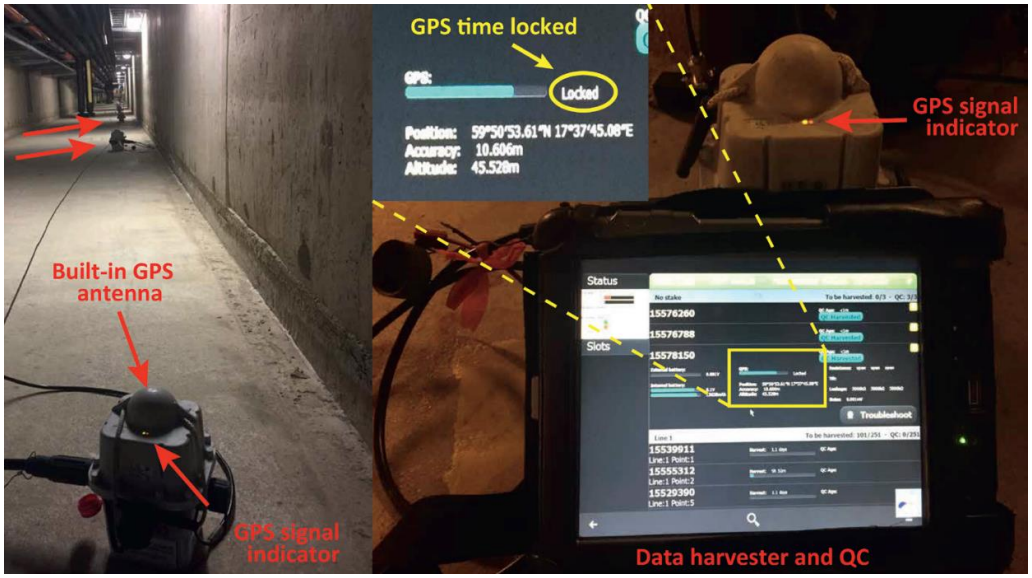

Figure 1. First test was done in a utility tunnel at Uppsala University simulating a tunnel seismic survey using commonly used wireless seismic recorders/ sensors (20 were used) for examining the performance of the GPS-time system. Flashing green-red light indicator on the recorder means locking to GPS-time signal. An accuracy of 10 microseconds was observed already at this stage and encouraged for a full-scale work in a real mining condition.

2. How-to and what-for showcases

Seismic data were acquired using both cabled and nodal seismic recorders, two perpendicular profiles on the surface comprising 650 recorders (Profiles 6 and 7), and 453 seismic recorders deployed along four exploration tunnels (or drifts) approximately 650 m below the ground surface where the two surface profiles positioned (Figure 2). Neves-Corvo is an active mine, operating seven days a week, and in three shifts. All our activities had to be well synchronized, controlled, and approved by the head mining office. These four exploration tunnels were also used for down-dip drilling; hence, they were not calm at the time of the data acquisition. During two deployment days, seismic receivers were distributed along four profiles in the exploration tunnels, namely, GP2, GP3, GP4, and GV5 and the surface array. As the seismic source, a recently developed e-Vib was used in the mine and a 250-kg drophammer on the surface. In the exploration tunnels, the GPS-time transmitter was used for data synchronization of 423 cabled recorders (only the central units) and 30 wireless recorders on average spaced at 5 m intervals. The time-synchronization between different element of the arrays implies the media between the surface and the tunnels can be scanned like an MRI scanning device. The Neves-Corvo

dataset is unique and a world-class of its kind and can be treated differently: (1) for surface-tunnel traveltime tomography to build velocity model for depth imaging workflows, (2) treating each dataset differently for imaging the deposits and their host rocks or (3) combining all the datasets. Some aspects of the survey are published in Donoso et al. (2021) and Brodic et al. (2021). The data from the exploration tunnels, while may be subject to complex 3D effects, because the recorders and sources are closer to the Lombador deposits should better image the deposits, even better and more successful than a VSP survey.

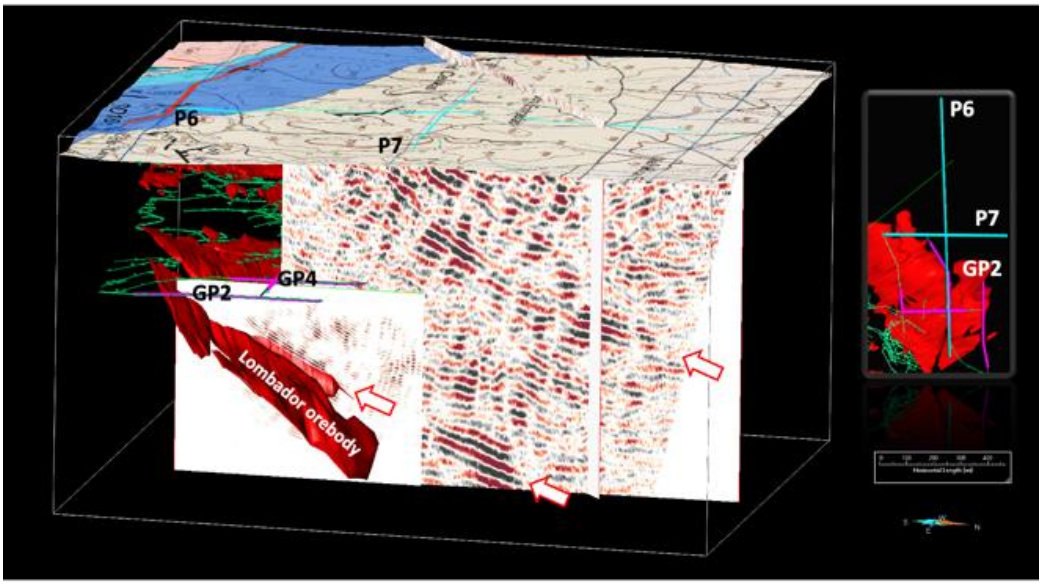

Figure 2. Data are shown as migrated stacked sections for surface profile P6 and the tunnel data separately. The higher resolution reflection of the Lombador deposit in the tunnel data clearly illustrates the added-value the GPS-time transmitter system provided in this work. In addition, the image can guide assay drilling better under the exploration tunnels.

Realized from the Neves-Corvo survey, the GPS-time transmitter was partly ruggedized for a new experiment; this time utilizing fiber-optic or distributed acoustic sensing (DAS) technologies as receivers. Inspired by the quality data from the Neves-Corvo survey, both cabled-connected geophones (drilled into the tunnel floor) and a straight-fiber optic cable in a mining tunnel at 3000 m depth in the South Deep (Figure 3) and nodal recorders were laid out on the surface to record synchronized data among all these receivers utilizing the transmitter for both data sampling and zero-source time tagging. Given the enormous challenges encountered around the logistics in an operating world-class gold mine, we finally managed to acquire over 200 shots in the mining tunnel and used the GPS-time transmitter for passive data recording of mining noise. This work breaks a record of any active and time-synchronized seismic survey in the world, thanks to the GPS-time transmitter realized earlier opening new possibilities for more innovative survey designs and in-mine seismic studies.

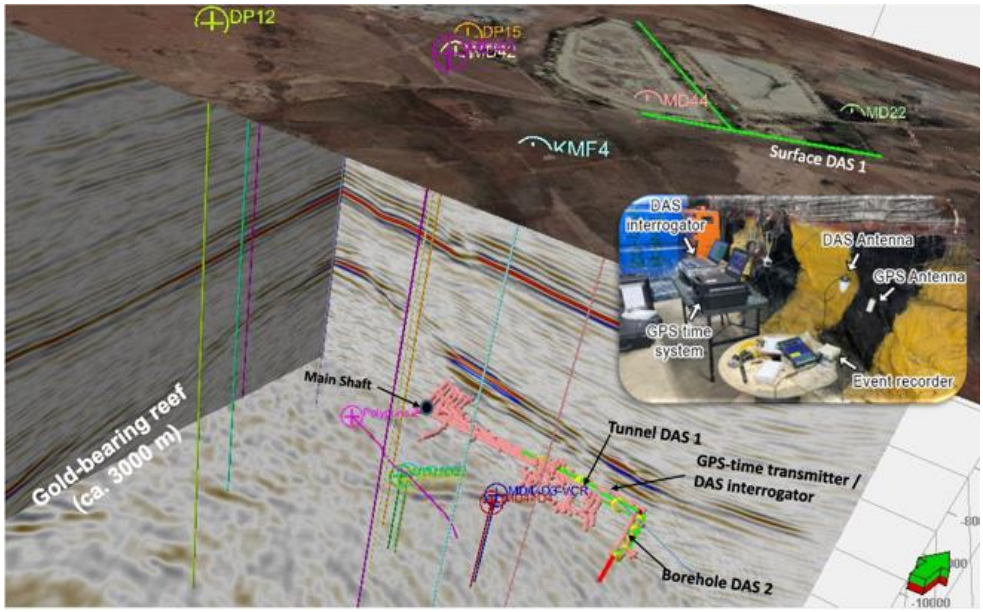

Figure 3. The South Deep in-mine/surface synchronized DAS and nodal array acquisition was conducted in June 2023 utilizing the GPS-time transmitter to the DAS interrogator and for time tagging seismic shots.

3. Conclusions

A GPS-time transmitter along with innovative ways of acquiring time-synchronized in-mine seismic data have been developed. Two case studies are shown (1) from the Neves-Corvo mine (Portugal) for imaging the tier-1 Lombador deposit below four exploration tunnels at approximately 650 m depth and (2) South Deep gold mine at 3000 m depth. Various recorders were successfully time-synchronized including nodal, and central acquisition systems, time-tagging units, and DAS interrogators. Furthermore, the GPS-time transmitter allows to also innovate new imaging solutions and workflows for improved targeting and rock mass characterization.

Acknowledgments

This work is partly supported by Smart Exploration Research Centre (www.smartexploration.se). The Smart Exploration Research Centre has received funding from the Swedish Foundation for Strategic Research (SSF) under grant agreement no. CMM22-0003. This is publication SE24-006. Many institutions and individuals were behind these experiments for which they are thanked.

References:

Brodic, B., Malehmir, A., Pecheco, N., Juhlin, C., Carvalho, J., Dynesius, L., van den Berg, J., de Kunder, R., Donoso, G., Sjölund, T., Araujo, V., 2021. Innovative seismic imaging of VMS deposits, Neves-Corvo, Portugal — Part I: In-mine array. Geophysics, 86, B165–B179.

Donoso, G., Malehmir, A., Brodic, B., Pecheco, N., Carvalho, J., Araujo, V., 2021. Innovative seismic imaging of VMS deposits, Neves-Corvo, Portugal — Part II: Surface array. Geophysics, 86, B181–B191.

Malehmir, A., Dynesius, L., Sjölund, T., 2020. Mining and mineral exploration system and methods for performing time-accurate measurements in a mine. Patent (Swedish Intellectual Property Office, granted on 17-11-2020), SE 543 288 C2.

Malehmir, A., Markovic, M., Papadopoulou, M., Högdahl, K., Ask, M., Strømme, M., Pitcairn, I., Martin, T., Zack, T., Majka, J., Svensson, M., Hamerslag, R., 2024. Smart Exploration Research Centre: Knowledge and Innovation for Exploration of Critical Raw Materials. First Break, 42, 89–93.

A new regional reflection seismic profile across the Peräpohja belt, northern Finland

M. Malinowski[1], T. Niiranen[2], T. Luhta[1] and L. Sito[3]

[1]Geological Survey of Finland, Espoo
[2]Geological Survey of Finland, Rovaniemi
[3]Geopartner Geofizyka Ltd., Krakow
E-mail: michal.malinowski@gtk.fi

A new 70-km long reflection seismic profile was acquired across the Palaeoproterozoic Peräpohja belt in northern Finland to shed new light on its structural framework. Single-receiver and single-source acquisition was implemented, resulting in excellent data quality. Survey layout was optimized for the ability to extract 3D reflector orientations as constraints for the 3D geological model. Initial seismic processing results reveals rich and coherent reflectivity in the top 15 km of the crust.

Keywords: reflection seismics, mineral exploration, structural geology

1. Introduction

Reflection seismics is indispensable for understanding the structural framework of the crust and providing important input for mineral system studies, as evidenced by studies from Canada (e.g., Haugaard et al. 2021) and Australia (e.g., Korsch and Doublier, 2016). Inherent non-uniqueness in interpreting data from the 2D crooked seismic profiles acquired over complex geological structures can be reduced by performing 3D reflector orientation analysis (Calvert, 2017; Calvert and Doublier, 2018). However, it requires good azimuthal coverage of the subsurface points, which can be achieved by recording additional cross-spreads. Having this in mind, a new reflection seismic profile was designed and acquired across the Paleoproterozoic Peräpohja belt (PB) in northern Finland as a part of the REPower-CEST "Clean Energy System Transition" project's work package devoted to critical raw materials. This work package aims at formulating a national exploration concept and testing it at PB, which was chosen as a study area for its known mineral systems and potential. In addition to seismic reflection data, a dense regional gravity network is being measured. Ultimately, all available geophysical and geological data will be integrated into a 3D geological model of the PB.

2. Geological background

The PB consists of supracrustal sequence of mica schists, greywackes, black shales, quartzites, carbonate rocks and dominantly mafic volcanic rocks deposited between c. 2.44 Ga and 1.92 Ga during multiple rifting and extensional stages of the Archean basement (Köykkä et al. 2019; Piippo et al. 2019). The 2.44 Ga layered intrusions, 2.22 Ga, 2.14 Ga, 2.13 Ga and 2.08 Ga mafic dykes within and at the Southern margin of the PB represent the intrusive activity during repeated extensional phases (Köykkä et al., 2019 and references therein). The supracrustal sequence of the PB was multiply deformed during the Svecofennian Orogenic stages between 1.92 and 1.77 Ga when the rocks were metamorphosed in greenschist to amphibolite-facies conditions (Lahtinen et al. 2015; Hölttä & Heilimo 2017; Piippo et al. 2019). Complex deformation resulted formation of complex fold interference pattern and intrinsic network of thrust and shear zones (Fig. 1). In the middle part of the stratigraphical sequence of the PB occurs a basin wide Petäjäskoski fm (Pfm) mainly composed of quartzites, siltstone/mudstone rocks, albite schists, and carbonate rocks (Kyläkoski et al. 2012; Köykkä et al. 2019). Kyläkoski et al. (2012) described thick sequences of collapse breccias within the Pfm and interpreted them

being a result of dissolution of evaporate-bearing sequences during the metamorphism of the rocks and further suggested that the belt scale sodic alteration described in PB rocks was the result of brines linked to the dissolution of the evaporite-bearing units.

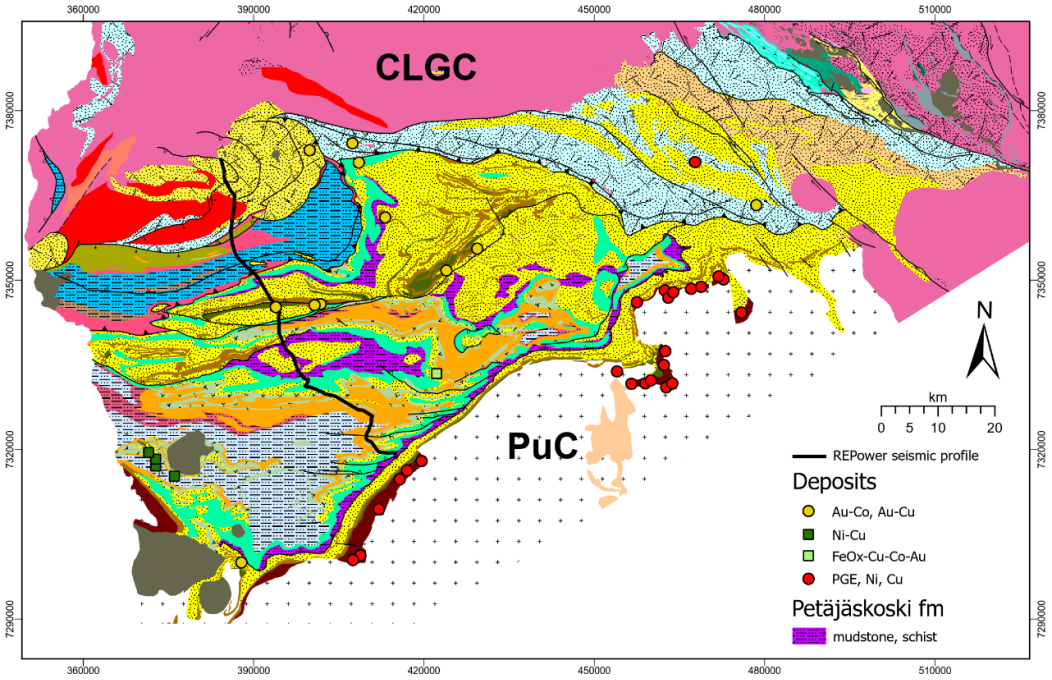

Figure 1. Bedrock map of the Peräpohja belt with location of main CRM-bearing mineral deposits and location of the new seismic profile. CLGC = Central Lapland Granitoid Complex, PuC = Pudasjärvi Complex (Bedrock of Finland 2024; Mineral deposits of Finland 2024).

High salinity brines are capable of leaching and transporting especially iron and base metals, but also gold, and the role of evaporites in formation of epigenetic, polymetallic deposits occur in PB and similar-aged Central Lapland and Kuusamo Belts. In PB, a number of epigenetic Au-Co, Au-Cu, and FeOx-Cu-Co-Au deposits have been discovered (Fig. 1). Common features for these are, besides clear structural control, a broad spatial correlation to Pfm and albitized rocks. Thus, it is likely that the two critical mineral systems components of the hydrothermal epigenetic polymetallic deposits in PB are the structural framework acting as pathway for the mineralizing fluids and locally as trap for the mineralization, and Pfm which potentially acted as the source for the metal carrying ligand (Cl^-). The PB hosts also a small number of magmatic Ni-Cu deposits (Fig. 1). Evaporate units typically host besides K- and Na-bearing chlorides also sulfur in the form of e.g. gypsum or anhydrite. Therefore, the Pfm may have played a role as a potential sulfur source for magmatic Ni-Cu mineral systems in the PB.

3. Seismic data acquisition and initial data analysis

Seismic data acquisition took place during three weeks in September 2024. 70-km long profile runs along the Mellakoski – Tervola – Sompujärvi transect (Fig. 1), mostly along the paved and gravel roads (except for Tervola bypass where forest roads were used). Receivers were spaced at 5 m interval along the main line (with nominal symmetric spread of 2600 channels and 6500 m offset). In order to improve azimuthal coverage required by the 3D reflector orientation analysis (Calvert, 2017), eight additional cross-spreads were layout along the profile with 25 m

station spacing. The full layout consisted of 17065 receiver stations. A single nimble node with piezoelectric sensor was deployed at each receiver position (Fig. 2a).

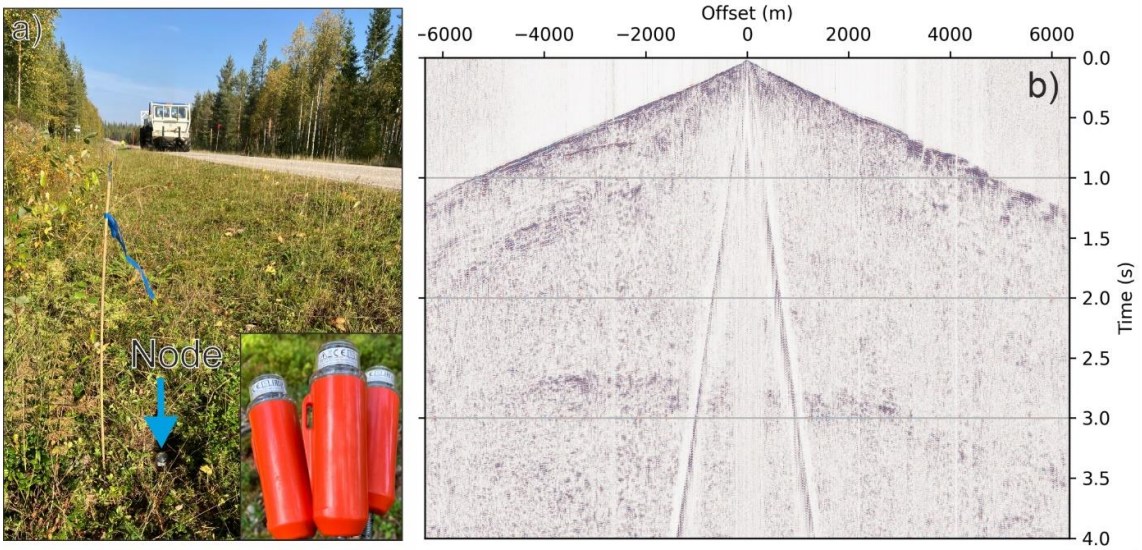

Figure 2. Picture of the nodal sensor and the Vibroseis truck (a). Shot gather example (b).

A single HEMI-60 Vibroseis truck (61,000lb peak force) was used as a source with 40 s long linear sweep of 10-150 Hz (repeated 2 times at each Vibropoint, VP). A total of 2809 VPs were acquired with nominal spacing of 25 m. Acquired dataset offers great flexibility in processing - dense station spacing facilitate static correction and noise removal, enabling also digital group forming if needed for increased signal-to-noise ratio. Additional cross-spreads greatly improved the azimuthal coverage of mid-points along the profile. The data quality is very good with first-arrivals visible in some of the shot gathers beyond the nominal spread up to 18-20 km. Reflections are also clearly distinguishable in the raw shot gathers (Fig. 2b). Initial processing revealed rich and coherent reflectivity throughout most of the profile down to ca. 15 km depth (Fig. 3). Further improvements are expected through the application of refraction statics, velocity analysis and optimized stacking coupled with the 3D reflector orientation analysis.

Figure 3. Depth-converted unmigrated brute stack along the REPower seismic profile. NMO correction and time-depth conversion with V=6000 m/s. View from SW.

4. Discussion and conclusions

Advances is seismic data acquisition techniques since the FIRE (Kukkonen and Lahtinen, 2006) and HIRE projects (Kukkonen et al. 2009) enable recording from thousands of wireless receivers deployed with much tighter spacing for improved resolution and longer offsets. It is also possible to obtain sufficient energy from a single Vibroseis truck rather than an array of trucks (5 to 3 used in FIRE and HIRE, respectively). REPower profile is a good example how the new technologies make the regional seismic acquisition more cost-effective, as well as how they reduce its environmental impact.

5. Acknowledgements

Financial support for the green transition by the European Union (number 151, P5C1I2, NextGenerationEU) via REPower-CEST “Clean Energy System Transition” project. Thanks to Geopartner Geofizyka Ltd. and GTK’s team for efficient seismic data acquisition.

References:

Bedrock of Finland—DigiKP, 2024. Digital map database [Electronic resource]. Geological Survey of Finland [referred 3.10.2024]

Calvert, A.J., 2017. Continuous estimation of 3-D reflector orientations along 2-D deep seismic reflection profiles. Tectonophysics, 718, 61-71.

Calvert, A.J. and Doublier, M.P., 2018. Archaean continental spreading inferred from seismic images of the Yilgarn Craton, Nat. Geosci., 11, 526–530.

Haugaard, R., Justina, F.D., Roots, E., Cheraghi, S., Vayavur, R., Hill, G., Snyder, D., Ayer, J., Naghizadeh, M., Smith, R., 2021. Crustal-Scale Geology and Fault Geometry Along the Gold-Endowed Matheson Transect of the Abitibi Greenstone Belt. Economic Geology 116, 1053–1072.

Hölttä, P., Heilimo, E., 2017. Metamorphic map of Finland. In: Nironen, M. (Ed.), Bedrock of Finland at the scale 1:1 000 000 – Major stratigraphic units. Metamorphism and tectonic evolution. Geol. Surv. Finl., Spec. Pap. 60, 77–128.

Korsch, R.J., Doublier, M.P., 2016. Major crustal boundaries of Australia, and their significance in mineral systems targeting. Ore Geology Reviews 76, 211–228.

Kyläkoski, M., Hanski, E., Huhma, H., 2012. The Petäjäskoski Formation, a new lithostratigraphic unit in the Paleoproterozoic Peräpohja Belt, northern Finland. Bull. Geol. Soc. Finl. 84, 85–120.

Köykkä J., Lahtinen R., Huhma H. 2019. Provenance evolution of the Paleoproterozoic metasedimentary cover sequences in northern Fennoscandia: Age distribution, geochemistry, and zircon morphology. Precambr. Res 331:105364.

Kukkonen, I.T. and Lahtinen, R. 2006 (Eds.). Finnish reflection experiment FIRE 2001-2005. Geological Survey of Finland, Special Papers, vol 43.

Kukkonen, I.T., Heikkinen, P.J. and HIRE Working Group, 2009, Project HIRE: High resolution seismic reflection surveys in ore exploration of crystalline rock areas. In: XXIV GEOFYSIIKAN PÄIVÄT.

Lahtinen, R., Sayab, M., Karell, F., 2015. Near–orthogonal deformation successions in the poly–deformed Paleoproterozoic Martimo belt: implications for the tectonic evolution of Northern Fennoscandia. Precambr. Res. 270, 22–38.

Mineral deposits of Finland, 2024. Digital map database [electronic resource]. Geological Survey of Finland. Espoo [referred 3.10.2024].

Piippo, S., Skyttä, P., Kloppenburg, A., 2019. Linkage of crustal deformation between the Archaean basement and the Proterozoic cover in the Peräpohja Area, northern Fennoscandia. Precambr. Res. 324, 303–323.

Microbiological aspects of sampling the St1 superdeep boreholes in Espoo, southern Finland

H. Miettinen[1], M. Nyyssönen[1], M. Nuppunen-Puputti[2] , R. Kietäväinen[3], I. Kukkonen[3], V. Nenonen[3], A. Karjalainen[4], J. Rytkönen[5] and M. Bomberg[1]

[1]VTT, Tekniikantie 21, ESPOO, P.O.Box 1000, FI-02044
[2]VTT, Kemistintie 3, ESPOO, P.O.Box 1000, FI-02044
[3]Dept. of Geosciences and Geography, University of Helsinki, P.O.Box 68, FIN-00014, Finland
[4]St1 Lähienergia Oy, Espoo, Finland
E-mail: Malin.Bomberg@vtt.fi

Espoo superdeep boreholes OTN2 and OTN3 were sampled in multidisciplinary collaboration. Microbiological part focused on obtaining microbiologically reliable uncontaminated fluid samples from the depth of 5 km where microbial communities were expected to be sparse. Several aspects needed to be considered in securing viable microorganisms such as high pressure and salinity as well as keeping the samples anoxic. Contamination control was essential including both extensive disinfection of sampling devices but also negative controls. The main objectives of microbial sampling were to detect and identify microbial communities present in the superdeep subsurface with DNA-based methods and to grow and identify possible viable microbial cells.

Keywords: High temperature, high pressure, bacteria, archaea, salinity, subsurface, biosphere

1. Introduction

Sampling in superdeep environments requires know-how and sophisticated equipment functional in both high pressure and high temperature conditions. Enabling this kind of demanding sampling, participation of specialized sampling team was needed. GFZ-Potsdam provided the superdeep sampling equipment and expertise directly feasible for pressurized fluid samples. However, collaboration was needed to adapt the sampling procedures applicable for reliable microbiological sampling.

Based on the earlier studies on the St1 DeepHeat boreholes OTN1, OTN2 and OTN3 in Otaniemi, Finland (Kukkonen et al., 2023; Purkamo et al., 2020) the conditions of the sample environments were expected to be extreme for microbial life. The conditions are anoxic and the anticipated temperature at 5 km depth was near 100 °C, hydrostatic pressure over 500 bar and total dissolved solids near 200 g/l. In such conditions life in any form is rare and highly specialised to survive or to even reproduce. At the moment some hyperthermophilic bacteria and archaea are known to be able to grow at temperatures over 100 °C, some archaea upto 122 °C at high-pressure (Takai et al., 2008). The abundance of microorganisms in the deep subsurface generally decreases with depth but is mostly dependent on the energy sources available for their metabolism rather than the actual depth. Thus, it was anticipated that finding life in the depths of 5 km at temperatures near 100 °C with high-pressure and salinity would be hard but, if successful, highly rewarding. However, false positive findings can occur if special measures are not done properly to avoid contamination when sampling a microbial community that is likely sparse.

2. Microbiological sampling aspects

Samples for microbiological studies were collected from the OTN2 and OTN3 boreholes in September, 2023 in Otaniemi, Finland (Fig 1A) with two positive displacement samplers (Leutert, Germany). Extensive measures to limit sample contamination were planned. The

Figure 1. A) Sampler device coming out of the borehole, **B)** Drying of disinfected sampler parts **C)** Releasing the sample from the sampler via silicon tube and needle to collection bottle, gas flowing forward to water in a jug.

sampler device interior and all small removable parts were disinfected thoroughly with 70% ethanol before sampling (Fig 1B), even though the high temperature and pressure during the sampling that lasted over an hour at 5 km, was considered to reliably kill all living microorganisms originating from other sources than the sample fluid itself. All materials such as glass bottles, silicon tubes and syringes used in the sample collection and handling were treated to render them DNA free. Preventing contamination totally in field conditions is extremely difficult, especially when utilizing DNA-based methods, as they detect DNA originating from both live and dead microorganisms. For this reason, negative control samples were taken from the sampler devices by filling the sampler with sterile water and releasing it the same way as the real samples. These control samples will be used to identify the possible background contamination originating from the sampling environment and equipment and will be used to identify the intrinsic deep biosphere from the contamination during data analysis.

The deep groundwater of the site is presumably anoxic and the possible microbial communities consist of anaerobic microorganisms, which rely on oxygen-free environments to survive. Even a short exposure to oxygen may kill the most sensitive obligately anaerobic microorganisms. In our work we aimed to culture hyperthermophilic anaerobic microorganisms in the laboratory. Oxygen contamination of the samples was avoided by replacing air with nitrogen gas from all used materials and handling the samples in an anaerobic glove box. Similarly, the two different culture media used for culturing microorganisms from the sample fluids were anaerobic providing energy either for autotrophic (use of inorganic compounds for growth) or heterotrophic (need organic compounds for growth) microorganisms (Fig 2).

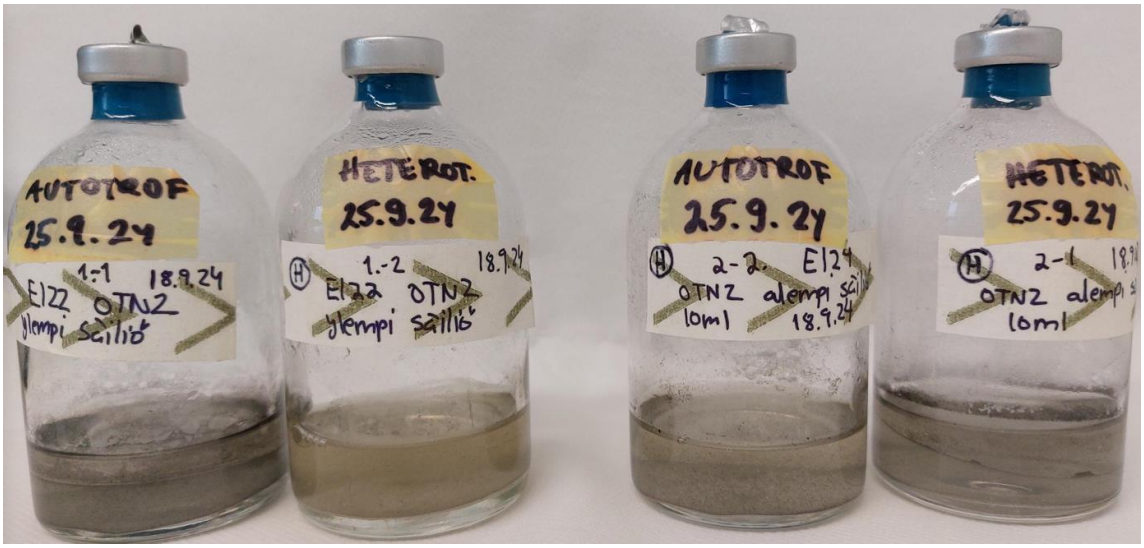

Figure 2. Culture bottles of OTN2 fluid samples growing at 80 °C in autotrophic or heterotrophic media with N_2, CH_4 and H_2 gas mixtures after two weeks.

Still, another matter that could affect the survival of microorganisms was the effect of the high pressure originally in the samples. If the pressure is abruptly reduced cells may burst and die. The pressure was released from the samples by letting the water-gas mixture slowly flow out of the sampler to a rubber stopper sealed sample collection bottle filled with nitrogen gas, via a sterile silicon tube equipped with a needle pushed through the rubber stopper of the bottle (Fig. 1C). From the collection bottle the extra gas was again led via a needle and tube into a water-filled jug so that the gas flow rate was visibly slow.

The first results from the previous sampling in June 2023 from fluid overflow of the OTN3 borehole, that based on this year's findings was likely fluid originating from the deep,

showed that the bacterial community consisted, to approximately 90%, of the phylum Bacteroidota, genus *Proteiniphilum*, and approximately 10% of the Firmicutes phylum (Fig. 3A). This is in line with the qPCR results (Fig. 3B) indicating that ca 10% of the community consists of sulfate reducing bacteria, which are prevalent within the Firmicutes class Clostridia.

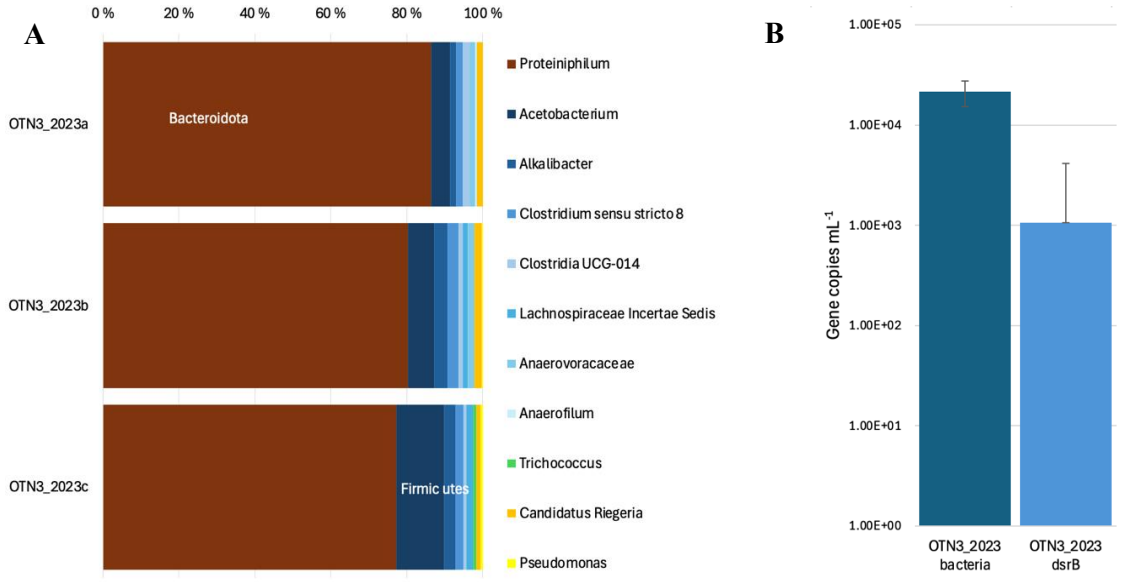

Figure 3. OTN3 overflow fluid microbiological results from the 2023 sampling. **A)** Predominant bacterial genera results with DNA sequencing, **B)** Estimated number of bacterial and sulfate reducer (dsrB) marker genes with quantitative PCR.

3. Conclusions

The objective of the microbiological sampling was to reliably 1) detect and identify microbial communities present in the deep subsurface with DNA-based methods and 2) to grow and identify possible viable microbial cells present in the samples. Following months will show if the goals will be realized.

References:

Takai, K., Nakamura, K., Toki, T., Tsunogai, U., Miyazaki, M., Miyazaki, J., Hirayama, H., Nakagawa, S., Nunoura, T., Horikoshi, K. 2008. Cell proliferation at 122°C and isotopically heavy CH_4 production by a hyperthermophilic methanogen under high-pressure cultivation. PNAS, 105, 10949-10954. https://doi.org/10.1073/pnas.0712334105

Kukkonen, I.T., Heikkinen, P.J., Malin, P.E., Renner, J., Dresen, G., Karjalainen, A., Rytkönen, J., Solantie, J. 2023. Hydraulic conductivity of the crystalline crust: Insights from hydraulic stimulation and induced seismicity of an enhanced geothermal system pilot reservoir at 6 km depth, Espoo, southern Finland. Geothermics 112 (2023) 102743. https://doi.org/10.1016/j.geothermics.2023.102743

Purkamo, L., Kietäväinen, R., Nuppunen-Puputti, M., Bomberg, M.,Cousins, C. 2020. Ultradeep microbial communities at 4.4 km within crystalline bedrock: Implications for habitability in a planetary context. Life, 10(1), Article 2. https://doi.org/10.3390/life10010002

Metamorphic insights into the Archean Basement of the Carajás Province and its Affinity with the Karelia and Kola Provinces

A.C. Nascimento[1, 2], D.C. Oliveira[1] and E. Heilimo[2]

[1] Institute of Geosciences (IG), University Federal do Pará (UFPA), Box 1611, 66075-100, Belém, Pará, Brazil
[2] Department of Geography and Geology, University of Turku, Finland
E-mail: aline.nascimento@ig.ufpa.br

This study examines the gneisses and migmatites of the Carajás Province, comparing them with the Archean basement of the Karelia and Kola Provinces. In the Carajás Province, migmatites include stromatic and dilatant to net-structured metatexites, schollen and schlieren diatexites, and rare patch metatexites. These migmatites consist of a orthogneiss and amphibolite paleosome, a quartz-feldspathic leucosome, and a biotite-rich melanosome. U-Pb SHRIMP and LA-ICP-MS zircon dating reveals protolith crystallization at 2.95–2.93 Ga, with peak metamorphism and partial melting at 2.89–2.84 Ga, closely aligning with the peak of regional metamorphism recorded by the granulites of Carajás. In the Karelia and Kola Provinces, migmatites are similarly dominated by metatexites, with tonalite-trondhjemite-granodiorite (TTG) gneisses being commonly migmatized; however, the presence of diatexites is significant in comparison with Carajás. Morphologically, both provinces exhibit well-developed stromatic structures, though Karelia and Kola Provinces migmatites often display more pronounced folding and banding. Geochemically, Karelia and Kola Provinces migmatized-TTGs tend to be more felsic and lower in mafic content compared to Carajás. Geochronologically, the Karelia and Kola Provinces record slightly younger TTG formation ages, around 2.80 Ga, with metamorphism peaking at 2.70–2.69 Ga, demonstrating comparable but slightly offset tectonothermal histories between the two regions. Thus, while both provinces share significant geological traits, key distinctions exist in their migmatite morphology, geochemistry, and age distribution.

Keywords: partial melting, geochronology, Carajás Province, Karelia Province, Kola Province.

1. Background

The Archean basement of both the Carajás and the Fennoscandian shields Archean Provinces (eg. Karelia and Kola Provinces) are characterised by a complex assembly of rock types, including gneisses, TTG (Tonalite-Trondhjemite-Granodiorite) suite granitoids, and greenstone belts, shaped by multiple tectono-metamorphic events (Chekulaev et al., 2022; Nascimento et al., 2023; Halla et al., 2024). In the Carajás Province, migmatized TTGs dominate, featuring stromatic and net-structured metatexites, schollen diatexites, occasional patch metatexites, and absence of diatexites. The presence of these migmatitic rocks suggests a dynamic crustal evolution driven by partial melting and differentiation processes (Nascimento et al., 2023). In comparison, the Karelia and Kola Provinces showcases migmatites of stromatic, schollen, and diatexite morphologies. These migmatites, dated between 2.95 and 2.70 Ga, similarly reflect high-grade metamorphic conditions, with geochemical signatures pointing to juvenile magmatic contributions alongside significant crustal recycling (Käpyaho et al., 2007; Mikkola et al., 2011; Chekulaev et al., 2022; Halla et al., 2024).

This study compares the occurrence, morphology, and ages of migmatites from both provinces, contributing to a broader understanding of Archean tectonic regimes and crustal processes. Studying migmatized TTGs in these provinces is crucial for unraveling the complexities of continental growth and metamorphic evolution during the Archean era.

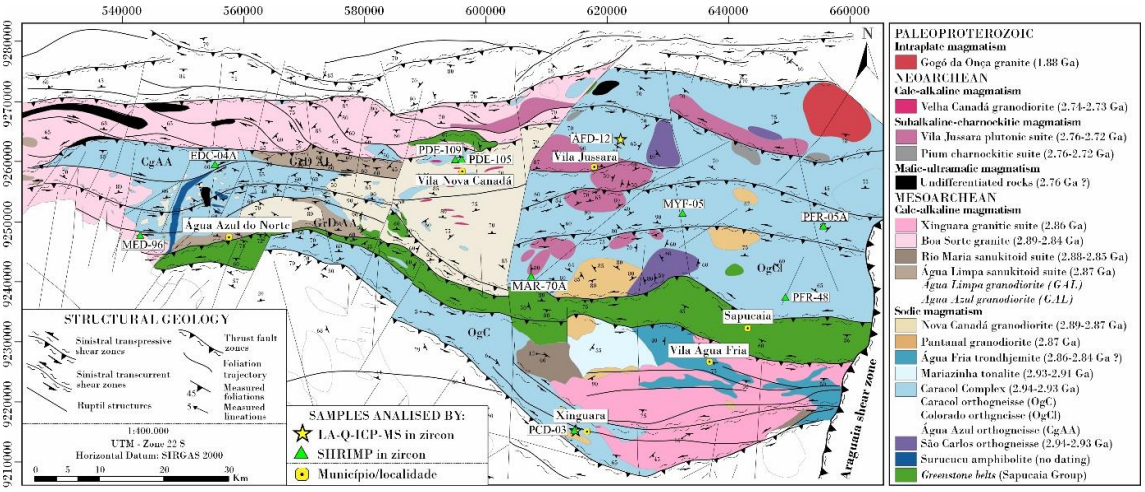

Figure 1. Geological map of the Carajás Province with the location of the analysed samples.

2. Methods and materials

The samples were crushed, pulverised, and homogenised at the Sample Preparation Laboratory (OPA) of the Institute of Geosciences at UFPA (Brazil). U-Pb zircon dating of 8 samples of orthogneisses from Carajás Province were performed using sensitive high-resolution ion microprobe (SIMS) at the GeoLab/IGc/USP Laboratory (University of São Paulo, Brazil), secondary ion mass spectrometer coupled with a high-resolution and sensitivity ion microprobe (SHRIMP IIe/MC) and a high-resolution Laser Ablation Multicollector Inductively Coupled Plasma Mass Spectrometry (LA-MC-ICP-MS), Neptune model, Thermo Finnigan brand, equipped with an Nd 213 nm laser probe, LSX-213 G2 model by CETAC.

3. Preliminary results and discussion

The field features indicating migmatization are exposed in extensive rock outcrops of the Carajás Province. The identified migmatite components are: i) palaeosome composed of tonalitic-trondhjemitic orthogneiss; ii) palaeosome of amphibolite; iii) leucosome of tonalitic and leucogranitic compositions; iv) biotite melanosome; v) segregated neosome of granodioritic-granitic composition; vi) non-segregated neosome of tonalitic-trondhjemitic composition. The main morphologies identified are: i) patch metatexite; ii) stromatic metatexite; iii) dilation to net-structured metatexite; iv) schollen and schlieren diatexite. The homogeneous diatexites are absent in Carajás Province.

There are two types of palaeosome: the first is represented by a dark grey medium-grained (3–6 mm) orthogneiss, with mafic content varying between 8–30%. Biotite and/or amphibole (~13–20%) are the main mafic phases, while titanite, zircon, allanite, opaques, epidote, apatite, and zoisite form the primary accessory mineralogy (~7%). Secondary mineralogy includes epidote, muscovite, chlorite, scapolite, and carbonate (~3%). The second paleosome type is medium-grained (2–6mm) amphibolite with granoblastic to granonematoblastic texture. Some samples contain biotite. Accessory minerals are titanite, opaques, epidote, and apatite. The leucosome component of the neosome is light grey to pinkish in colour, medium to coarse-grained (4–10 mm) and has a granodiorite to leucogranite compositions. The mafic residue occurs as melanosome, primarily composed of hornblende and biotite. The mineral paragenesis indicates medium to high-grade regional metamorphism, consistent with amphibolite facies (Nascimento et al., 2023). In constrast, the migmatites from Karelia and Kola Provinces are characterized by a stromatic structure and significant homogeneous diatexites, with rafts of amphibolite being common in the Kola Province and rare in the Karelia Province. In general, the mesosomes show locally faint layering defined by

alternating darker and lighter layers composed of plagioclase, quartz and biotite. Retrograde epidote and muscovite are common (Käpyaho et al., 2007). In both regions, the spatial-temporal association of migmatites are linked to ductile shear zones, suggesting deformation during partial melting, segregation, and melt migration.

New geochronological data provided upper intercept ages of 2944 ± 4 Ma (MSWD = 1.5), 2948 ± 9 Ma (MSWD = 1.40), and 2936 ± 5 Ma (MSWD = 0.29) for the orthogneisses from Carajás Province (all with 2σ errors). These ages are interpreted as representative of the crystallisation age of the protoliths of these rocks. Separate migmatite structures were not dated yet. Additionally, zircon populations dating between 2890 ± 5 Ma and 2843 ± 8 Ma were identified, representing the peak of regional metamorphism in the studied area. Similarly, for the Karelia and Kola Provinces, most zircon grains in the mesosomes yield ages between 2.90 Ga and 2.79 Ga, with cores of 2.94 Ga in one sample (Käpyaho et al., 2007; Joshi et al., 2024).

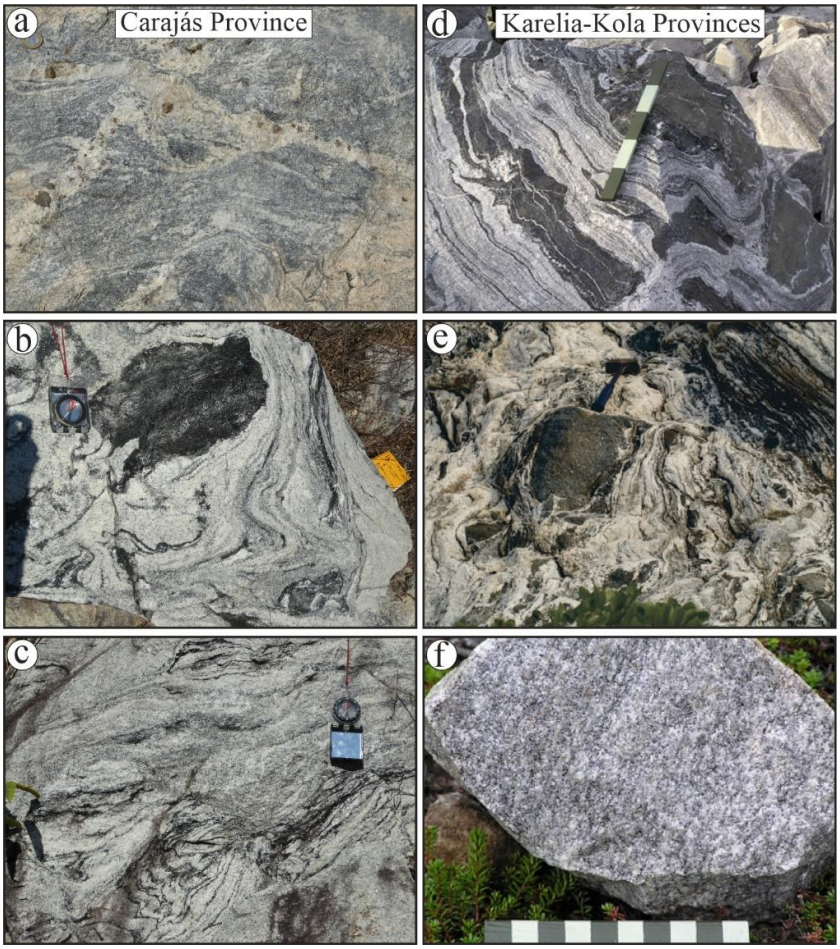

Figure 2. Field relations of the Carajás Province and its correlation with the Kola Province: (a) dilatant to net-structured metatexite migmatite, where the leucosome is located in dilatational sites oriented in at least two distinct directions; (b) schollen diatexite migmatite with remaining palaeosome fragments of amphibolite, displaying signs of assimilation; (c) schlieren migmatite with flow-induced structures indicated by the orientation of micas and elongated minerals; (d) metatexite in the Kola Province basement; (e) amphibolite diatexite migmatite with flow structure; (f) homogeneous diatexite migmatite. Kola Province photos are source from Halla et al. (2024).

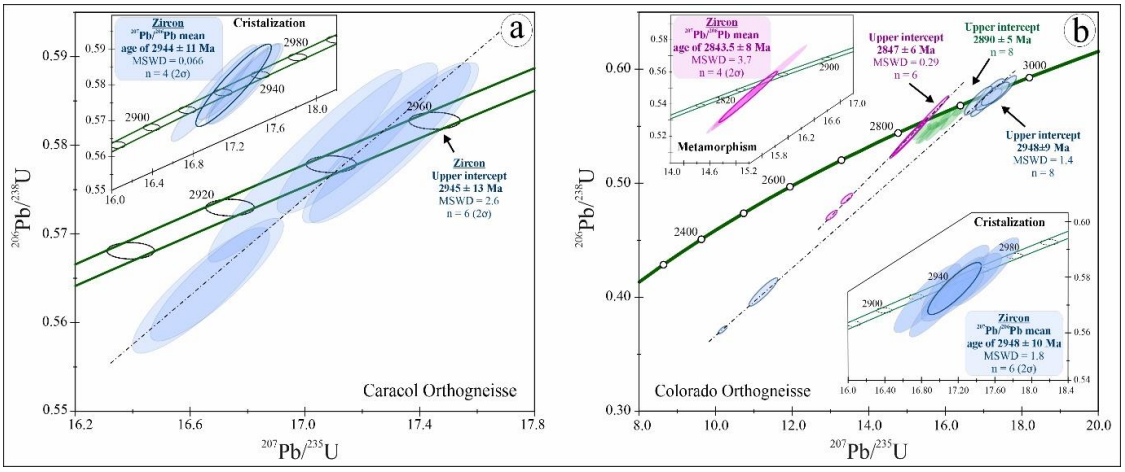

Figure 3. Concordia U-Pb diagrams of representative samples from the migmatized gneisses of the Carajás Province: (a) Caracol orthogneiss, (b) Colorado orthogneiss.

4. Conclusions

Migmatites provide crucial insights into the metamorphic history of the Archean basement in the Carajás Province and reveal its affinity with the Karelia and Kola Provinces. In the Carajás, migmatites exhibit a variety of morphologies, including stromatic and net-structured metatexites, as well as schollen and schlieren diatexites. The presence of tonalitic-trondhjemitic orthogneiss, amphibolite palaeosomes, and biotite-rich melanosomes suggest high-grade metamorphic conditions (upper amphibolite facies). U-Pb zircon geochronology dates the protoliths of these gneisses to 2.95–2.93 Ga, with peak regional metamorphism at 2.89–2.84 Ga. Similar characteristics are found in the Karelia and Kola Provinces, where migmatites show complex morphologies and represent significant crustal evolution processes. However, for the Karelia and Kola Provinces, the presence of homogeneous diatexites is more significant, which indicates higher metamorphic conditions and degree of partial melting compared to the Carajás Province. The study of migmatites helps us to understand the felsic continental crust formation and its differentiation.

5. References

Chekulaev, V.P., Arestova, N.A., Egorova, Y.S., 2022. The Archean Tonalite-Trondhjemite-Granodiorite Association of the Karelian Province: Geology, Geochemistry, Formation Stages and Conditions. Stratigr. Geol. Correl., 30, 183–200.

Halla, J., Joshi, K.B., Lutinen, A., Heilimo., E., Kurhila, M., 2024. On the origin of Archaean TTGs by migmatization of mantle plume-related metabasalts: Insights from the Lake Inari terrain, Arctic Fennoscandia. Precambrian Research, 407, 107407.

Joshi, K.B., Halla, J., Kurhila, M., Heilimo, E., 2024. Prolonged parallel chronology of distinct TTG types in the Lake Inari terrain, Arctic Fennoscandia: Implications for a stationary plume-related source. Precambrian Research, 408, 107418.

Marangoanha, B., Oliveira, D.C., Dall'Agnol, R., 2019. The Archean granulite-enderbite complex of the northern Carajás province, Amazonian craton (Brazil): Origin and implications for crustal growth and cratonization. Lithos, 350–351, 105275.

Mikkola, P., Huhma H., Heilimo, E., Whitehouse, M., 2011. Archean crustal evolution of the Suomussalmi district as part of the Kianta Complex, Karelia: Constraints from geochemistry and isotopes of granitoids. Lithos, 125, 287–307.

Nascimento, A.C., Oliveira, D.C., Silva, L.R., Gabriel, E.O., Leite-Santos, P.J., 2023. Origem, afinidades petrológicas e significado tectônico da Suíte Sanukitoide Água Limpa do Subdomínio Sapucaia, sudeste da Província Carajás (Cráton Amazônico). In: Simpósio de Geologia da Amazônia – SBG. Santarém (PA), Abstract.

Käpyaho, A., Hölttä, P., Whitehouse, M.J., 2007. U-Pb zircon geochronology of selected Archaean migmatites in eastern Finland. Bulletin of the Geological Society of Finland, 79, 95–115.

Origin and tectonic significance of Archean sanukitoids: correlation between the Carajás and Karelia Provinces

A.C. Nascimento[1, 2], D.C. Oliveira[1] and E. Heilimo[2]

[1] Institute of Geosciences (IG), University Federal do Pará (UFPA), Box 1611, 66075-100, Belém, Pará, Brazil
[2] Department of Geography and Geology, University of Turku, Finland
E-mail: aline.nascimento@ig.ufpa.br

Sanukitoid-affinity granitoid plutons in the Carajás Province (Amazonian Craton) share notable geochemical and isotopic similarities with those in the Karelia Province. In both regions, these rocks exhibit high concentrations of Mg, Cr, Ni, K, Ba, and Sr, and display isotopic signatures indicative of mixed juvenile and recycled crustal sources. U–Pb zircon dating from Carajás places the crystallization age of these sanukitoids at 2.87 Ga, with Hf isotopic values suggesting the incorporation of Paleoarchean crustal material (Hf-T_{DM}^{C} of 3.0–3.2 Ga). Nd isotopic data corroborates the Hf data with model ages ranging between 2.9–3.1 Ga and εNd(t) values from –0.6 to +2.9. These features are consistent with the tectonic setting of syntectonic emplacement in a collisional environment, characterized by slab break-off and the partial melting of an enriched mantle wedge. Comparatively, the Karelia sanukitoids also demonstrate high-Mg, Cr, and Ni contents and a mixed isotopic signature of juvenile and recycled material. The εHf(t) vary from +2.74 to -3.74, Hf-T_{DM}^{C} of 3.0–2.95 Ga and εNd(t) from -2.2 to +1.4 for the Karelia sanukitoids. However, Karelia sanukitoids are younger than Carajás sanukitoids, dating to 2.74–2.70 Ga. The tectonic settings are analogous, both reflecting post-subduction processes involving mantle-crust interactions and crustal thickening. The geochemical and isotopic affinities between the Carajás and Karelia sanukitoids are strong, but the key difference lies in their ages, with Carajás sanukitoids being approximately 150 million years older.

Keywords: Sanukitoids, crustal evolution, correlation, Carajás Province, Karelia Province.

1. Background

The Carajás Province, located in the southeast of the Amazonian Craton, is considered its main preserved Archean core (Almeida et al., 1981; Fig. 1a, b). Geological mapping in the Água Azul do Norte area (Carajás Province; Fig. 1c) led to the identification of two sanukitoid-affinity batholiths, composed of granodiorites with subordinate tonalites and monzogranites, distributed along extensive E-W shear zones that define terrane boundaries (Gabriel and Oliveira, 2014). The Água Azul sanukitoid batholith is located in the southern part of the area, while the Água Limpa sanukitoid batholith lies to the north. Both intrude the basement formed by greenstone belt and migmatised tonalite-trondhjemite-granodiorite (TTG) units, and are crosscut by biotite granites. In this study, U–Pb–Hf zircon and whole-rock Nd isotopic data are integrated with a geochemical review of these rocks, aiming to discuss the origin and tectonic significance of sanukitoid-type magmatism in the Carajás Province, and to propose correlations with similar rocks in the Karelia Province (Finland).

2. Methods and materials

The in-situ U-Pb zircon analyses were made using secondary ion mass spectrometry (SIMS), sensitive high-resolution ion microprobe (SHRIMP IIe model), at the GeoLab Laboratory/IGc/USP (University of São Paulo), with data published in Nascimento et al. (2024, in press). The Hf analyses on zircon were obtained from the same spot or domain of concordant U-Pb age at the Isotopic Geology Laboratory (Pará-Iso/UFPA) of the Geosciences Institute of UFPA, using a high-resolution Laser Ablation Multicollector Inductively Coupled Plasma Mass Spectrometry (LA-MC-ICP-MS), Neptune model, Thermo Finnigan brand, equipped with an Nd 213 nm laser probe, LSX-213 G2 model by CETAC. The whole-rock Nd isotopic data were

obtained at the Pará-Iso/UFPA Laboratory. A Finnigan MAT 262 mass spectrometer was used, equipped with seven movable Faraday cup collectors and a central electron multiplier.

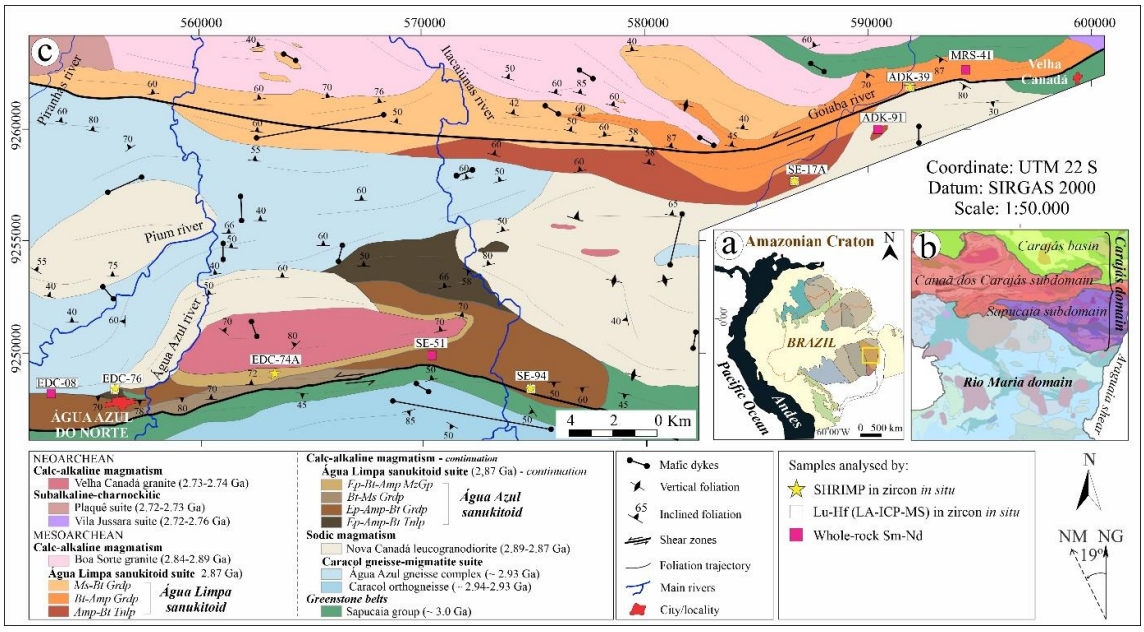

Figure 1. Location map of the study area. (a) Location of the Carajás Province in relation to the Amazonian Craton. (b) Division of the Carajás Province into the Carajás Domain (Sapucaia subdomain, Canaã dos Carajás subdomain, and Carajás Basin) and the Rio Maria Domain (Oliveira et al., 2022; Silva et al., 2022). (c) Semi-detailed local map of the studied area (Gabriel and Oliveira, 2014).

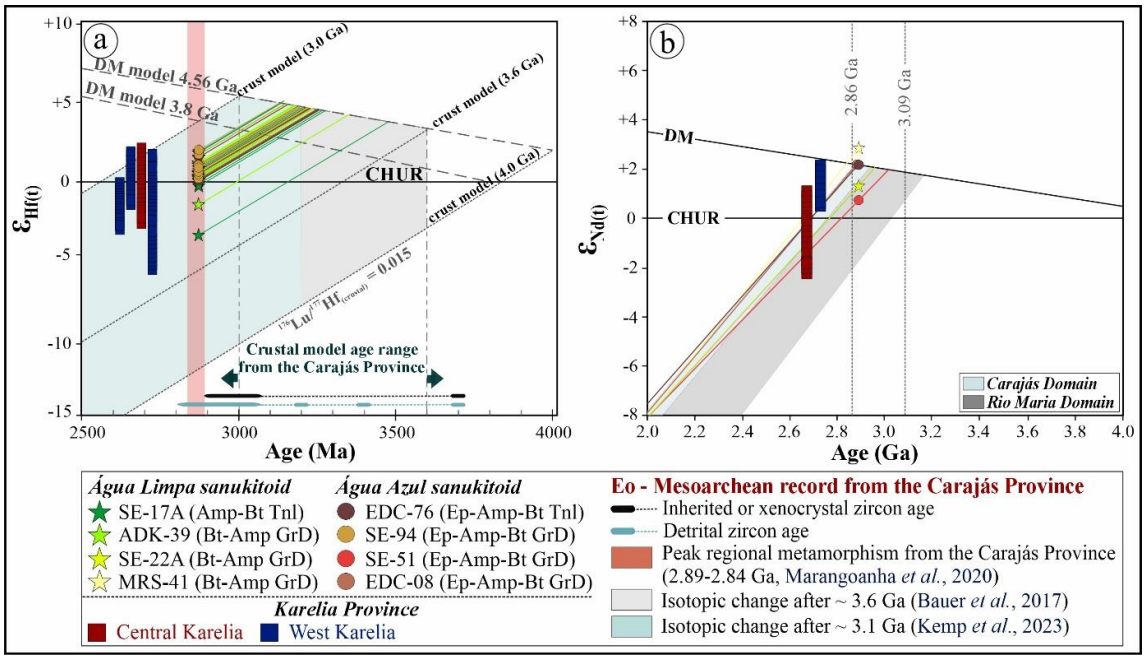

Figure 2. U-Pb-Hf zircon and whole-rock Nd isotopic data from the Carajás Province sanukitoids and comparison with Karelia sanukitoids: (a) ƐHf(t) versus Age (Ma) evolution diagrams and (b) ƐNd(t) versus Age (Ga). Karelia Province samples are source from Heilimo et al. (2010, 2013).

3. Preliminary results and discussion

The sanukitoids from Carajás Province consist of plagioclase, quartz, and alkali feldspar, with biotite and amphibole as the main ferromagnesian minerals. Primary accessory minerals include epidote, opaques, titanite, allanite, zircon, apatite, muscovite, and occasionally tourmaline, while secondary accessories include chlorite, scapolite, white mica, carbonate, and epidote (Gabriel and Oliveira, 2014). Karelia sanukitoids are metamorphosed with plagioclase, quartz, and alkali feldspar, with biotite and hornblende ± pyroxene as mafic minerals. As accessory titanite, opaque, apatite and zircon are common, while secondary minerals contain epidote, allanite, chlorite, sericite, saussurite, muscovite and carbonatite minerals (Heilimo et al., 2010 and references therein). The studied sanukitoids are predominantly metaluminous, with high #Mg (64–49), Cr (383–102 ppm), and Ni (117–32 ppm) values, aligning them with the high-Mg granodiorites of the Karelia Province (Heilimo et al., 2010; 2013). They exhibit rare earth element (REE) patterns characterised by high light REE (LREE) contents and moderate to strong fractionation of heavy REE (HREE) [La_N/Yb_N (170–18)], along with weak or absent negative Eu anomalies (Eu/Eu* 1.21–0.66) (Gabriel and Oliveira, 2014; Nascimento et al., 2024, in press).

U-Pb SHRIMP geochronology on zircon provided concordant ages of 2.87 Ga, interpreted as the crystallisation age for both sanukitoid plutons. Lu-Hf data obtained for both sanukitoid plutons yielded subchondritic to suprachondritic ε_{Hf} values varying from –3.3 to +2.1. Crustal model ages are Palaeoarchaean (Hf-T_{DM}^{C} = 3.2–2.9 Ga), indicating a Mesoarchaean juvenile origin at 2.87 Ga (suprachondritic component), but involving recycled Palaeoarchaean crust (subchondritic component). Whole-rock Nd isotopic data yielded mainly suprachondritic ε_{Nd} values (–0.6 to +2.8) and Mesoarchaean model ages (Nd-T_{DM} = 3.0–2.9 Ga), indicating a juvenile origin with the involvement of recycled crust in the mantle, corroborated by Hf isotopic data from zircon. For the 2.74–2.70 Ga Karelia sanukitoids, subchondritic to suprachondritic ε_{Hf} values (–6.1 to +1.7) and Mesoarchean crustal model ages (Hf-T_{DM}^{C}) of 3.0–2.9 Ga were obtained by Heilimo et al. (2013). Whole-rock Nd isotopic data yielded suprachondritic ε_{Nd} values (–2.2 to +1.7) and a Meso- to Neoarchaean model age (Nd-T_{DM} = 3.0–2.7 Ga), indicating a juvenile origin with the involvement of recycled crust in the mantle; hovewer, Karelia sanukitoids are younger than Carajás sanukitoids.

Subduction related tectonic setting is one possible tectonic scenario for mantle enrichment and sanukitoid formation (e.g. Heilimo et al., 2010; 2013). Additionally, the sanukitoids from the Carajás Province were emplaced syntectonically during the regional metamorphic peak of the province (2.89–2.84 Ga; Marangoanha et al., 2019). This suggests that the formation of these rocks is better explained by a post-subduction collisional scenario involving crustal thickening and slab break-off, which led to partial melting of the previously metasomatised mantle wedge to generate the sanukitoid-type magmas, similar to the processes described for the sanukitoids of the Karelia Province (Heilimo et al., 2013).

4. Conclusions

Based on the U-Pb SHRIMP geochronological data on zircon the Carajás Province sanukitoids crystallised ages of 2.87 Ga. U–Pb–Hf isotopic data on zircon and whole-rock Nd data indicate a juvenile origin (supracrustal component) at 2.87 Ga, with the involvement of recycled crustal material in the mantle (subcrustal component). This occurred in a collisional setting, characterised by crustal thickening, slab break-off, and partial melting of a previously enriched mantle wedge during the peak of regional metamorphism (2.89–2.84 Ga), leading to the formation of the Carajás Province sanukitoids. The sanukitoids from the Karelia Province exhibit strong geochemical and isotopic similarities with those from the Carajás Province, particularly in terms of their high Mg, Cr, Ni, K, Ba, and Sr contents, and mixed juvenile and

recycled crustal sources. However, the Karelia sanukitoids are slightly younger, with crystallisation ages of 2.74–2.70 Ga (Heilimo et al., 2010; 2013), and reflect a more evolved stage of mantle-crust interactions.

5. References

Almeida, F.F.M., Hasui, Y., Brito Neves, B.B., Fuck, R.A., 1981. Brazilian Structural Provinces: an introduction. Earth Science Review, 17, 1−29.

Gabriel, E.O., Oliveira, D.C., 2014. Geologia, petrografia e geoquímica dos granitoides arqueanos de alto magnésio da região de Água Azul do Norte, porção sul do Domínio Carajás, Pará. Boletim do Museu Paraense Emílio Goeldi Ciências Naturais, 9, 533–564.

Heilimo, E., Halla, J., Andersen, T., Huhma, H., 2013. Neoarchean crustal recycling and mantle metasomatism: Hf–Nd–Pb–O isotope evidence from sanukitoids of the Fennoscandian shield. *Precambrian Research*, 228, 250−266.

Heilimo, E., Halla, J., Hölttä, P., 2010. Discrimination and origin of the sanukitoid series: geochemical constraints from the Neoarchean western Karelian Province (Finland). Lithos, 115, 27–39.

Oliveira, D.C., Silva L.R., Nascimento A.C., Marangoanha B., 2022. Geologia Regional da Província Carajás, sudeste do Cráton Amazônico: Proposta litoestratigráfica e implicações para a compartimentação tectônica. *In*: II Congresso Amazônico de Mineração, Metalurgia e Materiais – COAMA. Marabá (PA), *Anais*, CD-rom.

Marangoanha, B., Oliveira, D.C., Dall'Agnol, R., 2019. The Archean granulite-enderbite complex of the northern Carajás province, Amazonian craton (Brazil): Origin and implications for crustal growth and cratonization. Lithos, 350–351, 105275.

Nascimento, A.C., Oliveira, D.C., Gabriel, E.O., Leite-Santos, P.J., 2024 in press. Geology, geochemistry, and zircon SHRIMP U−Pb geochronology of Mesoarchean high-Mg granitoids: Constraints on petrogenesis, emplacement timing, and deformation of the Água Limpa suite in the Carajás Province, SE Amazonian Craton. The Geological Society of London, 6, 1–30.

Silva, L.R., Oliveira, D.C., Nascimento, A.C., Lamarão, C.N., Almeida, J.A.C., 2022. The Mesoarchean plutonic complex from the Carajás province, Amazonian craton: Petrogenesis, zircon U-Pb SHRIMP geochronology and tectonic implications. Lithos, 432–433, 106901.

Generation of faults and associated damage zones in crystalline rocks

K. Nikkilä[1], P. Skyttä[2], N. Nordbäck[3], J. Engström[3]

[1]Åbo Akademi University
[2]Structural Geology Company
[3]Geological Survey of Finland
E-mail: kaisa.nikkila@abo.fi

In this study, we will demonstrate how strike-slip fault zones form in isotropic rapakivi granites. We will also show the different stages of fault zone formation, from initiation to the culmination as a gouge-bearing fault zone. Our findings indicate that fault nucleation consistently begins with the formation of en echelon arrays, in the absence of precursor joints. This contrasts with many previous studies worldwide, where pre-existing joints are the primary mechanism of fault formation.

Keywords: fault zone, brittle deformation, crystalline bedrock, rapakivi granite, fracture

1. General

The development of faults, particularly strike-slip faults, has been studied for decades (Segall and Pollard, 1983; Kim et al., 2003). A widely accepted model suggests that fault development begins along pre-existing extensional fractures, such as joints, which then become linked, allowing for increased displacement and finally to the formation of a continuous fault plane.

Many of the studies on fault development focus on sedimentary rocks (e.g. Myers and Aydin, 2004). In these rocks, in addition to the pre-existing fractures, the style of fault growth is often interpreted to depend on factors such as layer thickness and/or the compositional differences of the layers. However, in crystalline bedrock, such features are not present. For example, many intrusive rocks, like granites, are homogeneous and mechanically relatively isotropic. Nevertheless, it has been interpreted that in crystalline bedrock, pre-existing microstructures such as microcracks and grain boundaries may influence the formation of fractures, and further, in granites the field observations have shown that the initial stages of fault growth are associated with pre-existing structures like joints or dikes (Crider, 2015). However, in many places within the crystalline bedrock, such as in Finland, precursor fractures may have been healed due to later metamorphic events (Pennacchioni and Mancktelow, 2013), suggesting that these pre-existing features may play only a minor role in fault generation in the crystalline bedrock. This was also concluded in the studies by Skyttä et al. (2021) and Nordbäck et al. (2024), who suggested that jointing postdates faulting. These studies were conducted in the Rapakivi granites in Finland, which have not been affected by ductile deformation.

The brittle deformation in the crystalline bedrock of Olkiluoto, southwestern Finland, has been studied using structural and isotopic methods (Mattila and Viola, 2014; Marchesini et al., 2019; Prando et al., 2020; Nordbäck et al., 2022). Recently, Nordbäck et al. (2024) and Skyttä et al (2021) have continued the research to the rapakivi granites in southern Finland focusing on structural analysis. These studies from Finland have shown that faults were generated in several stages between 1.75 Ga and 1.0 Ga. Further, the studies done in the rapakivi granites indicate that the faults mainly appear as multiple narrow fault traces, which may have tip damage fractures (such as wing cracks) or have been linked together by stepover fractures. However, small scale faults within outcrops rarely have visible slickenside surfaces available for determining the fault kinematics (Nordbäck et al., 2024). Nevertheless, the tip damage fractures help determine the slip sense, but the amount of slip is rarely visible, as are the fault

cores with gouge. These studies have focused on the timing and stress fields of the brittle deformation, especially the faulting events in Finland. However, they have paid less attention to fault generations and different types of faults in the crystalline bedrock.

In this study, we show how isotropic rapakivi granite deform, how fractures evolve into strike-slip fault planes, and continue to evolve to eventually form fault zones within the crystalline bedrock. We show that fault planes in our study only develop via en echelon arrays in rapakivi granites, whereas joints as precursors are absent. Our case study show that fault gouge only exists in highly fragmented fault zones, and how the different fault zone types can be observed in various scales.

2. Study area

We conducted our studies in the Getaberget, Åland Islands, Southwest Finland, where high-quality ice-polished outcrops expose 1.58 Ga Mesoproterozoic Rapakivi granites. The semi-continuous outcrops and homogenous, isotropic lithology are ideal for studying fault generation, as they reveal the natural variability of faulting and fracturing processes without structural inheritance from pre-existing anisotropies, such as foliation or shear zones.

3. Material and methods

Our dataset includes high-resolution orthophotographs derived from UAVs (Unmanned Aerial Vehicle), digitized fracture tracelines from these orthophotographs, as well as field photographs and observations. We utilized data collected by Nordbäck et al. (2024). The methodology for obtaining the orthophotographs and the traceline digitization are found in (Nordbäck and Ovaskainen, 2022).

We used orthophotographs for field mapping to identify faults, and to select representative examples of common fault types in the Rapakivi granites. Field mapping focused on fault planes and fault zones with strike-slip displacement. For each type, we measured the dip and dip direction of the fault plane, related fractures, and kinematics. When possible, we also measured slip-surface lineation, core type, and damage zone width. Fault zones associated with aplite or clastic dikes were omitted.

We have divided the fault types into six different categories: shear fracture, en echelon, isolated fault, single step-over, multiple step-over, and gouge-bearing fault zone. The five first mentioned have been classified into three different scales: small (width < 1 m), medium (width 1-3m), and large (width > 3m). The gouge-bearing fault zones are examples of fault zones with one or multiple cores (with gouge).

3. Results

In the study area, all fault zones are formed by one or multiple fault planes, thus the primary stage of faulting is the development of a fault plane (Fig. 1A and B). Fault planes have been observed to develop from tensional en echelon arrays that during the initial stages of faulting develop parallel to the least principal stress. As the deformation progresses, the en echelon arrays connect through linking fractures, eventually creating a continuous surface, known as a fault plane. En echelon arrays can be found at all scales but are more commonly observed at small and medium scales. The fault planes then evolve into isolated faults, or single and multiple oversteps (Fig. C-D).

Isolated faults are fault planes with progressively grown tip-damage zones characterized by horse tails. Isolated faults are distant from other fault planes, and their tip-damage zones can be fragmented, showing two or three different sets of fractures at their tips. Isolated faults can be found at medium to large scales.

When two or more fault planes are subparallel and closely spaced, they link through *single or multiple oversteps*. These oversteps develop from the tip damages, eventually connecting them. The slip sense and step senses are the same, that is right-lateral kinematics and right stepping structures.

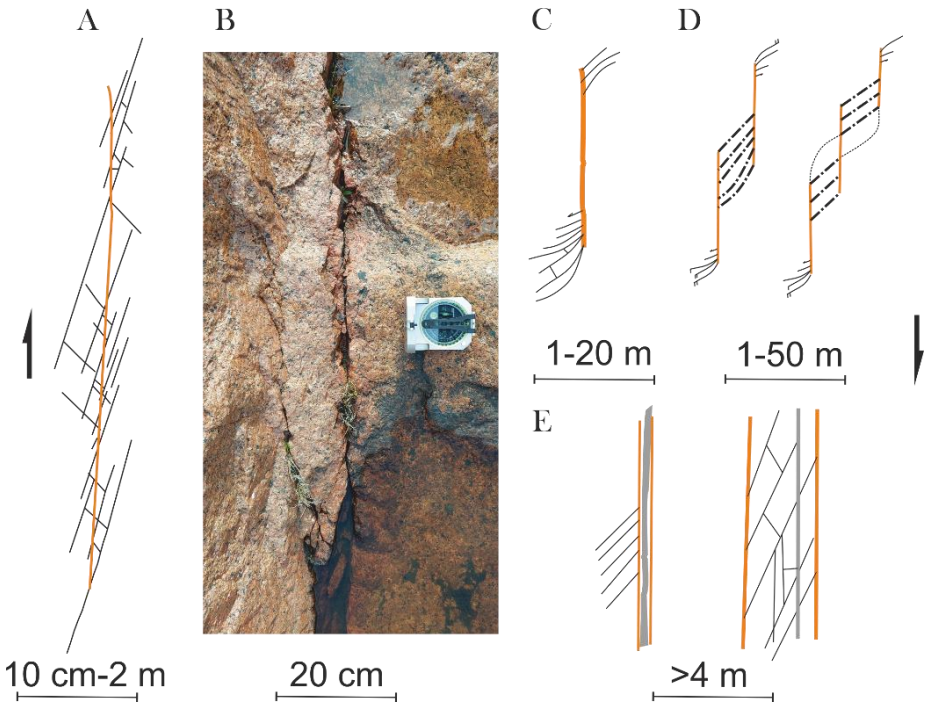

Figure 1. Simplified fault zone propagation model in rapakivi granites. Orange indicates the fault planes and grey gouge-bearing core. A) In the first stage, en echelon arrays nucleate and connect via linking fractures, usually forming at a sub-orthogonal angle. These linking fractures eventually create a continuous fault plane. B) En echelon arrays and fault plane in the field C) In the second stage, the fault planes grow, characterized by horse tails. D) In the third stage, the fault planes are connected by single or multiple oversteps. E) In the final stage, gouge-bearing fault zones (asymmetric or fault-bounded fractures) develop.

Since the step-over fractures have developed primary by propagation of the horse tail or en echelon fractures, i) the first set of linking fractures are parallel to those, while ii) the second set of linking fractures develops sub-perpendicular or at a high angle to the fault planes, and iii) the third set of fractures connect and crosses the linking fractures and are antithetic to the fault planes. The last ones can be found in a large-scale single oversteps, pull-aparts, but are lacking on multiple oversteps. Multiple oversteps generate if there are several parallel fault planes. The distance between fault planes, and thus oversteps, can vary within the same fault zone, ranging from centimetres to meters. Step-over fractures show systematic variation in dip with relative to their length: fractures at wider oversteps are the most moderate dipping (~70 degree).

Gouge-bearing faults are large-scale fault zones with one or more gouge-bearing cores (Fig. 1E). They can be divided into two types: (i) asymmetric faults with one main core, and (ii) fault-bounded fractures with highly fragmented zone and several subparallel fault planes or cores (with or without gouge). They may have four fracture sets: i) parallel and ii) sub-perpendicular to en échelons, iii) parallel and iv) sub-perpendicular to fault planes. Gouge-bearing fault zones often involve mineral alteration.

4. Summary

In the formation of a fault zone in rapakivi granites, the process begins with the nucleation of en echelon arrays (Figure 1). This is followed by the development of the fault plane through these arrays. The third stage involves the creation of oversteps, leading to the development of two to three linking fracture sets, resulting in a highly fragmented area. Finally, the process culminates in the formation of a gouge-bearing core.

References:

Crider, J. G., 2015. The initiation of brittle faults in crystalline rock. Journal of Structural Geology, 77, 159-174.

Kim, Y. S., Peacock, D. C. P., Sanderson, D. J., 2003. Mesoscale strike-slip faults and damage zones at Marsalforn, Gozo Island, Malta. Journal of Structural Geology, 25(5), 793-812.

Mattila, J., & Viola, G., 2014. New constraints on 1.7 Gyr of brittle tectonic evolution in southwestern Finland derived from a structural study at the site of a potential nuclear waste repository (Olkiluoto Island). Journal of Structural Geology, 67, 50-74.

Nordbäck, N., Mattila, J., Zwingmann, H., Viola, G., 2022. Precambrian fault reactivation revealed by structural and K-Ar geochronological data from the spent nuclear fuel repository in Olkiluoto, southwestern Finland. Tectonophysics, 824, 229208.

Nordbäck, N., Ovaskainen, N., 2022. Getaberget drone orthomosaic dataset, doi: 10.5281/ZENODO.4719627.

Nordbäck, N., Skyttä, P., Engström, J., Ovaskainen, N., Mattila, J., Aaltonen, I., 2024. Mesoproterozoic Strike-Slip Faulting within the Åland Rapakivi Batholith, Southwestern Finland. Tektonika, 2(1), 1-26.

Pennacchioni, G., Mancktelow, N. S., 2013. Initiation and growth of strike-slip faults within intact metagranitoid (Neves area, eastern Alps, Italy). Bulletin, 125(9-10), 1468-1483.

Prando, F., Menegon, L., Anderson, M., Marchesini, B., Mattila, J., & Viola, G., 2020. Fluid-mediated, brittle–ductile deformation at seismogenic depth–Part 2: Stress history and fluid pressure variations in a shear zone in a nuclear waste repository (Olkiluoto Island, Finland). Solid Earth, 11(2), 489-511.Segall, P., & Pollard, D. D., 1983. Joint formation in granitic rock of the Sierra Nevada. Geological Society of America Bulletin, 94(5), 563-575.

Skyttä, P., Ovaskainen, N., Nordbäck, N., Engström, J., & Mattila, J., 2021. Fault-induced mechanical anisotropy and its effects on fracture patterns in crystalline rocks. Journal of Structural Geology, 146, 104304.

Strike-Slip Faulting and Hydrothermal Alteration in the Vehmaa Rapakivi Batholith: Insights into Reservoirs in Crystalline Rocks and Geothermal Potential in Southern Finland

Nicklas Nordbäck[1], Alan Bischoff[1,2], Kaisa Nikkilä[3], Daniel Carbajal-Martinez[1], Jon Engström[1], Pietari Skyttä[4], Andy Nicol[5], Nikolas Ovaskainen[1] and Steffi Burchardt[6]

[1]Geological Survey of Finland
[2]University of Turku, Finland
[3]Åbo Akademi University, Finland
[4]Structural Geology Company, Finland
[5]University of Canterbury, New Zealand
[6]University of Uppsala, Sweden
E-mail: nicklas.nordback@gtk.fi

Here we report on brittle deformation and post-magmatic hydrothermal alteration within the rapakivi granites of the Vehmaa Batholith, Southern Finland. We observed that mineral alteration and porosity are structurally controlled and mainly occur in association to NW–SE striking faults along precipitation of mineral assemblages typical of hydrothermal processes. The results of fault kinematic paleostress suggest two stages of Proterozoic strike-slip faulting, as previously interpreted from the Åland rapakivi. Our new results advance the understanding of the brittle deformation and thermal evolution of the Fennoscandian crust during the Meso–Neoproterozoic, providing valuable insights into the potential of crystalline rocks as geothermal reservoirs within granitic settings.

Keywords: Tectonics, crystalline reservoirs, geothermal energy, hydrothermal alteration

1. Rationale

Reservoirs in crystalline rocks are typically formed by post-emplacement tectonics and hydrothermal activity, which can result in fracturing and dissolution pore networks. Ancient crystalline terranes, such as the Fennoscandian Shield, often experience multiple tectonic and magmatic events, leading to a complex history of fault reactivation and hydrothermal activity that can be challenging to unravel. The emplacement of rapakivi granites during the Paleo–Mesoproterozoic marks the end of a series of major orogenic and magmatic events in Southern Finland. Consequently, their anorogenic character and limited post-emplacement tectonic deformation provide an ideal setting for studying the mechanisms resulting in crystalline reservoir formation. To enhance understanding of these unconventional reservoirs, we investigate the effects of brittle deformation and hydrothermal alteration in the Vehmaa rapakivi Batholith, Southwest Finland.

2. Methods

We employed a multiscale approach including regional-scale lineament interpretation from magnetic and electromagnetic aerogeophysical maps (Hautaniemi et al. 2005), LiDAR data (National Land Survey of Finland, 2019) and bathymetric data (EMODnet Bathymetry Consortium, 2018). Mesoscale (meters to hundreds of meters) interpretation involved drone photogrammetry, fieldwork, and paleostress analysis, while at the microscale (mm to cm), we conducted microscopic petrography and petrophysical laboratorial tests from key lithologies.

3. Characterization of brittle structures within the Vehmaa Batholith

Our 1:200 000 scale lineament analysis of the Vehmaa rapakivi granite revealed two main sets of lineaments with NNW and ENE trends, which contrast with the regional NNE orientation of major lineaments within the surrounding Paleoproterozoic bedrock (Figure 1). The NNW lineaments are relatively continuous over several kilometers, while the ENE lineaments typically terminate against the NNW lineaments, suggesting that the ENE lineaments are younger.

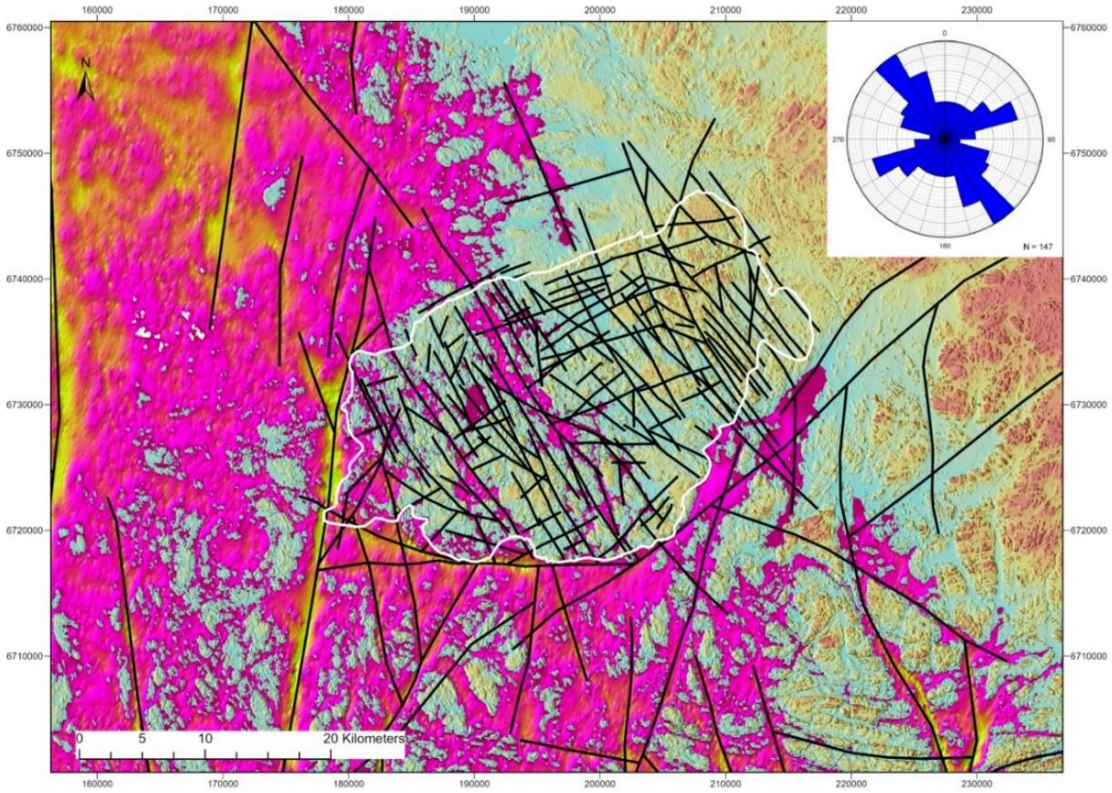

Figure 1. The regional-scale lineaments as interpreted on integrated geophysical and topographic data. Lineaments were interpreted at a 1:200 000 map scale within the Vehmaa Batholith (outlined in white), while a 1:500 000 map resolution was used for extending and interpreting the major lineaments of the surrounding areas. Rose plot displays lineament strikes within the batholith. Source rasters comprise LiDAR (blue-red colour scale) and bathymetry data (yellow-magenta colour scale).

In outcrop and drone photogrammetry, faults and fractured zones extend over tens to hundreds of meters and aligning consistently with the location and orientation of larger lineaments. The most prominent fault sets exhibit NW trends and strike-slip character (Figure 2A). Furthermore, ENE trending strike-slip faults are also present, though they do not form a well-defined set but exhibit instead scattered E to NE trends (Figure 2A). Paleostress analysis reveals two distinct stress regimes: one characterized by WNW–ESE compression and another by NNE–SSW compression, associated with transpressive and transtensive conditions, respectively (Figures 2B and 2C).

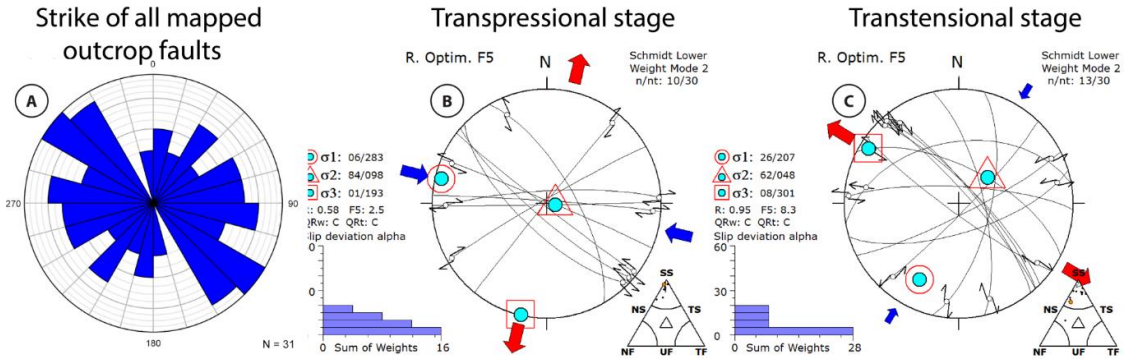

Figure 2. Fault orientation data and paleostress analysis results based on kinematic field observations. (**A**) Strike of mapped fault planes. Paleostress inversion with Wintensor software resulted in the identification of two separate faulting stages: (B) transpressional and (C) transtensional.

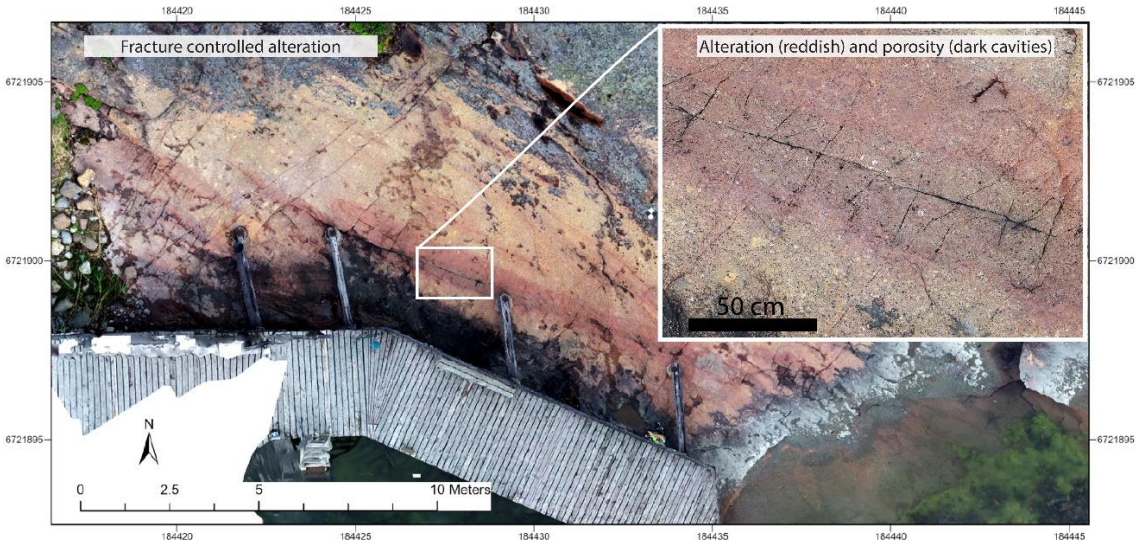

Figure 3. A drone orthomosaic image from an outcrop near Vuosnainen harbor, Kustavi, reveals fracture-controlled alteration (visible from dark reddish staining) and porosity (dark cavities) associated with NW–SE striking faults.

4. Relationship between faulting, mineral alteration, and crystalline reservoir formation

Our field and drone mapping revealed that many NW-trending strike-slip faults within the Vehmaa Batholith correlate with zones of pervasive mineral alteration (Figures 3 and 4). Typical mineral paragenesis within the alteration zones is chlorite, prehnite, and zeolite, indicating hydrothermal events of nearly 300 °C. Typically, the fractured and altered rocks within these zones display substantial porosity of ~10% and laboratory-measured permeabilities exceeding 2×10^{-15} m^2 under 50 MPa confining pressure. The strike-slip fault networks are hundreds-to-thousands of meters in total length and could form crystalline reservoirs with volumes exciding 1 km^3, which are promising targets for geothermal resources. Our findings particularly highlight that hydrothermal alteration linked to these faults can sustain high permeability even at depths >2 km, an observation consistent with the results of Bischoff et al., (2024).

Figure 4. An outcrop-overview of a right-lateral strike-slip fault associated with zeolite, prehnite and chlorite alteration.

5. Conclusions

Our study of the Vehmaa rapakivi granite reveals that the batholith was affected by substantial, low-displacement strike-slip faulting and subsequent hydrothermal alteration. The most substantial alteration zones are mainly within NW–SE striking fault zones. The high-temperature (>200 °C) mineral assemblages infilling the strike-slip faults and fractures suggest Proterozoic hydrothermal processes. Results of the conducted paleostress analyses are compatible with those in the Åland rapakivi Batholith (Nordbäck et al., 2024), which further links to stress stages and faulting stages within the Olkiluoto site in Southwestern Finland (Nordbäck et al., 2022). These findings indicate that the majority of brittle post-rapakivi deformation occurred between 1.55 and 1.2 Ga (Nordbäck et al., 2024). By advancing our understanding of the brittle tectonic and thermal history that shaped the Fennoscandian crust during the Meso–Neoproterozoic, our study contributes to the identification of potential geothermal targets in southern Finland and other crystalline settings worldwide.

References:

Bischoff, AP., Heap, MJ., Mikkola, P., Kuva, L., Reuschlé, T., Jolis, Em., Engström, J., Reijonen, H., Leskelä, T. (2024). Hydrothermally altered shear zones: a new reservoir play for the expansion of deep geothermal exploration in crystalline settings. Geothermics. https://doi.org/10.1016/j.geothermics.2023.102895

EMODnet Bathymetry Consortium, 2018. EMODnet Digital Bathymetry (DTM 2018). https://doi.org/10.12770/18FF0D48-B203-4A65-94A9-5FD8B0EC35F6

Hautaniemi, H., Kurimo, M., Multala, J., Leväniemi, H., Vironmäki, J., 2005. The "Three in One " Aerogeophysical Concept of Gtk in 2004. Geological Survey of Finland, Special Paper 39, 21–74, 2005.

National Land Survey of Finland, 2019. Laser scanning 2008-2019 by National Land Survey of Finland., https://www.maanmittauslaitos.fi/en/maps-and-spatial-data/expert-users/product-descriptions/laser-scanning-data

Nordbäck, N., Mattila, J., Zwingmann, H., Viola, G., 2022. Precambrian fault reactivation revealed by structural and K-Ar geochronological data from the spent nuclear fuel repository in Olkiluoto, southwestern Finland. Tectonophysics 824, 229208. https://doi.org/10.1016/j.tecto.2022.229208

Nordbäck, N., Skyttä, P., Engström, J., Ovaskainen, N., Mattila, J., Aaltonen, I., 2024. Mesoproterozoic Strike-Slip Faulting within the Åland Rapakivi Batholith, Southwestern Finland. Τεκτονικα 2, 1–26. https://doi.org/10.55575/tektonika2024.2.1.51

Rock surface attaching deep biosphere microbes and their functionality (DEEPFUN)

M. Nuppunen-Puputti[1], R. Kietäväinen[2], L. Purkamo[3], I. Kukkonen[2] & M. Bomberg[1]

[1]VTT, Espoo, Finland
[2]University of Helsinki, Helsinki, Finland
[3]Geological Survey of Finland, Espoo, Finland
E-mail: maija.nuppunen-puputti@vtt.fi

Microbial life occupies deep subsurface to multiple kilometres depths. These microorganisms exist both in the aquatic phase of deep groundwater as free-floating cells, and as sessile biofilms within fractures and pores of rocks, adhering to mineral surfaces. Outokumpu deep drill hole has facilitated research of deep life down to 2.5 km depth. The DEEPFUN project had a special focus on mapping and characterizing the ability of microbes to form biofilms under in-situ conditions in the Outokumpu deep bedrock, as well as in the laboratory conditions in microcosm experiments. These microbial communities were characterized with molecular biological methods such as amplicon sequencing and their functional capabilities were estimated with metagenomic analysis. DEEPFUN noted differences between planktic and biofilm community structures. Biofilm lifestyle emphasized heterotrophy, various carbon and sulfur related metabolic pathways and recycling of dead biomass. Sulfate reducing bacteria were commonly found over mica schist surfaces. Therefore, we suggest that evaluation of both planktic and sessile communities is crucial for understanding the overall impact of microbes on deep subsurface biogeochemical cycles.

Keywords: Outokumpu, biofilms, deep biosphere, mica schist

1. Introduction and background

Microbial life on Earth exists not only in the surface environments but also extends down multiple kilometres into the bedrock. This environment, with its microbes known as "intraterrestrials", is called the deep biosphere and hosts a large proportion of the total global biomass (Magnabosco et al., 2018). The deep subsurface is an extreme environment for life as it has no straight access to solar driven carbon cycle or energy, and instead relies more on recycling existing local resources including surrounding minerals, dissolved gases and dead biomass. Microbial life in the deep is considered slow, but microbes can react very fast when conditions change and new resources, like C-1 compounds, become available (Rajala et al., 2015).

The Outokumpu scientific deep drill hole, located in the Northern Karelia, Finland, has granted opportunity to study deep life within Precambrian bedrock. The Outokumpu subsurface hosts five different water types and geochemistry as well as microbial communities change according to the depth (Kietäväinen et al., 2013, Purkamo et al. 2016). Whereas previous projects investigated deep groundwater microbial communities, the DEEPFUN project aimed to understand the biofilm formation processes in the deep bedrock, characterize rock-surface-hosted microbial communities and their functionality as well as understand microbe-mineral interactions in mica schist biofilms (Nuppunen-Puputti et al., 2021, 2022, 2023, Nuppunen-Puputti 2023).

2. DEEPFUN project overview

The DEEPFUN project utilized two different sampling and study approaches. **First,** biofilm formation on rock and glass surfaces was studied using the in-situ incubation traps that were incubated at the depths of 500 m and 967 m (Figure 1). The samplers were placed at the depths of the open fracture zones with fluid in-flow towards the drill hole for a 6-month period. The

in-situ biofilm traps contained both open and closed chambers, allowing gas exchange and capture of water samples, in addition to the incubation of rock and glass specimens. **Second,** the packer-isolated fracture zone at a depth of 500 m was sampled for groundwater, which was used for microcosm experiments with rock specimens. This allowed also laboratory incubations with added substrates to promote microbial growth.

The microbial communities were characterized from the water and rock samples using molecular biological and microscopical methods such as group-specific amplicon sequencing (bacteria, fungi, archaea), quantitative PCR, metagenomic analyses and scanning electron microscopy (SEM) combined with energy-dispersive X-ray spectroscopy (EDS).

Figure 1. Field sampling in the Outokumpu deep drill hole site. This operation aimed to incubate rock specimens under in-situ conditions at the depths of 500 m and 967 m over a 6-month period. **A)** Assembling and attaching biofilm traps into the cable. **B)** Conducting microbiological sampling in an anaerobic field glove box after the experiment. **C)** Harvesting fluid samples from the closed in-situ biofilm traps.

3. Findings from the DEEPFUN project

The dominant groups in all mica schist biofilms were Bacteria and Fungi, with only a very low abundance of Archaea. The mica schist surfaces hosted a variety of attached microbial cell types, including rods, cocci and spirilli and long tubular filamentous cells (Figure 2).

The microbial community structure observed in the in-situ incubations differed from those developed in microcosm experiments. The highest diversity and evenness were observed in the bacterial communities formed under in-situ conditions. Similarly, groundwater-dwelling bacterial communities differed from those attached to surfaces. Different substrates also selected for different microbial groups.

Functional analysis of the metagenome assembled genomes (MAGs) from the mica schist biofilms showed that a heterotrophic lifestyle prevailed, also other carbon and sulfur cycle related metabolisms were important. Many MAGs contained genes encoding enzymes for digestion of complex compounds, indicating potential capabilities to use dead microbes, “necromass”, as their a source of carbon and/or energy.

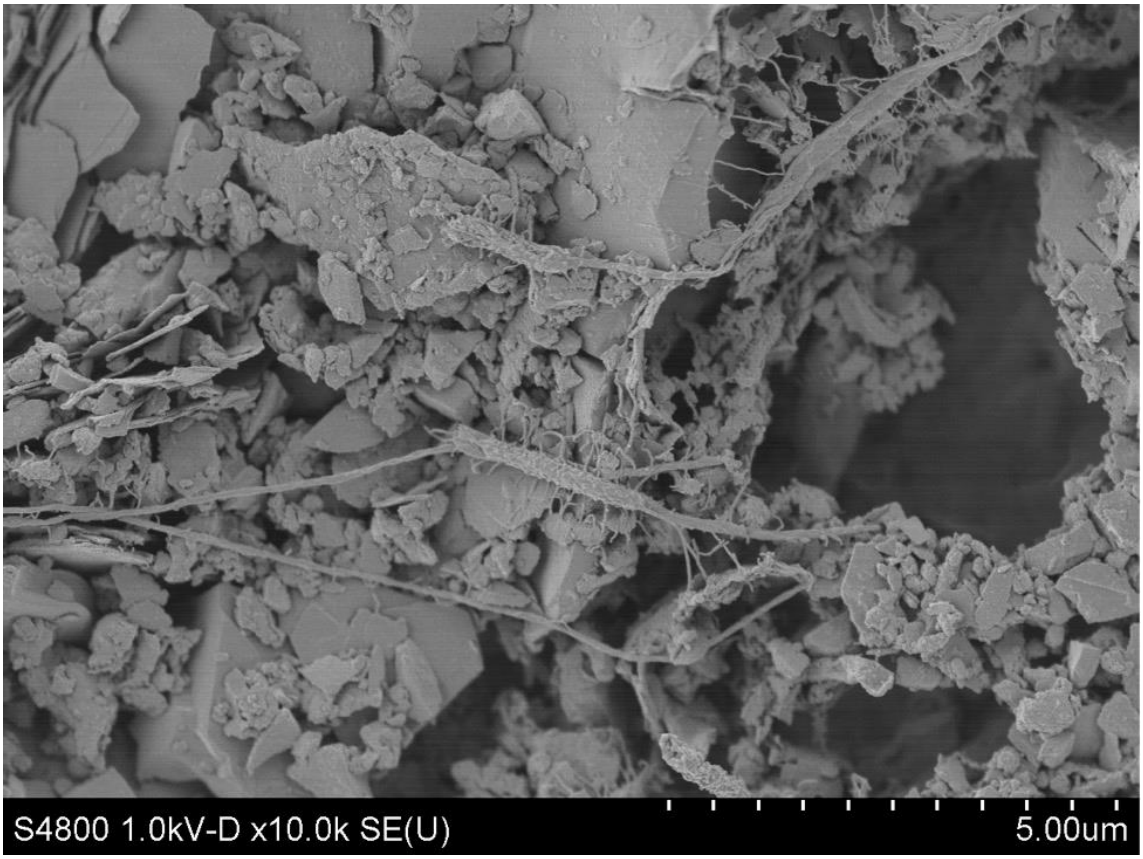

Figure 2. Attached microbial cells on the surface of the mica schist after an 8-month incubation in microcosms with groundwater originating from a depth of 500 m, visualized with SEM. Image by Mari Raulio.

4. Conclusions

The deep groundwater and sessile rock surface microbial communities in the Outokumpu deep subsurface differed from each other. This is an important aspect to consider when planning deep subsurface sampling campaigns and/or modelling activities for bedrock biogeochemical cycles. Biofilm community genomes showed ubiquitous heterotrophic traits and potential for recycling of necromass. Sulfate reducers were more common on mica schist surfaces compared to the water phase, indicating possible benefits from interactions with minerals.

Acknowledgements

DEEPFUN was mainly funded by Maj and Tor Nessling Foundation, while sampling was done in the Research Council of Finland project “Deep Life”. DEEPFUN would like to acknowledge Mirva Pyrhönen, Tarja Eriksson, Mari Raulio, Aino Soro, Pauliina Rajala, Merja Itävaara, Lasse Ahonen, Arto Pullinen, Satu Vuoriainen, Leo Harinen, Nina Hendriksson, Arja Henttinen, Eetu Aalto, Pasi Heino and Esko Karppanen

References:

Kietäväinen, R., Ahonen, L., Kukkonen, I. T., Hendriksson, N., Nyyssönen, M., & Itävaara, M. 2013. Characterisation and isotopic evolution of saline waters of the Outokumpu Deep Drill Hole, Finland: Implications for water origin and deep terrestrial biosphere. *Applied Geochemistry*, *32*, 37-51. https://doi.org/10.1016/j.apgeochem.2012.10.013

Magnabosco, C., Lin, L. H., Dong, H., Bomberg, M., Ghiorse, W., Stan-Lotter, H., Pedersen, K., Kieft, T. L., van Heerden, E., & Onstott, T. C. 2018. The biomass and biodiversity of the continental subsurface. *Nature Geoscience*, *11*, 707-717. https://doi.org/10.1038/s41561-018-0221-6

Nuppunen-Puputti, M., Kietäväinen, R., Purkamo, L., Rajala, P., Itävaara, M., Kukkonen, I., & Bomberg, M. 2021. Rock Surface Fungi in Deep Continental Biosphere—Exploration of Microbial Community Formation with Subsurface In Situ Biofilm Trap. *Microorganisms*, *9*(1), 1-29. Article 64. https://doi.org/10.3390/microorganisms9010064

Nuppunen-Puputti, M., Kietäväinen, R., Raulio, M., Soro, A., Purkamo, L., Kukkonen, I., & Bomberg, M. 2022. Epilithic microbial community functionality in deep oligotrophic continental bedrock. *Frontiers in Microbiology*, *13*, 826048. Article 826048. https://doi.org/10.3389/fmicb.2022.826048

Nuppunen-Puputti, M., Kietäväinen, R., Kukkonen, I., & Bomberg, M. 2023. Implications of a short carbon pulse on biofilm formation on mica schist in microcosms with deep crystalline bedrock groundwater. *Frontiers in Microbiology*, *14*,Article 1054084. https://doi.org/10.3389/fmicb.2023.1054084

Nuppunen-Puputti, M. 2023. Epilithic microbial communities and their functionality in the deep continental bedrock. [Dissertation, University of Helsinki]. University of Helsinki. http://urn.fi/URN:ISBN:978-951-51-9310-0

Purkamo, L., Bomberg, M., Kietäväinen, R., Salavirta, H., Nyyssönen, M., Nuppunen-Puputti, M., Ahonen, L., Kukkonen, I., Itävaara, M., 2016. Microbial co-occurrence patterns in deep Precambrian bedrock fracture fluids. Biogeosciences 13, 3091–3108. https://doi.org/10.5194/bg-13-3091-2016

Rajala, P., Bomberg, M., Kietäväinen, R., Kukkonen, I., Ahonen, L., Nyyssönen, M., & Itävaara, M. 2015. Rapid reactivation of deep subsurface microbes in the presence of C-1 compounds. *Microorganisms*, *3*(1), 17-33. https://doi.org/10.3390/microorganisms3010017

Dark oxygen in the deep geobiosphere of the geological repository (DODGE)

M. Nyyssönen[1], M. Nuppunen-Puputti[1], M. Kuusiluoma[2], A. Delgado[3], M. Bomberg[1] and R. Kietäväinen[2]

[1] VTT Technical Research Centre of Finland, Espoo, Finland
[2] University of Helsinki, Department of Geosciences and Geography, Helsinki, Finland
[3] Andalucian Earth Sciences Institute (IACT), Stable Isotopes Biogeochemistry Lab, Granada, Spain
E-mail: mari.nyyssonen@vtt.fi

In Finland and Sweden, the spent nuclear fuel repositories are situated at a depth of 400 – 450 m below the ground surface in bedrock chambers where strictly anoxic conditions are predicted to decrease the rate of biotic and abiotic processes that could adversely affect the long-term stability of the repository sites. Recently, the presence and production of oxygen in the dark deep subsurface has been demonstrated which may necessitate a re-evaluation of the biogeochemical processes that affect the long-term safety of the deep geological repository environment. The objective of the SAFER2028 funded DODGE project is to evaluate the presence of free oxygen in continental deep groundwater environments, understand its origin and production pathways, and assess its effects on microbial processes in the deep biosphere. The project contains both field and laboratory studies and is planned for 2 years. During the first year, fluid sampling, laboratory incubations, and hydrogeochemical and microbiological analyses have been performed to examine the O_2 and H_2 content in the dissolved and gas phase, to determine isotopic composition and source of these gases, and to assess the microbial communities and their metabolic potential affecting the production and consumption of oxygen and hydrogen as well as related cycles of redox sensitive nutrients in the deep geobiosphere.

Keywords: Dark oxygen, gas isotopes, microbiology, metagenomics, geological repository

1. Background

The disposal of highly radioactive spent nuclear fuel in Finland is based on the multi-barrier KBS-3 concept. The repository is constructed in the bedrock to a depth of ca. 420 - 450 m below the surface, and copper-sheeted cast iron canisters containing the spent fuel rods will be submerged in bentonite clay buffer in pits excavated into the floor of the disposal tunnels. The tunnels will be backfilled with bentonite clay and rock, sealed with concrete and allowed to fill with local surface- and groundwater. In the beginning, the conditions in the repository will be warm and oxic, but over time the repository will cool down and become oxygen free as a result of microbial and abiotic processes. According to model calculations, oxygen will be spent within approximately 200 years (King et al. 2010). The resulting anoxicity will limit microbial and chemical processes and thus reduce e.g., corrosion of the canisters.

Radiolysis of water and oxidation of sulfide minerals have been considered as potential processes providing the deep subsurface with reactive and potentially corrosive components, such as molecular hydrogen and oxygen, as well as H_2O_2 (Lefticariu et al. 2010; Li et al. 2022; Lin et al. 2005; Ershov & Gordeev 2008). Microbial activity can also affect the physical, chemical, and hydrological properties of the bedrock groundwater environment (Sohlberg et al. 2015), bentonite (Miettinen et al. 2022) and canisters (Carpén et al. 2018). Recent research has revealed that oxygen may be produced microbially within the dark, anoxic deep geobiosphere, in adequate amounts to support microbial aerobic processes (Ruff et al., 2023). Studies have also shown surprisingly often that aerobic microbial processes, which are dependent on available oxygen to proceed (Pedersen et al. 2008; Purkamo et al. 2015; Bomberg et al. 2019; Nuppunen-Puputti et al. 2022; Ruff et al. 2023), are present and active in the deep anoxic geobiosphere, thus challenging the models predicting the conditions and scenarios in the deep geological repositories.

3. Objectives

The overall objective of the DODGE project is to evaluate whether abiotic or biotic processes could produce oxygen and hydrogen that could serve as electron donors and acceptors in the deep otherwise anoxic subsurface and how this affects the models of the engineered barrier system (EBS) in the conditions of the final repository for spent nuclear fuel in Olkiluoto, Finland. More specific aims are to 1) evaluate the possibility of the production of dark oxygen in-situ. 2) identify the source of the microbially produced oxygen and hydrogen in microcosms studies using substrates with labelled oxygen, and 3) study the microbial processes affected by or affecting the production and consumption of dark oxygen and hydrogen and related cycles of redox sensitive nutrients in the deep geobiosphere.

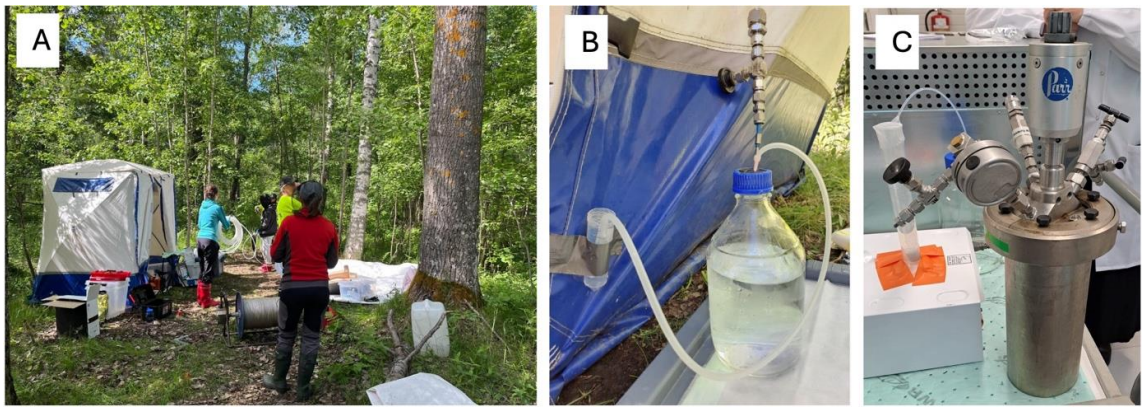

Figure 1. A) Groundwater sampling from Kopparnäs, Inkoo, B) Set up for collecting anaerobic groundwater samples, C) Pressure reactor for incubating groundwater samples at *in situ* conditions.

3. Results

First year of the project has focused on sampling of natural groundwater from Olkiluoto and from an analogue site in Inkoo (Kopparnäs) at depths relevant to the final repository (Figure 1). Hydrogeochemical analyses have been performed to examine the O_2 and H_2 content in the dissolved and gas phase and to determine isotopic composition and source of these gases. Microbiological analyses have included evaluation of the microbial community metabolisms through metagenomic and metatranscriptomic sequencing and assembly of a laboratory experiment to test hypotheses regarding dark microbial oxygen production under repository-relevant conditions (Figure 2).

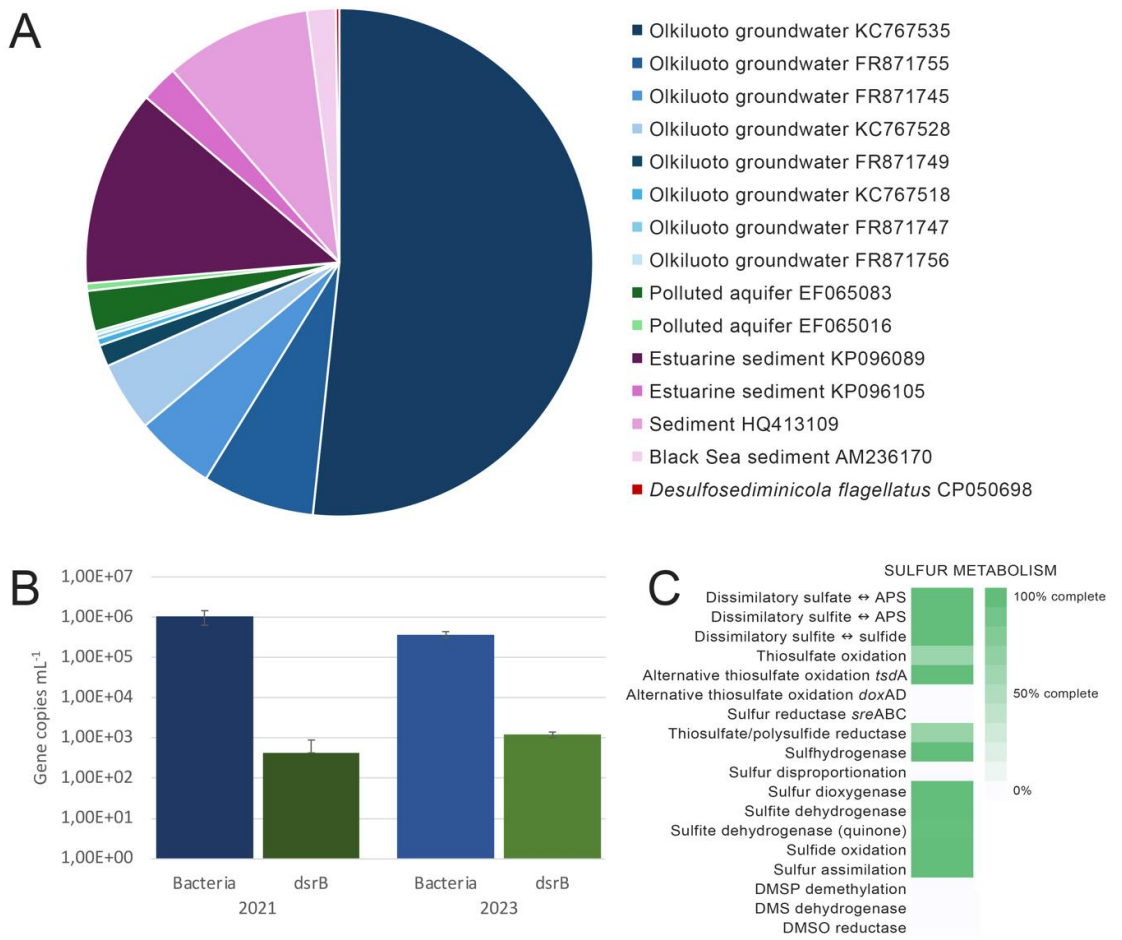

Figure 2. A) The relative abundance of different *dsr*B genes detected by amplicon sequencing in Kopparnäs (R-307) at approximately 126 – 130 m depth in 2021. B) The number of bacterial 16S rRNA gene and *dsr*B gene copies mL^{-1} groundwater in borehole R-307 in 2021 and 2023. C) The sulfur metabolisms detected in R-307 in 2021. Each metabolic pathway is represented by a colored box indicating the completeness of the pathway as detected by metagenomic sequencing. Dark green indicated 100% completeness, i.e. all needed genes for the process to proceed were detected, white indicates that none of the needed genes were found.

4. References

Bomberg, M., Claesson Liljedahl, L., Lamminmäki, T., Kontula, A. 2019. Highly diverse aquatic microbial communities separated by permafrost in Greenland show distinct features according to environmental niches. Frontiers in Microbiology, 10, 1583.

Carpén, L., Rajala, P., Bomberg, M. 2018. Corrosion of copper in anoxic ground water in the presence of SRB. Corrosion Science and Technology, 17 2018(4), 147-153.

Ershov, B.G. Gordeev, A.V., 2008. A model for radiolysis of water and aqueous solutions of H2, H2O2 and O2. Radiation Physics and Chemistry 77, 928-935.

Lefticariu, L., Pratt, L.A., LaVerne, J.A., Schimmelmann, A. 2010. Anoxic pyrite oxidation by water radiolysis products — A potential source of biosustaining energy. Earth and Planetary Science Letters, 292, 57-67.

Li, L., Wei, S., Lollar, B. S., Wing, B., Bui, T. H., Ono, S., ... & van Heerden, E. 2022. In situ oxidation of sulfide minerals supports widespread sulfate reducing bacteria in the deep subsurface of the Witwatersrand Basin (South Africa): Insights from multiple sulfur and oxygen isotopes. Earth and Planetary Science Letters, 577, 117247.

Lin, L.H., Slater, G.F., Sherwood Lollar, B., Lacrampe-Couloume, G., Onstott, T.C. 2005. The yield and isotopic composition of radiolytic H2, a potential energy source for the deep subsurface biosphere. Geochimica et Cosmochimica Acta 69, 893–903.

Miettinen, H., Bomberg, M., Bes, R., Tiljander, M., Vikman, M. 2022. Transformation of inherent microorganisms in Wyoming-type bentonite and their effects on structural iron. Applied Clay Science, 221, 106465.

Nuppunen-Puputti, M., Kietäväinen, R., Raulio, M., Soro, A., Purkamo, L., Kukkonen, I., Bomberg, M. 2022. Epilithic microbial community functionality in deep oligotrophic continental bedrock. Frontiers in Microbiology, 13, 826048.

Pedersen, K., Arlinger, J., Eriksson, S. et al. 2008. Numbers, biomass and cultivable diversity of microbial populations relate to depth and borehole-specific conditions in groundwater from depths of 4–450 m in Olkiluoto, Finland. ISME Journal 2, 760–775.

Purkamo, L., Kietäväinen, R., Miettinen, H., Sohlberg, E., Kukkonen, I., Itävaara, M., Bomberg, M. 2018. Diversity and functionality of archaeal, bacterial and fungal communities in deep Archaean bedrock groundwater. FEMS microbiology ecology, 94(8), fiy116.

Ruff, S.E., Humez, P., de Angelis, I.H. et al. 2023. Hydrogen and dark oxygen drive microbial productivity in diverse groundwater ecosystems. Nature Communications 14, 3194.

Sohlberg, E., Bomberg, M., Miettinen, H., Nyyssönen, M., Salavirta, H., Vikman, M., Itävaara, M. 2015. Revealing the unexplored fungal communities in deep groundwater of crystalline bedrock fracture zones in Olkiluoto, Finland. Frontiers in Microbiology. Frontiers 6, Article 573.

Structural studies of Wiborg rapakivi batholith in Geoenergialoikka -project to support utilization of geothermal energy in Kymenlaakso

C. Patzer[1], T. Luhta[1], M. Cyz[1], E. Koskela[1], V. Laakso[1], M. Malinowski[1], J. Mursu[2] and T.Luoto[1]

[1]Geological Survey of Finland, Espoo
[2]Geological Survey of Finland, Kuopio
E-mail: cedric.patzer@gtk.fi

In Geoenergialoikka project a new concept is tested to find most suitable locations for geothermal wells using geodata and geophysical studies, to increase the probability of success of geothermal projects.

Keywords: geothermal energy, geophysical modelling, Wiborg rapakivi batholith

1. Introduction

Geoenergialoikka (Geoenergy Leap) -project aims to speed up usage of low-carbon geothermal energy. Success of recent medium-deep and deep geothermal energy projects in Finland was assessed in a survey conducted by Geological Survey of Finland (GTK) (Arola et al., 2024). None of the ten projects evaluated achieved their goals within the timeframe and resources initially planned. One of the major obstacles encountered were unexpected weak zones in the bedrock. To enhance the probability of success of geothermal projects, structural geological studies prior to drilling were recommended in the report. The drilling site should first be evaluated based on existing geological and geophysical data, and later more detailed studies can be made on the chosen drilling site. In Geoenergialoikka this concept is tested in Kymenlaakso where Geoenergialoikka partner South-Eastern Finland University of Applied Sciences (XAMK) and project coordinator GTK are building a test and development environment consisting of one 800m deep geothermal well and a test drill hole.

2. Geological and geophysical background

Kymenlaakso is almost entirely on the Wiborg rapakivi batholith (Fig. 1). Structural studies needed for geothermal well location recommendations are thus essentially studies of the structures of the batholith. Main background studies used in preliminary assessments were geophysical interpretations by Elo and Korja (1993) and more recent reprocessing and interpretation of airborne geophysical datasets by Leväniemi and Kuusela (2015). Preliminary detection of possible zones of weakness was based also on GTK's Lineaments 1:500 000 interpretations (available via https://hakku.gtk.fi/) and earthquake data published by the Institute of Seismology University of Helsinki (available via https://www.seismo.helsinki.fi/EQs/query.php).

3. Geophysical studies in Geoenergialoikka

Within Geoenergialoikka we are currently performing two sets of geophysical studies, regional and local. In regional studies (Fig. 1) we aim to study the nature of several major lineaments in the area as well as the depth extent of the rapakivi batholith, an important input in the estimation of heat production. Magnetotelluric (MT) and co-located gravity measurements will be used to derive conductivity and density models, which will shed light on the depth extent and possible lateral variation of the thickness of the batholith. In addition, two reflection seismic lines were

measured to study some major lineaments in Kymenlaakso, and the contact between rapakivi and surrounding rocks.

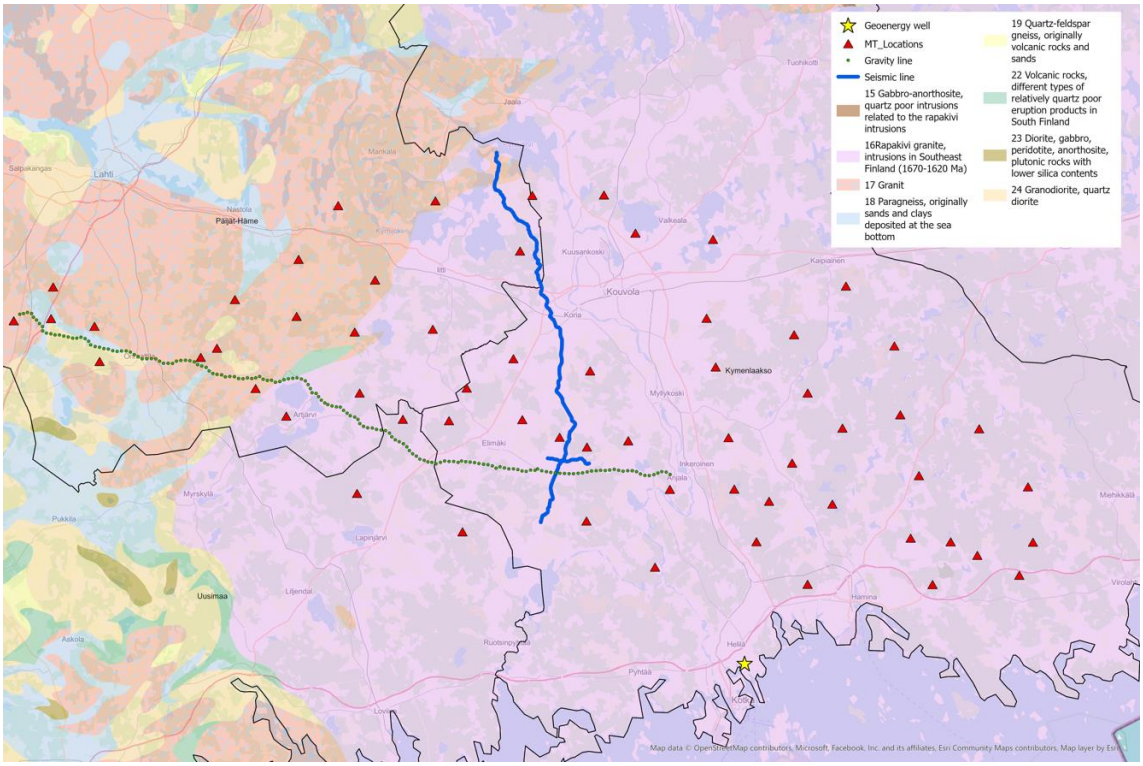

Figure 1. Geoenergialoikka study area in Kymenlaakso, most important lithological units, regional geophysical surveys and geothermal well site hosting local studies.

Local studies include gravity, reflection seismics, and passive seismics measurements at the future geothermal well location to exclude possibility of local weak bedrock zones. After drilling, DAS-VSP measurements will be used to provide detailed picture of the bedrock surrounding the well, and later mapping possible changes due to heat extraction. Geophysical modelling will be supported by an extensive petrophysical study, that will also provide thermal properties of rapakivi for heat production modelling.

4. Acknowledgements

Geoenergialoikka project is partly funded by the European Union Just Transition Fund, just transition for discontinuing the use of peat in regions. Thanks to GTK Geophysics Field Team for making our measurements happen.

References:

Arola, T., Martinkauppi, A., Piipponen, K., Vallin, S. and Wiberg M., 2024. Keskisyvän ja syvän geotermisen energian hankkeet Suomessa. GTK Open File Research Report 20/2024, 22 pages.

Elo, S., and A. Korja. Geophysical interpretation of the crustal and upper mantle structure in the Wiborg rapakivi granite area, southeastern Finland. Precambrian Research 64.1-4 (1993): 273-288.

Leväniemi, H. and Kuusela, J., 2015. Rapakivi structures revealed: reprocessing the Wiborg rapakivi batholith airborne datasets. GTK Archive Report 116/2014, 14 pages.

Contribution of the IAG to Lithosphere Research

M. Poutanen[1]

[1]Finnish Geospatial Research Institute FGI
National Land Survey of Finland
Vuorimiehentie 5, 02150 Espoo, FINLAND
E-mail: markku.poutanen@nls.fi

The International Association of Geodesy (IAG) is a scientific organisation in the field of geodesy. The IAG coordinates, collects, and analyses data from geodetic networks and observing stations. Twelve IAG Services provide the geodetic infrastructure and products for a wide range of disciplines and users. In this presentation, we describe the contributions of IAG products to solid Earth research both globally and regionally.

Keywords: geodesy, geodetic observations, IAG, lithosphere

1. Introduction

Geodesy is the science of determining the shape of the Earth, its gravity field, and its rotation as functions of time. With modern instrumentation and analytical techniques, geodetic methods can observe variations on scales ranging from large, secular trends to very small, transient deformations — all with increasing spatial and temporal resolution, high accuracy, and decreasing latency.

The International Association of Geodesy (IAG), one of the oldest scientific organisations, dates back to 1862 and is a constituent association of the International Union of Geodesy and Geophysics (IUGG) (Poutanen and Rózsa, 2020). The IAG promotes scientific cooperation and research in geodesy on a global scale, coordinating, collecting, and analysing data from geodetic networks and observing stations. The IAG's structure includes several components, such as four Commissions, twelve International Scientific Services, and the Global Geodetic Observing System (GGOS) (IAG, 2024).

The IAG Services are responsible for collecting and analysing observations in their specific fields and generating respective products. As part of the IAG, the Global Geodetic Observing System (GGOS) works together with the IAG Services to facilitate the production of geodetic products that are fundamental to both science and society (GGOS, 2024).

The essential products of geodesy are reliable and up-to-date geodetic reference frames. These are necessary for determining accurate time-dependent coordinates and their temporal variations, as well as for describing the Earth's orientation in space, particularly for GNSS positioning. Equally important is the understanding of global mass redistribution due to the melting of ice sheets and changes in the Earth's geopotential and gravity field. For this we need a gravity reference frame.

In the following sections, we examine some of these services and products more closely and explore how they contribute to solid Earth research.

2. Reference Frames and Crustal Deformation

The accuracy, reliability, and timeliness of the reference frame must be sufficient for monitoring and modelling Earth's rotation and orientation in space, studying deformations of the solid Earth, observing mass variations in geophysical fluids, understanding the dynamic interactions between geophysical fluids and the solid Earth, and determining the precise orbits of Earth-orbiting satellites.

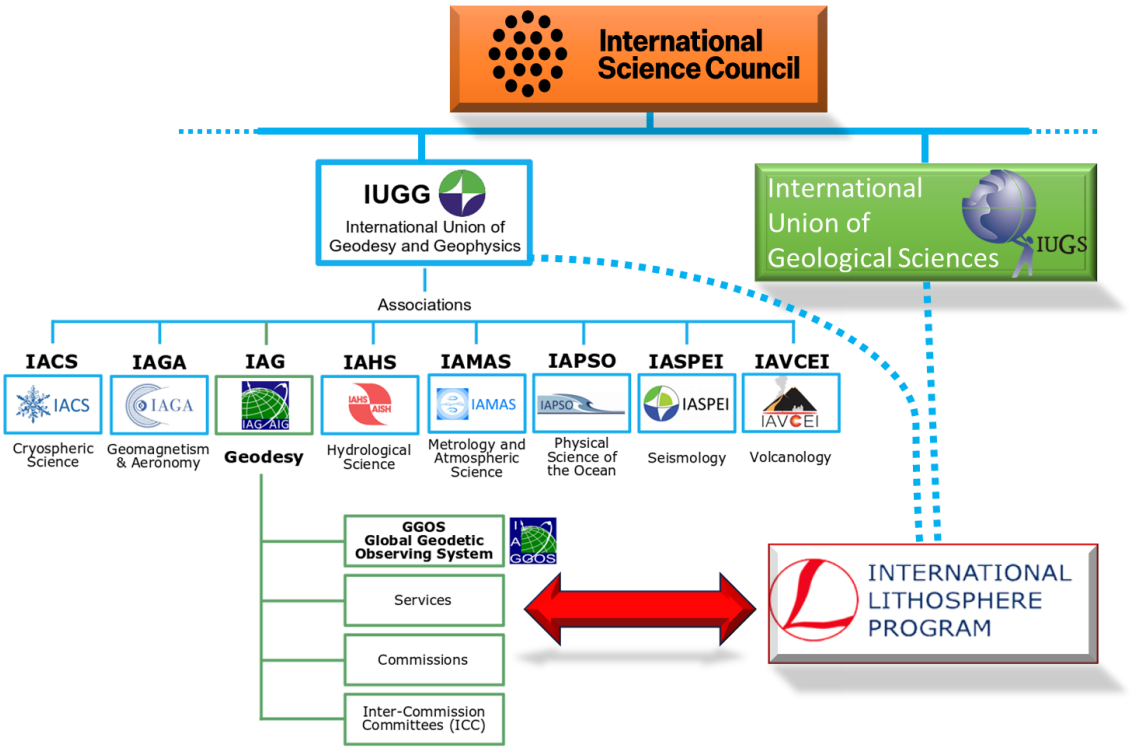

Figure 1. The International Lithosphere Program (ILP) is a joint scientific initiative of the IUGG and IUGS. As one of the associations of the IUGG, the IAG provides crucial data for lithosphere research as well. (IUGG/IAG part of the picture courtesy GGOS, 2024.)

The International Earth Rotation and Reference Systems Service (IERS) collects, archives, and distributes products, including the International Celestial Reference Frame (ICRF), the International Terrestrial Reference Frame (ITRF), Earth orientation information (both long-term and near-real-time), and products related to global geophysical fluids, such as mass and angular momentum distribution.

As shown in Fig. 2, maintaining such a reference frame requires a full set of geodetic techniques and contributions from several IAG Services. The three most important services providing data to IERS for maintaining the ITRF are:

- The International GNSS Service (IGS) provides GNSS data, coordinates, and velocities from more than 500 permanent and continuously operating stations. IGS also plays a critical role in linking other observing techniques at multi-technique sites.
- The International VLBI Service for Geodesy and Astrometry (IVS) supports operations within the Very Long Baseline Interferometry (VLBI) network. The main products of IVS are the scale and orientation of the global network, particularly the Earth Orientation Parameters (EOP), which are crucial for the functionality of GNSS.
- The International Laser Ranging Service (ILRS) contributes to the accurate determination of satellite ephemeris, including GNSS satellites, and to the realisation of the Earth's centre of mass and its temporal variation. This is the origin of the global reference frame.

The accuracy requirement for the ITRF is 1 mm in position and 0.1 mm/year in velocity (Plag and Pearlman, 2010). While this requirement has not yet been fully met, the stability of the latest versions of the ITRF is already close to these demands.

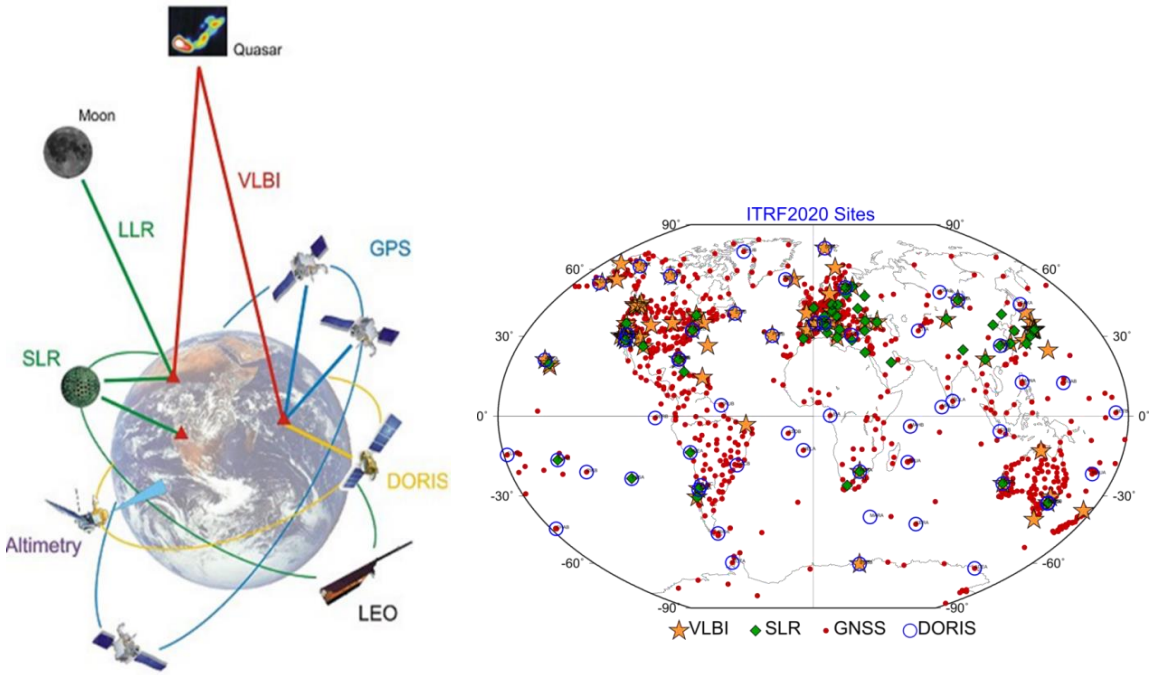

Figure 2. The use of modern **s**pace geodetic techniques is crucial for global reference frames, precise satellite positioning and Earth exploration. The global multi-technique geodetic network is used for creating and maintaining the ITRF. The latest version is ITRF 2020 (Altamimi et al., 2023).

The IAG recommends the International Terrestrial Reference Frame (ITRF) as the standard terrestrial reference frame for positioning, satellite navigation, Earth science applications, and the definition and alignment of national and regional reference frames. The importance of geodetic reference frames has also been recognised by the United Nations. In February 2015, the UN General Assembly adopted a geospatial resolution, "A Global Geodetic Reference Frame for Sustainable Development" (UN, 2015). This work is being continued by the Sub-Committee on Geodesy of the UN Committee of Experts on Global Geospatial Information Management (UN-GGIM) and the UN Global Centre of Excellence (GGCE), where the IAG is a key collaborator.

High accuracy, consistency, and long-term stability are required to precisely monitor global change phenomena such as sea level rise, ice sheet changes, and crustal deformation, as well as for a variety of precise positioning applications. Conversely, the better we understand the geophysical processes affecting the geodetic network, the better we will be able to maintain the reference frame in the future.

3. Gravity data services

Surface deformation models are crucial for the maintenance of geodetic reference frames. In addition to measuring changes in coordinates, these models also contain information about geophysical processes. This includes, for example, active seismic regions, where earthquakes cause displacements in station positions and velocities. Equally important are changes in gravity.

Precise knowledge of the gravity field is fundamental for understanding the Earth's shape, its interior, mass distribution, mass transport, and the dynamics of the mantle and crust. Global gravity field models are indispensable for understanding the Earth system and are also relevant to many other disciplines in the geosciences.

The International Terrestrial Gravity Reference System (ITGRS) is defined by the instantaneous acceleration of free-fall and is complemented by a set of conventional models. The International Terrestrial Gravity Reference Frame (ITGRF) is the realisation of the ITGRS. It is maintained through absolute gravity measurements traceable to SI units (GGOS, 2024).

The International Gravity Field Service (IGFS) serves as an umbrella organisation that coordinates gravity field-related data collection, validation, archiving, and dissemination. The IAG services contributing to the IGFS are ICGEM – International Centre for Global Earth Models, IDEMS – International Digital Elevation Model Service, IGETS – International Geodynamics and Earth Tide Service, ISG – International Service for the Geoid, and BGI – International Gravimetric Bureau.

The global gravity field and its temporal variations have been observed since the early 2000s by gravity satellites. This has allowed us to improve the accuracy of the global geoid model to the centimetre level. Regional and local geoid models, as well as gravity research, benefit significantly from the improved accuracy of the global geoid model.

Ground-based observations are carried out using absolute gravimeters, superconducting gravimeters, spring gravimeters, and the latest instrument, the quantum gravimeter. These are crucial for gravity field research, as the resolution of satellite techniques is limited to around 100 km. Detailed gravimetric data provide insights into the internal structure of the Earth. Lithosphere studies are one of the important disciplines utilising geodetic gravity data.

4. Summary

We have briefly discussed the IAG Services and their connection to solid Earth research. The indirect connections are even more significant, with GNSS positioning as an example. Without the geodetic network and space geodetic observations, precise GNSS positioning would not be possible. However, the relationship works in both directions: the better we understand phenomena in the lithosphere, the more we improve our understanding of the processes that affect the reference frame and gravity networks.

References:

Altamimi, Z., Rebischung, P., Collilieux, X. et al., 2023. ITRF2020: an augmented reference frame refining the modeling of nonlinear station motions. J Geod 97, 47. https://doi.org/10.1007/s00190-023-01738-w

GGOS, 2024. Global Geodetic Observing System. https://ggos.org (Referenced 10.10.2024)

IAG, 2024. International Association of Geodesy, https://iag-aig.org (Referenced 10.10.2024)

Plag, H.-P. and Pearlman, M., 2009 (Eds.). The Global Geodetic Observing System: Meeting the Requirements of a Global Society on a Changing Planet in 2020, Geoscience Books, Springer Berlin. 332 pp

Poutanen, M., and Rózsa, S., 2020 (Eds.). The Geodesist's Handbook 2020. Journal of Geodesy, 94(11), 109. 349 p. https://doi.org/10.1007/s00190-020-01434-z

UN, 2015. United Nations General Assembly resolution 69/266, A global geodetic reference frame for sustainable development A/RES/69/266. http://ggim.un.org/documents/A_RES_69_266_E.pdf

The Lapland Granulite Belt: new P–T–t results and tectonic ideas

J. M. Pownall[1], K.A. Cutts[2], K. Hiltunen[1] and V. Yliknuussi[1]

[1]Department of Geosciences & Geography, University of Helsinki, Gustaf Hällströmin katu 2, Helsinki, Finland
[2]Geological Survey of Finland (GTK), Vuorimiehentie 5, Espoo, Finland
E-mail: jonathan.pownall@helsinki.fi

The Paleoproterozoic (*c.* 1900 Ma) Lapland Granulite Belt (LGB) comprises extensive garnet-sillimanite metapelitic gneisses hosting mafic opx-bearing sheet-like intrusive bodies. Here we present (1) new field observations of the LGB and contact relations with adjacent units; (2) *in situ* Lu-Hf garnet ages for several LGB samples; and (3) the results of preliminary phase equilibria modelling using MAGEMin (Riel et al., 2022), utilising major element EPMA maps analysed with XMapTools software (Lanari et al., 2014). These new results tentatively indicate peak metamorphic conditions of 830–900°C at 6.5–8.0 kbar at *c*. 1919 ± 10 Ma. Tectonic models involving underplating by associated anorthositic bodies will be explored as a mechanism for achieving hot and widespread granulite-facies conditions.

Keywords: Lapland, Paleoproterozoic, granulite, Lu-Hf, garnet, thermobarometry

1. Background

The Lapland Granulite Belt (LGB), a Paleoproterozoic (circa 1910–1880 Ma) granulite-facies metamorphic complex, extends across arctic Finland, Norway, and Russia's Kola Peninsula (see Fig. 1). Studied in detail by Eskola (1952), the Finnish exposures of these rocks were pivotal in defining granulites as a distinct metamorphic facies. The complex includes extensive and fairly monotonous grt + sill ± crd pelitic migmatites containing centimeter- to kilometer-scale enderbitic (qtz + pl + opx ± cpx) and noritic (pl + opx ± hbl) layers, which were emplaced as mafic intrusions (Tuisku et al., 2006). Notably, the southwestern edge of the belt features a significant anorthosite body, known as the Angeli Anorthosite.

The 'Inari Orocline' (Lahtinen and Huhma, 2019) is concave along its northeastern edge (see Fig. 1). This arc is flanked by the Archean–Paleoproterozoic Karelian Craton to the southwest and the Archean Inari Craton to the northeast. The convergence of these cratons around 1930–1910 Ma (Daly et al., 2006; Lahtinen and Huhma, 2019) is argued to have driven predominantly collisional orogenesis of the intervening supracrustal rocks, leading to prolonged high-temperature regional metamorphism and melting (approximately 850°C, ~7 kbar) during a single, extended (~60 Myr) tectonic cycle (Tuisku et al., 2006).

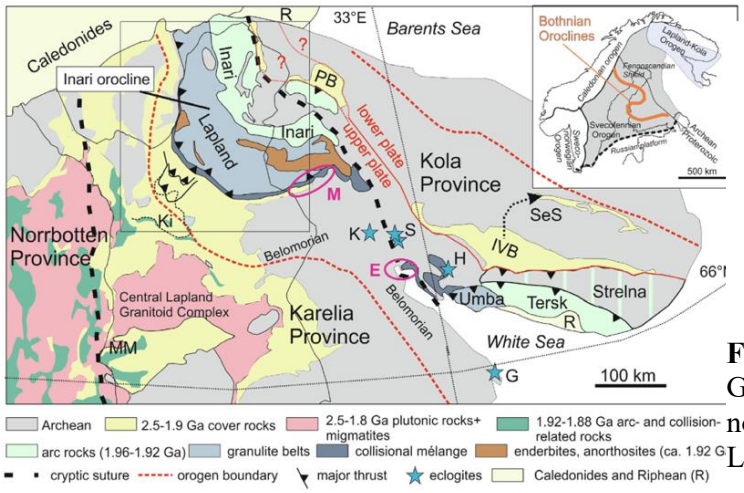

Figure 5. The Lapland Granulite Belt location within northern Fennoscandia (from Lahtinen and Huhma, 2019)

2. Previous work and aims of current study

Previous studies of the Lapland Granulite Belt's metamorphic history primarily concentrated on P–T characterisation by phase equilibria modelling of typical bulk compositions (Hölttä and Heilimo, 2017) or by petrogenetic grid analysis and cation exchange thermometry (Tuisku et al., 2006); however, detailed sample-specific phase equilibria modeling, trace-element thermometry, and elemental mapping techniques have not yet been applied to these metamorphic rocks.

In this study, we introduce new field observations, Electron Probe Micro Analyzer (EPMA) maps, P–T modeling, and *in situ* Lu-Hf garnet dating for a collection of garnet-bearing granulites and mafic enderbites from the Lapland Granulite Belt (specifically the Inari, Ivalo, and Kárášjohka areas) and the neighboring Inari Terrane (including the adjoining Kaamanen Complex). The aim of this study is to determine higher-resolution pressure–temperature–time (P–T–t) histories for different components of the LGB in order to better understand the tectonic history for the Lapland region, and more broadly for high-temperature Paleoproterozoic orogens.

3. New Lu-Hf garnet ages

In situ Lu-Hf garnet geochronology (following the method of Simpson et al., 2021) yielded ages for Lapland Granulite Belt granulites (1919 ± 16 Ma) and adjacent Kaamanen Complex gneisses (1919 ± 10 Ma; Fig 2a) that are consistent within uncertainty, and consistent also with previously reported Lapland granulite U-Pb zircon ages (1919 ± 3 Ma; Tuisku and Huhma, 2006).

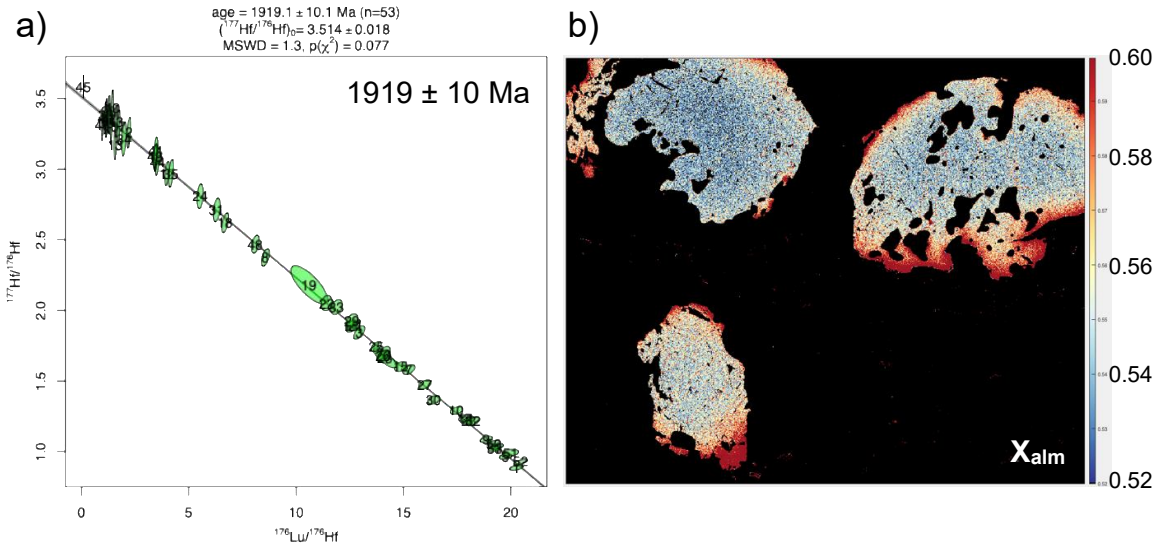

Figure 2. a) Inverse Lu–Hf isochron plot of sample LL20-28 and calculated age of 1919 ± 10 Ma; **b)** EPMA element map of sample LL20-28, processed by XMapTools, displaying only garnet and its almandine ($Fe_3Al_2Si_3O_{12}$) content (X_{alm}).

4. New P-T results from phase equilibria modelling

Thin sections of three LGB samples (2 metapelites and 1 enderbite), from which Lu-Hf garnet dating has been performed, have been mapped for major element chemistry by electron microprobe (EPMA) at HelLabs, University of Helsinki, with the maps being analysed and characterised by XMapTools software (Lanari et al., 2014). Local bulk compositions calculated

by XMapTools have been modelled by MAGEMin (Riel et al., 2022), a newly-developed Gibbs free energy minimisation programme, to produce P–T pseudosections. P–T path segments interpreted from these pseudosections are very similar between all three samples. Modelled $X_{almandine}$ and X_{pyrope} contents of zoned garnets (e.g., Fig. 2b) indicate peak P-T conditions of 830–900°C at 6.5–8.0 kbar, with the rocks cooling and decompressing first to ~750°C at ~4–6 kbar (summarised in Fig. 3). Garnet–orthopyroxene cation exchange thermometry applied to the enderbitic sample suggests higher peak temperatures, greater than 900°C. These results are in broad agreement with Tuisku et al. (2006).

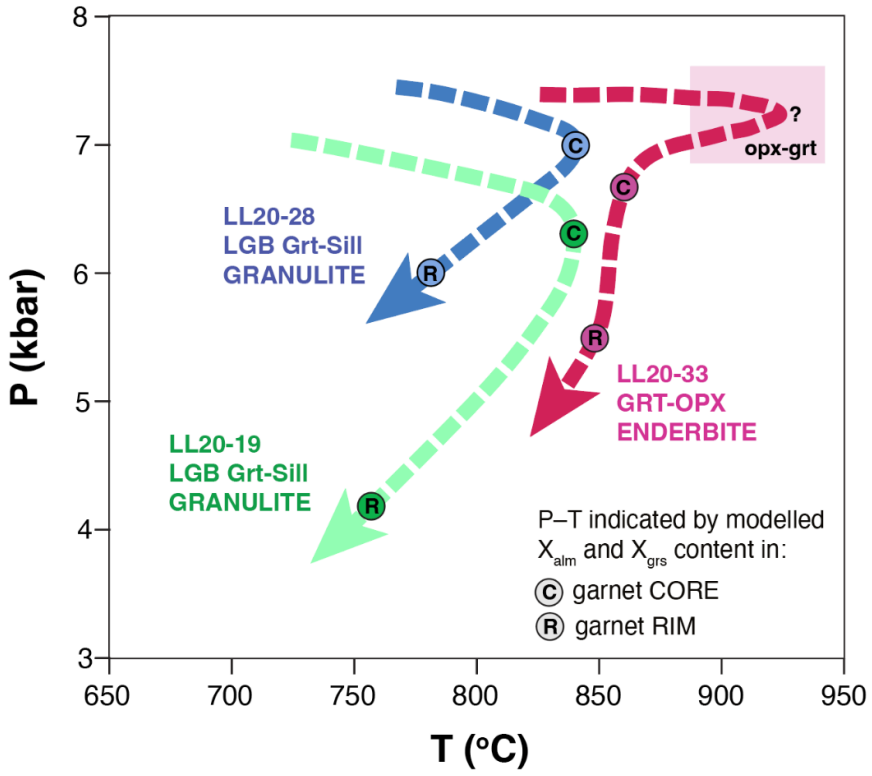

Figure 3. Summary of interpreted pressure-temperature (P–T) paths determined by phase equilibria modelling (MAGEMin P–T pseudosections, not shown here) for two garnet-sillimanite granulite samples (LL20-19 and LL20-28) and one garnet-orthopyroxene enderbite sample (LL20-33). The 'C' and 'R' circles mark the P–T condition indicated by modelled almandine (X_{alm}) and grossular (X_{grs}) content of garnet in core and rim regions, respectively. The pink 'opx-grt' box indicates the approximate temperature results of opx-grt thermometry (multiple calibrations), calculated for a 7 kbar pressure.

5. Current thoughts and tectonic ideas to further test

This project is very much a work-in-progress. These new P–T–t results, recording a high-temperature metamorphic event (830–900°C; 6.5–8.0 kbar) at c. 1919 Ma appear to so far support the findings of previous studies (Tuisku and Huhma, 2006; Tuisku et al., 2006).

However it is not clear by which mechanism these granulite-facies conditions were generated. Recent fieldwork (August 2024) has shown the Angeli Anorthosite body shares finely inter-banded sheared contacts with LGB granulites along the southwestern boundary.

The anorthosites were also found to structurally underlie the LGB granulites. It is quite possible that the anothosite body is far larger than it's outcrop area, potentially underplating a large portion of the granulite complex at least in the southwest. We are exploring the model that (1) these anorthosites are instrumental in supplying heat to the LGB rocks, and that (2) potentially, the mantle melt region from which the anothosites must have fractionated may have also generated the mafic magmas occuring today as the enderbitic-noritic component of the LGB. Under this scenario, major lithospheric extension–possibly by some form of slab rollback or trench retreat–was likely the fundamental driver of mantle exhumation, melting, and mafic sill emplacement. The project will continue to test this hypothesis.

References:

Daly, J.S., Balagansky, V.V., Timmerman, M.J., Whitehouse, M.J., 2006. The Lapland–Kola orogen: Palaeoproterozoic collision and accretion of the northern Fennoscandian lithosphere, in: Gee, D.G., Stephenson, R.A. (Eds.), European Lithosphere Dynamics. Geological Society of London.

Eskola, P., 1952. On The Granulites Of Lapland, American Journal of Science, 250, 133–171.

Hölttä, P., Heilimo, E., 2017. Metamorphic Map of Finland, Geological Survey of Finland Special Paper, 60, 77–128.

Lahtinen, R., Huhma, H., 2019. A revised geodynamic model for the Lapland-Kola Orogen, Precambrian Research, 330, 1–19.

Lanari, P., Vidal, O., De Andrade., V., Dubaq, B., Lewin, E., Grosch, E.G., Schwartz., S., 2014. XMapTools: A MATLAB-based program for electron microprobe X-ray image processing and thermobarometry, Computers & Geosciences, 62, 227–240.

Riel, N., Kaus, B.J.P., Green, E.C.R., Berlie N., 2022. MAGEMin, an Efficient Gibbs Energy Minimizer: Application to Igneous Systems, Geochemistry, Geophysics, Geosystems, 23, 10.1029/2022GC010427.

Simpson, A., Gilbert, S., Tamblyn, R., Hand, M., Spandler, C., Gillespie., J., Nixon, A., Glorie., S., 2021. In-situ Lu–Hf geochronology of garnet, apatite and xenotime by LA ICP MS/MS, Chemical Geology, 577, 120299.

Tuisku, P., Huhma, H., 2006. Evolution of migmatitic granulite complexes: Implications from Lapland Granulite Belt, Part II: Isotopic dating, Bull Geol Soc Finland 78, 143–175.

Tuisku, P., Mikkola, P., Huhma, H., 2006. Evolution of migmatitic granulite complexes: Implications from Lapland Granulite Belt, Part I: Metamorphic geology, Bull Geol Soc Finland 78, 71–105.

International Union of Geodesy and Geophysics (IUGG)

S. Silvennoinen[1*], T. Luoto[2] and the Finnish National Committee of Geodesy and Geophysics

[1]Department of Geosciences and Geography, University of Helsinki, Helsinki, Finland
[2]Geological Survey of Finland, Espoo, Finland
[*]Corresponding author, e-mail: sonja.silvennoinen@helsinki.fi

Structure and strategy

The International Union of Geodesy and Geophysics (IUGG), founded in 1919, is a non-governmental scientific organization dedicated to advancing, promoting, and communicating knowledge of the Earth, its space environment, and the dynamical processes causing change. IUGG promotes and coordinates scientific studies (physical, chemical, and mathematical) of the Earth and its environment in space and encourages application of this knowledge to societal needs, such as mineral commodities, mitigation of natural hazards, and environmental preservation. In particular, IUGG focuses on the physics and chemistry of the Earth's interior, surface, fresh waters, cryosphere, oceans and atmosphere, as well as relevant studies of other planets.

Currently, IUGG has 73 member countries in Africa, Asia, Europe, North and Central America, Oceania, and South America and scientists in the member countries can participate in IUGG activities through the National Committees of IUGG. IUGG is composed of eight semi-autonomous Associations: International Association of Cryospheric Sciences (IACS), International Association of Geodesy (IAG), International Association of Geomagnetism and Aeronomy (IAGA), International Association of Hydrological Sciences (IAHS), International Association of Meteorology and Atmospheric Sciences (IAMAS), International Association for the Physical Sciences of the Oceans (IAPSO), International Association of Seismology and Physics of the Earth's Interior (IASPEI), and International Association of Volcanology and Chemistry of the Earth's Interior (IAVCEI). IUGG also has Union Commissions and a Working Group that promote research on particular interdisciplinary problems: Climatic and Environmental Change (CCEC), Data and Information (UCDI), Geophysical Risk and Sustainability (GRC), Mathematical Geophysics (CMC), Planetary Sciences (UCPS), Study of the Earth's Deep Interior (SEDI), and the Working Group on History (WGH). Through the Associations and Commissions, IUGG undertakes research, assembles observations, gains insights, coordinates activities, liaises with other scientific bodies, plays an advocacy role, contributes to education, and works to expand capabilities and participation on a global scale.

Endeavours

The IUGG Associations and Commissions run frequent symposia and workshops on timely topics in the respective disciplines and the IUGG General Assembly is arranged every four years. IUGG has initiated many collaborative efforts that have led to highly productive interdisciplinary research programs, e.g. the International Lithosphere Program (ILP – a joint activity of IUGG and the International Union of Geological Sciences), Global Geodetic Observing System (GGOS), Extreme Natural Hazards and Societal Implications (ENHANS), International Year of Deltas (IYD), Mathematics of Planet Earth (MPE), World Data System (WDS), World Climate Research Program (WCRP), and International Geosphere-Biosphere Program (IGBP). IUGG also runs publishing activities, the Special Publication Series of IUGG (Cambridge University Press) as well as Association-affiliated journals and books, among them

the Journal of Geodesy (IAG), the Hydrological Sciences Journal (IAHS), and the Bulletin of Volcanology (IAVCEI).

To best respond to the challenges of the changing Earth environment and society, special attention is paid to (1) encouraging early career scientists to participate in international science activities, e.g. through appropriate Association-level strategies and travel grants; (2) enhancing the possibilities of countries and agencies to provide free access to data and information, and to initiate collaborative projects with a regional and global scope; and (3) contributing to the education of future generations of geoscientists, taking into account challenges and inequities such as gender inequalities, the need to offer education for individuals with diverse backgrounds, and the need for greater cross-disciplinary knowledge. The Finnish National Committee of Geodesy and Geophysics has representatives for each of the Associations of IUGG and Finland has been actively involved in the activities of IUGG from the outset.

Online resources

https://geofysiikanseura.yhdistysavain.fi/kansalliskomiteat/geodeettis-geofysikaalinen-kansa/
https://linkedin.com/company/sggkk/

Tectonic assembly of the SW Fennoscandian margin

T. Slagstad[1], E.A.F. Østnes[2], B.E. Sørensen[2]

[1]Geological Survey of Norway, Trondheim, Norway
[2]Department of Geosciences, NTNU, Trondheim, Norway
E-mail: trond.slagstad@ngu.no

The late Mesoproterozoic Sveconorwegian Orogeny reworked the southwestern margin of the Fennoscandian Shield between ca. 1140 and 930 Ma. The last decade or so has seen relatively vigorous debate about the tectonic significance of the Sveconorwegian Orogeny, with some workers arguing that it represents continent-continent collision and amalgamation of Baltica to the Rodinian supercontinent, whereas others argue that it formed as part of an accretionary margin requiring the presence and subduction of a large, long-lived ocean. In a series of recent papers (Slagstad et al., 2020, 2024), we showed that the pre-1020 Ma orogenic evolution must have taken place some unconstrained distance west of the present-day Norwegian coastline and involved a series of accretionary events. Between ca. 1020 and 990 Ma, reduced magmatic activity and high-pressure metamorphism at the eastern front of the orogen marks wholesale thrusting of the Sveconorwegian Province at least 500 km eastward onto (or into) SW Fennoscandia. The lost lithosphere that was overridden by the Sveconorwegian Province was most likely continental, suggested by the lack of arc magmatism and a transition to less radiogenic Hf isotopic compositions after 980 Ma. The presence of this subducted continental lithosphere could explain the anomalously low seismic velocities observed under much of the Sveconorwegian Province. Here, we present the first direct evidence of the hypothesised lateral shear zone that accommodated juxtaposition of the Sveconorwegian lithospheric block with more interior parts of Fennoscandia.

Keywords: Fennoscandia, Sveconorwegian, Mesoproterozoic, crustal growth, continental subduction

1. Introduction

Two years ago, we compiled a large database of crystallisation ages and Hf data from Precambrian basement in Norway, Sweden and Finland, and supplemented the database with 90 new zircon U–Pb/Hf analyses, spanning geographically from N Norway (Troms) to SW Norway. The goal of the work was to provide new information about the ca. 1.8–1.4 Ga growth of the western Fennoscandian margin. However, the distribution of ages and Hf compositions showed that the Sveconorwegian Province represented a major deviation from models involving more or less westward growth in an Andean-type setting (Figures 1 and 2). A further compilation of pre- to syn-Sveconorwegian magmatism (1.3–0.9 Ga) also showed contrasts in pre- and early-orogenic evolution, consistent with significant separation of the Sveconorwegian Province and its foreland until between 1020 and 990 Ma. The data pointed to late-Mesoproterozoic reworking of the margin, with translation of a large lithospheric block, constituting most of the Sveconorwegian Province, over distances of several 100 km. Here, we present new field observations that document the presence of a several kilometres wide and almost 100 km long sinistral shear zone that likely accommodated at least 500 km of eastward movement (constrained to west of the Norwegian coastline, as explained below).

2. Geological background

The Sveconorwegian Orogeny was a long-lived orogenic event and is commonly said to have lasted between ca. 1140 and 930 Ma. However, a defining feature of the orogeny is the disparate tectonic histories of tectonically bound units making up the orogen. For example, high-pressure metamorphism in the central Bamble and Kongsberg lithotectonic units between 1140 and 1120 Ma took place while extension and sedimentation were taking place in the Telemark unit. Sedimentation in Telemark ceased at ca. 1100 Ma, coinciding with rapid cooling of Bamble at

this time, suggesting thrusting of Bamble (and Kongsberg) onto Telemark at this time. Other important contrasts include high-pressure metamorphism in the Eastern Segment at ca. 990 Ma, whereas the crust in the western part of the orogen appears to have remained thin and characterised by high- to ultrahigh-temperature metamorphism and voluminous magmatism. This long-lived orogenic evolution and contrasts in metamorphic and magmatic histories formed the basis for reinterpreting the Sveconorwegian Orogeny as an accretionary rather than collisional orogen.

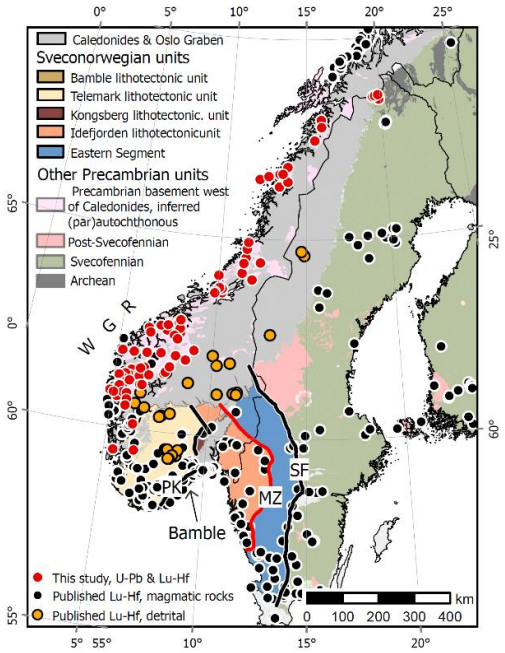

Figure 1. Simplified geologic map of western Fennoscandia and the Sveconorwegian Province with new samples in red and previously published Lu–Hf isotopic data in black and orange. Thick, black lines are Sveconorwegian shear zones. MZ–Mylonite Zone, PK–Porsgrunn–Kristiansand Shear Zone; SF–Sveconorwegian Front, WGR–Western Gneiss Region.

3. Zircon U–Pb and Hf data, ages of metamorphism constrain allochthoneity

Figure 2 shows compilations of zircon U–Pb crystallisation ages and Hf isotopic compositions (model ages, T_{DM}s). The map shows that contrary to a gradual younging towards the west (along profile A–A') in central Norway and Sweden, there is a jump from >1650 Ma crust in the Eastern Segment to <1650 Ma crust in the structurally overlying Idefjorden unit (profile C–C'). The jump coincided with the Mylonite Zone, a major tectonic zone associated with top-to-east thrusting around 990 Ma. Although less sharp, a similar jump in crystallisation age is observed along the north–south B–B' profile in the western gneiss region. These jumps roughly delineate the Sveconorwegian Province, with the exception of the Eastern Segment, and the Hf model age map shows that the Province is characterised by more juvenile crust than observed north and east of the Province. Figure 3 shows that this age and isotopically defined domain is also characterised by a magmatic and metamorphic history that is distinct from surrounding crust. For example, voluminous magmatism between ca. 1180 and 980 Ma is lacking north and east of the Sveconorwegian Province, as is high-grade metamorphism between 1140 and 990 Ma. After ca. 990 Ma eastward thrusting on the Mylonite Zone, a similar magmatic and metamorphic record exists both within and around the Province.

The contrasting crystallisation ages, isotopic composition, metamorphic and magmatic history inside and outside the Sveconorwegian Province is most easily explained if we assume that the Sveconorwegian Province is allochthonous.

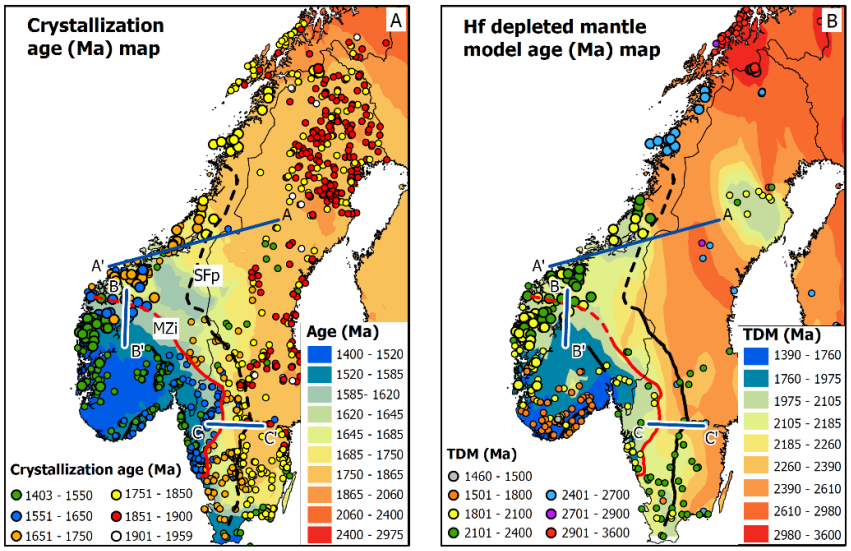

Figure 2. (A) U–Pb crystallisation ages plotted on a crystallisation-age map based on interpolation between all data points. (B) Median, two-stage depleted mantle Hf model ages (T_{DMS}) plotted on an interpolated grid of T_{DMS}s. Profiles A–A', B–B', and C–C' highlight trends and steps in ages and Hf isotopic compositions.

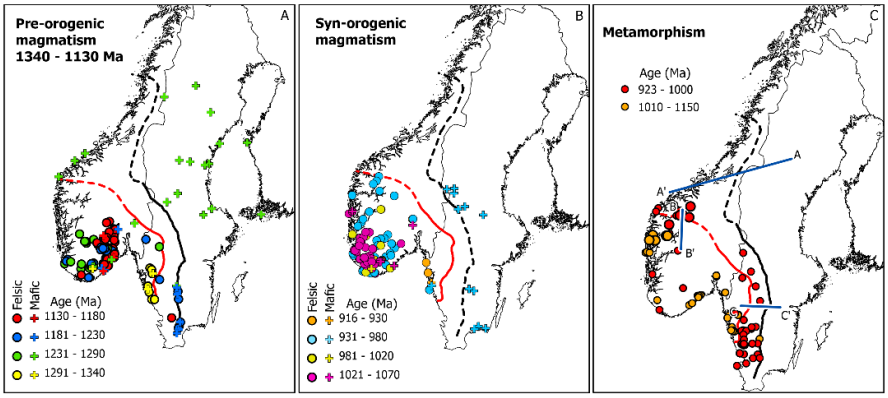

Figure 3. (A) Age and distribution of pre-Sveconorwegian (>1130 Ma) magmatism, subdivided into felsic and mafic compositions. Intermediate compositions are subordinate. (B) Age and distribution of syn-Sveconorwegian (1130–915 Ma) magmatism, subdivided into felsic and mafic compositions. (C) Map showing the distribution of Sveconorwegian metamorphic ages, divided into pre- and post-1000 Ma.

4. Tectonic model

One persistent, puzzling feature has been that roughly north–south trending major structures within the Province disappear under the Caledonian nappes and do not reappear in basement windows northwest of the nappes. It now appears that most of these features relate to an earlier period of orogenic activity, involving significant north-south lateral shearing, that took place outboard of the western coastline of Norway. This is illustrated in Figure 4, which shows that the piece of lithosphere currently referred to as the Sveconorwegian Province has crystallisation ages and isotopic compositions consistent with formation outboard of the present-day western coastline of Norway. During the Sveconorwegian Orogeny, this lithospheric block was thrust eastwards, overriding the pre-existing lithosphere there.

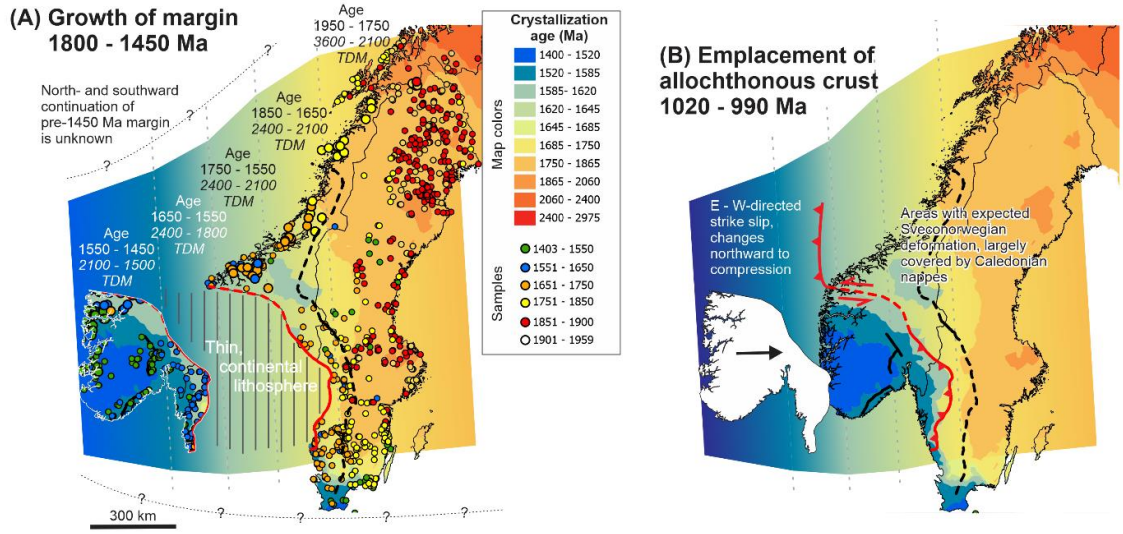

Figure 4. Schematic tectonic model. (A) Westward growth of the margin between 1800 and 1450 Ma, most likely in a retreating arc setting. Assuming dominantly westward growth of the margin, as indicated by crust outside the Sveconorwegian Province, the ages and isotopic compositions of rocks constituting the Province appear to have formed at least 500 km west of their current position. (B) Between ca. 1020 and 990 Ma, units located in both hanging and footwall to the Mylonite Zone experienced strong deformation and high-grade metamorphism, suggesting that they were juxtaposed around this time. No arc magmatism is recorded during this period, suggesting that the intervening, subducted crust was continental rather than oceanic.

5. Conclusions

The Sveconorwegian lithosphere most likely formed west of the present-day Norwegian coastline and the first 150 Myr of Sveconorwegian orogenesis took place here, prior to eastward thrusting of the entire lithospheric block between 1020 and 990 Ma. Although the preserved Sveconorwegian Province has a tectonic history clearly compatible with accretionary tectonics, further work is needed to elucidate the character of the larger ("pan-Sveconorwegian") orogenic system.

6. References

Slagstad, T., Marker, M., Roberts, N.M.W., Saalmann, K., Kirkland, C.L., Kulakov, E., Ganerød, M., Røhr, T.S., Møkkelgjerd, S.H.H., Granseth, A., Sørensen, B.E., 2020. The Sveconorwegian orogeny – Reamalgamation of the fragmented southwestern margin of Fennoscandia. Precambrian Research 350, 105877.

Slagstad, T., Skår, Ø., Bjerkan, G., Coint, N., Granseth, A., Kirkland, C.L., Kulakov, E., Mansur, E., Orvik, A.A., Petersson, A., Roberts, N.M.W., 2024. Subduction and loss of continental crust during the Mesoproterozoic Sveconorwegian Orogeny. Precambrian Research 409, 107454.

Critical raw materials of the Estonian Precambrian basement: Any new targets?

A. Soesoo[1,2,3], S. Nirgi[1] and J. Solano Acosta[2]

[1]Geological Survey of Estonia, F.R. Kreutzwaldi 5, 44314 Rakvere, Estonia
[2]Institute of Geology, Tallinn University of Technology, Ehitajate tee 5, Tallinn, 19086, Estonia
[3]Department of Geology, University of Tartu, Ravila 14a, 50411, Tartu, Estonia
E-mail: alvar.soesoo@gmail.com

In this presentation, we will describe the geology of the Estonian Precambrian basement rocks and provide an overview of basement metallogenesis, along with new directions for further studies. We will also present new data on the Märjamaa rapakivi, which reveals high concentrations of rare earth elements (REEs).

Keywords: Critical metals, mineralisation, Precambrian basement, Estonia

1. The Precambrian basement of Estonia

The Estonian Paleo- to Meso-Proterozoic metamorphic and igneous rock basement can be regarded as a southern extension of the Fennoscandian Shield within the East European Craton. It consists of two major units: amphibolite facies rocks in northern Estonia and primarily granulite facies rocks in southern Estonia. These rock complexes are similar to those found in southern Finland. Since the crystalline rocks are covered by a sedimentary layer that ranges from 100 to 780 meters in thickness, geological information about the crystalline rocks mainly derives from studies of drill core samples and geophysical investigations (Puura et al. 1983; Soesoo et al. 2004; Bogdanova et al. 2015).

Based on geophysical, petrological, and geochemical studies, the Estonian basement can be divided into two primary geological units: the North Estonian amphibolite facies unit and the South Estonian granulite facies unit. These units are separated by the Paldiski-Pskov tectonic zone. The basement also includes six structural-petrological zones: the Tallinn, Alutaguse, Jõhvi, West-Estonian, Tapa, and South-Estonian zones. These zones vary in rock composition, genesis, geophysical properties, and degree of metamorphism.

2. Metal resources in the Lower Proterozoic rocks

Over the past century, more than 500 boreholes have been drilled to explore the crystalline basement of Estonia. A significant portion of these drill cores is preserved and available at the Geological Survey of Estonia rock archive. Between 1990 and 2018, however, very few studies of the crystalline basement were conducted. Recent investigations have greatly enhanced our understanding of metal genesis and the overall geology of the basement.

Historically, occurrences of several metals have been documented (Figure 1). Reported metals include copper, zinc, lead, iron, and others, along with known occurrences of gold and silver. Among the magnetic anomalies identified in the basement, the most notable is the Jõhvi magnetic anomaly, which was discovered as early as 1924. These anomalies are primarily attributed to magnetite-rich gneisses (the Jõhvi and Sakusaare anomalies) and sulphide-graphite-bearing gneisses (the Uljaste, Haljala, and Assamalla anomalies). The first drill holes targeting the Jõhvi anomaly were drilled between 1937 and 1939.

Drill core studies indicate that the complex of magnetite-rich gneisses may reach thicknesses of up to 100 meters and exhibit a wide range of chemical compositions, with total iron content varying from 15% to 46% by weight. The rocks also show unusually high manganese content, ranging from 1% to 6% by weight. Large-scale mineralisation is associated

with specific rock types, such as garnet-pyroxene, pyroxene-garnet, pyroxene gneisses, and garnet-amphibole, amphibole-garnet, and biotite-amphibole gneisses (Soesoo et al. 2004; Soesoo et al. 2021; Nirgi and Soesoo, 2021).

Sulphide mineralisation, including associations of pyrite and pyrrhotite, as well as minor chalcopyrite, arsenopyrite, galena, sphalerite, and iron arsenide (loellingite), indicates a complex and possibly multiphase mineralisation history for these rocks. Chalcopyrite typically occurs alongside pyrite and pyrrhotite, while loellingite and arsenopyrite are often associated with quartz-feldspar veining, which may also contain gold and silver (Nirgi and Soesoo 2021). The Jõhvi rocks bear similarities to those found in Bergslagen, Sweden, and potentially to Orijärvi in southern Finland. Significant anomalies of sidero-chalcophile sulphide-graphite-bearing gneisses are also present in other regions of northern Estonia, with copper, lead, and zinc concentrations reaching as high as 5.6% in some areas (Figure 1).

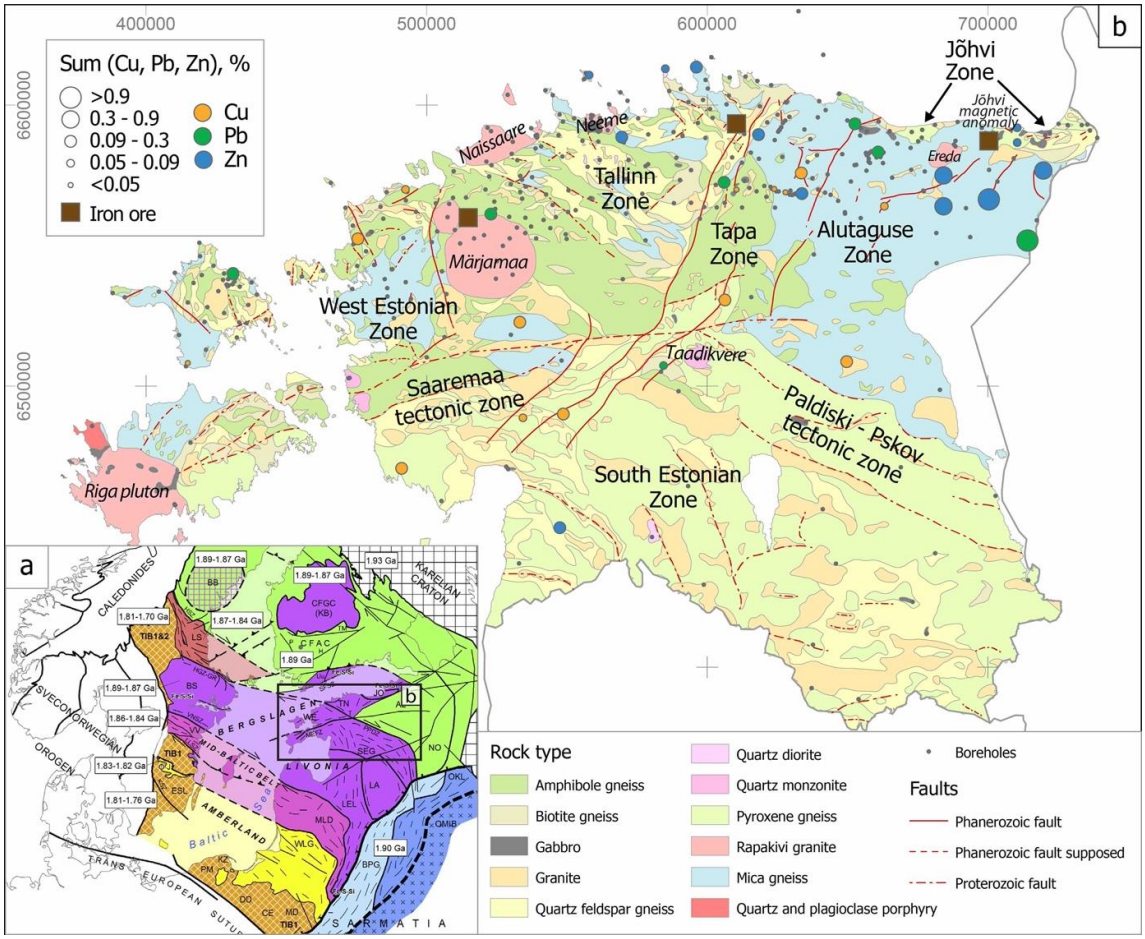

Figure 1. Main geological zones of the Estonian basement and metal occurrences.

3. New studies of historical drill cores

Studies of both historical and recent drill cores have become increasingly important for the exploration of critical minerals. The archive contains approximately ten kilometres of crystalline basement drill core, and the research goal is to analyse these cores for critical and other base metals. A new study employs a modern automated scanning technique using the Geotek MSCL-XYZ instrument to identify critical raw materials and associated elements in selected drill cores from northern Estonia.

The first phase of the study focused on crystalline rock intervals from 22 promising cores to collect comprehensive geochemical, mineralogical, and petrophysical data. Currently, about three kilometres of drill core have been scanned. As a result, various element associations linked to critical raw materials were identified, including mineral systems such as Ni-Co-Cr, Mo-W-Bi, Sn-Zn-Cd, Cu-Ni, Nb-Y-P, K-Sn-Rb-Ga, and Au-Ag-As-Sb-Bi-W-Se-Sn. The study has produced a list of specific depth intervals with mineral potential that warrant further investigation (Figure 2).

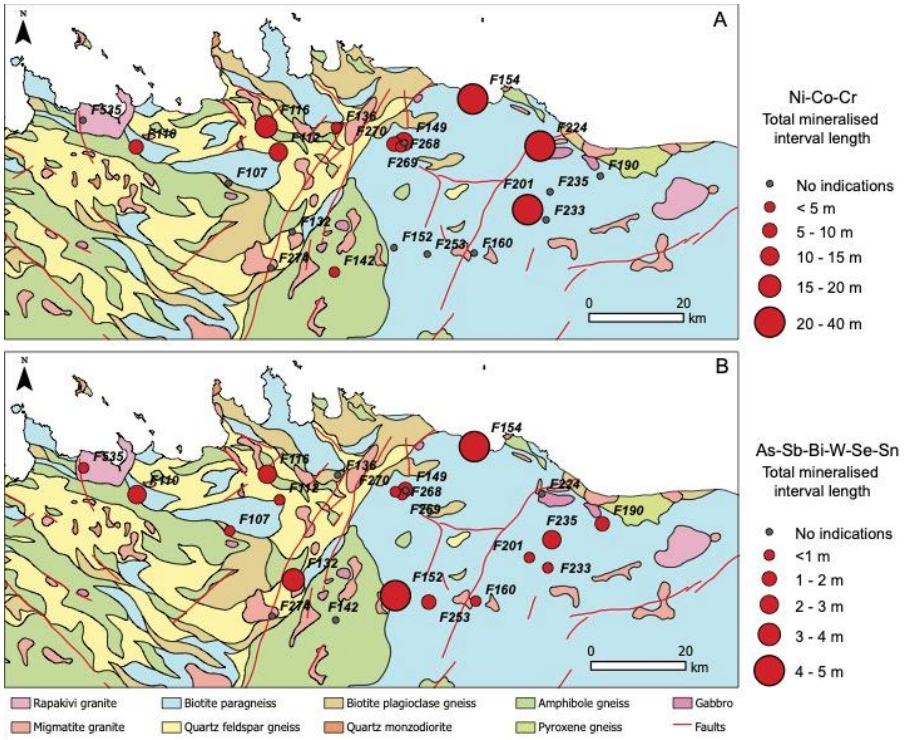

Figure 2. The results of the Geotek MSCL-XYZ instrument scans for critical metals in the 22 selected drill cores in NE Estonia.

4. The Estonian rapakivi granite plutons: REE-rich Märjamaa pluton

The Fennoscandian anorogenic anorthosite-rapakivi plutons developed between 1.67 and 1.45 billion years ago within the Svecofennian juvenile crust. Geophysical studies and drilling have revealed five stock-like rapakivi granite plutons in Estonia: Naissaare, Neeme, Märjamaa, Taebla, and Ereda, all located beneath a 150 to 300-meter-thick late Neoproterozoic and Palaeozoic sedimentary cover (Soesoo, 1993).

The Märjamaa pluton consists of porphyritic potassium-rich granitoid rocks. Its center is composed of highly magnetic granodiorite (quartz monzonite; 62-68 wt% SiO_2), which is surrounded by porphyritic hornblende-bearing biotite granite. We propose that the Märjamaa pluton formed as a result of intraplate magmatism through multiple intrusive phases. The main phase of the intrusion occurred at 1629 ± 7 million years ago, followed by a second phase at 1626 ± 3 million years ago, and a third phase, which includes the Kloostri satellite, at 1622 ± 4.9 million years ago (A. Soesoo, unpublished data; C. Potagin, MSc thesis).

Recent studies have also established high to very high concentrations of rare earth elements (REEs) in certain parts of the Märjamaa pluton, with total REE levels reaching up to 3600 ppm (La up to 840, Ce – 1468, Pr – 187, Nd – 700, Sm – 112, Gd – 93, Tb – 12, Dy – 54,

Ho – 11, Er – 26). This suggests a potential new target for REEs related to specific granitoid magmatism.

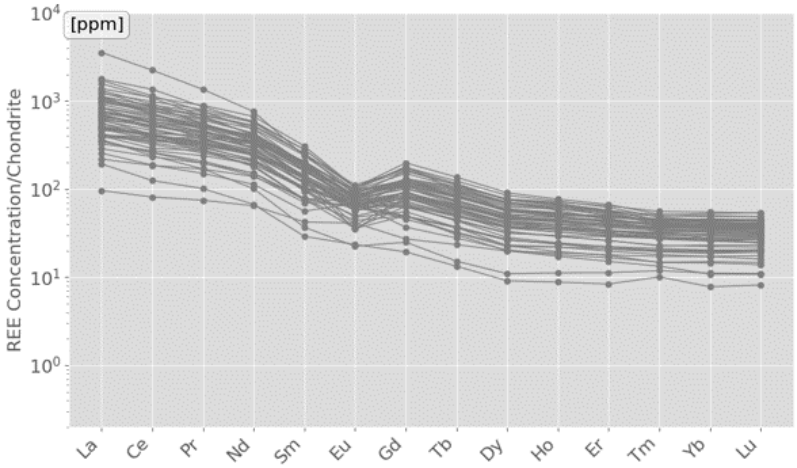

Figure 3. Chondrite-normalised REE compositions of the Märjamaa rapakivi granites.

5. Conclusions

The Precambrian basement rocks of Estonia exhibit geological and metallogenic similarities to those in Bergslagen, Sweden, and possibly Orijärvi in southern Finland. A modern automated scanning technique using the Geotek MSCL-XYZ instrument has identified various mineral systems, including Ni-Co-Cr, Mo-W-Bi, Sn-Zn-Cd, Cu-Ni, Nb-Y-P, K-Sn-Rb-Ga, and Au-Ag-As-Sb-Bi-W-Se-Sn. Additionally, a recent geochemical study revealed high to very high concentrations of rare earth elements (REEs) in certain sections of the Märjamaa rapakivi pluton, with total REE levels reaching up to 3600 ppm.

References:

Bogdanova, S., Gorbatschev, R., Skridlaite, G., Soesoo, A., Taran, L., Kurlovich, D., 2015. Trans-Baltic Palaeoproterozoic correlations towards the reconstruction of supercontinent Columbia/Nuna. Precambrian Research, 259, 5-33.

Puura, V., Vaher, R., Klein, V., Koppelmaa, H., Niin, M., Vanamb, V., Kirs, J., 1983. Kristallicheskij fundament Estonii, Moscow, 208 pages.

Nirgi, S., Soesoo, A., 2021. Geology and geochemistry of a Paleoproterozoic iron mineralization in north-eastern Estonia. Proceedings of the Karelian Research Centre of the Russian Academy of Sciences, 10, 25-43.

Soesoo, A., Puura, V., Kirs, J., Petersell, V., Niin, M., All, T., 2004. Outlines of the Precambrian basement of Estonia. Proceedings of the Estonian Academy of Sciences, Geology, 53, 149-164.

Soesoo, A., 1993. Estonian porphyraceous potassium granites: petrochemical subdivision and petrogenetical interpretation. Proceedings of the Estonian Academy of Sciences. Geology, 42, 97-109.

Soesoo, A., Nirgi, S., Urtson, K., Voolma, M., 2021. Geochemistry, mineral chemistry and pressure–temperature conditions of the Jõhvi magnetite quartzites and magnetite-rich gneisses, NE Estonia. Estonian Journal of Earth Sciences, 70, 2, 71-93.

Geophysical and Geochemical characterisation of the Märjamaa Rapakivi granite, Estonia.

JD. Solano-Acosta[1], A. Soesoo[1,2,3] and R. Hints[1]

[1]Department of Geology, Tallinn University of Technology, Tallinn, Estonia
2 Geological Survey of Estonia, F. R. Kreutzwaldi 5, 44314 Rakvere, Estonia
3Department of Geology, University of Tartu, Ravila 14a, 50411, Tartu, Estonia
E-mail: juan.solano@taltech.ee

The Märjamaa A-type granitoid, part of the Anorthosite-Rapakivi Granite Complex (ARGC), dates to 1.62 billion years ago. It was studied using gravimetric and magnetic potential field methods and whole-rock geochemistry for its three phases. The residual potential field data showed that Phase I had higher anomalies, while Phase III had less intensity. On the other hand, Phase II showed a negative anomaly. Derivative methods of the potential field data were used to better delineate and characterise the geometries of each phase, with the deepest part following the samples of Phase I and the shallower parts for Phase II and III. The major elemental data for the three phases complemented the geophysical insights. The overall trend indicated an increase in SiO_2 content and a decrease in mafic mineral contributions. This marked a transition towards a more felsic composition as the system evolved from Phase I through Phase III. Petrogenetic analysis revealed minor variations in crystallisation pressures across the three phases of magmatic evolution, starting at around 3.9 kb with initial temperatures around 740°C. These trends highlighted the progressive evolution of magmatic conditions across the phases, with shifts in mineral content and thermal dynamics illustrating the geochemical and petrogenetic development of the system. This study presents the geodynamical and geochemical evolution of the tripartite emplacement of the Märjamaa granite.

Keywords: Geophysical Characterization, Geochemical Evolution, Märjamaa Rapakivi Granitoid, Phase Differentiation

1. General

Rapakivi granites, commonly recognised by their distinctive feldspar textures, hold a crucial position within anorogenic magmatic suites across the Fennoscandian Shield. These granites and associated anorthosites and ferrodioritic dikes contribute to the broader Anorthosite-Rapakivi Granite Complexes (ARGC), which have proven valuable in understanding crustal evolution and tectonic settings. The ARGC suite in Fennoscandia is defined by diverse compositional characteristics, ranging from ultramafic to peraluminous. Notably, these formations have been key in reconstructing post-orogenic tectonic events, as they are often found in regions with minimal deformation, preserving original intrusive structures and magmatic textures (Ramo et al., 1995; Sharkov, 2010).

The Märjamaa pluton in Estonia showcases the typical mineralogical and geochemical characteristics of the ARGC. This pluton, along with other minor intrusions such as the Naissaare and Taebla bodies, is connected to the more significant magmatic events that influenced the southern Fennoscandian Shield (Fig. 1). The Märjamaa pluton is characterised by pink, coarse-grained textures, mainly consisting of microcline megacrysts within a syeno- to monzogranitic matrix. Geophysical methods such as gravity and magnetic surveys have detected anomaly signatures over this granite. Additionally, integrating major elemental geochemical analysis provides comprehensive evolutionary models. This study explores the geophysical and major geochemical anomalies associated with the Märjamaa pluton to understand the processes influencing the emplacement and evolution of these granitoid complexes within Fennoscandia.

2. Geological context

Before unifying around 1.8 billion years ago, Fennoscandia, Sarmatia, and Volgo-Uralia regions

developed under distinct tectonic and metamorphic conditions shaped by significant orogenic events. During the Paleoproterozoic era, the Svecofennian orogeny spurred extensive crustal growth in Fennoscandia between 2.1 and 1.79 billion years ago through the accretion of microcontinents and volcanic arcs onto the Karelian craton, culminating in a collision with Volgo-Sarmatia around 1.84–1.79 billion years ago to form a united continental block. This orogenic activity melded the Svecofennian crust with the Archean core of the Fennoscandian Shield, leading to granite intrusions and interactions with volcanic belts in southwestern Finland (Fig.1b). Around 1.64 billion years ago, a phase of crustal extension across southern Finland and northern Estonia promoted the formation of basaltic dike swarms and the emplacement of Anorthosite-Rapakivi Granite Complexes from lower crustal melting and mafic magma movement, followed by the Gothian orogeny between 1.73 and 1.48 billion years ago which likely developed new crustal belts to the west through terrane accretion.

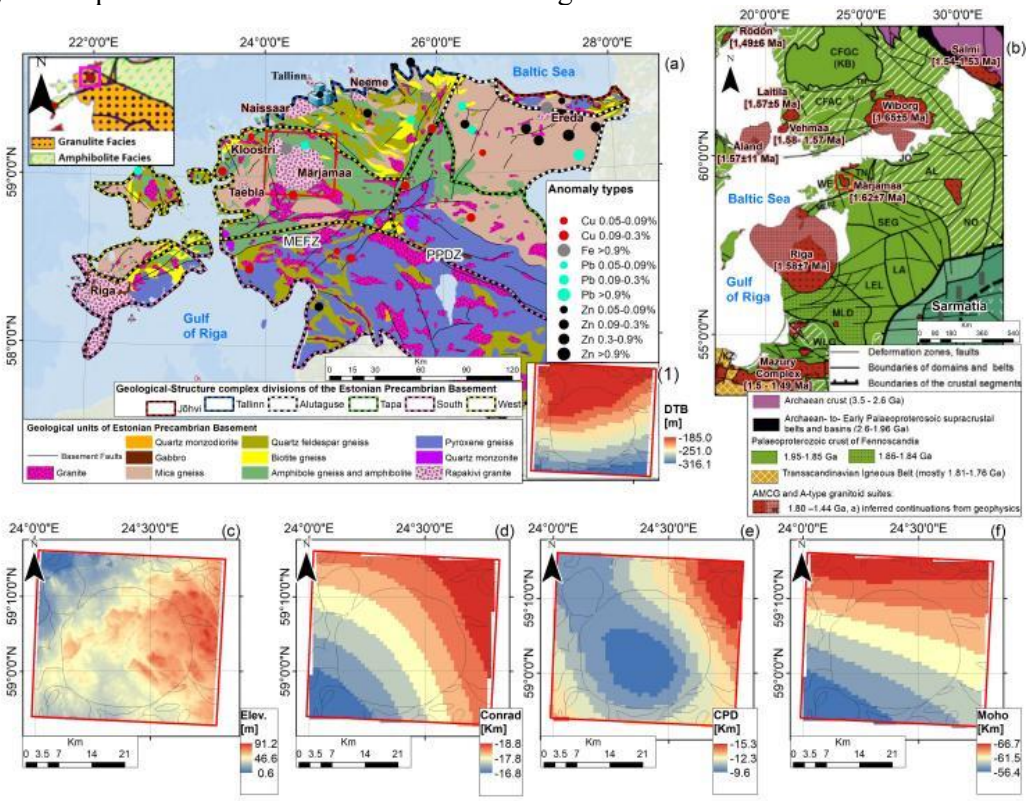

Figure 1. Geological Setting of the Study Zone: (a) Precambrian map displays Estonia's basement and key geochemical anomalies sourced from the Geoportal of the Land Board of the Republic of Estonia. It features depth-to-basement measurements and outlines major tectonic domains, with the study areas of Märjamaa and Kloostri granitoids highlighted in red. (b) Fennoscandian Rapakivi granitoids over the Palaeoproterozoic crust, more detailed in *Bogdanova et al.,2015*. (c-f) Additional geophysical data, including elevation (c), Conrad discontinuity (d), Curie Point Depth (e), and Moho discontinuity (f), are detailed in *Solano-Acosta et al.,2023.*

Estonian Anorthosite-Rapakivi Granite Complexes, including the Märjamaa, Neeme, Ereda, Naissaare, and Taebla plutons, are identified as porphyritic potassium granites of Rapakivi age, characterised by a coarse to medium-grained, pinkish-grey appearance with prominent microcline porphyroblasts. The Märjamaa pluton, in particular, with its asymmetrically rounded shape spanning about 40 x 25 km, consists of coarse-grained, pink-grey porphyritic granites

and is occasionally intersected by aplites, intruding the Proterozoic West Estonian gneisses with sharp geological contacts. According to *Klein et al. (1994)* Märjamaa evolutionary sequence is tripartite: the central portion contains melanocratic granodioritic compositions representing the earliest phase of crystallisation from iron-rich melts (Phase I), surrounded by more leucocratic granites enriched in microcline with reduced biotite content (Phase II), and finally, the northwestern Kloostri (Fig.1a) sector features leucogranitic compositions marked by the absence of hornblende and the presence of muscovite and fluorite, indicating a high degree of magmatic differentiation (Phase III). Tripartite phase boundaries are presented in Figure 2.

3. Methods And Results

The geometries of the Märjamaa granitoid were analyzed using Bouguer and magnetic anomaly data from the Estonian Geological Service. The potential dataset for the Märjamaa pluton, which includes Bouguer and magnetic data, underwent a detailed analysis. This involved using regional-residual anomaly separation and advanced derivative techniques to identify the underlying geological structures (Fig.2 a-c). The MAGMAP tool within the Geosoft Oasis Montaj software was used to analyse regional anomalies and subtract them from filtered data, resulting in residual grids highlighting shallower crustal sources. Deeper sources were suggested by regional anomalies such as the Moho discontinuity (Fig.1f). A reduction-to-pole (RTP) transformation further aligned the magnetic anomaly peaks directly over their sources,

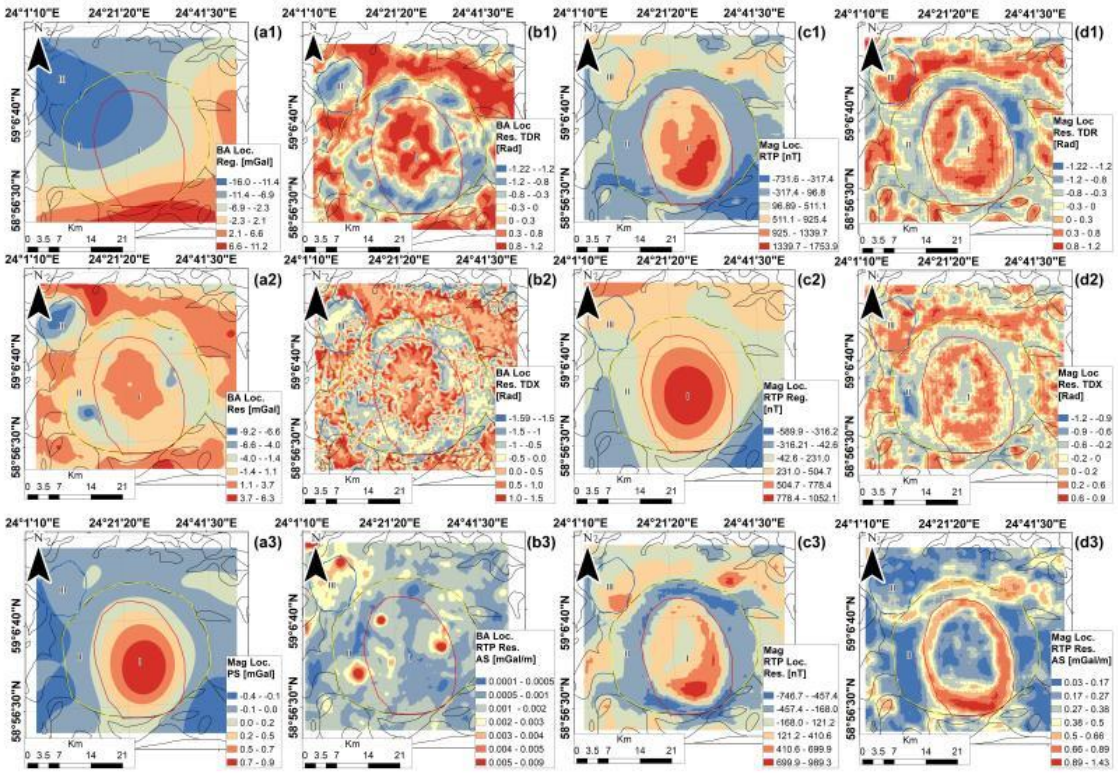

Figure 2. Geophysical wave-cut and residual derivative results. (a1) Bouguer regional map, (a2) Bouguer residual map, (a3) Pseudo-gravity map derived from RTP magnetic data. (b) Bouguer residual derivatives: (b1) , Total Derivative Ratio (TDR), (b2) Total Derivative Cross (TDX), (b3) Analytic Signal (AS). (c1) Magnetic Reduce-To-Pole (RTP) map, (c2) RTP regional map, (c3) RTP residual map. (d) RTP residual derivatives: (d1) TDR, (d2) TDX, (d3) AS. Each grid indicates the three Märjamaa Phases.

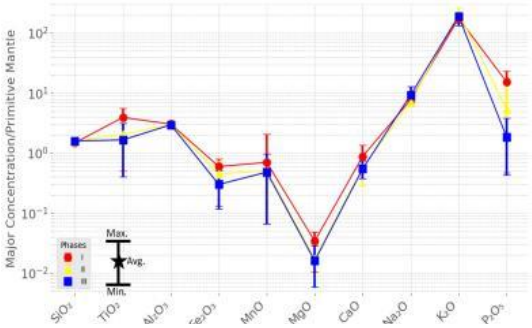

Figure 3. Major elemental distribution of the *Kivisilla et al. (1999),* normalised to the Primitive Mantle (PM)**.**

making interpretations simpler (Fig.2c1). To enhance the delineation of the geological features, various derivative methods, including Total Derivative Ratio (TDR), Total Derivative Cross (TDX), and Analytic Signal (AS), were applied for each residual potential result (Fig.2 b-d). These techniques sharpened the gradients over edges and produced clearer images of the subsurface features, effectively mapping lineaments, fault systems, dykes, and the granitoid geometries across the study area.

The Märjamaa granitoid, thoroughly analysed by *Kivisilla (1999)* using the Wet-Chemistry method, provides a comprehensive dataset revealing whole-rock major elemental compositions across its tripartite phases (Fig.3). The geochemical data shows an increasing trend of SiO_2 from 66.69% in Phase I to 71.59% in Phase III, with corresponding decreases in FeO* and Mg#, indicating a shift from mafic to more felsic compositions as the magmatic system evolves. These shifts are supported by detailed CIPW norm calculations. The Märjamaa granitoid exhibits FeO/(FeO + MgO) ratios of 0.73, 0.91, and 0.85 in Phases I, II, and III, respectively, indicating variable oxidizing conditions. In comparison, Laurentia's magnetite-series granites, with ratios between 0.80 and 0.88, show more oxidizing conditions, whereas its ilmenite-series granites, with ratios above 0.88, are more reduced. Finnish Rapakivi granites, displaying a wider ratio range from 0.79 to 1.00, typically manifest traits of reduced A-type granites. Petrogenetic analysis from the major elemental data indicates that temperature and pressure analyses detail Phase I with a temperature of 734.6°C and pressure of 3.9 kbar, Phase II with the highest temperature of 746.6°C and pressure of 3.96 kbar, and Phase III cooling slightly to 737.8°C with a reduced pressure of 3.8 kbar. Water content also fluctuates, decreasing from 7.7% in Phase I to 7.3% in Phase II, then slightly increasing to 7.5% in Phase III.

4. Discussion

The geophysical and geochemical analysis of the Märjamaa rapakivi granitoid's tripartite phases reveals distinct characteristics: Phase I is marked by deep anomalies, higher magnetic and gravimetric readings, and lower silicic affinities. Phase II displays the highest temperature and pressure and negative potential anomalies. Conversely, Phase III shows higher magnetic and negative residual Bouguer anomalies, indicating a shallower emplacement.

References:

Bogdanova, S., Gorbatschev, R., Skridlaite, G., Soesoo, A., Taran, L., Kurlovich, D., 2015. Trans-baltic palaeoproterozoic correlations towards the reconstruction of supercontinent Columbia/Nuna. Precambrian Research 259, 5–33.

Kivisilla, J., Niin, M., Koppelmaa, H., 1999. Catalogue of chemical analyses of major elements in the rocks of the crystalline basement of Estonia. Eesti Geoloogiakeskus.

Klein, V., Konsa, M., Niin, M., 1994. On mineralogy of the porphyrous potassium granites of small massifs in the northern Estonian basement. Proceedings of the Estonian Academy of Sciences, Geology

Rämö, O.T., Haapala, I., 1995. One hundred years of rapakivi granite. Mineralogy and Petrology 52, 129–185.

Solano-Acosta, J.D., Soesoo, A., Hints, R., 2023. New insights of the crustal structure across Estonia using satellite potential fields derived from wgm 2012 gravity data and emag2v3 magnetic data. Tectonophysics

Sharkov, E., 2010. Middle-proterozoic anorthosite–rapakivi granite complexes: An example of within-plate magmatism in abnormally thick crust: Evidence from the east European craton. Precambrian Research 183, 689–700.

Is the Estonian Alutaguse Section of Eastern Fennoscandia a continuation of the Southern Svecofennian Finnish Terranes, or is it akin to the Swedish Bergslagen region?

JD. Solano-Acosta[1], A. Soesoo[1,2,3], R. Hints[1] and S. Graul[1]

[1] Department of Geology, Tallinn University of Technology, Tallinn, Estonia
[2] Geological Survey of Estonia, F. R. Kreutzwaldi 5, 44314 Rakvere, Estonia
[3]Department of Geology, University of Tartu, Ravila 14a, 50411, Tartu, Estonia
E-mail: juan.solano@taltech.ee

This research explores the geochemistry of Paleoproterozoic metasedimentary and metavolcanic units in the Alutaguse region of North Estonia and the South Svecofennian (SS) zones, including Ladoga, Saimaa, Häme Belt, and Uusimaa Belt, to better understand the tectonic evolution of the Svecofennian Orogeny in Eastern Fennoscandia. Metasedimentary units consist of micaceous gneisses (± Grt ± Crd ± Sil), while metavolcanics include amphibolites and pyroxenic gneisses. Historical and new data show that High-SiO_2 (>63 wt%) metasediments have felsic origins similar to the Upper Continental Crust (UCC), whereas Low-SiO_2 (≤63 wt%) metasediments, resembling graywackes and shales, indicate mafic to intermediate origins similar to Post-Archean Australian Shale (PAAS). Various weathering indices, including CIA, PIA, CIW, and ICV for metasediments, and AI, CCPI, WIP, and SI for metavolcanics, were applied to reveal these geochemical trends. The metavolcanics are classified as subalkaline, with geochemical signatures pointing to asthenospheric mantle origins for Alutaguse and subducted oceanic crust origins for SS. Tectonic affinity analyses indicate a predominant oceanic arc setting in both regions. High concentrations of CaO and MnO in Alutaguse and Uusimaa metasediments suggest a genetic link, positioning Alutaguse as a backarc of 1.90-1.89 Ga back-arc to the Uusimaa belt, followed by the accretion of the Uusimaa and Häme belts around 1.87 Ga, marking the closure of the Svecofennian ocean. The Alutaguse zone probably developed as a back-arc to the Tallinn-Uusimaa belt after the accretion of the Bergslagen microcontinent. This interpretation is supported by geophysical anomalies correlated with Zn-Pb-Fe mineralisation, which shows similarities to Bergslagen's VMS provinces and warrants further investigation.

Keywords: Svecofennian Orogeny, Alutaguse zone, South Svecofennian (SS) zone; Geochemistry; Metasediments; Metavolcanics; Weathering indices; Provenance; Tectonic setting

1. General

The Estonian Paleoproterozoic crystalline basement remains largely hidden beneath extensive Lower Paleozoic strata, limiting direct study. Most knowledge comes from drill cores and geophysical data, revealing high-grade Paleoproterozoic metavolcanic and metasedimentary rocks in northern Estonia, divided into the Tallinn, Alutaguse, and Jõhvi structural zones (Fig.1). These zones contain 1.92–1.88 Ga rocks, closely resembling those found in southwestern Finland and central Sweden's Bergslagen region (Bogdanova et al., 2015) (Fig.1a). The Alutaguse zone, interpreted as a folded metasedimentary basin that developed after the back arc of the closure of the Tallinn volcanic belt, remains poorly understood due to limited geochemical and geochronological studies, leaving its origin and development open to debate (Soesoo et al., 2020) (Fig.1b).

This study integrates new geochemical data and geophysical analysis of Bouguer gravity and magnetic anomaly data to further investigate the Alutaguse zone (Fig.1d). By analysing major, trace, and rare earth elements (REE) in metasedimentary and metavolcanic rocks, we aim to identify the composition and origin of the source material, detect weathering patterns, and infer tectonic settings. Additionally, geophysical analysis provides further insights into the subsurface structure and evolution of the zone, contributing to a broader understanding

of the geodynamic processes that shaped this region during the Svecofennian orogeny and its connection to the Proterozoic history of the Estonian basement.

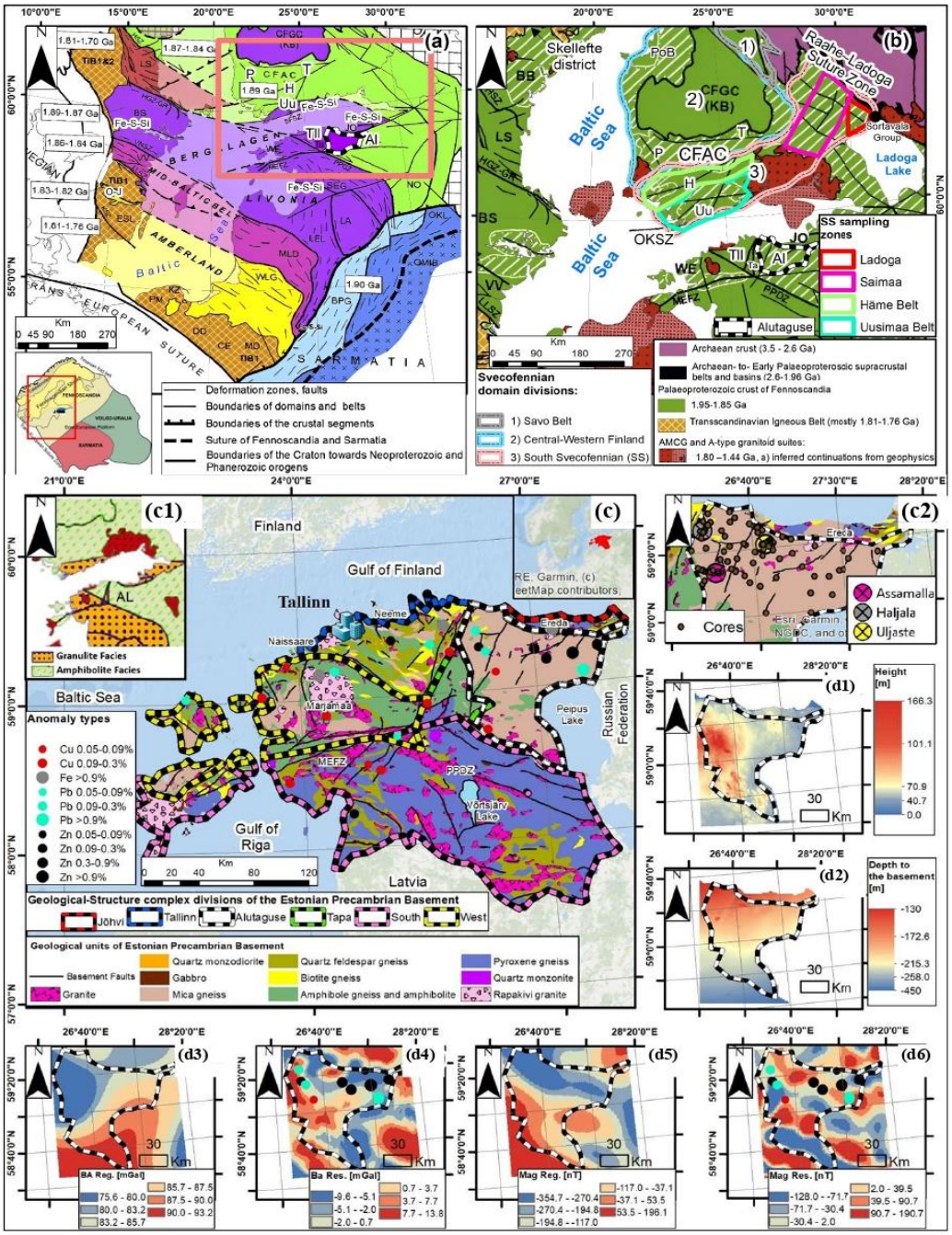

Figure 1. Geological setting of the study area highlighting key features: a) Crustal structure of the Central and Southern Svecofennian orogens crossing the Baltic Sea. b) Major Paleoproterozoic tectonic zones in Fennoscandia. c) Geological map of the Estonian Precambrian basement showing geochemical anomalies (after Soesoo et al., 2020), with red symbols for Rapakivi lithologies (after Bogdanova et al., 2015). Inset: rock distribution of granulite and amphibolite. c1) Zoomed map of the Alutaguse zone, showing core locations and metallogenic zones. d) Geophysical maps of the Alutaguse zone: topography, depth to the basement, Bouguer anomalies, and magnetic anomalies.

2. Methodology

This study focusses on the geochemical characterisation of metasediments and metavolcanic rocks from the Alutaguse and SS regions (Fig.1b). Major elemental data were supplemented with findings from Kivisilla et al. (1999) and trace element data from the Estonian Geological Service. We incorporated data from Rasilainen et al. (2007) and Kotova et al. (2009) for the SS region. Analytical methods involved advanced techniques, ensuring precise results, with average concentrations shown in Figure 2. Potential methods were also used (Fig.1d).

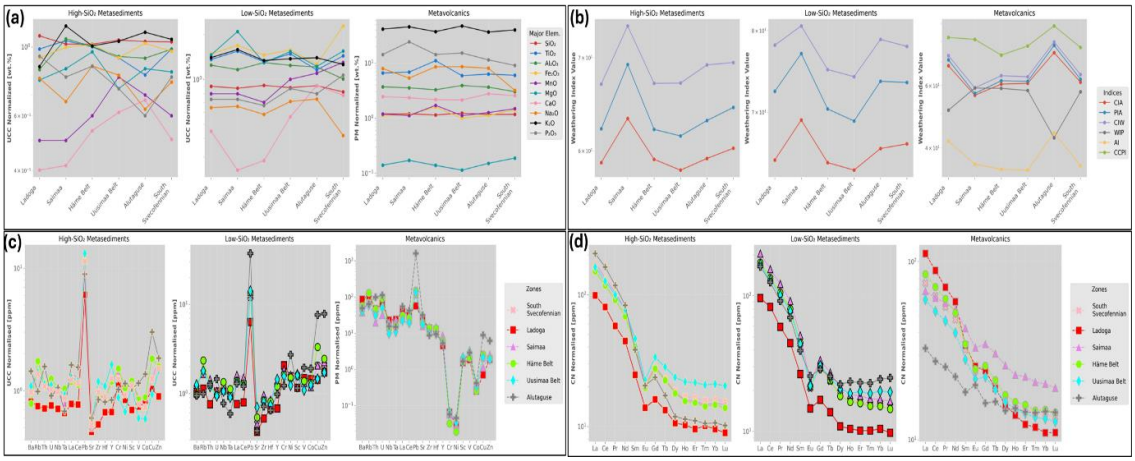

Figure 2. Bivariate average geochemical trends of the Alutaguse and South Svecofennian (SS) zones. a. Major elemental data. b. Weathering indices. c. Trace elements. d. Rare Earth Elements (REE).

3. Contributions and future research

For the Low-SiO_2 and High-SiO_2 meta-sediments, rifting settings dominate most of the samples (Figs. 3a, 3b). Ternary plots of La-Th-Sc (inset) and Th-Sc-Zr/10 (background) suggest a continental island arc (CIA) tectonic setting (Fig. 3c). In contrast, metavolcanic units are more closely aligned with calc-alkaline volcanic arc-basalt (VAB) origins, as indicated by the Hf/3–Th–Nb/16 plot (Fig.3d). Major elemental analysis highlights that the magma primarily originates from mafic basaltic sources (Fig. 3e). Furthermore, the Ba / Th and U/Th ratios vs. Th/Nb emphasise the subduction influence over the SS samples, with sediment melt predominating in the Alutaguse sediments, suggesting a back-arc rifting process (Fig.3f). Our primary contribution is elucidating the back-arc origin of the Alutaguse zone, likely linked genetically to the Uusimaa units (Fig.3f). This inference stems from the high CaO and MnO content observed in the metasediments (Fig.2a). Furthermore, we propose that the most plausible model for Fennoscandia evolution involves a double subduction collision, culminating in the amalgamation of Bergslagen with southern Proto-Fennoscandia around 1.87–1.86 Ga. We recommend further study of the metasedimentary and metavolcanic units in the Tallinn zone to determine whether they are part of the Uusimaa belt in Estonia or represent a separate arc predating the Uusimaa belts. If the latter occurred, they may have originated similarly to the adjacent northern arc belts, suggesting that the Estonian basement is closely tied to the geodynamic evolution of the Bergslagen microcontinent (Fig.3g).

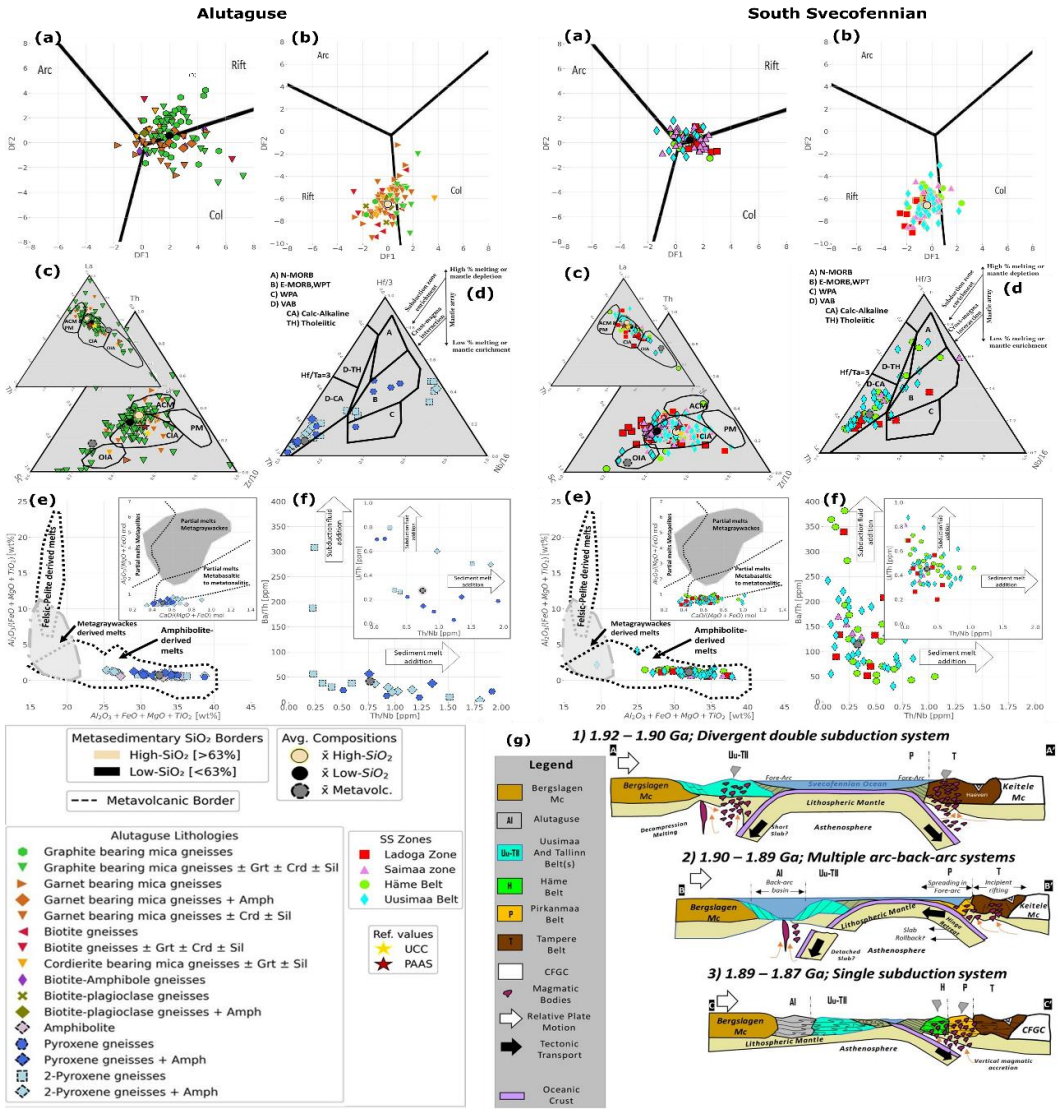

Figure 3. Geochemical plots between the Alutaguse and SS a-c) metasedimentary and d-f) metavolcanic units involving major elemental tectonic discriminant functions. g) Schematic geodynamic model (after Kukkonen and Lauri, 2009; Kara, 2021) illustrating the evolution of Southern Finland and Northern Estonia within the context of the region's evolution.

References:

Kara, J. (2021) Evolution of the Svecofennian Bedrock in Southern Finland - Spatial and temporal changes in the mantle-derived magmatism and mantle-crust interaction. Docthoral thesis - University of Turku.

Kivisilla, J. et al. (1999) Catalogue of chemical analyses of major elements in the rocks of the crystalline basement of Estonia. Eesti Geoloogiakeskus.

Kotova, L. et al. (2009) Source rocks and provenances of the ladoga group siliciclastic metasediments (Svecofennian foldbelt, baltic shield): Results of geochemical and sm-nd isotopic study. Stratigraphy and Geological Correlation, 17, 1–19

Kukkonen, I. and Lauri, L. (2009) Modelling the thermal evolution of a collisional Precambrian orogen: High heat production migmatitic granites of southern Finland. Precambrian Research, 168(3-4), 233–246.

Rasilainen, K. et al. (2007) The Rock Geochemical Database of Finland: Manual. Geological Survey of Finland.

Soesoo, A. et al. (2020) The evolution of the Estonian Precambrian basement: geological, geophysical and geochronological constraints., (2), 18–33.

Solano-Acosta, J. D. et al. (2023). New insights of the crustal structure across Estonia using satellite potential fields derived from WGM-2012 gravity data and EMAG2v3 magnetic data. Tectonophysics, 846, 229656

Influence of the Transscandinavian Igneous Belt on the post-orogenic shoshonitic magmatism in Finland

O. Teräs[1], K. Nikkilä[1], P. Mikkola[2], A. Kotilainen[3], O. Eklund[1] and O.T. Rämö[3]

[1]Åbo Akademi University, Department of Geology and Mineralogy, Turku, Finland
[2]Geological Survey of Finland, Kuopio, Finland
[3]University of Helsinki, Department of Geosciences and Geography, Helsinki, Finland
E-mail: oliver.teras@abo.fi

The role of the Transscandinavian Igneous Belt (TIB) in post-orogenic magmatism in western and southern Finland may be pivotal to the understanding of the post-orogenic crustal evolution of the Svecofennian province. This research characterizes the whole-rock geochemical, U-Pb zircon, and whole-rock Sr-Nd isotopic signatures of two post-orogenic shoshonitic intrusions, the Tistronskär monzodiorite and the Loukee high-Ba-Sr granite, dated at 1805 ± 4 Ma and 1794 ± 13 Ma, respectively. We explore the contribution of TIB-related magmatism to the generation and melting of enriched mantle sources for shoshonitic melts. This study demonstrates that shoshonitic intrusions likely originated from an enriched mantle domain, metasomatized by subducted sediments. The shoshonitic magmas are suggested to have formed during a period of lower crustal delamination in a post-orogenic setting, where TIB-related processes were crucial in promoting mantle-derived magmatism in western and southern Finland.

Keywords: Svecofennian orogeny, Transscandinavian Igneous Belt, post-orogenic magmatism, shoshonitic intrusions

1. Introduction

The Svecofennian orogeny (1.92–1.76 Ga) in Finland is characterized by a series of tectonic and magmatic events, which culminated in the emplacement of post-orogenic shoshonitic intrusions in the Svecofennian province (Fig. 1A; Nironen, 2017). The Transscandinavian Igneous Belt (TIB; Högdahl et al., 2004) may have played a significant role in influencing post-orogenic magmatism, particularly delivering sedimentary material through subduction to the mantle depths. In western and southern Finland, the Tistronskär monzodiorite and Loukee high-Ba-Sr granite represent examples of such magmatic activity, as they both show mantle source affinities and thus were likely formed primarily from mantle melts.

2. Geological Setting

Post-orogenic intrusions, such as the Tistronskär monzodiorite and Loukee granite, are situated in western and southeastern Finland, respectively (Fig. 1A). These areas may have been influenced by TIB magmatism, as oceanic slab subduction may have caused the upper mantle to melt in post-orogenic settings. Post-orogenic rocks from western Finland to Russian Karelia exhibit mantle-like geochemical and isotopic signatures and suggest that the mantle source was modified by subduction delivered sediments.

It has been suggested that the carbonated subduction-modified mantle reflected by high LREE, K, Ba, Sr and P_2O_5/TiO_2 values of post-orogenic basic intrusions from western Finland to Russian Karelia coincides with the Transscandinavian Igneous Belt magmatism in western Sweden (Andersson et al., 2006). However, the eastern continuous of TIB-related slab under the Svecofennian province is uncertain. The 1.80 Ga post-orogenic basic/acidic magmatism is widespread from western Finland to Russian Karelia and thus provides an opportunity to examine this issue.

3. Results

New U-Pb zircon data indicate crystallization at 1805 ± 4 Ma for the Tistronskär monzodiorite and 1794 ± 13 Ma for the Loukee granite. Both intrusions show high LREE, K, Ba, Sr and P_2O_5/TiO_2 values and thus showing a shoshonitic affinity. The geochemistry of these rocks supports fractional crystallization of a melt derived from an enriched mantle source, modified by subduction-related metasomatism. Initial εNd values of the intrusions are compatible with enriched mantle-derived origin with minimal crustal interaction.

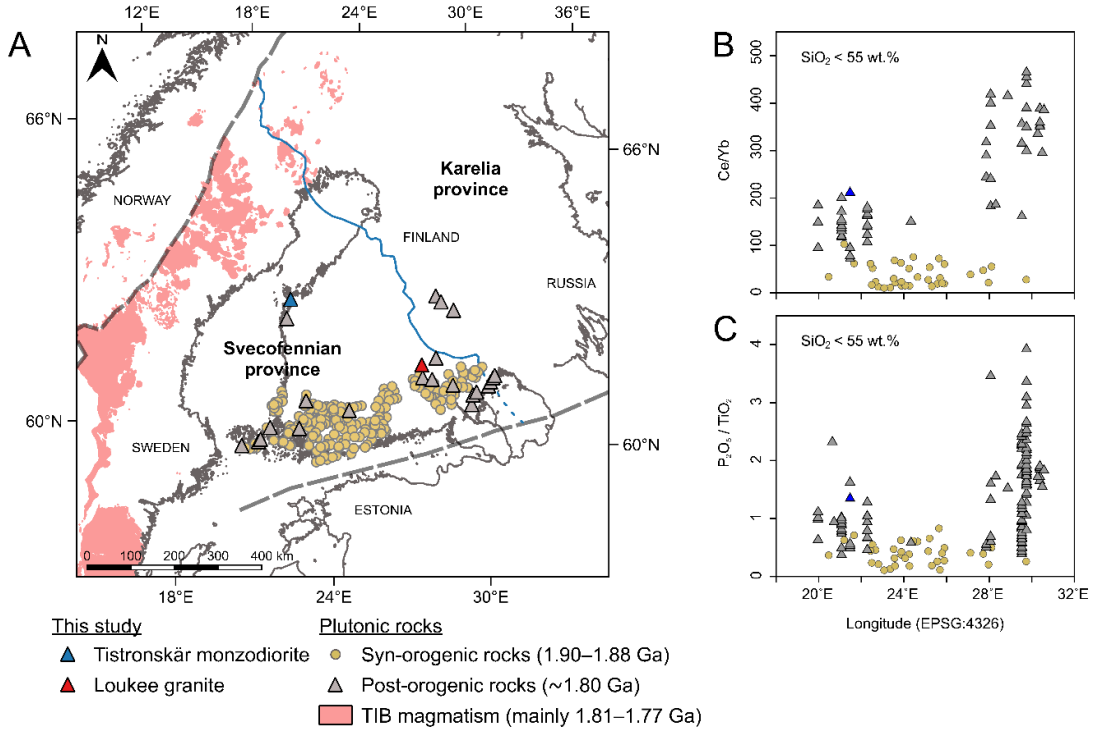

Figure 1. (A) Post-orogenic magmatism in the Svecofennian province at 1.81–1.75 Ga. Longitude versus Ce/Yb (B) and P_2O_5/TiO_2 (C) plots illustrating geochemical trends from west to east through the Svecofennian province. Syn-orogenic plutonic rocks (1.90–1.88 Ga) are marked with circles (DigiKP, 2024; Kara et al., 2018) and shoshonitic post-orogenic plutonic rocks with triangles (Konopelko, 1997; Eklund et al., 1998; Väisänen et al., 2000; Andersson et al., 2006; Rutanen et al., 2011; Woodard et al., 2014). Sources for TIB granitoids are from the SGU database. TIB = Transscandinavian Igneous Belt. Province boundaries are shown by solid/broken lines.

4. Discussion

The role of the TIB magmatism in triggering post-orogenic magmatism may be central to the formation of the shoshonitic intrusions in Svecofennian province. Slab break-off and lithospheric delamination caused by TIB activity likely induced upper mantle melting, which, in turn, produced the shoshonitic magmas emplaced in western and southern Finland. These processes explain the long-lasting magmatic activity, spanning several million years (1.81–1.76 Ga), and highlight the regional controls on magmatism during the late stages of the Svecofennian orogeny.

The availability of hydrous fluids (e.g., from a nearby subducting plate, TIB magmatism, Fig. 1A) could facilitate lower crust eclogitization (Krystopowicz and Currie 2013). This

eclogite phase change itself could induce lower crust weakening and could initiate lower crust delamination in western and southern Finland. This is consistent with the notion that a phase transformation in the lower crust from mafic granulite to eclogite plays a major role in the development of delamination (Meissner and Mooney 1998; Krystopowicz and Currie 2013). Thus, there may be a link between the availability of hydrous fluids (e.g., from a nearby subducting plate), lower crust eclogitization, and delamination. The Ce/Yb and P_2O_5/TiO_2 ratio increase (Figs. 1B and 1C) from west (nearby TIB) to east (Russian Karelia) in the post-orogenic rocks may support a spatial control of upper mantle enrichment processes underneath the Finnish Svecofennian.

5. Conclusion

This study gives new insights into the mechanisms driving post-orogenic magmatism in the Svecofennian province. The influence of TIB-related processes, including slab break-off and delamination, are important in generating post-orogenic magmatism in western and southern Finland. Fractional crystallization of mantle-derived magmas played a crucial role in generating the observed shoshonitic magmatic rocks and their geochemical traits.

References:

Andersson, U.B., Eklund, O., Fröjdö, S., Konopelko, D., 2006. 1.8 Ga magmatism in the Fennoscandian Shield; lateral variations in subcontinental mantle enrichment. Lithos 86, 110-136.

DigiKP, 2024. Digital map database, Spatial data products, Rock geochemical data of Finland. Geological Survey of Finland, Espoo. Page visited 13.5.2024. https://hakku.gtk.fi/en/locations/search

Eklund, O., Konopelko, D., Rutanen, H., Fröjdö, S., Shebanov, A.D., 1998. 1.8 Ga Svecofennian post-collisional shoshonitic magmatism in the Fennoscandian shield. Lithos 45, 87-108.

Högdahl, K., Andersson, U.B., Eklund, O., 2004. The Transscandinavian Igneous Belt (TIB) in Sweden: A review of its character and evolution. Geological Survey of Finland, Special Paper 37, 1-123.

Kara, J., Väisänen, M., Johansson, A., Lahaye, Y., O'Brien, H., Eklund, O., 2018. 1.90-1.88 Ga arc magmatism of central Fennoscandia: geochemistry, U-Pb geochronology, Sm-Nd and Lu-Hf isotope systematics of plutonic-volcanic rocks from southern Finland. Geologica Acta 16, 1-23.

Konopelko, D.L., 1997. Postorogenic intrusions of the NW Ladoga region with special references to apatite-bearing potassium ultramafic rocks. PhD thesis, St. Petersburg University, Russia, pp. 200.

Krystopowicz, N.J., Currie, C.A., 2013. Crustal eclogitization and lithosphere delamination in orogens. Earth and Planetary Science Letters 361, 195-207.

Meissner, R., Mooney, W., 1998. Weakness of the lower continental crust: a condition for delamination, uplift, and escape. Tectonophysics 296, 47-60.

Nironen, M., 2017. Guide to the Geological Map of Finland – Bedrock 1:1 000 000. Geological Survey of Finland, Special Paper 60, 41-76.

Rutanen, H., Andersson, U.B., Väisänen, M., Johansson, Å., Sören, F., Lahaye, Y., 2011. 1.8 Ga magmatism in southern Finland: Strongly enriched mantle and juvenile crustal sources in a post-collisional setting. International Geology Review 53, 1622-1683.

SGU database, 2024. Digital map database, Products and services. Geological Survey of Sweden, Upsala. Page visited 13.5.2024. https://apps.sgu.se/kartvisare/kartvisare-bergets-alder.html

Väisänen, M., Mänttäri, I., Kriegsman, L.M., Hölttä, P., 2000. Tectonic setting of post-collisional magmatism in the Palaeoproterozoic Svecofennian Orogen, SW Finland. Lithos 54, 63-81.

Woodard, J., Kietäväinen, R., Eklund, O., 2014. Svecofennian post-collisional shoshonitic lamprophyres at the margin of the Karelia Craton: Implications for mantle metasomatism. Lithos 205, 379-393.

EPOS-FI - The Finnish node of the European Plate Observing System

A. Tsampas[1], A. Korja[2], E. Moen[1] and EPOS-Finland Consortium

[1]Institute of Seismology, P.O. Box 68, FIN-00014 University of Helsinki
[2]Department of Geosciences and Geography, P.O. Box 64, FIN-00014 University of Helsinki
E-mail: anestis.tsampas@helsinki.fi

EPOS-Finland (EPOS-FI, formerly known as the FIN-EPOS consortium) is an umbrella organization comprising distributed National Research Infrastructures (NRIs) in Solid Earth Sciences. It serves as the Finnish national node of the European Plate Observing System (EPOS). EPOS-FI has been established to provide state-of-the-art research facilities academia, offer modern and competent services to society, and facilitate Finnish actions in EPOS-ERIC (http://www.epos-eu.org/). The Finnish participation in EPOS is promoted and developed by the EPOS-FI council, which consists of representatives from the involved organizations. The Council is responsible for establishing the long-term NRI plan, coordinating the data quality and visibility of the infrastructures associated with EPOS-FI, and enhancing their transnational access for both scientific and societal purposes. Additionally, it oversees participation in European/Nordic initiatives related to EPOS and works to expand the user base of EPOS data. The coordination office of EPOS-FI is located at the Institute of Seismology, University of Helsinki. Also, Finland is currently working towards a national governmental process to join EPOS ERIC as a member state in 2025.

Keywords: EPOS, national node, National Research Infrastructure (NRI), Thematic Core Services (TCS), consortium, Findable Accessible Interoperable and Reusable (FAIR) data management, databases, metadata.

1. General

EPOS is a pan-European multidisciplinary distributed Research Infrastructure (RI) that integrates data, data products, and facilities for the solid Earth science community in Europe (https://www.epos-eu.org/). Easily accessible solid Earth science data and services facilitate innovative multidisciplinary research aimed at enhancing our understanding of the physical processes of the solid Earth that influence risk factors such as earthquakes and volcanic eruptions. In 2018, the European Commission granted EPOS the legal status of a European Research Infrastructure Consortium (ERIC). Based in Italy, EPOS ERIC currently includes fourteen member countries: Belgium, Denmark, France, Greece, Iceland, Italy, the Netherlands, Norway, Poland, Portugal, Romania, Slovenia, and the United Kingdom, with Switzerland participating as an observer (Atakan et al., 2022).

EPOS-FI is the Finnish national node of EPOS and one of the landmark Research Infrastructures (RIs) recognized by the European Strategy Forum on Research Infrastructures (ESFRI) (see https://www.esfri.eu/; Cocco et al., 2022; Cocco and Montone, 2022). The collaborative community of Finnish universities and research institutes involved in EPOS-FI owns and operates National Research Infrastructures (NRIs) dedicated to solid Earth science, including observatories, laboratories, and data centers throughout Finland.

2. EPOS-FI Contribution of Data and Services

The TCSs of EPOS facilitate integration among specific scientific communities and focus on collecting and disseminating observations of geological, geochemical, and geophysical processes within the Earth and its near space.

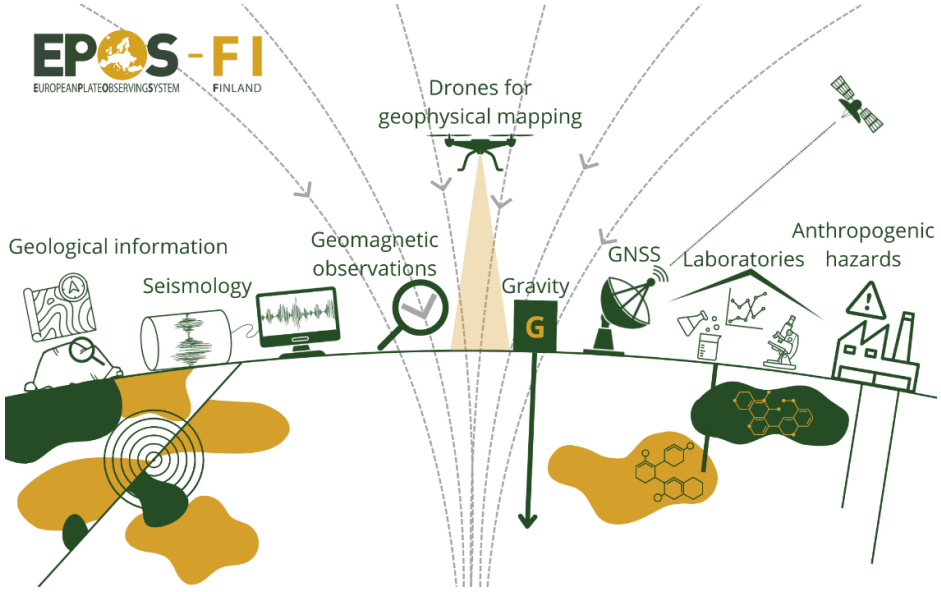

Figure 1. A graphical representation of the integrated sources of Finnish solid Earth science data related to EPOS.

Finnish NRIs are owned, hosted, and operated by universities and research institutes, also known as EPOS-FI consortium partners, which play a governmental role in the provision of field-specific geoscientific data. These institutions include the University of Helsinki, the University of Oulu, the Geological Survey of Finland (GTK), the Finnish Meteorological Institute (FMI), the Finnish Geospatial Research Institute of the National Land Survey (NLS), the VTT Technical Research Centre of Finland Ltd, and the CSC IT Center for Science Ltd. EPOS-FI data (see also Figure 1) are utilized by academia, government, and industry, as well as by millions of indirect users across broader society. These users include those involved in satellite and flight routing, navigation systems, mobile networks, and the exploration and extraction of raw materials.

The NRIs hosted by EPOS-FI partner organizations provide data to both national and international data centers, as well as to the EPOS Thematic Core Services (TCS) (Figure 2). The data and services offered by EPOS-FI partners are partially accessible through separate Finnish databases. They also offer Open Access, Findable, Accessible, Interoperable, and Reusable (FAIR) geoscientific data management for both science and society. They also provide online data to international data centers and specific fields related to several EPOS TCSs, including Seismology, Anthropogenic Hazards, GNSS Data and Products, Geomagnetic Observations, Geological Information and Modeling, and Multi-Scale Laboratories. The FAIR principles ensure effective data management and enhance the transparency and reproducibility of research. These principles were published by Wilkinson et al. (2016). Moreover, the EPOS data portal offers easy access to data, data products, and services, along with comprehensive metadata that includes links to sources and publications (https://www.epos-eu.org/dataportal/; Bailo et al., 2023).

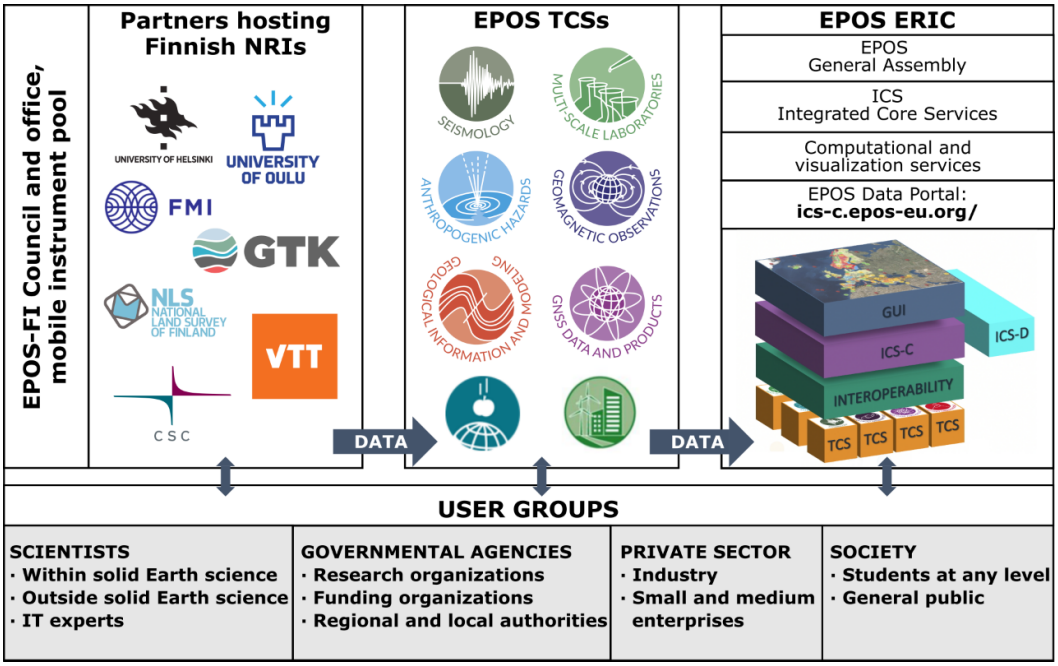

Figure 2. Structure of EPOS-FI and data delivery to EPOS TCSs.

NRIs comprise the Finnish permanent seismic, geodetic and geomagnetic observatory networks, geophysical and geochemical laboratories, laboratories for national timekeeping, a mobile geoscientific instrument pool FINNSIP (https://finnsip.fi/; Hillers et al., 2024), data and computing centers, and data portals. The instrumentation forms the basis for the Finnish reference frames for national time, space and positioning, geomagnetic field as well as seismic monitoring.

The mobile Finnish Seismic Instrument Pool (FINNSIP) is one of the largest seismic instrument pools in Europe, with over 1300 instruments. The FINNSIP is owned and maintained by Finnish universities and research institutions, with coordination provided by the Institute of Seismology, University of Helsinki. Other parties of the FINNSIP consortium include Aalto University, the Geological Survey of Finland (GTK), and the Universities of Oulu and Turku.

FINNSIP was established between 2020-2024 and currently comprises 46 broadband seismometers and digitizers, 5 accelerometers, and 1229 and 71 Geospace and SmartSolo autonomous geophone units, respectively. The selected instruments facilitate a diverse range of acquisition methods and monitoring capabilities. The governance and funding phase of the pool (FLEX-EPOS project, part of the FIN-EPOS project) will conclude in December 2024. Following this period, the pool will continue to operate, supporting both domestic and international collaborations for research or commercial projects with public or private entities.

3. Conclusions

The data and metadata from the NRIs related to the EPOS-FI infrastructure, along with the information they generate, play a crucial role in fostering a safe society and facilitating the movement of information, goods, and people.

Furthermore, the collection of data and metadata requires a long-term commitment at the national level. Continuous global time series and long-term openly accessible measurements are invaluable, forming an irreplaceable foundation for scientific research and societal

development. In this context, EPOS-FI facilitates the collection and long-term storage of information in a manner that supports the achievement of these objectives.

4. Acknowledgements

The national FIN-EPOS coordination and participation in EPOS ERIC and FLEX-EPOS have been granted with FIRI funding from the Academy of Finland for 2021–2024 by funding decisions 328984 and 328776, 328778-328782, 328784, 328786. Nordic EPOS – A FAIR Nordic EPOS Data Hub -project receives financial support from the NordForsk Research Infrastructure Hubs 2020–2022 call, decision number 97318.

References:

Atakan, K., Cocco, M., Orlecka-Sikora, B., Pijnenburg, R., Michalek, J., Rønnevik, C., Olszewska, D., Górka-Kostrubiec, B., Drury, M.R., 2022. National EPOS initiatives and participation to the EPOS integration plan. Annals of Geophysics, 65, 2, DM211; doi.org/10.4401/ag-8758.

Bailo, D., Paciello, R., Michalek, J., Cocco, M., Freda, C., Jeffery, K., Atakan, K., 2023. The EPOS multi-disciplinary Data Portal for integrated access to solid Earth science datasets. Sci Data 10, 784; doi.org/10.1038/s41597-023-02697-9.

Cocco, M., Freda, C., Atakan, K., Bailo, D., Contell, K.S., Lange, O., Michalek, J., 2022. The EPOS Research Infrastructure: a federated approach to integrate solid Earth science data and services. Annals of Geophysics, 65, 2, DM208; doi.org/10.4401/ag-8756.

Cocco, M., Montone, P., 2022. EPOS a Research Infrastructure in solid Earth: open science and innovation. Annals of Geophysics, 65, 2; doi.org/10.4401/ag-8835.

Hillers, G., Koivisto, E., Haapanala, P., Kukkonen, I., Courbis, R., Ding, Y., Fordell, T., Heinonen, S., Junno, N., Juntunen, A., Komminaho, K., Kozlovskaya, E., Leveinen, J., Moisio, K., Näränen, J., Oksanen, T., Skyttä, P., Tanskanen, E., Tiira, T., 2024. FINNSIP - The mobile Finnish Seismic Instrument Pool (in press).

Wilkinson, M. D., Dumontier, M., Aalbersberg, Ij. J., Appleton, G., Axton, M., Baak, A., Blomberg, N., Boiten, J.-W., da Silva Santos, L. B., Bourne, P. E., Bouwman, J., Brookes, A. J., Clark, T., Crosas, M., Dillo, I., Dumon, O., Edmunds, S., Evelo, C. T., Finkers, R., Gonzalez-Beltran, A., Gray, A. J. G., Groth, P., Goble, C., Grethe, J. S., Heringa, J., 't Hoen, P. A. C., Hooft, R., Kuhn, T., Kok, R., Kok, J., Lusher, S. J., Martone, M. E., Mons, A., Packer, A. L., Persson, B., Rocca-Serra, P., Roos, M., van Schaik, R., Sansone, S.-A., Schultes, E., Sengstag, T., Slater, T., Strawn, G., Swertz, M. A., Thompson, M., van der Lei, J., van Mulligen, E., Velterop, J., Waagmeester, A., Wittenburg, P., Wolstencroft, K., Zhao, J., Mons, B., 2016. The FAIR Guiding Principles for scientific data management and stewardship. Scientific Data, 3, 160018; doi.org/10.1038/sdata.2016.18.

Magnetotellurics over Kainuu belt, Finland

J. Tuomiranta[1], C. Patzer[2], J. Kamm[2] and J. Salminen[1]

[1]Department of Geosciences and geography, P.O. Box 64, 00014 University of Helsinki
[2]Geological Survey of Finland, P.O. Box 96 02151 Espoo, Finland
E-mail: jasmiina.tuomiranta@helsinki.fi

Understanding the subsurface electrical conductivity is particularly useful in regions with complex tectonic histories, as it provides critical information about geological history including metallogenic and tectonic evolution of the area. Both Kainuu belt as well as the Outokumpu belt are significant mineral provinces in Finland. Despite being genetically linked and having common geological history they are today spatially separated by about 40 km. The area has been studied in the past by 2D magnetotelluric (MT) measurements but due to the 3-dimensional structure of the area 2D interpretations are limited in scope. Therefore, we collected 27 additional MT sites to complement the existing data for subsequent 3D inversion. Here we present the preliminary 3D electric conductivity model of the Kainuu Belt, highlighting its potential deep connection to Outokumpu. The results indicate the presence of complex conductors, similar to those identified in previous studies, with the extension of measurements further south potentially linking these two geological regions.

Keywords: magnetotellurics, crustal resistivity, Kainuu belt

1. Introduction

The Fennoscandian Shield is one of the three main crustal segments of the East European Craton (Bogdanova et al., 2008). Its northeastern section consists of the Archean Karelian, Belomorian, and Kola provinces, while the southwestern part is made up of the Paleoproterozoic Svecofennian domain (Gaál and Gorbatschev, 1987). Paleoproterozoic intraplate rifting and subsequent orogenic events influenced the metallogeny of eastern Finland resulting in the formation of valuable metal deposits, including chromium, PGE, nickel, copper, and cobalt resources in Finland. Sediment hosted deposits formed at 2.1 - 1.95 Ga in the Kainuu belt (Talvivaara) and Outokumpu proto-ores were produced during the latest stages of rifting of the supercontinent Kenorland (Eilu and Lahtinen, 2013). While mineral deposits in the Kainuu belt and Outokumpu share a common geological history, they are at the surface spatially separated by several 10s of kilometres. However, there might be a connection between them at depth as also previously suggested by Vaittinen et al., (2012) based on conductivity model. That kind of connection would help in discovering new mineralizations and offering possible new insights into the metallogenic and tectonic history of the area.

The key tool to explore such deep crustal conductivity structures is the magnetotelluric (MT) method, which is a passive electromagnetic technique that measures natural variations of the Earth's electromagnetic field at the surface to infer subsurface (Simpson and Bahr, 2005). The goal of this work is to try to better understand the large-scale mineral systems at the Kainuu and Outokumpu regions in northern Karelia by complementing existing MT datasets from previous studies (e.g. Vaittinen et al., 2012) and creating 3D-model of the area. We extended the dataset from Vaittinen et al., 2012 southwards to confirm or refute the connection between Kainuu belt and Outokumpu region.

2. Methods and previous results

In June 2024 we collected 27 additional broad band MT stations measuring electric and magnetic fields to complement data from Vaittinen et al., 2012 and extent the survey area south towards Outokumpu (Figure 1). We used Metronix ADU dataloggers and MFS-07 induction coil magnetometers. Each site has been continuously recorded between 24 to 48 h with 128 Hz

sampling rate and 2 h with 4096 Hz at night. We used robust remote reference processing to obtain good quality MT transfer functions. The remote reference site was located near Sodankylä. We use ModEM software to (Kelbert et al., 2014) to derive a three dimensional electric conductivity model of the subsurface. The subsequent time series processing and inversions are currently ongoing work.

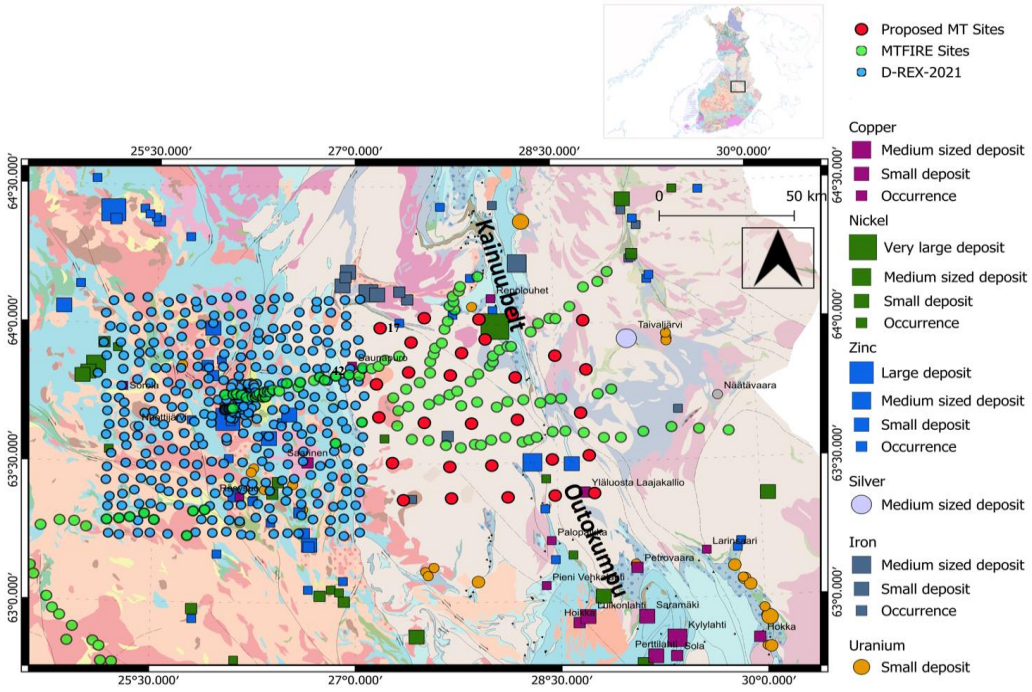

Figure 1. Kainuu belt and Outokumpu area Northern Karelia. Planned MT sites: Red dots. Existing sites from (Vaittinen et al., 2012): green dots. D-REx project (Kamm et al., 2022): blue dots. Mineral deposits: colored squares.

The national research project MT-Fire during years 2006-2008 by Toivo Korja was also partially overlapping with the research area from this project. Part of MT-Fire lines were crossing the Kainuu belt, and 2D inversion results of these suggested that there are no significant crustal conductors between the Kainuu belt and the Outokumpu region (Vaittinen et al. 2012). However, the moderate conductivity observed likely corresponds to shear zones between two Archaean complexes and the Archaean rocks in eastern Finland. The crust of Karelian province is highly resistive with only minor variations, including its Archaean lower crust, which contrasts with the more conductive lower crust of the Proterozoic Savo Belt and the granulitic lower crust of the Keitele microcontinent. Their model does show few possible complex conductors. The results were obtained along 2D lines and the interpretation in 3D settings will provide additional information about the area. In addition, Kamm et al. (2022) studied the nearby area of our measurement points (seen from Figure 1).

3. Results and discussion

Most of the newly measured sites show good to excellent data quality (site 042 in Figure 2, and on a map in Figure 1). However, some sites suffered from severe cultural noise contamination, resulting in loss of long period data. Additionally, we observe sites with phases outside the typical first/third quadrant, such as site 17 shown in Figure 2 and on a map on Figure 1. This suggests a complex three-dimensional subsurface structure, highlighting the significance of 3D inversion. The inversions are currently under process and results are primary in nature.

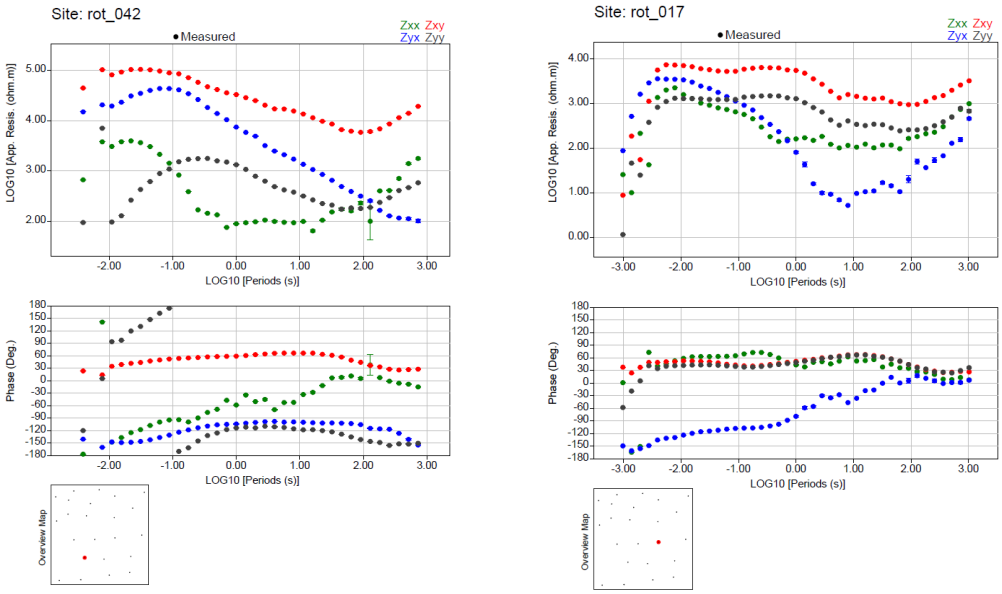

Figure 2. Apparent resistivity and phase curves of site 042 (left) and 017(right). Site 042 shows excellent data quality over the entire period range. Site 017 shows anomalous out of quadrant phase in the Zyx component for long period data.

The ongoing inversion processes and continued analysis of the data will provide more robust models of the subsurface, offering new insights into the geological history and the potential mineralization zones. These findings could not only advance our understanding of the metallogenic evolution of the Kainuu and Outokumpu belts but may also contribute to future mineral exploration in Finland. While the belts are spatially separated at the surface, the preliminary results suggest the presence of complex conductors below them, similar to those identified in earlier studies.

4. Conclusions

By expanding on previous 2D magnetotelluric (MT) measurements with 27 additional MT-sites and conducting a 3D inversion, we were able to explore the possible complex electrical conductivity patterns in the Kainuu and Outokumpu belt. The observed anomalous out-of-quadrant phases underscore the complexity of the subsurface structures, further highlighting the necessity of a 3D interpretation. The ongoing inversion processes will refine these findings, offering a clearer picture of the subsurface structure.

5. Acknowledgements

We want to thank Renlund foundation for financial support and CSC computing centre to allowing us to use their services.

References

Bogdanova, S.V., Bingen, B., Gorbatschev, R., Kheraskova, T.N., Kozlov, V.I., Puchkov, V.N. and Volozh, Y.A., 2008. The East European Craton (Baltica) before and during the assembly of Rodinia. *Precambrian Research*, *160*(1-2), 23-45.

Eilu, P. and Lahtinen, R., 2013. Fennoscandian metallogeny and supercontinent cycles. In *Proceedings of the 12th Biennial SGA Meeting. Sweden, Uppsala* (pp. 1632-1634).

Gaál, G. and Gorbatschev, R., 1987. An outline of the Precambrian evolution of the Baltic Shield. *Precambrian research*, *35*, 15-52.

Kamm, J., Mishra, P. K., Patzer, C., Autio, U., Vaittinen, K., Smirnov, M., Muhumuza, K., and Hill, G. 2022. 3D Magnetotelluric Study of the Crustal Architecture and Mineral System in Pyhäsalmi, Finland. AGU Fall Meeting Abstracts. Vol. 2022, GP33A–01

Kelbert, A., Meqbel, N., Egbert, G.D. and Tandon, K., 2014. ModEM: A modular system for inversion of electromagnetic geophysical data. *Computers & Geosciences*, *66*, 40-53.

Laajoki, K., Strand, K. and Härmä, P., 1989. Lithostratigraphy of the early Proterozoic Kainuu Schist Belt in the Kurkikylä-Siikavaara area, northern Finland, with emphasis on the genetic approach. *Bull. Geol. Soc. Finland*, *61*(Part 1), 65-93.

Lahtinen, R., Hölttä, P., Kontinen, A., Niiranen, T., Nironen, M., Saalmann, K. and Sorjonen-Ward, P., 2011. Tectonic and metallogenic evolution of the Fennoscandian shield: key questions with emphasis on Finland. *Geological Survey of Finland Special Paper*, *49*, 23-33.

Salminen, J., Lehtonen, E., Mertanen, S., Pesonen, L.J., Elming S.-Å., Luoto, T. 2021. The Precambrian drift history and paleogeography of Baltica. In: Pesonen, L.J., Salminen, J., Evans, D.A.D., Elming, S.-Å., Veikkolainen, T. (eds.) Ancient Supercontinents and the Paleogeography of Earth, Elsevier, 155–206. ISBN: 9780128185339.

Simpson, F. and Bahr, K., 2005. *Practical magnetotellurics*. Cambridge University Press.

Vaittinen, K., Korja, T., Kaikkonen, P., Lahti, I., & Smirnov, M. Y. (2012). High-resolution magnetotelluric studies of the Archaean-Proterozoic border zone in the Fennoscandian Shield, Finland. Geophysical Journal International, 188(3), 908-924.

Exploring the life and death of ancient orogens

D. Whipp[1], M. Häkkinen[1,2], L. Tuikka[1], A.-K. Maier[1], E. Muñoz[1], and S. Laaksonen[1]

[1]Institute of Seismology, University of Helsinki, Helsinki, Finland
[2]Department of Geosciences and Geography, University of Helsinki, Helsinki, Finland
E-mail: david.whipp@helsinki.fi

Ancient orogens offer a view into processes related to plate tectonics earlier in Earth's history. Ancient orogenic regions also commonly host valuable mineral deposits, making understanding their evolution from their tectonically active life to their post-tectonic death important for science and society. Here we provide some examples of how the evolution of ancient orogens can be understood using a variety of complementary approaches.

Keywords: orogen, numerical modelling, thermochronology, geodynamics, Fennoscandia

1. The challenge of understanding ancient orogens

Mountainous regions, or orogens, are one of the most striking manifestations of tectonic processes, with elevated topography shaped by the interactions between tectonics, erosion, climate, and biota (e.g., Starke et al., 2020). We can explore these interactions in modern orogens using a wide array of observable features, including surface elevations, geodetic measurements, seismicity, structural features, and many others. Ancient orogens, however, present a distinct challenge, often lacking key features that provide deeper insight into how various geological processes interacted and may have influenced the evolution of the orogen. These ancient settings, particularly of Archean and Paleoproterozoic age, are essential to study though, as deformed rocks of that age often host valuable mineral deposits that are important resources for the green transition. The question is: how can we understand the evolution of ancient orogens from their tectonically active period (or life) to their post-orogenic existence (or death)? Here we present a brief overview of the techniques used by the Helsinki University Geodynamics Group to study ancient orogens.

2. Reconstructing an ancient orogen's life

The metamorphic rocks that comprise the core of ancient orogens are one of the more useful records of the orogen's life (e.g., Liu et al., 2022). Through a combination of field observations, microstructural textures, bulk chemistry, phase equilibria calculations, and observed mineral assemblages it is possible to reconstruct the pressure-temperature-time (PTt) history of a metamorphic rock (Figure 1a). In the case of ancient orogens, this history can provide evidence of processes active within the upper to middle crust of the orogen. Although post-orogenic erosion leads to the later exposure of metamorphic rocks at the surface, the PTt history often reflects the life of the orogen. However, it can be challenging to link metamorphic PTt histories to past tectonic settings and infer something about the tectonic evolution of an orogen.

Numerical geodynamic models (e.g., Figure 1b) can simulate the tectonic evolution of orogens from millimeters to the scale of the upper mantle. These models incorporate various rheological behaviors including frictional plasticity and nonlinear viscosity, the transfer of heat and mass, and can be driven by gravitational forces to simulate tectonic plate-driving forces such as slab pull and ridge push. Beyond this, it is possible to use tracers in the models to record pressure and temperature as the model evolves, which can be compared to observed PTt histories (e.g., Figure 1a) to link metamorphic data to various tectonic settings.

3. Records of a dead orogen

Although ancient orogens may be active for tens of millions of years, the vast majority of their existence is in the post-orogenic, or dead, phase. During this time, erosion gradually removes the mountain topography and exposes the deeper levels of the orogen at the surface. Low-temperature thermochronology is an established technique for quantifying rates of rock exhumation over millions of years. However, erosion of dead orogens occurs at rates considerably slower than those during the orogen's life, presenting challenges to measuring thermochronometer ages due to slow cooling and the effects of radioactive decay damage on the diffusion of the daughter isotopes measured to determine ages. Fennoscandia presents an excellent opportunity for studying the extremely slow rates of erosion in a dead orogen using bedrock samples (Figure 1c) combined with inverse numerical models that incorporate the effects of radiation damage on mineral cooling ages (Figure 1d).

References:

Liu, Y., Mitchell, R. N., Brown, M., Johnson, T. E., & Pisarevsky, S. (2022). Linking metamorphism and plate boundaries over the past 2 billion years. *Geology*, *50*(5), 631-635.

Starke, J., Ehlers, T. A., & Schaller, M. (2020). Latitudinal effect of vegetation on erosion rates identified along western South America. *Science*, *367*(6484), 1358-1361.

Whipp, D. M., Kellett, D. A., Coutand, I., & Ketcham, R. A. (2022). Modeling competing effects of cooling rate, grain size, and radiation damage in low-temperature thermochronometers. *Geochronology*, *4*(1), 143-152.

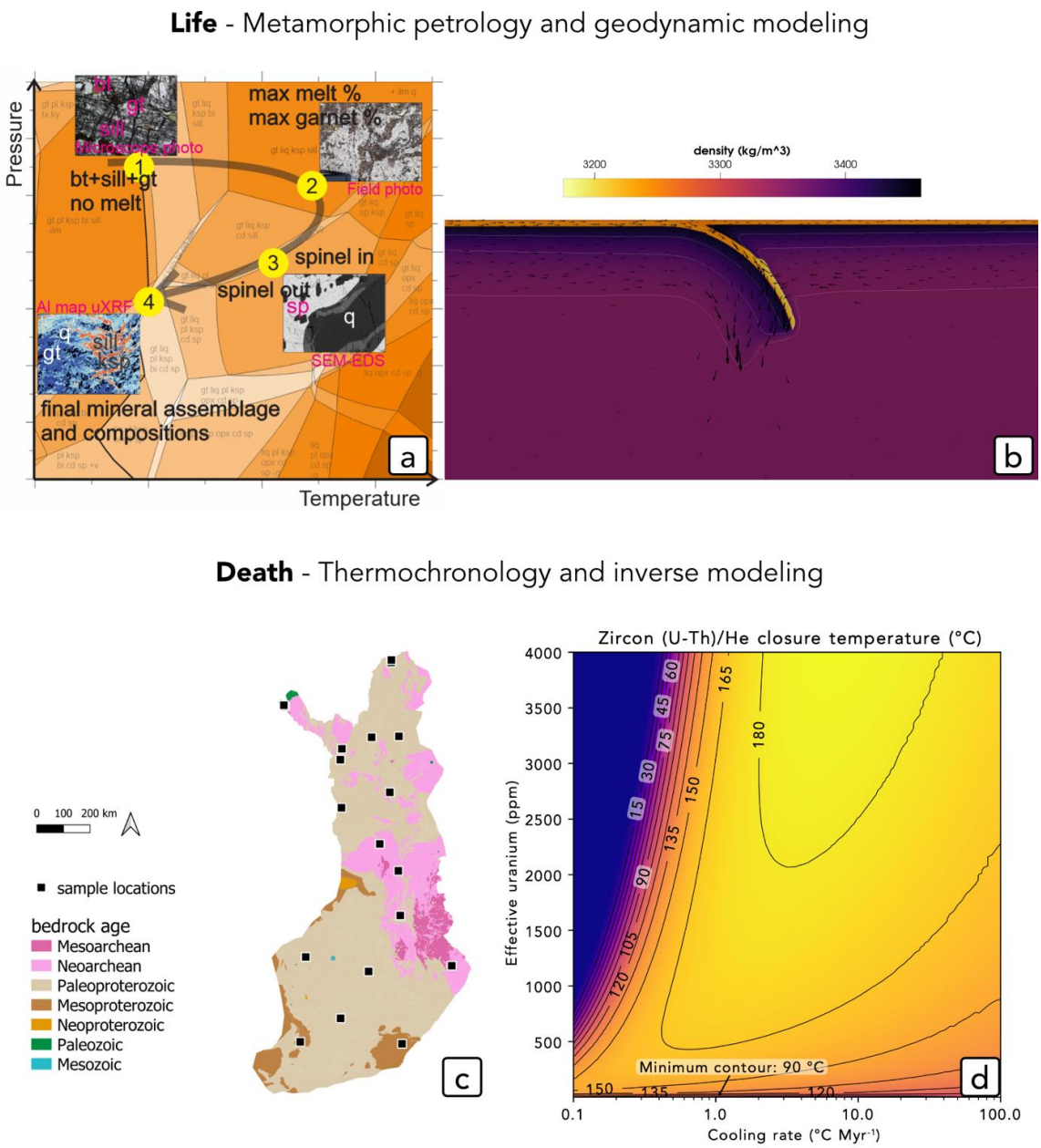

Figure 1. Approaches to studying the life and death of ancient orogens. (a) An example calculated pseudosection of stable metamorphic mineral phases with a reconstructed pressure-temperature-time (PTt) history (gray arrow). The PTt history incorporates (1) microtextures, (2) field observations, (3) electron microscope data, and (4) mineral assemblage and composition data. (b) An example of a 2D geodynamic model of gravity-driven subduction. (c) A map of Finland showing bedrock ages and sites visited in the summer of 2024 for bedrock sample collection for low-temperature thermochronology. (d) Predicted zircon (U-Th)/He thermochronometer effective closure temperatures as a function of cooling rate and effective uranium concentration. From Whipp/Kellett et al. (2022).

ISSN 0357-3060
ISBN 978-952-10-9614-3 (PDF)